VEER SURENDRA SAI UNIVERSITY OF TECHNOLOGY BURLA, ODISHA,

DEPARTMENT OF PRODUCTION ENGINEERING

Lecture Notes on

NON-TRADITIONAL MACHINING (NTM) COURSE CODE: BMS 401

7th Semester B. Tech in Production Engineering

MOUDULE- I

Introduction: Need for Non-Traditional Machining, Classification, Process Selection

Ultrasonic Machining: Principle, Transducer, Magnetrostrictive material, Analysis for material removal rate by Shaw, Effect of process parameters, Application.

1.1 INTRODUCTION

The industries always face problems in manufacturing of components because of several reasons. This may be because of the complexity of the job profile or may be due to surface requirements with higher accuracy and surface finish or due to the strength of the materials.

In the early stage of mankind, tools were made of stone for the item being made. When iron tools were invented, desirable metals and more sophisticated articles could be produced. In twentieth century products were made from the most durable and consequently, the most un-Machinable materials. In an effort to meet the manufacturing challenges created by these materials, tools have now evolved to include materials such as alloy steel, carbide, diamond and ceramics. A similar evolution has taken place with the methods used to power our tools. Initially, tools were powered by muscles; either human or animal. However as the powers of water, wind, steam and electricity were harnessed, mankind was able to further extend manufacturing capabilities with new machines, greater accuracy and faster machining rates.
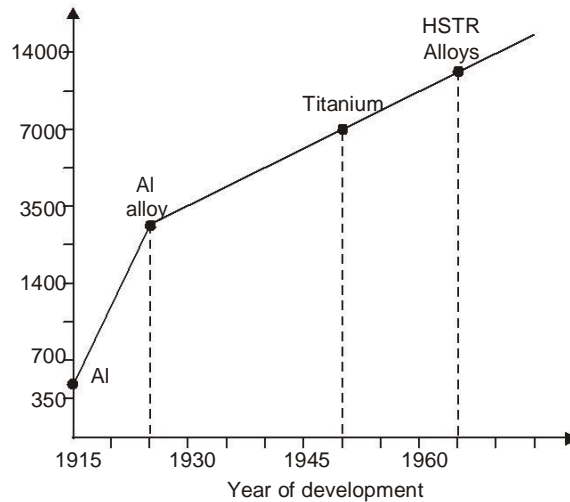
Trend of increase of material strength

Every time new tools, tool materials, and power sources are utilized, the efficiency and capabilities of manufacturers are greatly enhanced. Since 1940's, a revolution in manufacturing has been taking place that once again allows manufactuers to meet the demands imposed by increasingly sophisticated designs and durable but in many cases nearly unmachinable, materials.

In the Above figure Merchant had displayed the gradual increase in strength of material with year wise development of material in aerospace industry. This manufacturing revolution is now, as it has been in the past, centered on the use of new tools and new forms of energy. The result has been the introduction of new manufacturing processes used for material removal, forming and joining, known today as non-traditional manufacturing processes.

Non-traditional manufacturing processes harness energy sources considered unconventional by yesterday's standards. Material removal can now be accomplished with electrochemical reaction, high temperature plasmas and high-velocity jets of liquids and abrasives. Materials that in the past have been extremely difficult to form, are now formed with magnetic fields, explosives and the shock waves from powerful electric sparks. Material-joining capabilities have been expanded with the use of high-frequency sound waves and beams of electrons and coherent light. During the last 55 years, over 20 different non-traditional manufacturing processes have been invented and successfully implemented into production.

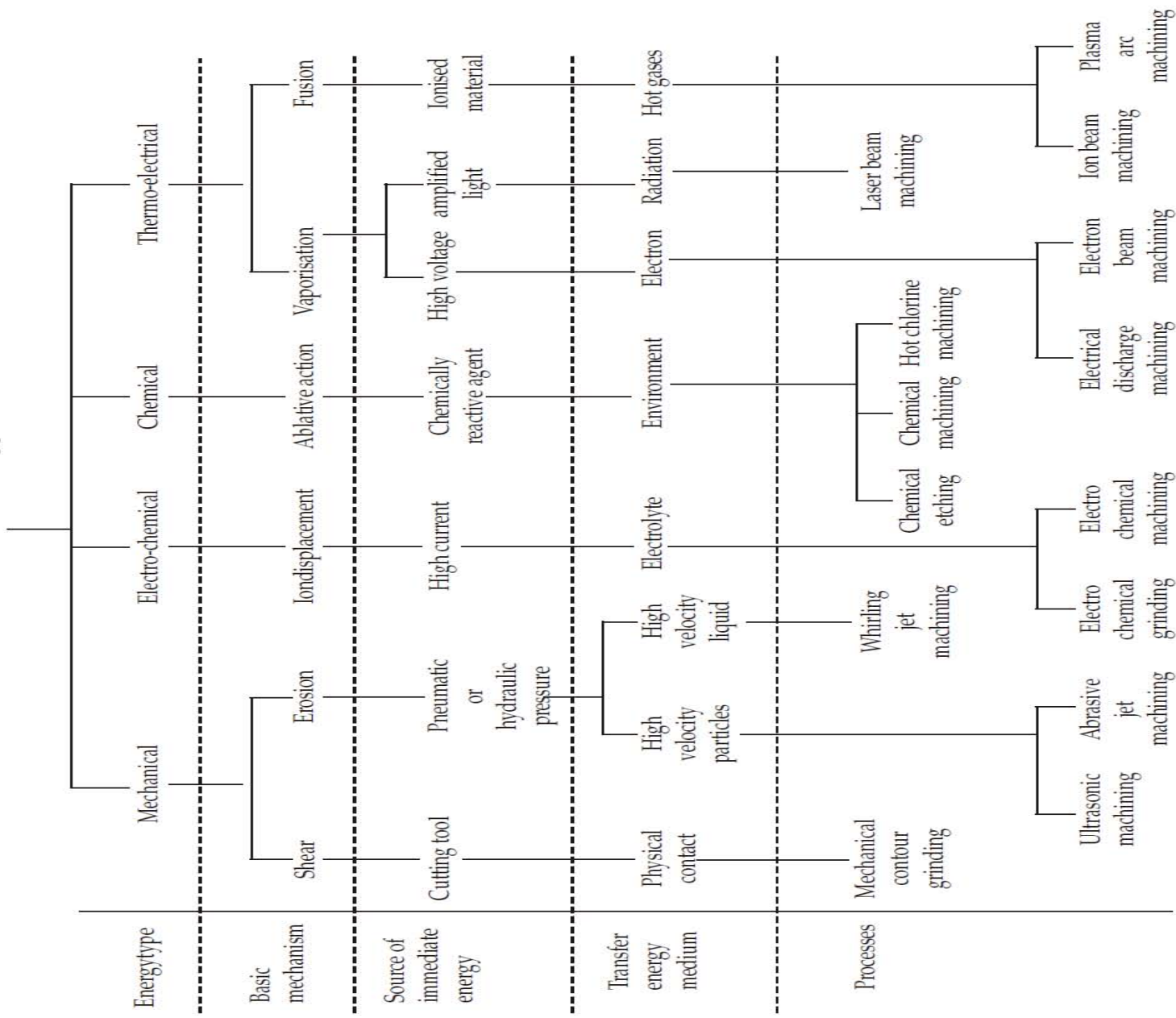## 1.2 CLASSIFICATION OF UNCONVENTIONAL MANUFACTURING PROCESSES

The non-conventional manufacturing processes are not affected by hardness, toughness or brittleness of material and can produce any intricate shape on any workpiece material by suitable control over the various physical parameters of the processes.

The non-conventional manufacturing processes may be classified on the basis of type of energy namely, mechanical, electrical, chemical, thermal or magnetic, apply to the workpiece directly and have the desired shape transformation or material removal from the work surface by using different scientific mechanism.
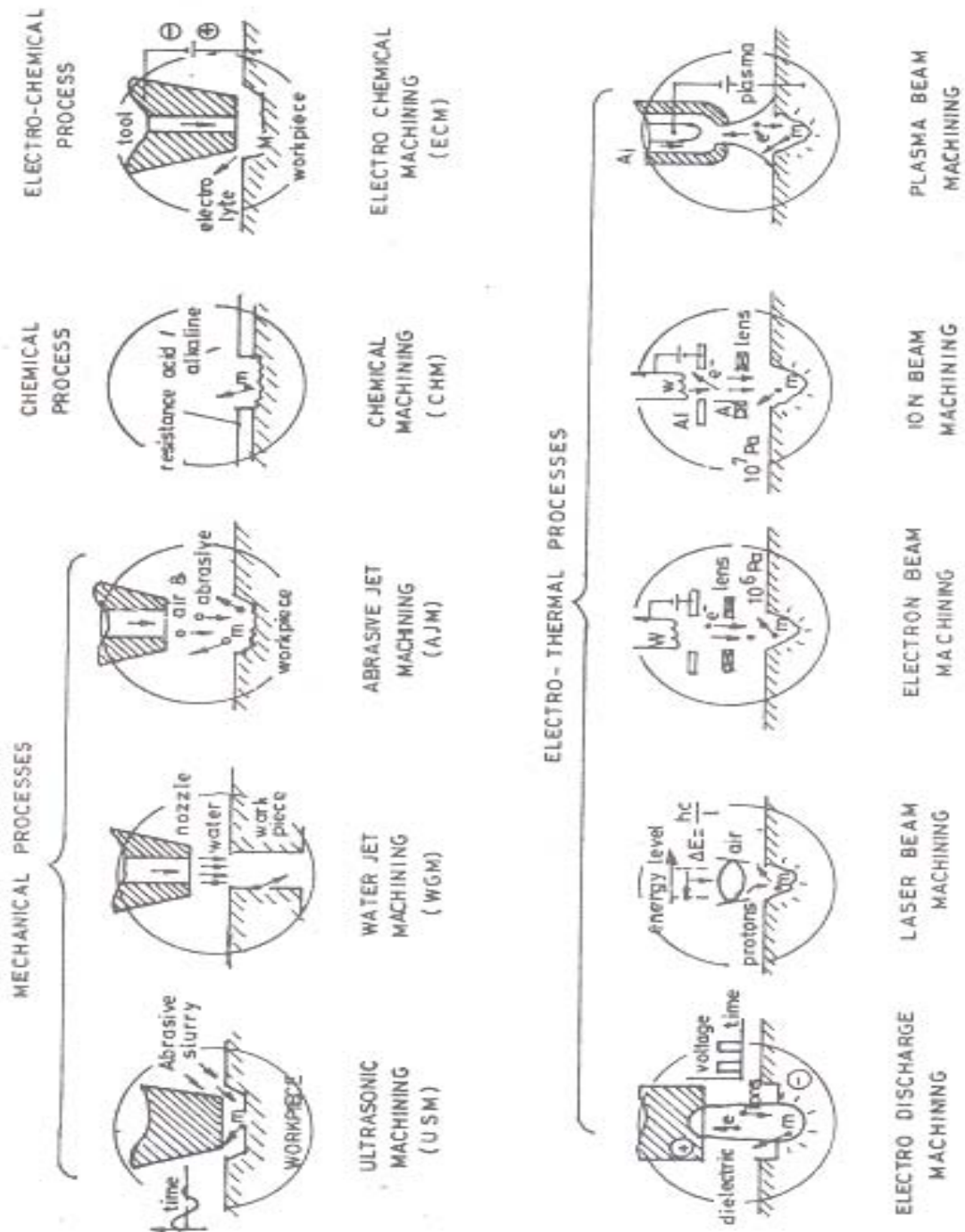
Thus, these non-conventional processes can be classified into various groups according to the basic requirements which are as follows :

    (*i*) Type of energy required, namely, mechanical, electrical, chemical etc.

   (*ii*) Basic mechanism involved in the processes, like erosion, ionic dissolution, vaporisation etc.

  (*iii*) Source of immediate energy required for material removal, namely, hydrostatic pressure, high current density, high voltage, ionised material, etc.

  (*iv*) Medium for transfer of those energies, like high velocity particles, electrolyte, electron, hot gases, etc. On the basis of above requirements, the various processes may be classified as shown

Non-conventional manufacturing processes

Energy type	Basic mechanism	Source of immediate energy	Transfer energy medium	Processes
Mechanical	Shear	Cutting tool	Physical contact	Mechanical contour grinding
	Erosion	Pneumatic or hydraulic pressure	High velocity particles	Ultrasonic machining / Abrasive jet machining
			High velocity liquid	Whirling jet machining
Electro-chemical	Ion displacement	High current	Electrolyte	Electro chemical grinding / Electro chemical machining
Chemical	Ablative action	Chemically reactive agent	Environment	Chemical etching / Chemical machining / Hot chlorine machining
Thermo-electrical	Vaporisation	High voltage	Electron	Electrical discharge machining / Electron beam machining
		amplified light	Radiation	Laser beam machining
	Fusion	Ionised material	Hot gases	Ion beam machining / Plasma arc machining

In these processes, as the machining mechanisms are quite different from each other shown in the figure below, the controlling parameters for machining differ from each other.

ELECTRO-CHEMICAL PROCESS — ELECTRO CHEMICAL MACHINING (ECM)

CHEMICAL PROCESS — CHEMICAL MACHINING (CHM)

MECHANICAL PROCESSES — ABRASIVE JET MACHINING (AJM), WATER JET MACHINING (WGM), ULTRASONIC MACHINING (USM)

ELECTRO-THERMAL PROCESSES — PLASMA BEAM MACHINING, ION BEAM MACHINING, ELECTRON BEAM MACHINING, LASER BEAM MACHINING, ELECTRO DISCHARGE MACHINING

1.3 COMPARATIVE ANALYSIS OF UNCONVENTIONAL MANUFACTURING PROCESSES

A comparative analysis of the various unconventional manufacturing processes should be made so that a guide-line may be drawn to find the suitability of application of different processes. A particular manufacturing process found suitable under the given conditions may not be equally efficient under other conditions. Therefore, a careful selection of the process for a given manufacturing problem is essential. The analysis has been made from the point of view of

     (*i*) Physical parameters involved in the processes;

    (*ii*) Capability of machining different shapes of work material;

   (*iii*) Applicability of different processes to various types of material, *e.g.* metals, alloys and non-metals;

    (*iv*) Operational characteristics of manufacturing

    (*v*) Economics involved in the various processes.

1.3.1 Physical parameters

The physical parameters of non-conventional machining processes have a direct impact on the metal removal as well as on the energy consumed in different processes. (Table 1.2)

TABLE 1.2. Physical Parameters of the Non-conventional Processes

Parameters	USM	AJM	ECM	CHM	EDM	EBM	LBM	PAM
Potential (V)	220	220	10	—	45	150000	4500	100
Current (Amp)	12 (A.C.)	1.0	10000 (D.C.)	—	50 (Pulsed D.C.)	0.001 (Pulsed D.C.)	2 (Average 200 Peak)	500 (D.C.)
Power (W)	2400	220	100000	—	2700	150	—	50000
Gap (m.m.)	0.25	0.75	0.20	—	0.025	100	150	7.5
Medium	Abrasive in water	Abrasive in gas	Electrolyte	Liquid chemical	Liquid dielectric	Vaccum	Air	Argon or hydrogen

From a comparative study of the effect of metal removal rate on the power consumed by various non-conventional machining processes shown in figure below.
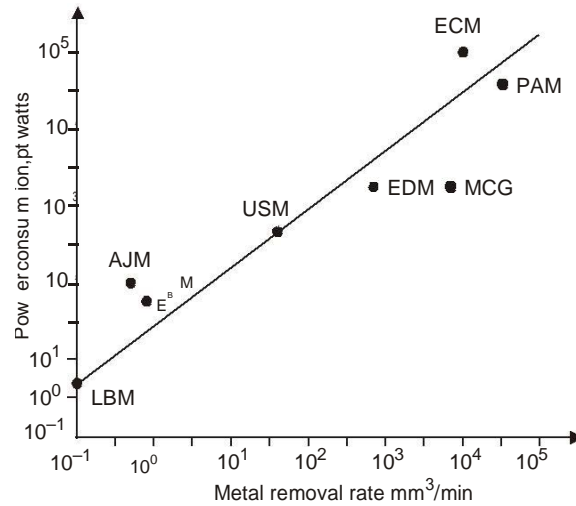
Effect of metal removal rate on power consumption.

It is found that some of the processes (*e.g.* EBM, ECM) above the mean power consumption line consume a greater amount of power than the processes (*e.g.* EDM, PAM, ECG) below the mean power consumption line. Thus, the capital cost involved in the processes (EBM, ECM etc.) lying above the mean line is high whereas for the processes below that line (*e.g.*, EDM, PAM, MCG) is comparatively low.

1.3.2 Capability to shape

The capability of different processes can be analysed on the basis of various machining operation point of view such as micro-drilling, drilling, cavity sinking, pocketing (shallow and deep), contouring a surface, through cutting (shallow and deep) etc.

TABLE 1.3. Shape Application of Non-conventional Processes

Process	Holes				Trough cavities		Surfacing		Trough cutting	
	Precision small holes		Standard		Precision	standard	Double contouring	Surface of revolution	Shallow	deep
	Dia < .025 mm	Dia > .025 mm	Length < 20 mm	Length > 20 mm						
USM	—	—	good	poor	good	good	poor	—	poor	—
AJM	—	—	fair	poor	poor	fair	—	—	good	—
ECM	—	—	good	good	fair	good	good	fair	good	good
CHM	fair	fair	—	—	poor	fair	—	—	good	—
EDM	—	—	good	fair	good	good	fair	—	poor	—
LBM	good	good	fair	poor	poor	poor	—	—	good	fair
PAM	—	—	fair	—	poor	poor	—	poor	good	good

For micro-drilling operation, the only process which has good capability to micro drill is laser beam machining while for drilling shapes having slenderness ratio L/D <20 the process USM, ECM and EDM will be most suitable. EDM and ECM processes have good capability to make pocketing operation (shallow or deep). For surface contouring operation, ECM process is most suitable but other processes except EDM have no application for contouring operation.

1.3.3 Applicability to materials

Materials applications of the various machining methods are summarised in the table 1.4 and table 1.5. For the machining of electrically non-conducting materials, both ECM and EDM are unsuitable, whereas the mechanical methods can achieve the desired results.

TABLE 1.4

Metals Alloys					
Process	*Aluminium*	*Steel*	*Super alloy*	*Titanium*	*Refractory material*
USM	Poor	Fair	Poor	Fair	Good
AJM	Fair	Fair	Good	Fair	Good
ECM	Fair	Good	Good	Fair	Fair
CHM	Good	Good	Fair	Fair	Poor
EDM	Fair	Good	Good	Good	Good
EBM	Fair	Fair	Fair	Fair	Good
LBM	Fair	Fair	Fair	Fair	Poor
PAM	Good	Good	Good	Fair	Poor

USM is suitable for machining of refractory type of material while AJM are for super alloys and refractory materials.

TABLE 1.5

	Non-Metals		
Process	*Ceramics*	*Plastic*	*Glass*
USM	Good	Fair	Good
AJM	Good	Fair	Good
ECM	—	—	—
CHM	Poor	Poor	Fair
EDM	—	—	—
EBM	Good	Fair	Fair
LBM	Good	Fair	Fair
PAM	—	Poor	—

1.3.4 Machining characteristics

The machining characteristics of different non-conventional processes can be analysed with respect to

(i) Metal removal rate

(ii) Tolerance maintained

(iii) Surface finish obtained

(iv) Depth of surface damage

(v) Power required for machining

The process capabilities of non-conventional manufacturing processes have been compared in table 1.6. The metal removal rates by ECM and PAM are respectively one-fourth and 1.25 times that of conventional whereas others are only a small fractions of it. Power requirement of ECM and PAM is also very high when compared with other non-conventional machining processes. This involves higher capital cost for those processes. ECM has very low tool wear rate but it has certain fairly serious problems regarding the contamination of the electrolyte used and the corrosion of machine parts. The surface finish and tolerance obtained by various processes except PAM is satisfactory.

TABLE 1.6

Process	*MRR* (mm^3/min)	*Tolerance* (μ)	*Surface* (μ) *CLA*	*Depth of surface damage* (μ)	*Power (watts)*
USM	300	7.5	0.2–0.5	25	2400
AJM	0.8	50	0.5–1.2	2.5	250
ECM	15000	50	0.1–2.5	5.0	100000
CHM	15	50	0.5–2.5	50	—
EDM	800	15	0.2–1.2	125	2700
EBM	1.6	25	0.5–2.5	250	150 (average) 2000 (peak)
LBM	0.1	25	0.5–1.2	125	2 (average)
PAM	75000	125	Rough	500	50000
Conventional machining	50000	50	0.5–5.0	25	3000

1.3.5 Economics of the processes

The economics of the various processes are analysed on the basis of following factors and given in Table 1.7.

Capital cost, Tooling cost Consumed power cost, Metal removal rate efficiency Tool wear.

TABLE 1.7

Process	*Capital cost*	*Tooling cost*	*Power consumption cost*	*Material removal rate efficiency*	*Tool wear*
USM	L	L	L	H	M
AJM	VL	L	L	H	L
ECM	VH	M	M	L	VL
CHM	M	L	H*	M	VL
EDM	M	H	L	H	H
EBM	H	L	L	VH	VL
LBM	L	L	VL	VH	VL
PAM	VL	L	VL	VL	VL
MCG	L	L	L	VL	L

* indicates cost of chemicals.

The capital cost of ECM is very high when compared with traditional mechanical contour grinding and other non-conventional machining processes whereas capital costs for AJM and PAM are comparatively low. EDM has got higher tooling cost than other machining processes. Power consumption is very low for PAM and LBM processes whereas it is greater in case of ECM. The metal removal efficiency is very high for EBM and LBM than for other processes. In conclusion, the suitability of application of any of the processes is dependent upon various factors and must be considered all or some of them before applying non-conventional processes.

Ultrasonic Machining (USM)

2.1 PROCESS

This is also an impact erosion process to machine materials where the work material is removed by repetitive impact of abrasive particles carried in a liquid medium in the form of slurry under the action of a 'shaped' vibrating tool attached to a vibrating mechanical system "Horn". The word 'shaped' explains that the process in capable of producing 3D, profiles corresponding to the tool shape. Basic scheme is as shown in Fig. 2.1.
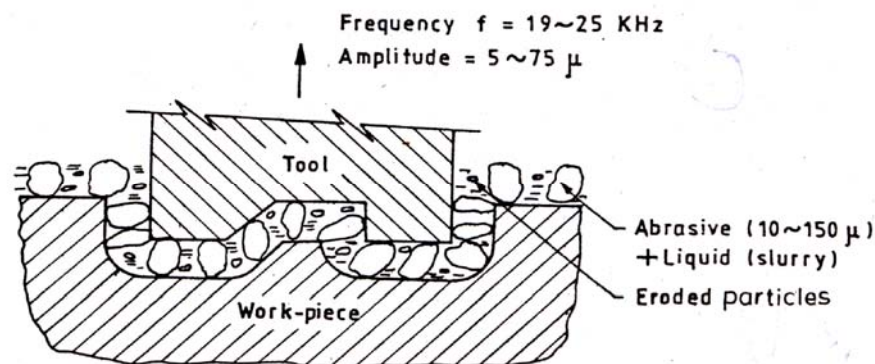
Fig. 2.1 Ultrasonic Machining

3.2 WORKING PRINCIPLE

The working principle is schematically shown in Fig. 2.2, where a shaped tool is given a mechanical vibration. This vibration causes the abrasive particles in the slurry to hammer against a stationary work piece to cause micro-indentations to initiate fracture in work material, observed as stock removal of the latter. The abrasives outside the domain of the tool remain inactive and so the removal process is an impact form machining process. The machined surface is approximately the inverse profile of the tool form. The machining rate is mainly dependent on the amplitude and frequency of impact.
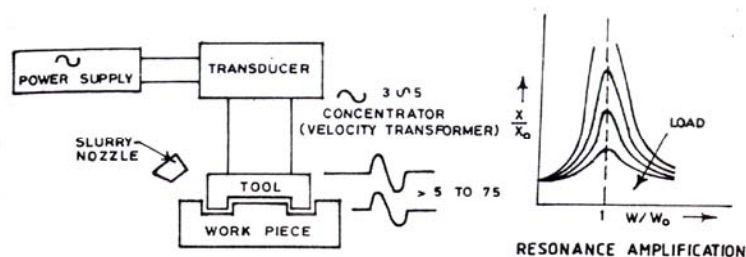
Fig. 2.2 Scheme of USM

The range of particle size used in the process generally lies between 10 and 150 microns, the amplitude of vibration is selected between 5 and 75 microns. The removal rate of material is also dependent on the rate at which the abrasive particles are hammered, i.e. the frequency of operation. Higher the frequency of operation better is the material removal rate. Higher frequency has some adverse effect on human being in shop floor. However, higher frequency of about 430 KHz was tried to produce vigorous agitation in the liquid, which in turn affected stray cutting effects on the work piece, whereas lower frequency does not have this effect. But higher frequency is utilised effectively to grind small parts.

Ultrasonic machining of hard materials in classified into two groups:

1.   Working with freely directed abrasives using high frequency (grinding).

2.   Precision ultrasonic machining under the purview of present deliberation.

The much more safer zone of ultrasonic machining is between 19 kHz and 25 KHz. So, the tool is to be vibrated with an amplitude of vibration of 5 to 75 microns at a frequency between 19 and 25 kHz.

Abrasive in a slurry form is more effective compared to abrasives in loose form, since the liquid would help removal of material due to cavitation effect during return stroke of the tool. Moreover, the liquid will help evenly distribution abrasive particles into the working gap.

Vibration to the tool is imparted from a transducer (Fig. 3.2) which is energised by a electronic generator. The transducer converts the electrical energy to mechanical vibration whose frequency corresponds to the electrical supply frequency.

Since the vibration amplitude achievable from the transducer generally does not exceed 3 to 5 microns,, it needs to be amplified on the principle of mechanical resonance by the concentrator (velocity transformer), between. The transducer and tool. This connector also serves as the tool holder. It has amplitude of vibration at about 3 to 5 micron corresponding to the transducer at one end required vibration amplitude of about 5 to 75 microns at tool end. The transducer along with the concentrator and tool is known as "ACOUSTIC HEAD"

Hence working principle of the machine tool will depend on:

Transducer   :   Type of material and its operational characteristics.

Concentrator :   Shape, material property.

Tool :   Material, shape and wear rate.

Abrasive slurry : Material, shape and size.

Operating parameters : Frequency, amplitude of vibration, static load.

Others : Mounting, feed mechanism, working temperature, etc.

The cutting process employs the mechanical vibration of the tool. The process cannot be of high efficiency unless most of the input electrical energy to the transducer and the resulting mechanical energy thus produced in the vibrator (horn) suffers minimum losses. And thereby the energy transmitted to the working zone and via the vibrator itself is dependent on the load to which it is coupled. The maximum efficiency is obtained by a proper matching of the two; the transducer and the vibrator.

Major working parts of this machine is the acoustic head (Fig. 3.3). The main function of this is to produce and propagate vibration in the tool. Energy is being drawn from the generator in electrical form and is converted to mechanical form either by of Piezoelectric or Magnetostriction method.

Though the former is easier for design, yet due to its non-availability, latter has been tried. The periodical shortening and lengthening of the transducer in synchronism with the generator frequency initiates the vibration. The inadequacy of this amplitude of vibration necessitates the use of a concentrator (Horn). The concentrator is simply a convergent wave-guide for designed amplitude at its far end. The two together form the vibrating system.
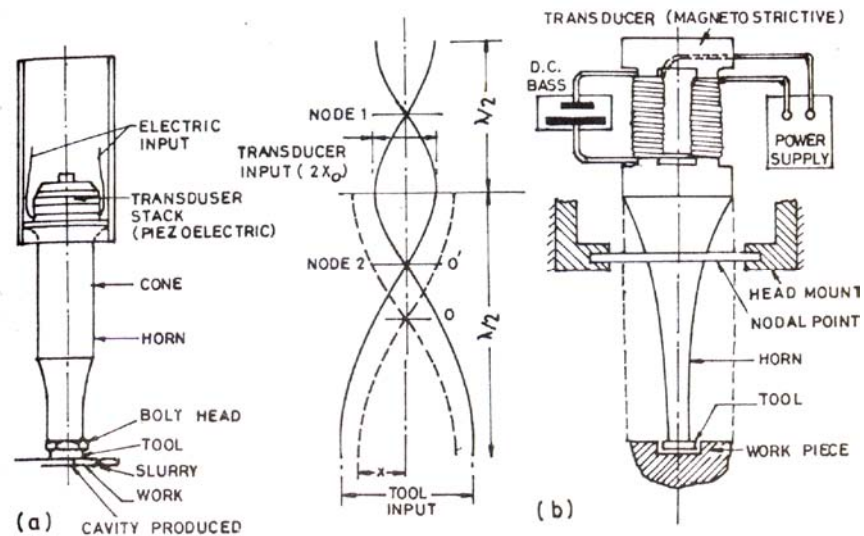
Fig. 3.3 Scheme of Acoustic Head.

vibrator is made resonating to obtain sufficient amplitude. The length of propagation is made half-wavelength (or occasionally a multiple of this). The concentrator becomes a

volume resonator tuned to the same frequency which produces best condition for maximum power transfer.

There is always a second channel for the energy to dissipate as waste through the holder 6 and the fixed part 6 of the feed-mechanism. To minimise the loss it is advisable to fix the holder at any nodal point of the vibrating system. From the above considerations it is seen that proper care must be taken while designing the different accessories of the machine in order to achieve maximum attainable efficiency of the machine.

3.2.1 Magnetostrictive transducers

There are some materials which exhibit change in dimension when they are magnetised. This property is known as magnetostriction or piezomagnetism. The change can be either positive or negative in a direction parallel to the magnetic field and is also independent of the direction of magnetic field.

Magnetostriction can be explained in terms of Domain theory. Domains are very small elements of material in the order of 10^{-8}-10^{-9} cm^3, called as dipoles. The forces cause the magnetic moments of the atoms to orient in a direction easier for magnetisation, coinciding with the directions of the crystallographic axes. In the cubic-lattice crystals (ferromagnetic) like iron and nickel there are six directions of easier magnetostriction. During unmagnetised condition all these axes remain in equal number causing the magnetic moment order less and unoriented domains, compensate one another. Under sufficient magnetic field, the magnetic dipoles (domains) orient themselves in the direction of magnetic field. This causes the material either to expand or contract till all the magnetic domains become parallel (magnetically saturated). When the material expands on the application magnetic field irrespective of its direction is called as positive-magnetostriction and similarly for negative- magnetostriction when it contracts.

Thus the strain produced (positive or negative) i.e. $\Delta l / l$ is very small of the order of 10^{-6} to

10^{-5}. The magnetostrictive curves for few commonly used materials are shown in Fig. 3.4 (a).

It is observed that most of the material exhibits positive-striction but for nickel it is negative. Some materials like iron and cast cobalt exhibit dual characters i.e. below about 350 Oersted of field intensity they behave positive and above that their properties reverse.

Practical materials, iron-cobalt, iron-aluminium (Alfer), and nickel have the highest magneto striction. An alloy of platinum (32%) and iron (68%) has exhibited highest magnetostriction of all ($\Delta l / l = 1.8$ X 10^{-4}) but of no use in practice for its high cost.

.

However, the property deteriorates at higher temperature and completely ceases above Curie-temperature of individual material. So consideration is to be provided while designing and developing the cooling system for magnetostrictive transducers, otherwise the natural frequency of the magnetostrictive core may change to detain the system from resonance.

Iron-aluminium alloy, Alfer displays similar magnetostriction as Nickel but owing to its higher resistivity its hysteresis loss is lower. Moreover, Alfter is stronger mechanically than nickel. Permendur has a special feature of high brittleness, cracks are to be avoided after stamping and should not be subjected to shocks or bending after annealing. It has got higher hysteresis loss than Alfer.

The magnetic properties of rolled sheets of magnetostrictive materials are anisotropic, particularly Permendur in the rolling direction and least in the perpendicular direction. Therefore, sheets cut at 45° to the rolling direction are best for making transducers.

3.2.2 Transducer Amplifications

Piezoelectric or Electrostrictive transducer developed so are for very high frequency application because of its growth size. If it is required to use this type of transducers with large radiating surface or at low frequency, it runs into difficulties since in the first case it is to obtain large enough crystals or manufacture large enough crystals units and in the second case similar considerations apply along with the fact that the radiation impedance becomes extremely high so that matching of the transducer to the generator becomes impossible. Both the difficulties may be overcome by using a sandwich transducers which consists of piece or pieces of transducer
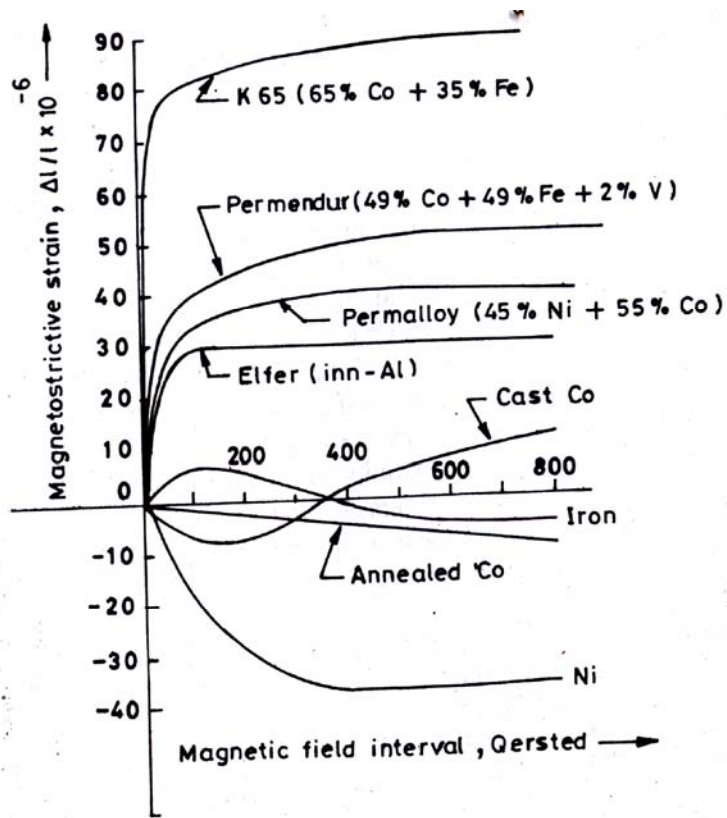
(a)
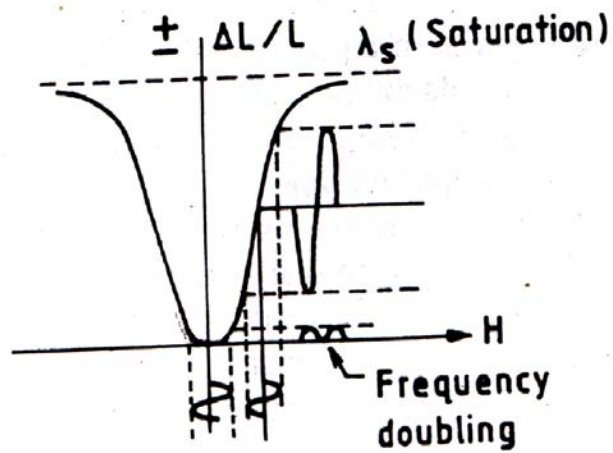
(b)

Fig. 3.4 Magnetostrictive Property of some Materials

materials cemented between two plates of non-piezoelectric materials. Using several pieces of transducer materials side by side the radiating surface can also be increased. Since the complete sandwich system (Fig. 3.3a) now form the resonating system, the operating frequency comes down mismatching with discrete transducer materials resonant frequency. However, this type of transducers are preferred for low power applications of ultrasonic machining and good quality factors are not achievable by these types of transducer. For high power applications (intensity > 0.5 watt/cm^2) the performance is not satisfactory. For very high power (above about 500 watt) the cost also becomes very high. For better quality and cheaper transducers, magnetostrictive types are preferred.

Magnetostrictive transducers are used in nearly all good quality ultrasonic machine tools. Their advantages are their high efficiency, easier manufacturability and higher reliability in the range of 15-30 kHz. It also needs cooperatively very low voltage supply. Unlike previous type of transducers, this type of transducer requires a closed magnetic path, hence a window type (Fig. 3.5) transducer is commonly preferred.
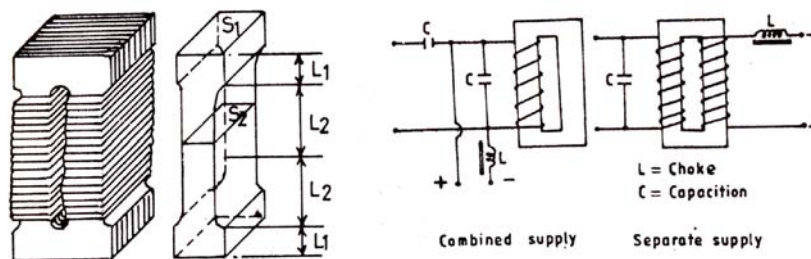
Fig. 3.5 Window Type Magnetostrictive Transducer

A magnetostrictive material in an alternating field vibrates at twice the frequency of field (frequency doubling) as follows from the symmetry of the magnetostrictive curve (Fig. 3.4b). Besides this the amplitude of mechanical vibration is small since the slope near zero magnetic field is very small. The system becomes non-linear and increases loss. All these undesired qualities are removed by shifting the excitation to one side of the linear portion of the electrostriction curve, i.e. by providing a steady field or a biasing magnetization. So a steady field superimposed on the alternating field would provide a steady undistorted and matched frequency mechanical vibration is obtained from the transducer (but with 180° out of phase).

Whatever type of transducers may be used, the losses in them are kept to minimum when the amplitude of vibrations are limited not to exceed 3-5 microns.

Since the required level of vibration at the tool end is more, the transducer vibration needs to be amplified many fold. This is done by means of the concentrator or the resonator which is nothing but a mechanical amplifier.

3.2.3 Concentrator

The concentrator provides the link between the transducer and tool and its main function is to amplify the amplitude of vibration as per requirements. This is also achieved through the principle of resonance (Fig. 3.2). If a proper length of any material whose natural frequency ω matches with the excitation frequency ω_0 with amplitude x_0, then at resonance, i.e. at $\omega / \omega_0 = 1$ the ratio x / x_0 increases, if it is not critically damped.

Now if a straight rod, preferably of a ductile material (Fig. 3.2) is chosen with length equal to its half wavelength of sound and allowed to resonate the free ends will vibrate with an amplitude $x > x_0$. The point will be at the center of the rod, i.e. at $0°$. But then the end which will be connected to the exciter, i.e. the transducer, will suffer from amplitude mismatch which does not allow the system to work smoothly.

If a taper rod is chosen in place (Fig. 3.3b) then the nodal point will be shifted from point 0 to 0' because change of center of mass, shifted towards the larger end. This provides the smaller and to vibrate at higher amplitude x while the larger and is at x_0 to match comfortably with the transducer. Thus a gain in amplification is achieved for amplitude of vibration and for this reason the concentrator, sometimes, is called as a mechanical amplifier or resonator and because of its taper shape and amplification, commonly known as a 'HORN'.

3.2.4   Nodal Point Clamping

Method of fixing the vibratory system as discussed earlier (consisting of transducer, horn and tool) to form the acoustic head is of very importance. It should be done in such a way that it makes a rigid system without enough loss in the mounting, so it has to be damped at the nodal points. Otherwise, losses are increased and fatigue failure is inhabitable. The dampening at nodal point at the transducer is not permitted because of electrical supplies and hence clamped at other nodal points are maintained as shown in Fig. 3.3.

3.2.5   Feed Mechanism

Feed system is to apply the static load between the tool and work piece during machining operation. The precision and sensitivity are of high importance. Feed may either be given to the acoustic had or to the work-piece as per the designer's choice, but in general, the feed motion is given the acoustic head so as to permit x-y positioning facility to the work piece (Fig. 3.6). In the figure (a) and (b) are for gravity feed devices where counter weights are used to apply the load to the head though a pulley and lever device respectively. In
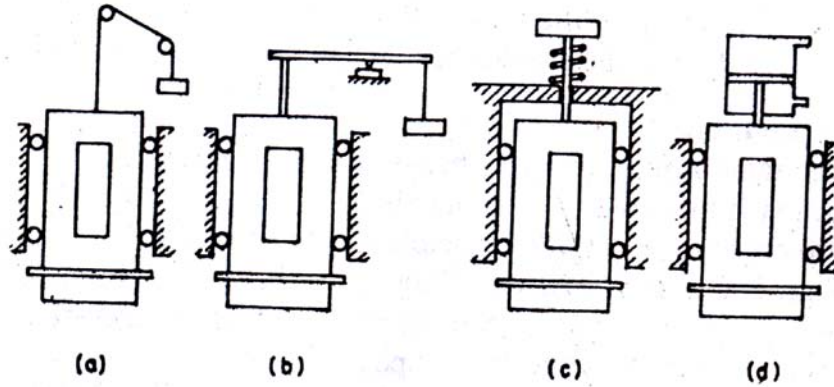
Fig. 3.6 Scheme of Different Types of Feed Systems

(c), a spring loaded system is shown; for high feed rate conditions either pneumatic or hydraulic system as shown in (d) may be preferred.

3.3 SELECTION OF PROCESS

Selection of the tool for particular profile generation are to be made from the material of the work-piece, tool and the abrasives used responsible for different types of wear occurring on the tool which is schematically explained in the Fig. 3.7.

The application and performances are given in Table 3.1.

Table 3.1 Typical Performance Characteristics (Obtained from a 700 W USM with a cold rolled steel and 32 micron boron carbide abrasive)

Material	Ratio of MRR to TWR	Max. machining area (cm^2)	Average penetration rate (mm/min)
Glass	100: 1	25.8	3.81
Ceramic	75: 1	19.4	1.51
Germanium	100 :: 1	22.6	2.16
WC	1.5 :: 1	7.7	0.25
Tool Steel	1 :: 1	5.6	0.13
Mother of Pearl	100 :1	25.8	3.81
Synthetic Ruby	2 :1	5.6	0.51
Carbon-graphite	100 :1	19.4	2.00
Ferrite	100 :1	22.6	3.18
Quartz	50 :1	19.4	1.65
B_4C	2 :1	5.6	0.20
Glass bonded mica	100 :1	22.6	3.18

3.4 MATERIAL REMOVAL RATE (MRR)

3.4.1 An Empericai Approach

This method is adopted in practice when the theory of analysis for MRR is not known. In this approach let us consider the following parameters that influences MRR:

(i) Abrasive grit (R).

(ii) Packing density (η), i.e. how closely the abrasives are packed in the slurry.

(iii) Amplitude of vibration (y_0) of the tool.

(iv) Frequency of vibration (f) or. angular frequency (ω) of the tool; ($\omega = 2\mu f$).

(v) Stress (σ) developed in the tool.

(vi) Hardness (*H*) of the work material.

Hence MRR can be expressed as a combined function of the above parameters as:

$$MRR = \vartheta(say) = \phi(R, \eta, y_0, f, \sigma, H) \tag{3.1}$$

To get the relation experimentally one must go through dimensionless parameters generated out of these variables

$$\left[\frac{Y}{Y_0 f}\right], \left[\frac{Y_0}{R}\right], \left[\frac{\sigma}{H}\right] and \left[\Upsilon l\right]$$
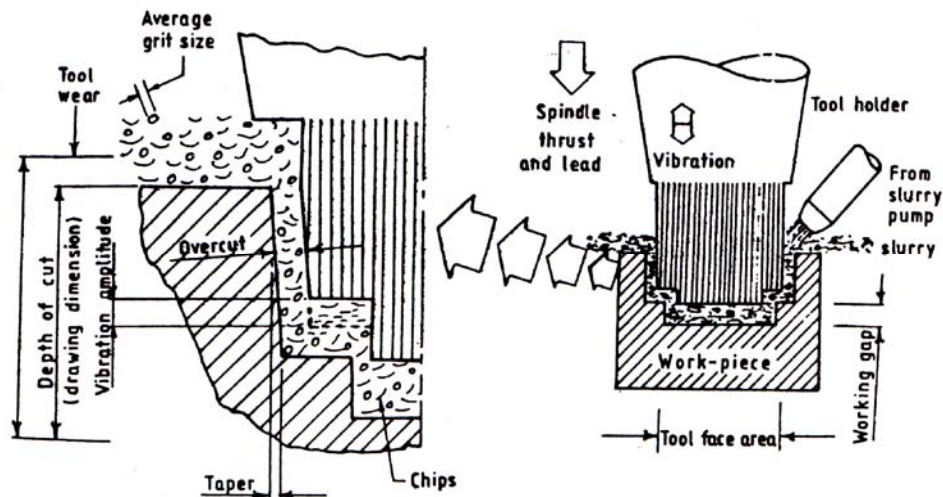
Fig. 3.7 USM Operating Terminology

Keeping $[Y_0/R]$ and $[\eta]$ constant one must plot the relation between $[\vartheta/Y_0R]$ and $[\sigma/H]$ as given below (say, but actually seen in experiments) This is done under a constant static load and slurry conditions. MRR

observed for varying work hardness H and the experiment is repeated for different value of Y_0. The curves are generally non-linear, so assuming first order non-linearity the log-log plot is given as (Fig. 3.8):

From the curves intercept $[C]$ against $[Y_0/R]$ we get

$$\log\left[\frac{\vartheta}{Y_0R}\right] = n\log\left[\frac{\sigma}{H}\right] + \log C$$
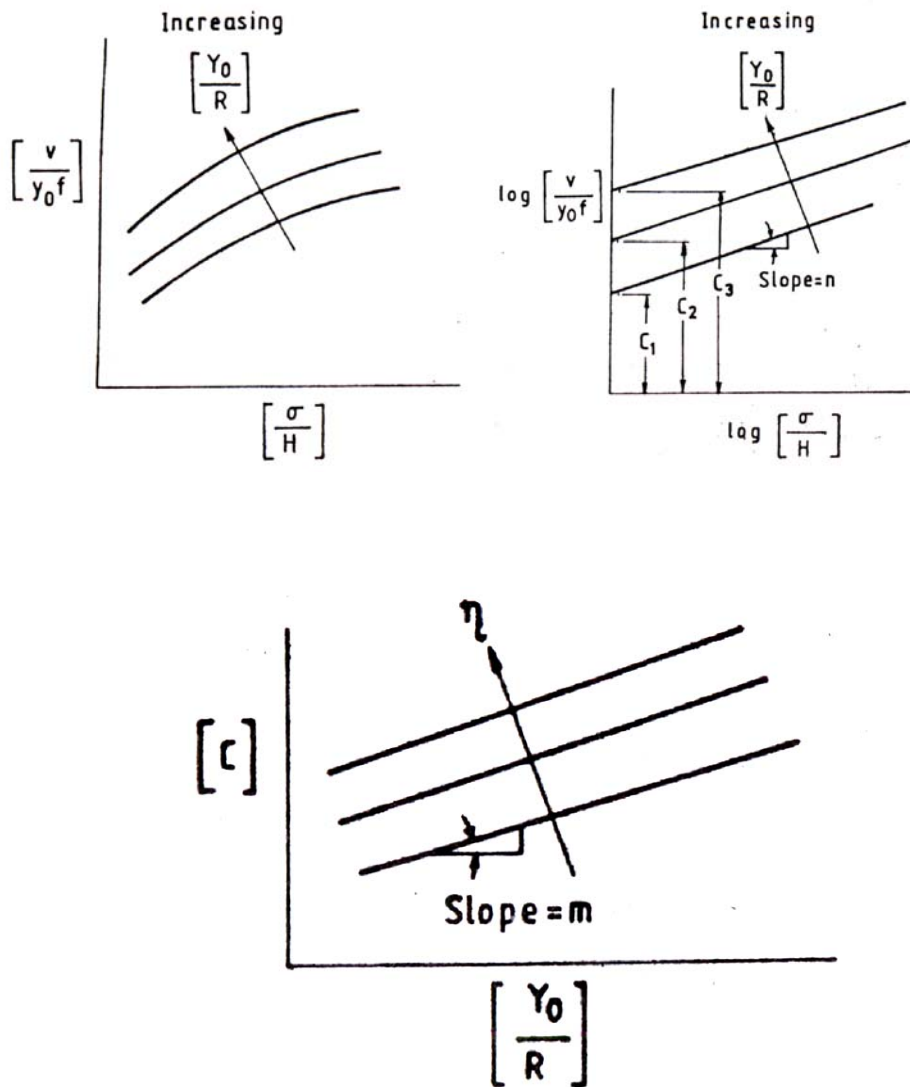
Fig. 3.8 Effect of Operating Parameters on MRR

or $\quad \left[\dfrac{\vartheta}{Y_0 f}\right] = C\left(\dfrac{\sigma}{H}\right)^n$ $\hspace{3cm}$ (3.2)

Now, the curves intercept [C] is plotted against [Y_0/R] to get their relations.-

This procedure may be conducted for different packing density (η) as follows. Hence relation of C with (Y_0/R) can be written (Fig. 3.8) as:

$$C = K(\eta)\left(\dfrac{Y_0}{R}\right)$$ $\hspace{3cm}$ (3.3)

where K is a function. Rewriting eq. 3.2, we get

$$\dfrac{\vartheta}{Y_0 f} = K(\eta)\left(\dfrac{Y_0}{R}\right)\left(\dfrac{\sigma}{H}\right)^n$$

$$= K_1\left(\dfrac{Y_0}{R}\right)\left(\dfrac{\sigma}{H}\right)^n$$

or $\quad \vartheta = K_1\left(\dfrac{Y_0^{\,2}}{R}\right)\left(\dfrac{\sigma}{H}\right)^n .f$ $\hspace{3cm}$ (3.4)

where $K_1 =$ is a constant.

3.4.2 An Analytic Approach (Cook's Model)

This model is based on the brittle fracture of the work materials and under following assumptions:

(i) The abrasive grits are spherical in nature.

(ii) Material removal (Fig. 3.9) is based on hemispherical fracture mechanism due to the indentation.

(iii) Tool and abrasive are rigid.
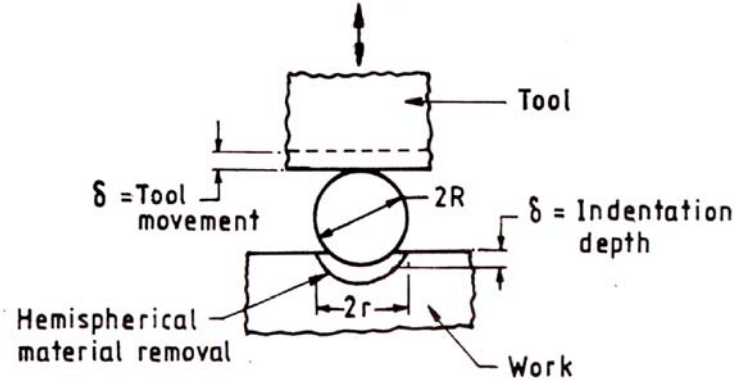
Fig. 3.9 Scheme of Material Removal Process

If R is the radius of the abrasive grit (average), r = radius of circular indentation and H the hardness of work material, then the volume of the material removed per impact t) is given by (Fig. 3.10):

$$\vartheta = \frac{1}{2}\left(\frac{4}{3}\pi r^3\right) = \frac{2}{3}\pi r^3 \tag{3.5}$$

Hence $\text{MRR/grit} = \vartheta.f = \frac{2}{3}\pi r^3 f \tag{3.6}$

where, f = frequency of operation.
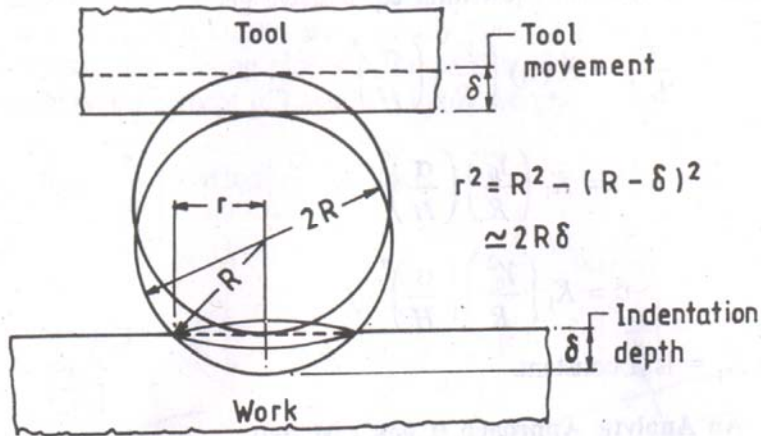
Fig. 3.10 Indentation Geometry

From the geometry of above figure, substituting the value of r, eq. 3.6 can be rewritten as:

$$\text{MRR/grit} = \frac{2}{3}\pi\left(2R\delta\right)^{3/2} f \tag{3.7}$$

If there are N number of grits per unit area, then total
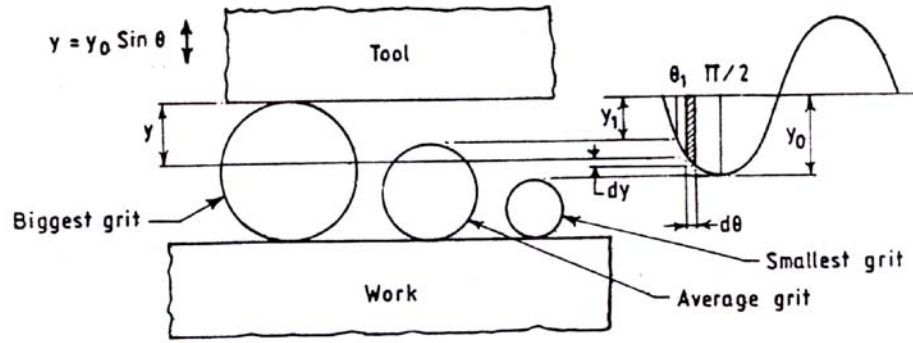
Fig. 3.11 Variable Indentation with the Tool Movement

$$\text{MRR} = \frac{2}{3}\pi \left(2R\delta\right)^{3/2} N f \tag{3.8}$$

Since the abrasives are not of same size to create actual indentation depth δ and number of abrasive particles per unit area are unpredictable, it becomes difficult to find the actual MRR. To eliminate these two terms, a force analysis is to be done as these are two contributing factors for forces on both tool and work. Figure 3.11 shows how the indentation will vary with movement of tool.

Actually, the force generated on the tool, and work due to a grit, is because of the tool movement from θ_1 to $\pi/2$. Hence, the average force per grit is given by

$$2\pi P_{avg} = \int_{\theta_1}^{\pi/2} P d\theta \tag{3.9}$$

where P = instantaneous force due to δ penetration.

But $P = \pi r^2 H = \pi 2R\delta H = K\delta$

where, $k = 2\pi RH$ is a constant, and

$\delta = y - y_1 = Y_0 \sin\theta - Y_0 \sin\theta_1$

(assuming a sinusoidal vibration of the tool).

So, $2\pi P_{avg} = \int_{\theta_1} \left(Y_0 \sin\theta - Y_0 \sin\theta_1\right) d\theta$

or $\dfrac{2\pi P_{avg}}{KY_0} = \int\limits_{\theta_1}^{\pi/2} \left(\sin\theta - \sin\theta_1.\theta\right) d\theta = \left[-\cos\theta - \sin\theta_1.\theta\right]_{\theta_1}^{\pi/2}$

or $\dfrac{2\pi P_{avg}}{KY_0} = \left[\cos\theta_1 - \sin\theta_1\left(\dfrac{\pi}{2} - \theta_1\right)\right]$ (3.10)

Now, right hand side of the expression is a function of 0,, i.e.:

$$\phi(\theta_1) = \cos\theta_1 - \sin\theta_1\left(\dfrac{\pi}{2} - \theta_1\right)$$

Here $\phi(\theta_1)$ is a mathematical function and can be solved numerically. Again, maximum indentation δ_{max} is given by

$$\delta_{max} = Y_0 - y_1 = Y_0(1 - \sin\theta_1)$$

$$\sin\theta_1 = 1 - \left[\dfrac{\delta_{max}}{Y_0}\right]$$

or $\theta_1 = \sin^{-1}\left[1 - \dfrac{\delta_{max}}{Y_0}\right]\theta_1 = \sin^{-1}\left[1 - \dfrac{\delta_{max}}{Y_0}\right]$ (3.11)

Assume different ratios of (δ_{max}/Y_0) to obtain values of θ_1, to calculate the values of $\phi(\theta_1)$. If plotted as in Fig. 3.12, it will give a relation between $\phi(\theta_1)$ and (δ_{max}/Y_0) as:
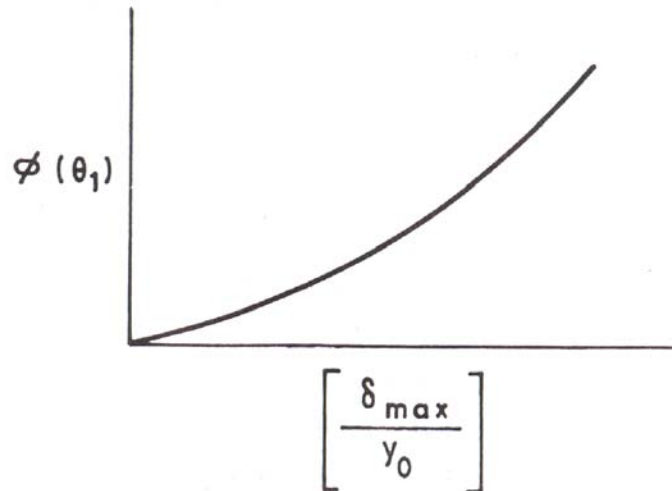
$$\phi(\theta_1) = \left(\delta_{max}/Y_0\right)^{3/2}$$

Fig. 3.12

Hence, $\dfrac{2\pi P_{avg}}{KY_0} = \left(\dfrac{\delta_{max}}{Y_0}\right)^{3/2}$ (3.12)

Now, consider the reaction forces on the tool. If the stress developed in the tool is o due to the impacts, then average force per grit,

$P_{avg} = \sigma / N$

Substituting above value in eq. 3.12

$\dfrac{2\pi\sigma}{KY_0 N} = \left(\dfrac{\delta_{max}}{Y_0}\right)^{3/2}$

or $\quad N = \dfrac{2\pi\sigma}{2\pi RHY_0}\left(\dfrac{Y_0}{\delta_{max}}\right)^{3/2} = \dfrac{\sigma}{RH}\dfrac{Y_0^{1/2}}{\delta_{max}^{3/2}}$ (3.13)

Total MRR is obtained by substituting the value of N in eq. 3.8 and rearranging as

$\text{MRR} = 5.9 R^{1/2}Y_0^{1/2}\left(\dfrac{\sigma}{H}\right)f \;\; \text{mm/sec}$ (3.14)

where R and Y_0 are in mm.

or $\;\; \text{MRR} = 4.17 D^{1/2}Y_0^{1/2}Y_0^{1/2}\left(\dfrac{\sigma}{H}\right)f \;\; \text{micron/sec}$ (3.15)

where, D is the abrasive grit size in micron (10^{-3} mm) and Y_0 the amplitude of vibration in micron (10^{-3} mm).
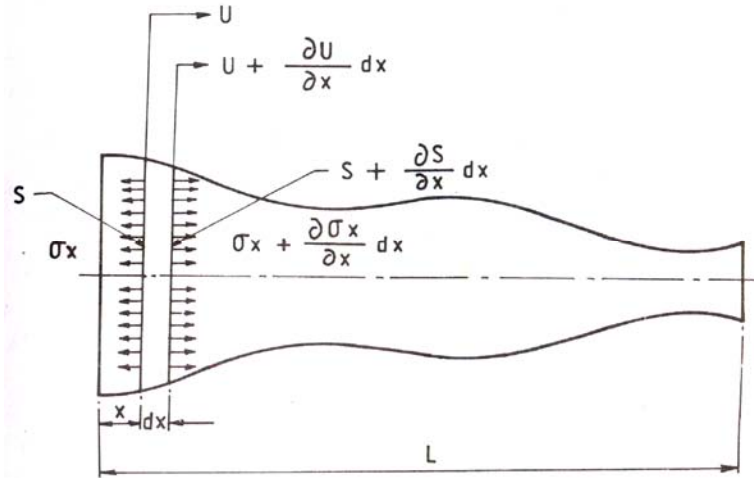
Fig. 3.13 Scheme of a Free-Free Vibration of a Non-uniform Bar

3.5 HORN DESIGN

The horn or the mechanical resonator is designed on the basis of axial vibration of an elrstic member with varying cross-section. Let us consider a free-free vibration of a non-uniform bar, in general as shown in Fig. 3.13, assuming (i) Plane wave propagation in the rod along the axial direction and (ii) Wave propagation along lateral directions are neglected.

An elementary section taken at distance x from one end of thickness dx will be subjected to different stress level due to a stress gradient of (5GX /5X) which will produce a strain in the elementary strip as

$$\text{Strain} = \frac{[U + (\partial U / \partial x)dx] - U}{dx} = \frac{\partial U}{\partial x} = \frac{\sigma_x}{E}$$

where U is the displacement of section x and x is the stress level on the section at x of area S.

Hence $\quad \sigma_x = E\dfrac{\partial U}{\partial x}$ $\hfill$ (3.16)

Due to vibration the elementary strip shall be acted upon by an accelerating force as

$$F_a = \frac{\rho}{g} \frac{\left(S + \dfrac{\partial S}{\partial x}\right)dx + S}{2} dx \frac{\partial^2 U}{\partial t^2}$$

neglecting $(dx)^2$ term,

$$F_a = \frac{\rho}{g} S\, dx \frac{\partial^2 U}{\partial t^2}$$

(3.17)

where p is the density of the material, and g the acceleration due to gravity. The constraining force acting on the elementary strip

$$F_c = \left(\sigma_x + \frac{\partial \sigma_x}{\partial x} dx \right)\left(S + \frac{\partial S}{\partial x} dx \right) - \sigma_x S$$

neglecting $(dx)^2$

$$F_c \cong S + \frac{\partial \sigma_x}{\partial x} dx + \sigma_x + \frac{\partial S}{\partial x} dx$$

(3.18)

Equating eqs. 3.17 and 3.18

$$S\frac{\partial \sigma_x}{\partial x} + \sigma_x + \frac{\partial S}{\partial x} = \frac{\rho}{g} S \frac{\partial^2 U}{\partial t^2}$$

(3.19)

Substituting the value of (σ_x) and $\partial \sigma_x / \partial x$ from eq. 3.16 in eq. 3.19

$$SE\frac{\partial^2 U}{\partial x^2} + E\frac{\partial U}{\partial x}\frac{\partial S}{\partial x} = \frac{\rho}{g} S \frac{\partial^2 U}{\partial t^2}$$

(3.20)

Now, the displacement equation for angular frequency w can be written as:

$$U = A\sin\,(wt) + B\cos t\,(wt)$$

from which $\dfrac{\partial^2 U}{\partial t^2} = \omega^2 U$

$$\frac{\partial^2 U}{\partial x^2} + \frac{1}{S}\frac{\partial U}{\partial x}\frac{\partial S}{\partial x} + \frac{\omega^2}{c^2} U = 0$$

(3.21)

Where $c = \sqrt{\dfrac{Eg}{\rho}} = $ velocity of sound in the material.

Case Study

For a uniform cylindrical rod, as $(\partial S / \partial x) = 0$, eq. 3.21 takes the form

$$\frac{\partial^2 U}{\partial x^2} + \frac{\omega^2}{c^2} U = 0$$

The solution of which is given by

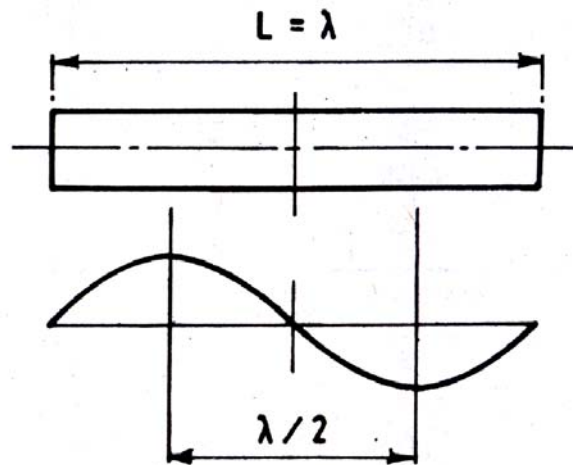$$U = A\sin\left(\frac{\omega}{c}x\right) + B\cos\left(\frac{\omega}{c}x\right)$$

Putting the boundary values as $U = 0$ at $x = 0$ and $x = L$,

$$L = \frac{n\pi}{\omega}\sqrt{\frac{Eg}{\rho}} \quad \text{(where } n = 1, 2, 3, \ldots\ldots\text{)}$$

First fundamental resonant frequency f_1 is given by

$$f_1 = \frac{1}{2L}\sqrt{\frac{Eg}{\rho}}$$

The length of resonating rod with a full wavelength is shown in Fig. 3.14.

Fig. 3.14 First Fundamental Mode of Vibration of a Uniform Rod
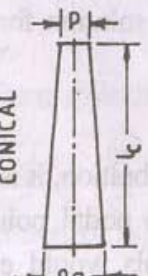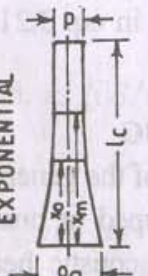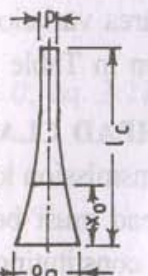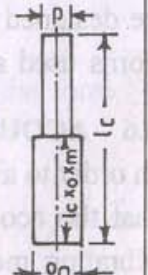
To obtain maximum vibration at the two extreme ends of the rod, the length should of half the wavelength, i.e. $\lambda/2$. Since the amplitude at both the ends are euqal giving a gain value of the amplitude amplification as 1 (one) and in ultrasonic applications there must be some gain for the amplification of the amplitude of vibration from the transducer end to the required level at the tool end.

For the above said reason, the hom is made from a tapered rod following a certain area variation law. Hence, solution for the length of the hom is to be designed using area variation law in eq. 3.21. The solution for different horns used are given in Table 3.2.

3.6 ACOUSTIC HEAD CLAMPING

In order to avoid transmission losses of the generated vibration, it is desirable lhat the acoustic head must be clamped at one of its nodal points of the yibrating members constituting the acoustic head. This would enable the system to run smoothly without any high frequency vibration in the structural

Table 3.2 Half Wave Ultrasonic Concentrator Calculation

TYPE OF CONCENTRATOR	FORMULA OF CURVE	THEORETICAL AMPLIFICATION FACTOR, k_a	RESONANCE HALF WAVE LENGTH, l_c, cm	CO-ORDINATE OF DISPLACEMENT NODE, x_o, cm
CONICAL	$D_x = D_o(1 - \alpha' x \times x)$; $\alpha' = \dfrac{D_o - d}{D_o \times l_o}$	$k_o = \sqrt{1 + \left(\dfrac{2\pi l_c}{\lambda}\right)^2}$; $k_o < N$	$l_c = \dfrac{\lambda}{2} \times \dfrac{(\alpha l_c)}{\pi}$, where (αl_c) roots of equation $\tan(\alpha l_c) = \dfrac{(\alpha l_c)}{\dfrac{(\alpha l_c)^2 \times N}{(1-N)\pi^2} + 1}$	$x_a = \dfrac{1}{\alpha} \times \arctan\left(\dfrac{\alpha}{\alpha'}\right)$; $\alpha = \dfrac{\omega}{V_s} = \dfrac{V_s}{\ }$
EXPONENTIAL	$D_x = D_o \times e^{-\beta x}$; $\beta = \dfrac{\omega}{c_1} \times \dfrac{\ln N}{l_o}$; $N = \dfrac{D_o}{d}$	$k_o = \dfrac{D_o}{d} = N$	$l_c = \dfrac{V_s}{2f}\sqrt{1 + \left(\dfrac{\ln N}{\pi}\right)^2}$	$x_a = \dfrac{l_o}{\pi} \operatorname{arc\,cot}\left(\dfrac{\ln N}{\pi}\right)$
CATENOIDAL	$D_x = d \times ch\,Y(l_a - x)$; $Y = \dfrac{1}{l_o} \times \sqrt{x^2 + (\ln N)^2}$; $N = \dfrac{D}{d}$	$k_o = \dfrac{N}{\cos(k'l)}$; $k_o > N$	$l_c = \dfrac{\lambda}{2\pi}\sqrt{(k'l)^2 + (\text{Arch } N)^2} = (k'l)$ roots of equation $k'l + \tan(k'l) = -\sqrt{1 - \dfrac{1}{N^2}} \times (\text{Arch } N)$	$x_o = \dfrac{1}{k} \times \arctan\left(\dfrac{k'}{Y} \times \coth Y \times l_c\right)$ where $k' = \sqrt{\alpha^2 - Y^2}$
STEPPED CYLINDRICAL	$D_x = D_o$ when $0 \leq x \leq l_o/2$; $D_x = d$ when $l_o/2 \leq x \leq l_c$	$k_o = \left(\dfrac{D_o}{d}\right)^2 = N^2$	$l_c = \dfrac{\lambda}{2} = \dfrac{V_s}{2 \times f}$	$x_o = \dfrac{l_o}{2} = \dfrac{V_s}{4 \times f}$

components of the machine ensuring longer and safer life time. Any one out of the total twelve methods of clamping shown in Fig. 3.15 may be used as per the designer's choice.
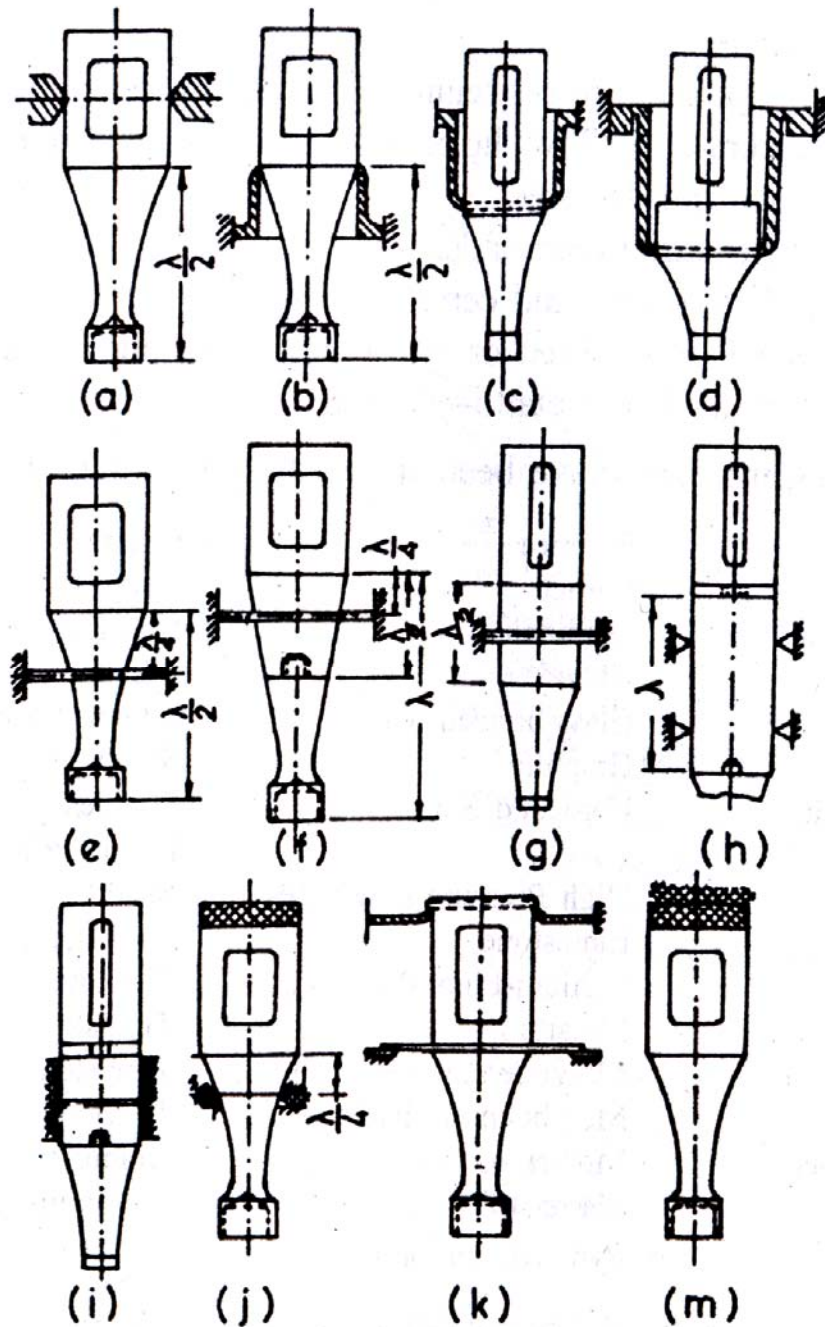
Fig. 3.15 Scheme of Different Nodal Point Clamping Devices

3.7 APPLICATIONS

Ultrasonic machining finds its application in processing material that cannot be machined by conventional cutting tool. Generally, it is used for conducting or non-conducting brittle materials. In recent years the use of ultrasonic machining in industries (ultrasonic welding in electronics industries as well) is increasing day by day.

Currently, principal fields of application are in the following areas:

- Manufacture of hard alloy wire drawing, punching and blanking dies, also making small complicated dies and punches of steel.

- Machining semi-conducting materials such as germanium and silicon.

- Machining ferrite and other special metallo-ceramic materials used in electrical installations.

- Making instruments and optical parts of glass, quartz, fluoride and barium titanate.

- Making components of porcelain and special ceramics.

- Cutting accurate shallow holes of rectangular or other section in cemented and nitrided steel.

- Cutting of industrial diamonds.

- Grinding glass, quartz and ceramics.

- Cutting holes with curved or spiral center line and cutting threads in glass and mineral or metallo-ceramic.

Following materials have been successfully machined by ultrasonic :

Agale	Formica	Quartz
Aluminium	Garnet	Ruby
Aluminium Oxide	Germanium	Sapphire
Barium Titanate	Glass	Silicon
Beryllium Oxide	Glass-bonded Mica	Silicon Carbide
Boron Carbide	Graphite	Silicon Nitrate
Boron Composites	Hardened Steel	Stainless Steel (hardened)
Brass	High Pressure Laminates	Stealite
Calcium	Limestone	Tool Steel
Carbides	Lithium-Fluoride	Ti-alloys
Carbon	Micarta	Tungsten
Ceramics	Molybdenum	Tungsten Carbide
Composite	Molybdenum disilicate	Thorium Oxide

Cold Rolled Steel	Mother of Pearl	Uranium Carbide
Febony	Plaster of Paris	Zirconium Oxide
Ferrite	Pyrolytic	Graphite

Cutting power or the ability cut using different abrasives ultrasonically shown Table 3.3.

Table 3.3

Abrasive	Knoop hardness	Relative cutting power
Diamond	6500-7000	1.0
Cubic Boron Nitride (CBN)	4700	0.95
Boron Carbide (B$_4$C)	2800	0.50-0.60
Silicon Carbide (SiC)	2480-2500	0.25-0.45
Aluminium Oxide (A1$_2$0$_3$)	2000-2100	0.14-0.16

3.8 OPERATIONAL SUMMARY

Typical values of USM operating parameters:

Power	200-4000 watts
frequency	15-30 kHz (most common -20 kHz)

Abrasive	
Type	Boron carbide (frequently) SiC (most common) A1$_2$O$_3$ (may also be used)
Size	mesh 120-1200
	μm 142-6
Concentration	20-60% by volume with water. Sometimes oil may be used for finishing operation
Flow	Ample (20~5°C) 2-5°C in desirable

Amplitude of vibration	5-70 μm (amplitude approx should remain between half to equal mean diameter of abrasive)
Tool tip force	0.45 to 45 kg. But generally 4.5 kg
Tool material	Mild steel, 303 stainless steel, monel, Molybdenum
Overcut and cutting gap	Twice the grit size (approx)

Area of cut	up to about 90 mm
Accuracy	± 25 μm (± 5 μm is possible)
Taper	5 μm per mm
Surface roughness, Ra	0.5 to 1.0 μm

3.9 LIMITATIONS

The USM process does not compete with conventional material removal operations on the basis of stock removal. Non-metal because of poor electrical conductivity that cannot be machined by EDM and ECM can very well be machined by USM.

MODULE-II

Abrasive Jet Machining: principle, Application, Advantage and disadvantages, variables in AJM, Water jet machining, Jet cutting equipment's, principle, advantage, Practical application.

Water Jet Machining: Jet Cutting Equipment's, principle, Advantages, Practical Applications.

Electrochemical machining: Principle Faraday's Law, Material Removal rate, Dynamics of ECM, processes, Tool Design, Advantages, Applications, Limitations, Electrochemical grinding, Deburring and Honing.

Abrasive Jet Machining (AJM)

1   PROCESS

Abrasive jet machining can be used to cut hard and brittle materials (e.g. germanium, silicon, mica, glass and ceramics) in a large variety cutting and deburring and the process is smooth and free from vibration. This is a process of removal of materials by impact erosion through the action of a concentrated, high velocity stream of the grit abrasives entrained in a high-velocity gas stream. It differs from conventional sand blasting process for its fineness of particle size and controllable machining parameters. The operating elements in AJM are Abrasive, Carrier Gas and Nozzle as schematically shown in Fig. 1.1.
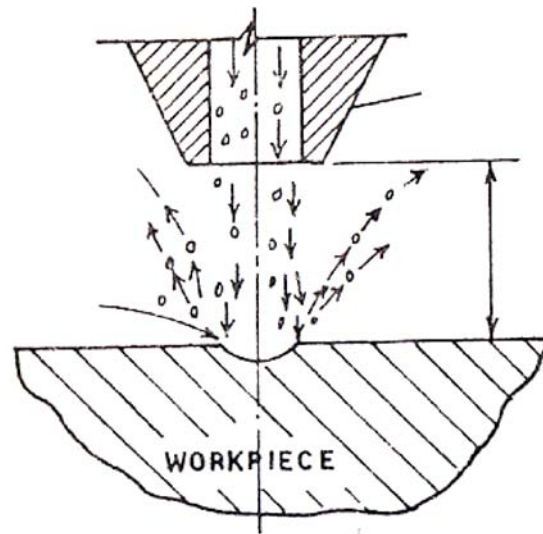
Fig. 1.1 Abrasive Jet Machining Principles

1.2 OPERATING PRINCIPLES

The variables that affect the cutting phenomena are:

(a)   Abrasive: composition, strength, shape, size, and mass flow rate.

(b)   Carrier gas: composition, pressure and velocity.

(c)   Nozzle: geometry, composition, nozzle-tip distance (stand off distant and its orientation).

The most common abrasives are Al_2O_3 and SiC available in 10, 27, 50 micron nominal diameters and the usage of the abrasives are given in fable 1.1.

Table 1.1 Recommended Use of Abrasives

Abrasives	Grain size micron	Operation
Al_2O_3	10, 27, 50	Cutting grooving
SiC	-do-	-do-
Sodium Bicarbonate	27	Light polishing below 50°C
lolomite	66	Etching and polishing
Glass beads	0.635-1.27 mm	Light polishing and fine deburring

The surface finish achieved by the process is dependent on the abrasive particle size and the materials machined as shown in Table 1.2.

Table 2.2 Surface Roughness Achievable

Mark Material	Abrasive Hardness	Grit size (micron)	Ra (micron)
Glass	Al_2O_3	10	150-200
	1800 H.V.	28	360-510
		50	970-1400
Stainless steel annealed	Al_2O_3	10	200-500
	1800 H.V.	25	250-530
		50	380-960
	SiC	20	300-500
	2600 H. V.	50	430-860
	Glass bead 500 H. V.	50	300-960

The Material removal rate is governed by the mass flow rate and velocity of the abrasive particles uniquely related to gas mass flow rate. These are well explained from Fig. 1.2 and typical data as shown in Figs. 1.3 and 1.4.

Again the jet coming out of the nozzle remains straight for some time and then flares out. So the accuracy and the cut area depends on the nozzle-tip-distance (NTD) from the work piece and the typical data are as shown in Figs. 1.5 and 1.6.
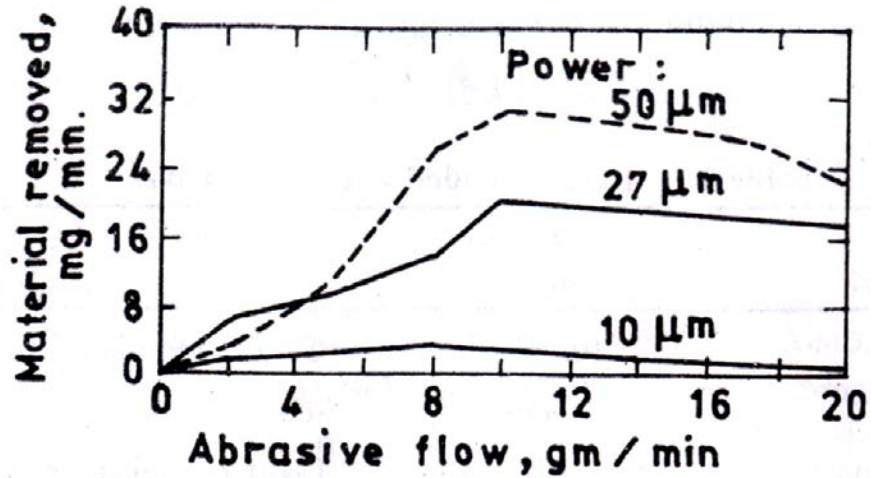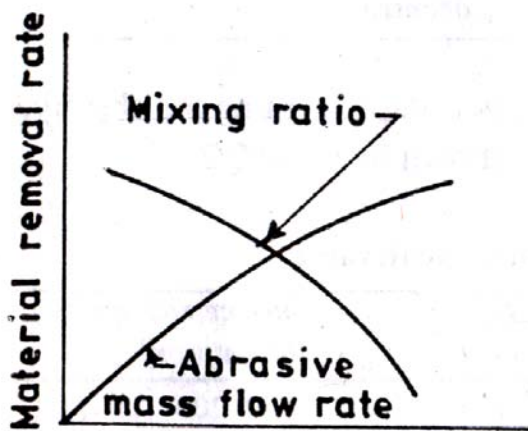
Fig. 1.2 Effect of Abrasive Flow Rate on MRR

Fig. 1.3 Effect of Abrasive Flow and Mixing Ratio on MRR
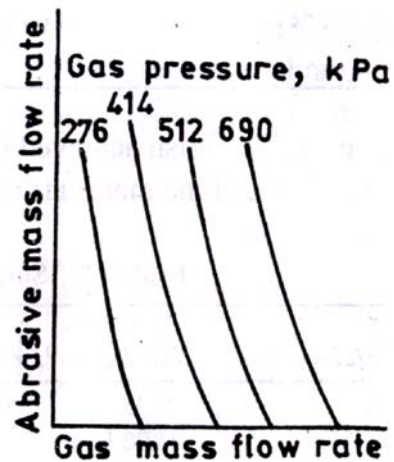

Fig. 1.4 Effect of Gas Flow on Abrasive Flow

1.3 EQUIPMENT

The basic unit is schematically shown in Figs. 1.7 and 1.8. It consists of gas supply unit, filter, pressure regulator, mixing chamber, nozzle assembly and the dust collecting chamber along with the work holding device. In the mixing chamber, the abrasive is allowed to flow into the gas stream. The mixing ratio is generally controlled by a vibrator. The particle and gas mixture comes out of the nozzle inside the machining chamber of the machine tool unit. The feed motion can be given either to the work holding device or to the nozzle.

1.4 MATERIAL REMOVAL RATE

The material is removed from work piece due to impact erosion of the high velocity particles. The Kinetic Energy of the particle is utilised to cause the micro-indentation in the work material and the material removal is a measure of the indentation.
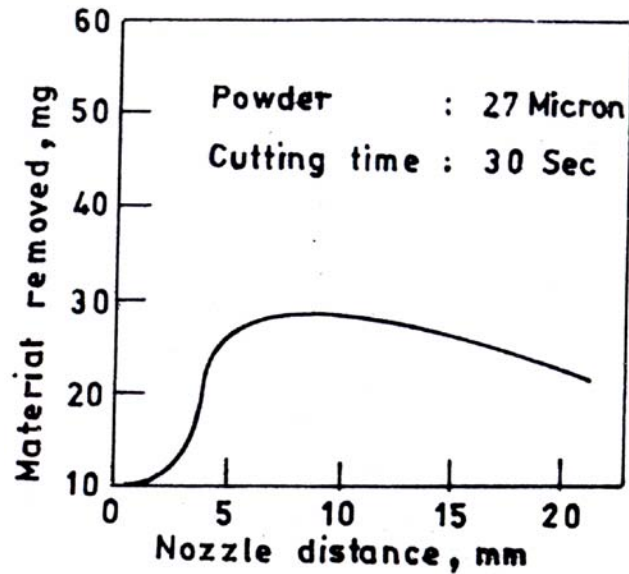

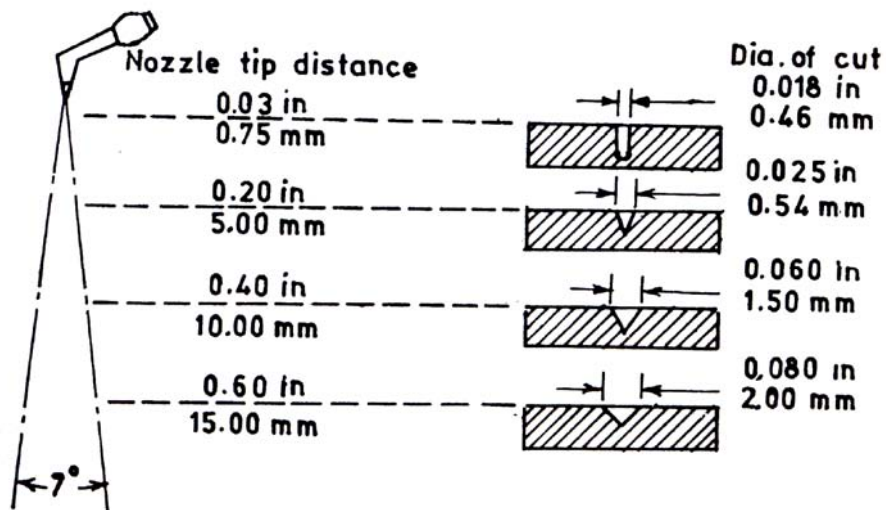**Fig. 1.5 Effect of NTD on Material Removal**

Fig. 1.6 Effect of NTD on Machining Accuracy

The model is based on the following assumptions:

- The abrasive particles are considered to be rigid and spherical bodies of diameter equal to the average grit size (Fig. 1.9a.).

- In case of a ductile work material, the material removed is equal to the volume of the indentation (Fig. 1.9b); and in case of a brittle work material, the volume of material removed is hemispherical whose diameter is equal to the chord length of the indentation.
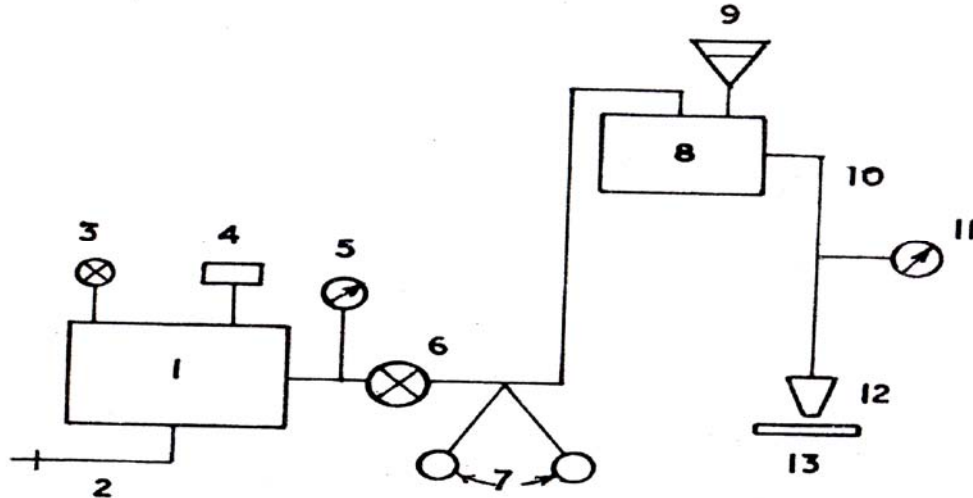
1. Compressor	2. Drain
3. Relief valve	4. Air filter cum drier
5. Pressure gauge	6. Opening valve
7. Pressure regulator	8. Mixing chamber
9. Abrasive powder	10. Air + Abrasive
11. Pressure gauge	12. Nozzle
13. Workpiece	

Fig. 1.7 Scheme of the AJM Set-up

From the geometry of Fig. 1.9, it can be proved that the relation between abrasive particle size d, indentation depth δ and half of the chord length r is

$$r^2 \square\, 2R\delta = d\delta \tag{1.1}$$

So the volumetric material removal per particle impact v is given by: For Brittle Materials (hemispherical brittle fracture)

$$v\left(\text{brittle}\right) = \left(2/3\right)\pi r^3 = \left(2/3\right)\pi\left(d\delta\right)^{3/2} \tag{1.2}$$

For ductile work material (material removal is equal to the indentation volume)

$$v\left(ductile\right) \cong \pi\delta^2\left[\left(d/2\right)-\left(\delta/3\right)\right], \text{ and neglecting } \delta^3 \text{ terms } \cong \left(\pi d\delta^2\right)/2 \tag{1.3}$$
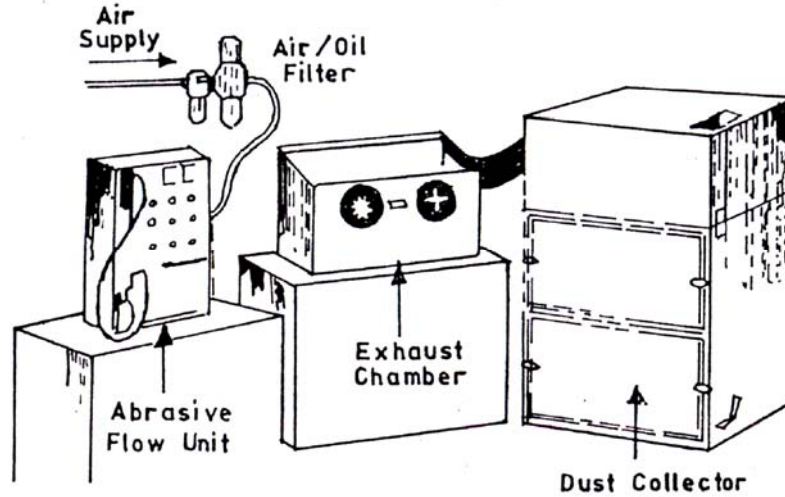
Fig. 1.8 General View of an Abrasive Jet Machine

So, if there are N number of particle impacts per unit time the material- removal-rate (MRR) equations are obtained from eqs. 2.2 and 2.3 as

$$\text{MRR (brittle)} = (2/3)\ \pi\ (d\delta)^{3/2}\ N \tag{1.4}$$

$$\text{MRR (ductile)} = \left[(\pi d\delta^2)/2\right] N \tag{1.5}$$

The unkonwn factors in the above two equations are δ and N. The estimation of δ can be derived from the energy balance equation as

K.E. = W.D. in the indentation of work material

Now K.E. possessed by the particle of mass m and density ρ, moving with a velocity 'U' just before the impact is

$$K.E. = \left(1/2\right)mU^2 = (1/2)\left[(\pi/6)d^3\rho\right]U^2 = (\pi/12)d^3\rho U^2 \tag{1.6}$$

he energy of impact will introduce a force P on the indenter to cause an indentation depth 5 in work material of hardness H. So W.D. in the indentation

$$W.D. = (1/2)P\delta = (1/2)(\pi r^2 H)\delta \tag{1.7}$$

Substituting the value of r from eq. 2.1 in 2.7 and equating to eq. 2.6

$$(\pi / 12) \, d^3 \, \rho \, U^2 = (1/2)(\pi d \delta H) \delta$$
$$= (1/2)\pi dH \delta^2 \qquad (1.8)$$
$$\delta^2 = (\rho / 6)\left[(dU)^2 / H\right]$$

The number of particles N striking the target can be estimated from the known value of abrasive mass flow rate, M as
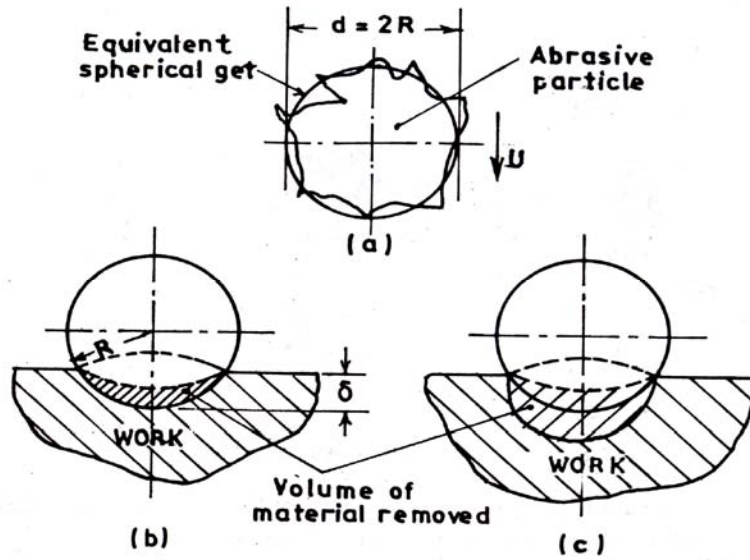
Fig. 1.9 Scheme of Material Removal Mechanisms

$$N = \frac{M}{\text{Mass of each particle}} = \frac{6M}{\pi d^3 \rho} \qquad (1.9)$$

The MRR equation can be determined by substituting the values of δ and N in the eqs. 2.4 and 2.5, as

$$\text{MRR(brittle)} = 1.04 \frac{MV^{3/2}}{\rho^{1/4} H^{3/4}} \qquad (1.10)$$

Similarly for ductile materials:

$$\text{MRR (ductile)} = 0.5 \frac{MV^2}{H} \qquad (1.11)$$

Equations 2.10 and 2.11 give the maximum possible material removal rate in case of AJM process for machining brittle materials and ductile materials respectively. The equations show that the velocity effects are more predominant than mass flow rate on material removal rate. It is interesting to note (Fig. 2.10) that under lower velocity conditions ductile material show lower

material removal rate for an angle of impingement of 90° (degree) than brittle materials. But at certain velocity U*, both material may exhibit similar property for impact erosion rate and above this velocity, ductile materials may erede very fast.
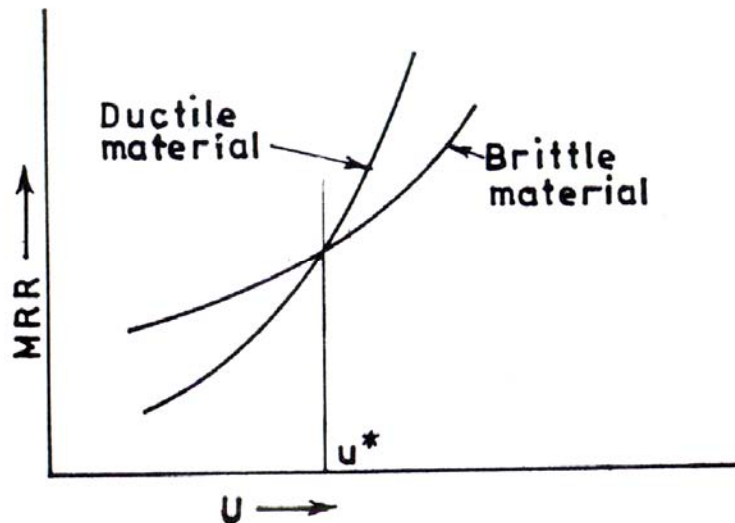
Fig. 1.10 Effect of Velocity on Material Removal Rate

1.5 APPLICATION

(a) This is used for abrading and frosting glass more economically as compared to etching or grinding.

(b) Cleaning of metallic smears on ceramics, oxides on metals, resistive coatings etc.

(c) Cutting and machining of fragile material like germanium, silicon etc.

(d) Register treaming can be done very easily and micro module fabrication for electrical contact, semiconductor processing can also be done effectively.

(e) It is a good method for debarring small hole like in hypodermic needles and for small milled slots in hard metallic components.

1.6 LIMITATIONS

The limitations in applicability of the process arise from the following reasons:

(a) The volumetric or stock removal rate is very low.

(b) Elastomers or soft plastics are not amenable to abrasive jet treatment.

(c) The accuracy of cutting is hampered by tapering effect and stray cutting] '

(d) A dust collecting chamber is a basic requirement to prevent atmospheric pollution to cause health hazards.

(e) Abrasive powders cannot be reused.

(f) Short stand-off distance when used for cutting, damages the nozzle.

(g) Abrasive particles may be embedded in the workpiece sometimes.

Water Jet Machining (WJM)

2.1   PROCESS

This employs a fine, high pressure (1500-4000 MN/cm^2), high velocity (up to twice the speed of sound) jet of water, which when bombarded on the work piece erodes the material.

High-pressure water jet has two properties which make it potentially useful in industries. They are, its destructive power and its application as a precision cutting tool.

A high-velocity water jet when directed at a target in such way that, its velocity in virtually reduced to zero on striking the surface. Practically, most of the kinetic energy of the jet of water is converted to very high pressure. In fact, at the initial phase (within first few milli-seconds) the transient pressure reaches several times greater than the normal stagnation pressure. This causes erosion if the local fluid pressure exceeds the strength of target material or in other words, the water jet will make a hole in the material if the pressure is high enough.

2.2   OPERATING PRINCIPLE

Many variables such as nozzle orifice diameter, water pressure, cutting feed rate and the stand distance affect the performance.

Generally, high cutting quality would be the result of the conditions: high pressure, large nozzle orifice, low feed rate and narrow stand off distance.

The equipment (Fig. 2.1) consist of three main units: (1) pump along with a intensifier to generate very high pressure (1-10 kbar); (2) cutting unit consisting nozzle and work table movement and (3) filtration unit to remove the debris from water after use.

A polymer (glycerin, polyethylene oxide) is added to the working fluid to prevent freezing and provide lubricating action in the intensifier plunger type pump.

2.3   MECHANISM OF JET CUTTING

Water-jet cutting or water-jet machining (WJM) is similar to laser beam machining (LBM) and electron beam machining (EBM) in the respect that a given amount of energy 10^{10} watt/mm^2) is concentrated onto a very small Point to cause material removal.
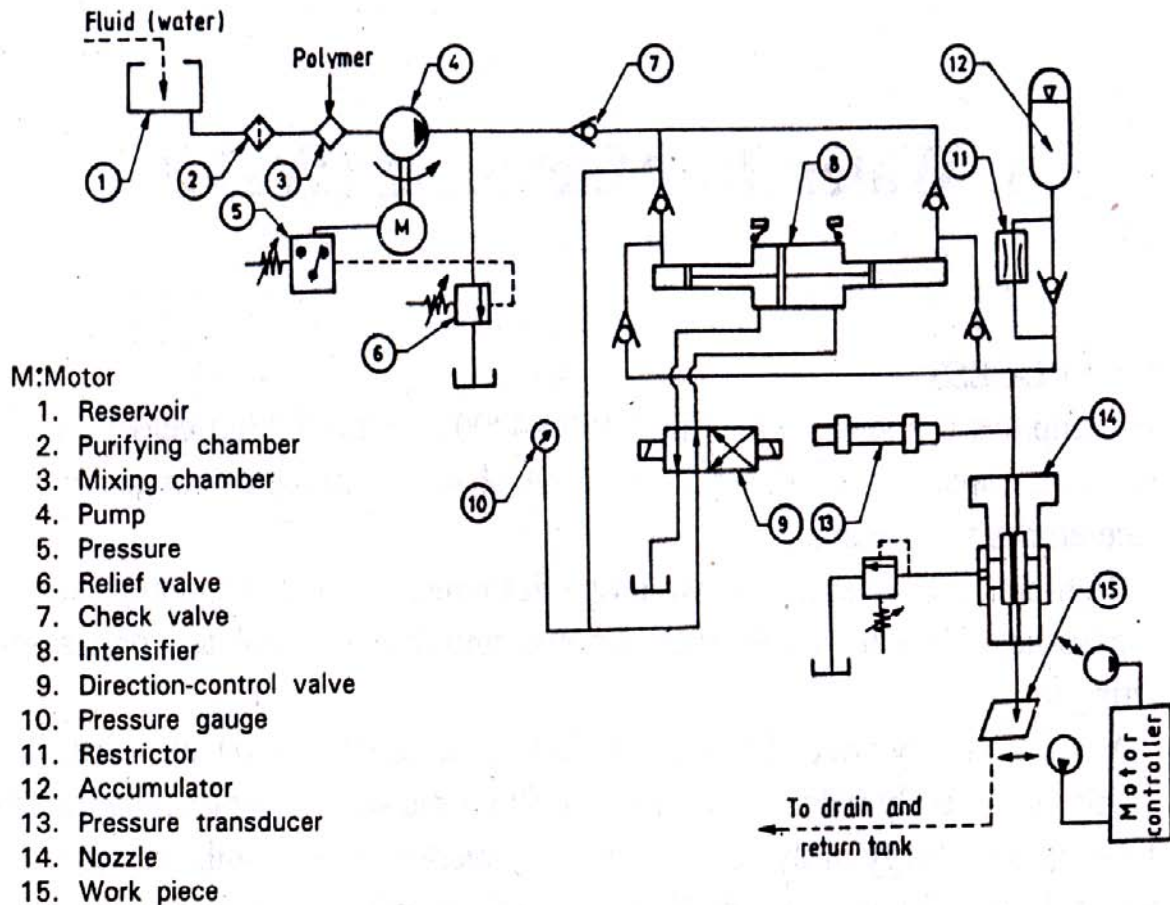
Fig. 2.1 Water Jet Cutting Unit

When a high velocity water-jet is directed to a target in such a way that on striking the surface its velocity is virtually reduced to zero then most of the' kinetic energy of the water is converted into pressure energy (called stagnation pressure). In fact, in the first few milliseconds after the initial impact the transient pressure generated may be as high as three times the normal stagnation pressure.

Thus the mechanism of water-jet cutting is erosion caused by localised compressive failure which occurs when the local fluid pressure exceeds the strength of the target material. In some ductile materials, it is involved with a shearing action caused by the high speed radial flow of the jet along the work piece. When quality cutting is not required, such as tunneling, other mechanisms like spalling caused by stress waves and the effect of stagnation pressure caused by cutting fluid penetrating cracks and pores are expected. Some are of the opinion that cavitation in

the jet also plays a role in eroding the target material. It is well known that a considerable localised damage, caused by erosion, can result from a cavitation bubbles collapsing against a solid.

2.4 PROCESS PARAMETERS

For successful utilisation of WJM process, it is necessary to analyse the following process criteria:.

> (i) Material Removal Rate (MRR).
>
> (ii) Geometry and finish of work piece.
>
> (iii)Wear rate of the nozzle (as nozzle is a costly item).

However, the process criteria are greatly influenced by various process parameters as enumerated below:

(i) MRR depends on the reactive force F of the jet.

Again,

Reactive force = Mass flow rate (m) x Jet velocity (V)

Hence, MRR α m α V

and the velocity depends on fluid pressure whereas mass flow rate depends on both- nozzle diameter d and fluid pressure P.

Hence, MRR α d α P

British Hydromechanic Research Association have found following empirical relationships:

$$v = 14.1 P^{1/2} \tag{2.1}$$

$$Q = 0.67 K \ N \ d^2 \ P^{1/2} \tag{2.2}$$

$$HHP = 1.11 \ K \ N \ d^2 \ P^{3/2} \tag{2.3}$$

$$F = 0.079 \ K \ N \ d^2 \ P \tag{2.4}$$

Where

V = maximum water jet velocity at nozzle outlet (m/s),

Q = water flow rate through nozzle (1/min),

HHP = hydraulic horsepower of jets (W),

F = reactive force of jet nozzle (N),

K = nozzle discharge co-efficient (dimensionless),

N = number of nozzles used (dimensionless),

P = pressure differential across the nozzle (bar),

d = nozzle orifice diameter (mm).

Apart from these, MRR is also greatly influenced by stand-off distance (SOD) of the nozzle tip from the surface of the material being cut.

It is found that MRR increases with the increase of SOD up to a certain limit after which it remains unchanged for a certain tip distances and then falls gradually. This is explained as follows. Small MRR at low SOD is due to a reduction in nozzle pressure with decreasing distance, whereas a drop in MRR at large SOD is due to a reduction in the jet velocity with increasing distance.

A large SOD affects accuracy and quality. Water flares out because of a peeling off' effect caused by air friction. Theoretically, any divergence causes the jet to cut less effectively and less accurately.

(ii)   Geometry and finish of work piece of depends on three factors:

(a)   Nozzle design.

(b)   Jet velocity, cutting speed and depth of cut

(c)   Properties (especially hardness) of the material being cut.

(iii)   Wear rate of the nozzle depends mainly on the hardness of the nozzle material, pressure (hence, velocity) of the jet and nozzle design.

From above it is clear that for a given material, the rate of cut, depth of cut and quality (keeping in mind the sealing problems, nozzle wear rate, etc.), a compromise has to be made and optimum values of various parameters discussed above are to be found out and used.

2.5 APPLICATIONS

1. WJM is used to cut many nonmetallic materials like Keplar, glass epoxy, graphite, boron, F.R.P. corrugated board, leather and many other brittle materials.

2. It is used mostly in shoe making industry and now has entered into steel plant to descale the chilled layer of steel ingots, in aircraft industries to profile cutting of FRP aircraft structures even glass windows.

Electrochemical Machining (ECM)

3.1 PROCESS

This is a process of anodic dissolution of work material by high current flowing through an electrolyte between shaped tool and work piece.

The principle is exactly same as electroplating where the anode goes into solution expecting the cathode deposition. In ECM, the electrolyte is so chosen that there is no plating (decomposition of metals) on the cathode (tool) so the tool shape remains unchanged and if a close gap (0.1-0.2 mm) is maintained between the tool and work, the machined surface takes the replica of the tool shape. The scheme is shown in Fig. 3.1.
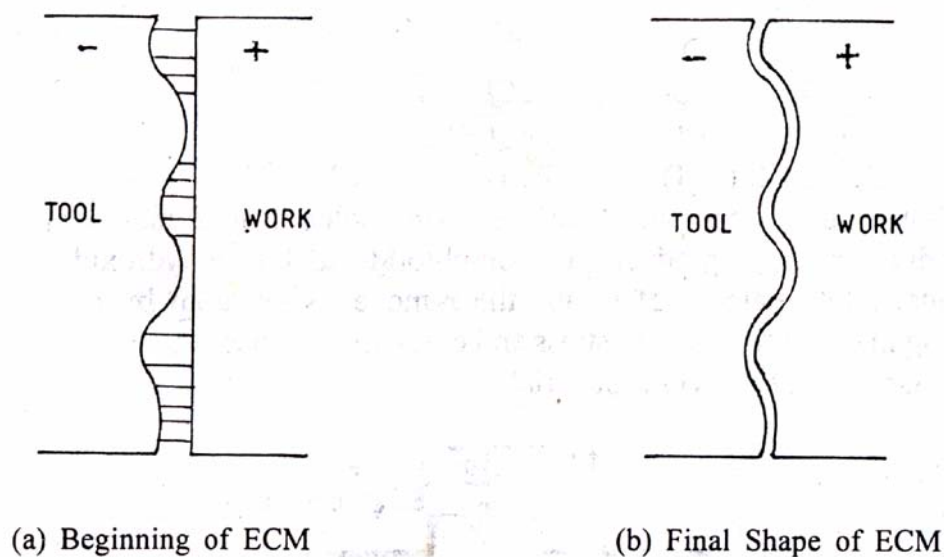


(a) Beginning of ECM   (b) Final Shape of ECM

Fig. 3.1 The ECM Scheme

## 3.2 PRINCIPLE OF OPERATION

In the electrolyte cell (ECM) the reactions take place at different levels electrolyte, cathode and anode (Figs. 3.2 and 3.3).

It is evident from the above schemes that when current is flown through a solution of NaCl in water, the ions formed and will proceed to produce the desired effects as:

$$NaCl \leftrightarrow Na^+ + Cl^-$$

$$H_2O \leftrightarrow H^+ + (OH)^-$$
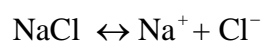
The positive ions move towards the cathode (tool) while negative ions move towards anode (work piece) to react. Let - us analyse the two possible reactions at the cathode and anode.

1. Cathode Reaction

$Na^+ + e^- = Na$

$Na + H_2O = Na\,(OH) + H^+$

$2H^+ + 2e^- = H_2 \uparrow$
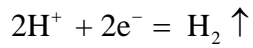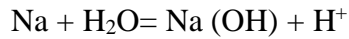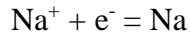
It shows that there is no deposition on tool but only gas is formed, whereas, in cathode in machining an iron specimen for example:

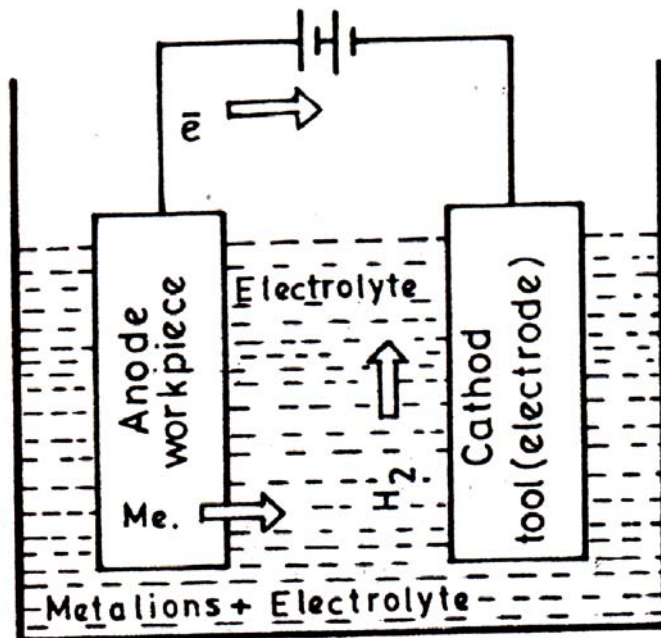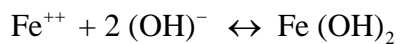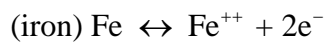Fig. 3.2 An Electrolyte Cell

2. *Anode Reaction*

(iron) Fe $\leftrightarrow$ $Fe^{++} + 2e^-$

$Fe^{++} + 2Cl^- \leftrightarrow FeCL_2$

$Fe^{++} + 2\,(OH)^- \leftrightarrow Fe\,(OH)_2$

$FeCl + 2\,(OH)^- \leftrightarrow Fe\,(OH)_2 + 2Cl^-$

It shows metal (work piece), i.e. Fe goes into solution and hence machined to produce reaction products as iron-chloride and iron-hydroxide as a precipitate. Interesting part is that the removal is an atom by an atom, resulting in higher finish with stress and crack free surface, and independent of the hardness of the work material.
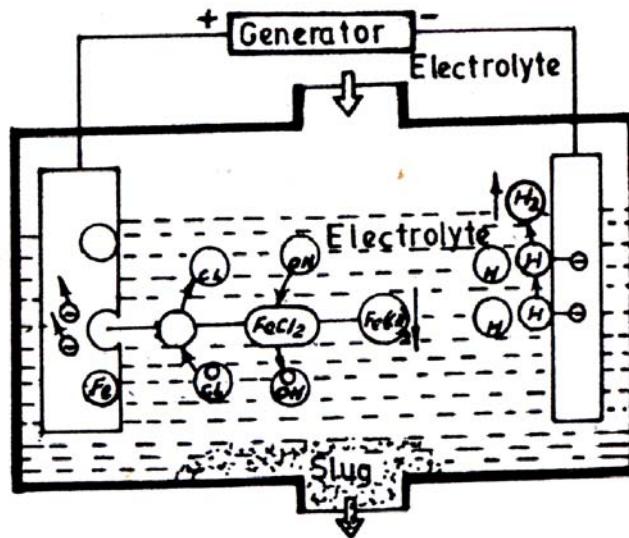
Fig. 3.3 Anodic Dissolution Proc.

As current flows, several phenomena occur at the electrode surfaces to oppose the very cause of it (make the above reactions to proceed). These emf opposing the flow are termed as anode and cathode overvoltage (Fig. 3.4) and include activation polarisation, concentration polarisation and ohmic vervoltag. When no current flows, electrochemical reactions occurring at an electrode are in equilibrium. However, to make the dissolution proceed, one has to apply a voltage in excess of electrode and activation polarisation potentials, i.e. about 2 volts maximum.

Fig. 3.4 Potential Profile in the Machining Gap

3.3 THE EQUIPMENT

An ECM system consists of a machining unit with a suitable fixture, electrolyte flow system, electrolyte filtration unit and the DC power source with feed control devices (Fig. 3.5).
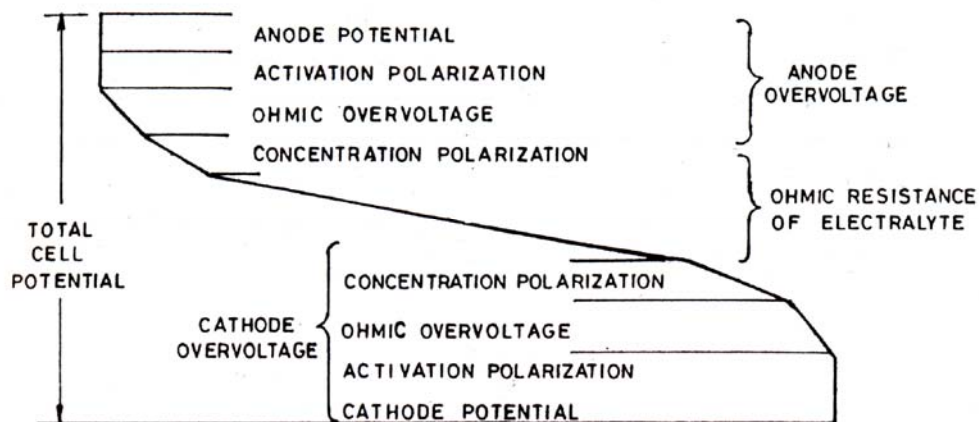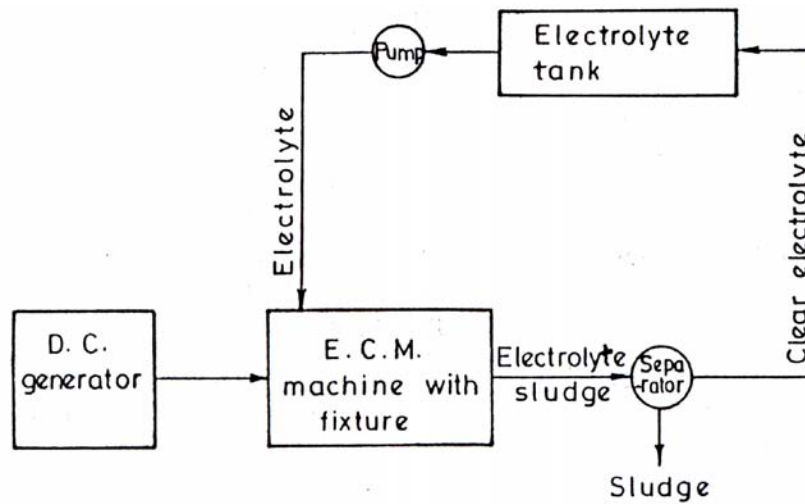

Fig. 3.5 A Basic Scheme of the Machine

The unit is more explicitly elaborated in Fig. 3.6. A tool (may require an insulation at the sides to prevent undesired machining on the sides) is mounted on the tool holder. The tool, in most of the cases are hollow, is to allow electrolyte to flow into the working gap. The tool holder is given a feed drive. The work is mounted on a fixture, insulated from the main body of the machine. The electrolyte is allowed to flow into the system at a high pressure and the reaction product along with the electrolyte flow into a tank and then the reaction product is separated from the electrolyte through the help of micro-filter or a centrifuge. Then the filtered electrolyte is pumped with metered quantity into the system. A DC voltage of 2 to 30 V is applied in between the tool and the work for machining operation. A fan is to be provided to constantly remove the gas evolved within the working gap at the cathode. However, the ECM machines may be of universal or special- purpose. Since the machining is done by electrical energy, the power supply has the most critical role in the system which needs further explanations.
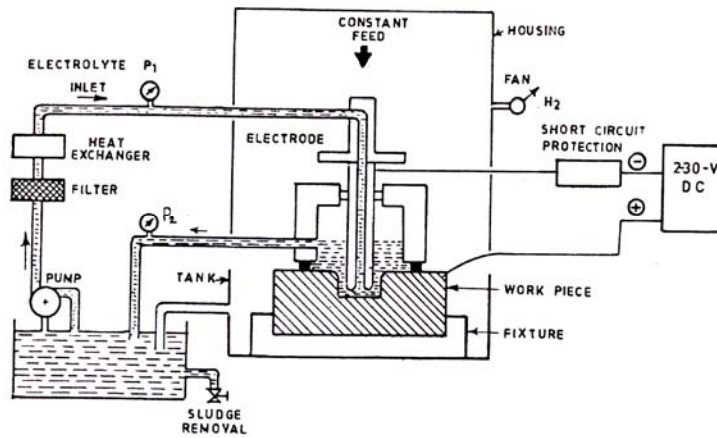
Fig. 3.6 Schematic Diagram of Electrochemical Drilling Machine

3.4 POWER SUPPLY AND CONTROL

Power supply for an ECM machine is usually the most expensive single item of the installation and may account for substantial part of the total extremely high cost of the complete machine.

The unit is a low voltage DC supply capable of delivering high current (10,000A or more) requirement. Since the power requirement is too high the three phase high voltage is stepped down through transformer and rectified (Fig. 3.7). It is also essential to provide adequate protective circuits for the transformer, rectifier and the machine itself against overload and short circuit conditions. The short circuit conditions can occur accidentally for various reasons since the gap between the tool and work is maintained too low (0.1 to 0.2 mm), mishandling or wrong fitting of the electrode or work piece, accumulation of conductive debris in the working gap or malfunction of the gap control system. It is also necessary to monitor the voltage and current continuously to quantify the MRR.

Fig. 3.7 Schematic Block Diagram of a Typical Power Supply for an ECM Machine

3.5 ANALYSIS OF MATERIAL REMOVAL
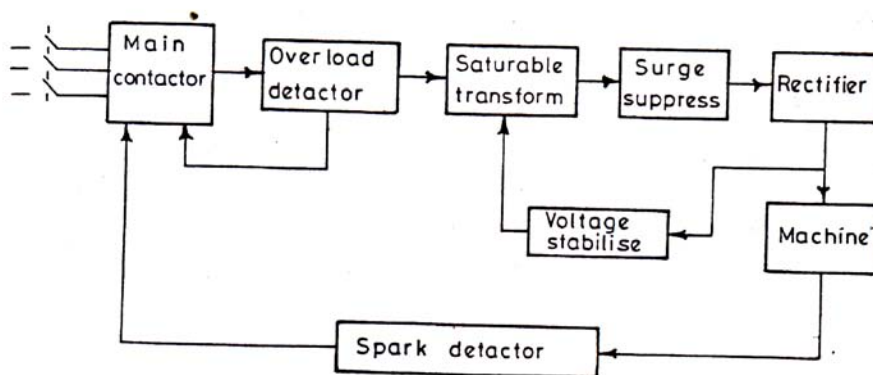
3.5.1 Basic Theory (Faraday's Laws)

The rate of dissolution (material removed) can be analysed from the basic fundamentals of electrochemistry given by Michael Faraday in his laws.

(a) The first law states that "the amount of chemical changes W produced (i.e. dissolved or deposited) is proportional to the amount of charge Q passed through the electrolyte", i.e.

$$W \, \alpha \, Q \tag{3.1}$$

(b) The second law proposes that the amount of change produced in the material is proportional to its electrochemical equivalent, of the ECE material, i.e.

$$W \, \alpha \, \text{ECE, but ECE} = M/v \tag{3.2}$$

where M is the atomic weight and v the valency.

From the two laws it can be written

$$w = \frac{1}{F}(ECE).Q$$

$$= \frac{1}{F}\frac{M}{v}Q \tag{3.3}$$

$$\text{or } W = \frac{1}{F}\left(\frac{M}{v}\right)It \tag{3.4}$$

where F is the Farday's constant = 96500 coulombs = 26.8 amp-hr, Q the charge (coulomb), I the current (ampere) and t the dissolution period.

Equation 6.4 gives the idea about the rate of dissolution of a single elemental material. Since most of the materials machined by this process are difficult-to-machine alloys of metals, the Faradic eq. 6.4 needs modification accordingly.

3.5.2 Dissolution of an Alloy

Generally an engineering material is in the form of an alloy consisting of different elements. So to find out the rate of dissolution, one must consider each element separately and combine them for the whole alloy. To start with, let us consider the alloy consisting of:

$1 - n$ = number of elements

$M_1..........M_n$ = atomic weights of individual elements

$v_1.......v_n$ = valency of the respective elements

$X_1..........X_n$ = percentage of the element present in the alloy

Now, if ρ is the density of the alloy and V_a the volume that goes into solution in a given time t, then the weight W of the first element present in the alloy is given by

$$W_1 = \frac{V_a \rho X_1}{100}$$

Similarly,

$$W_2 = \frac{V_a \rho X_2}{100}$$

$$W_n = \frac{V_a \rho X_n}{100}, \text{ and so on.}$$

The charge $(Q_1 - Q_n)$ taken by each element present in the alloy can be given by eq. 6.3 as:

$$Q_1 = \frac{W_1 F v_1}{M_1} = \frac{V_a \rho F}{100} \frac{v_1 X_1}{M_1}$$

Similarly,

$$Q_2 = \frac{W_2 F v_2}{M_2} = \frac{V_a \rho F}{100} \frac{v_2 X_2}{M_2}$$

$$Q_n = \frac{W_n F v_n}{M_n} = \frac{V_a \rho F}{100} \frac{v_n X_n}{M_n} \text{ and so on}$$

Now, the total charge, required for removing all the elements from the alloy will be

$$Q_{total} = Q_1 + Q_2 + ...+ Q_n \tag{3.5}$$

or $\quad Q_{total} = \dfrac{v_a \rho F}{100} \left[\dfrac{X_1 v_1}{M_1} + \dfrac{X_2 v_2}{M_2} + ...\dfrac{X_n v_n}{M_n} \right]$

or $\quad Q_{total} = \dfrac{v_a \rho F}{100} \sum\limits_{i=1}^{i=n} \dfrac{X_1 v_1}{M_1}$ \hfill (3.6)

Hence, volumetric material removal rate V_m per unit charge is given by

$$V_m = \frac{V_a}{Q_{total}} = \frac{100}{\rho F} \frac{1}{\displaystyle\sum_{i=1}^{i=n} \frac{X_1 v_1}{M_1}} \tag{3.7}$$

If current I flows for time t sec, then from eq. 6.6

$$Q_{total} = It = \frac{v_a \rho F}{100} \sum_{i=1}^{i=n} \frac{X_1 v_1}{M_1}$$

$$\text{or} \quad \text{MRR} = \frac{V_a}{t} = \frac{100}{\rho F} \frac{1}{\displaystyle\sum_{i=1}^{i=n} \frac{X_1 v_1}{M_1}} \tag{3.8}$$

3.6 DYNAMICS OF ECM PROCESS

One has an idea of how much material will be removed in a given time from a work piece for given current flowing through the electrolyte between the tool (electrode) and work piece. Now the problem arises whether one should allow the machining without any feed or give a feed. To solve this, let us consider an electrolyte flowing through a parallel gap h between the tool and work piece (Fig. 3.8)
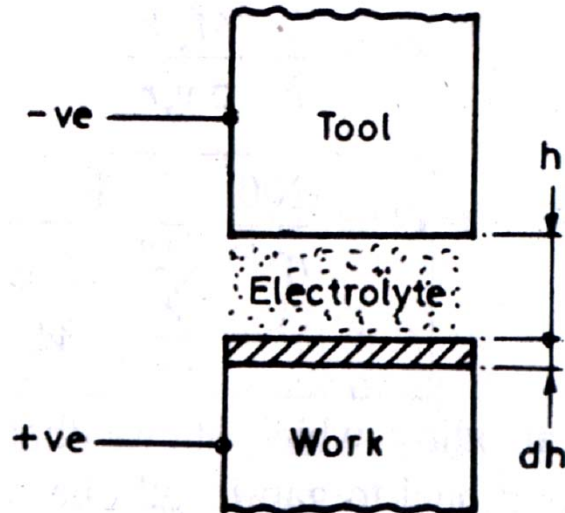
Fig. 3.8 ECM with No Feed

If the constant voltage V is supplied across the gap one should find out how the gap change takes place.

3.6.1 Zero Feed Rate

In other words, if no feed is given to the tool, how far dissolution would proceed. This would decide whether no-feed or if feed then how much of it.

Now if dh is the change in gap in a given time dt, area of cross section of tool (reaction area) is A and density of the material ρ, then the weight dissolved,

$$dw = \rho \, A \, dh = \frac{1}{F} \frac{M_x}{v_x} I dt \quad \text{(from eq. 6.4)}$$

$$\frac{dh}{dt} = \frac{1}{F} \frac{M_x}{\rho v_x} \frac{I}{A} \qquad\qquad (3.9)$$

i.e. the rate of change of gap is proportional to current density (I/A).

Now, if V is the applied D.C. voltage, R the resistance of electrolye and r the specific resistance of the electrolyte, then,

$$I = \frac{V}{R_e} = \frac{V}{\dfrac{rh}{A}} = \frac{VA}{rh} \qquad\qquad (3.10)$$

On substituting the value of I from eq. 6.10 in 6.9, one can rewrite

$$\frac{dh}{dt} = \frac{1}{F} \frac{M_x}{\rho v_x r} \frac{v}{h}$$

and for a constant voltage source

$$\frac{dh}{dt} = \frac{C}{h} \qquad\qquad (3.11)$$

where,

$$C = \frac{1}{F} \frac{M_x V}{\rho v_x r}$$

or $\quad C = \dfrac{100}{r\rho F} \dfrac{I}{\displaystyle\sum_{i=1}^{i=n} \dfrac{X_1 v_1}{M_1}}$

for an alloy which shows that the rate of change of gap is inversely proportional to gap length, i.e. with time the rate of change of gap or the dissolution rate falls.

Now let us examine if no feed is given, i.e. under zero feed rate condition how the gap varies with time.

We know

$$\frac{dh}{dt} = \frac{C}{h} \text{ or } hdh = Cdt$$

Integrating this within the limits

$$\int_{h_0}^{h_1} hdh = \int_0^t Cdt$$

or $\left(h_1^2 - h_0^2\right)/2 = Ct$

or $h_1^2 - h_0^2 = 2Ct$ (3.12)
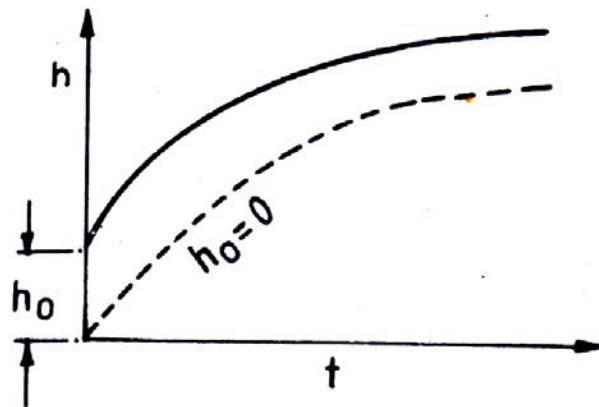
Fig. 6.9 Variation of Gap Length with Time

which gives the parabolic variation of gap shown in Fig. 3.9.

It shows that if we do not give any feed to the tool, the dissolution rate falls. Hence, it is necessary to give a feed to the tool.

3.6.2 Dynamics Under Given Feed Condition

If feed S is given to the tool, then eq. 3.11 is modified to

$$\frac{dh}{dt} = \frac{C}{h} - S$$ (3.13)

It is necessary to establish the feed rate because if S is high compared to rate of change of gap, then short circuit will result in stoppage of electro-chemical reaction. Hence, to establish a

relation for feed a steady state condition of electro-chemical reaction is to be established. Under this steady state condition

$$\frac{dh}{dt} = 0. \qquad \text{Hence } S = \frac{C}{h}$$ (3.14)

The gap under steady state condition h_e is

$$h_e = \frac{C}{S}$$ (3.15)

i.e. in steady state or equilibrium condition with a constant feed, the gap remains constant.

Now it is necessary to know how and when the equilibrium condition is reached. To establish this one must find out the behaviour of eq. 6.13 with respect to feed. The approach to the equilibrium gap can be found out by method of substitution of the equation, by reducing the variables to ECM ur:U since they are not dimensionally balanced.

In ECM units we can assume the equilibrium gap he to an unit for conversion of gap and time units.

$$\text{gap,} \qquad h' = \frac{h}{h_e} = \frac{Sh}{C}$$

gap,

$$\text{and time} \quad t' = \frac{St}{h_e} = \frac{S^2 h}{C}$$ (3.16)

$$\text{Hence,} \quad \frac{dh'}{dt'} = \frac{C}{S} \frac{C}{S^2} \frac{dh}{dt} = \frac{1}{S} \frac{dh}{dt}$$ (3.17)

$$\text{Hence,} \quad \frac{dh}{dt} = S \frac{dh'}{dt'}$$ (3.18)

Therefore, 6.13 is converted and expressed as

$$S \frac{dh'}{dt'} = \frac{S}{h'} - S$$

$$\text{or} \quad S \frac{dh'}{dt'} = \frac{1 - h'}{h'}$$ (3.19)

Now,

$$dt' = \frac{h'}{1 - h'} dh'$$

On integration

$$\int_0^{t'} dt' = \int_{h_0'}^{h_1'} \frac{h}{1-h'} \, dh'$$

or $\quad t' = \left[(1-h') - \log(1-h') \right]_{h_0'}^{h'}$

or $\quad t' = (h_0' - h_1') + \log \dfrac{h_0' - 1}{h_1' - 1}$ $\hfill$ (3.20)

The plot of above equation is shown in Fig. 6.10.

This shows that whatever the initial gap is given, it tends to a unit gap, i.e. equilibrium is reached, since the gap approaches the gap asymptotically.

Hence

$$h' = 1 \text{ or } \frac{Sh}{C} = 1$$

From which,
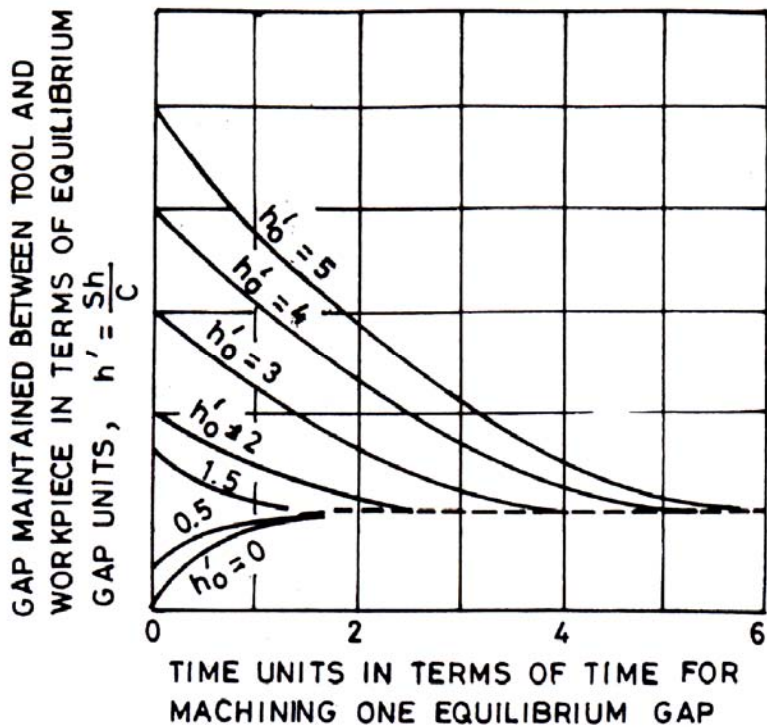
Fig. 3.10 Variation of Gap Length in ECM with Feed

$$S = \frac{C}{h} = \frac{M_x V}{v_x F \rho r} \frac{1}{h}$$

Where $C = \dfrac{M_x V}{v_x F \rho r}$

or $\quad S = \dfrac{M_x}{v_x F \rho} \dfrac{1}{rh} = \dfrac{M_x}{v_x F \rho} \dfrac{I}{A}$

i.e. $\quad S = \dfrac{M_x}{v_x F \rho} \dfrac{I}{A} = $ MRR $\hfill (3.21)$

It is seen that, in a constant feed rate ECM system, the machining process is inherently self-regulated since the MRR tend to approach the feed rate.

Another interesting phenomena is that a highest feed condition (for a limiting value of current) the equilibrium gap is minimum and produces a closer tolerance between the tool and the work surface, i.e. as production rate is increased the accuracy maintained is higher in ECM operation. Hence, it can be considered as one of the high production system.

3.7 HYDRODYNAMICS OF ECM PROCESS

It is clear that the material removal rate increases with current and the machine can be operated at the highest feed rate condition. The increased current will produce more heat in the electrolyte (Joule heating) that might reach a boiling condition and prevent the electrolytic reactions further. So it is necessary to allow sufficient flow of electrolyte through the gap schematically shown in Fig. 3.11 for a pair of parallel electrodes.
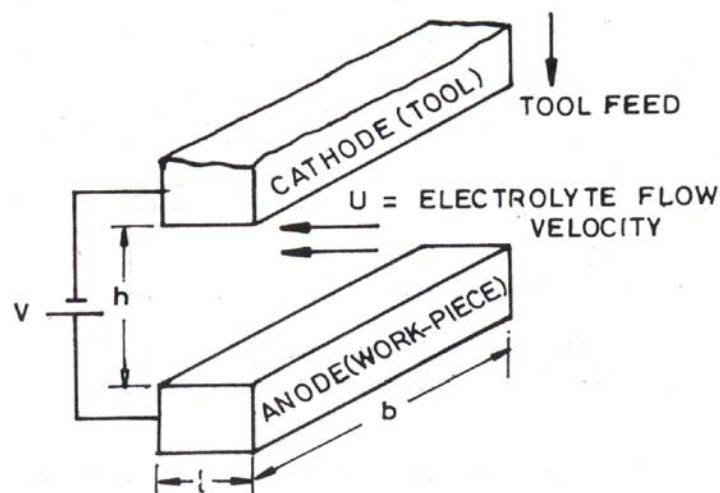
Fig. 3.11 Flow Through a Pair of Parallel Electrodes

Now the heat produced in the electrolyte due to the current I flowing through it

$$H = I^2 R_e = \frac{I^2 r h_e}{A}$$

If C_{pe} is the average specific heat of the electrolyte and specific resistance r is assumed to be constant

$$I^2 R_e = 4.187 \ q \ \rho_e C_{pe} \left(\theta_0 - \theta_i \right)$$

where q is the flow rate of the electrolyte, ρ_e the density of the electrolyte, θ_0 the outlet temperature of the electrolyte and θ_i the inlet temperature of the electrolyte.

It is also preferred that θ_0 should be as close to boiling temperature θ_b but never in excess for accelerated reaction.

Hence, $I^2 R_e = 4.187 \ q \ \rho_e \ C_{pe} \left(\theta_b - \theta_i \right)$ (3.22)

Now if we consider the current density in the gap, J is given by

$$J_c = \frac{I}{A}$$

where, A is the area of the tool.

Then,

$$\left(J_c^2 A^2 \right) \frac{r h_e}{A} = 4.187 q \ \rho_e \ C_{pe} \left(\theta_b - \theta_i \right)$$

or $J_c^2 = \dfrac{4.187 q \ \rho_e \ C_{pe} \left(\theta_b - \theta_i \right)}{h_e A}$ (3.23)

from which the flow rate of electrolyte to prevent boiling

$$q = \frac{I^2 r h_e}{4.187 A \ \rho_e \ C_{pe} \left(\theta_b - \theta_i \right)}$$ (3.24)

In the case of a rectangular electrode if the velocity of the electrolyte flow is U, then

$$q = U \ b \ h_e$$

Hence $U = \dfrac{I^2 r}{4.187 A \, \rho_e \, (\theta_b - \theta_i) b}$

Again, if V is the applied voltage

$$I = \frac{V}{R_e} = \frac{VA}{rh_e} \tag{3.25}$$

Since, $A = b \, l$, therefore

$$U = \frac{V^2 l}{4.187 \, rh_e^2 \, \rho_e \, C_{pe} (\theta_b - \theta_i)} \tag{3.26}$$

3.8 TOOL DESIGN

The first encounter with the process is that drilling a straight hole (Fig. 3.12a) involves a bare tool, while drilling the side of the tool also contributes to the machining process. Hence, taper is observed and the side takes of parabolic profile since machining on the side is for zero-feed rate condition (Sec. 3.6.1). The solution is to provide side insulation is shown in Fig. 3.12b.

Moreover, it has so far been assumed that the process of ECM to be of ideal in nature, i.e. the theory involved considers electric field solely within the limits of the gap and assumes that it obeys Ohm's and Faraday's laws.

With the flow of the electrolyte and machining at the highest feed-rate conditions, the work surface does not copy the replica (inverse profile) of the tool. The errors in machining are observed because:

(a) **Machining with a Bare Tool**   (b)   **Straight Hole Drilling with Side Insulation**
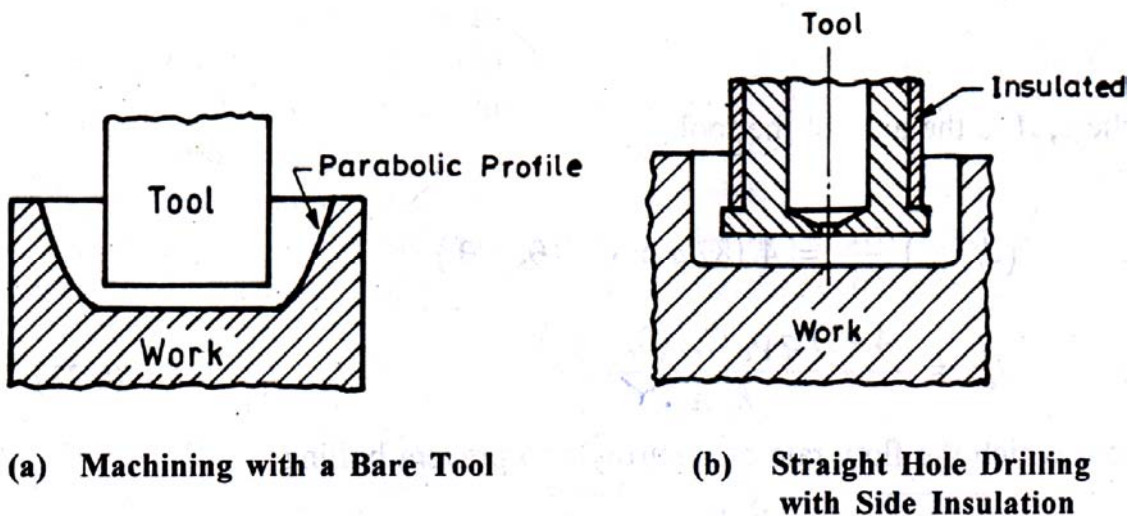
Fig. 3.12 Error due to Machining on Side and its Solution

- the electrolyte is heated up as it moves past the working gap and the temperature effect on the specific resistance of the electrolyte reflects on the machining rate at any point:

- flow of the electrolyte causes the reaction products at the cathode (gas bubbles) to move along affecting the change in resistance of the electrolyte.

- flow of the electrolyte once again causes the reaction products* produced at the work-surface (sludge and wear debris) to flow along to affect the change in resistance of electrolyte:

- the gap length along the curved surface changes, since the feed is given in a particular direction.

3.8.1 Heating of Electrolyte

Heating of the electrolyte (Joule heating) brings a change in the specific resistance. Assuming a linear variation of specific resistance with temperature as (Fig. 3.13).

$$r_x = r_i \left(1 \pm \alpha \ \theta_x \right) \tag{3.27}$$

the surface takes a parabolic profile with linear temperature variation. So the tool needs a corresponding change in profile to make a plane work surface (Fig. 3.13).
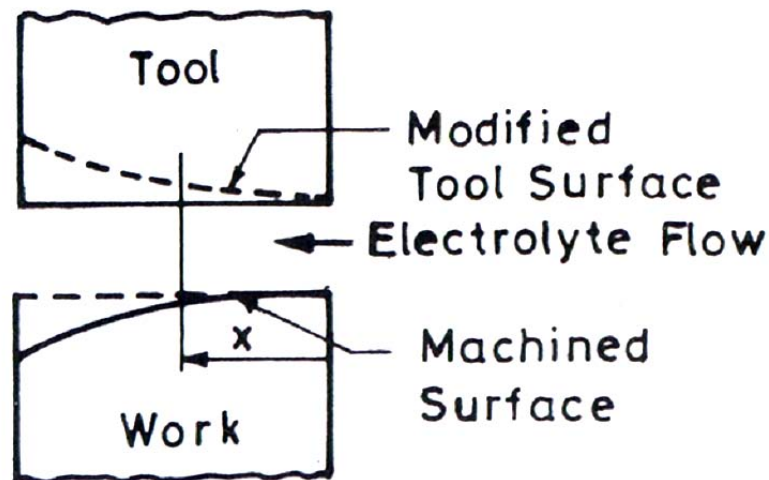
Fig. 3.13 Effect of Temperature on Surface Profile

3.8.2 Variation in Gas Bubble Concentration

Electrolyte induces the variation in gas-bubble concentration along its flow direction. The void fraction will produce a change in the resistance of the electrolyte in a way,

$$r_x = r_i\left(1 \pm \beta\, x\right) \tag{3.28}$$

where β is the coefficient of the change in resistance due to void fraction.
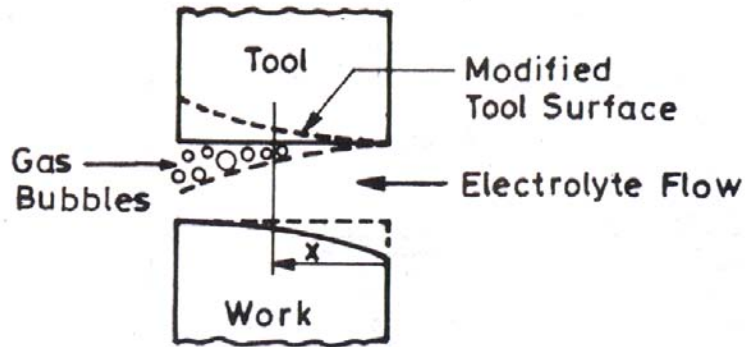
The corresponding machining error and necessary correction needed in the tool profile is shown in Fig. 6.14.

Fig. 6.14 Error Correction for Flow of Gas Bubbles

3.8.3 Variation in Sludge Concentration

The dielectric flow again induces the reaction products produced at the anode (work) surface to flow along with it. This causes the sludge concentration to increase continuously along the flow direction again bringing a change in the resistance of the electrolyte as

$$r_x = r_i\left(1 \pm \gamma\, x\right) \tag{3.29}$$

where γ is the coefficient in the change in resistance due to variation in sludge concentration.

Hence, the necessary correction needs to be provided.

3.8.4 Combined Effect

The combined effect of errors discussed above is summarised in Fig. 3.15.

In quantitative terms, electrolyte temperature and gas and sludge contents affect the distribution of local material removal rate in a plane parallel gap. The hydrogen evolving at the tool and sludge at the work piece produces three-phase layer (consisting of sludge, electrolyte and gas bubbles) at the electrode gaining in depth in the direction of the electrolyte flow.

Changes in the properties of the medium filling the gap entail change the pattern of heat generation (Fig. 6.16b), that affect the machined profile. So suitable correction is needed as shown above.
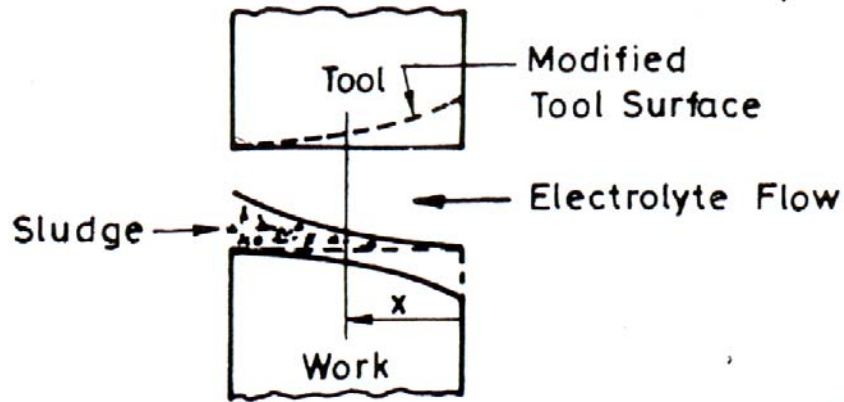
Fig. 3.15 Effect of Sludge Concentration
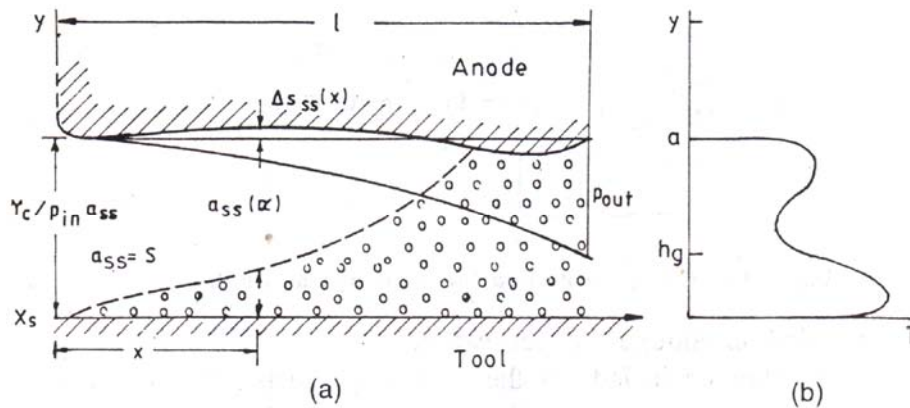
Fig. 3.16 Effect of Heat Build-up in the Electrolyte and Amount of Gas and Sludge in the Gap on the Distribution of Removal Rate in ECM Process

A point is to be noted here that the movement of the bubbles and sludge affects the coherency in machining process in a plane perpendicular to the flow is as shown in Fig. 3.17. So flow lines, equivalent to lay-lines as in the case of conventional machining processes, are observed along the electrolyte flow direction. This might be taken into advantage while orienting such lines in a desired direction so as to make the electrolyte flow in the same direction.

3.8.5 Effect of Feed Variation

While machining a contour (Fig. 3.18) the gap at different surfaces changes under equilibrium condition. Thereby, the rate of machining will affect the surfaces. So care must be taken to prevent inaccuracy under such conditions. One can redesign tool profile as discussed below.
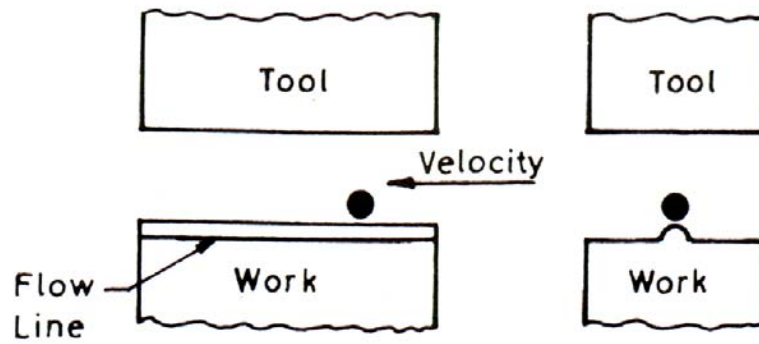
Fig. 3.17 Flow Lines in ECM
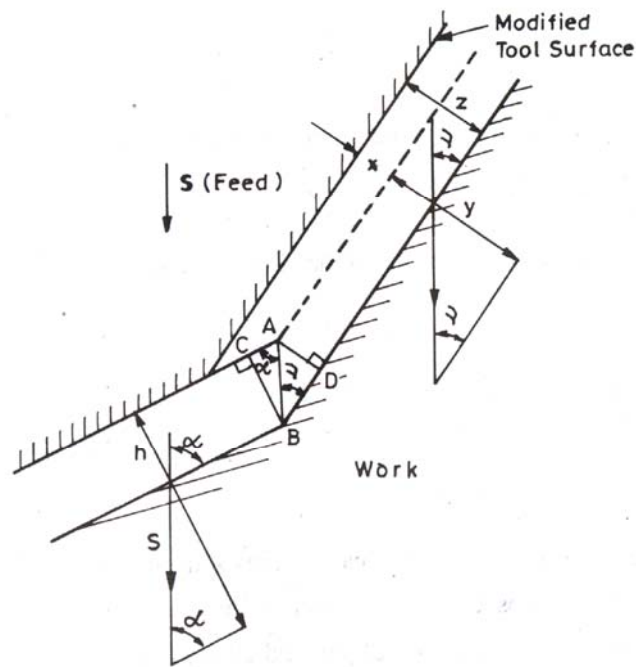
Fig. 3.18 Gap Under Equilibrium Condition and Correction for ECM Tool

The two surfaces inclined at an angle α and θ with the feed direction (Fig. 3.18) will produce unequal gap lengths of 'h' and y respectively. The machining on the surface inclined at an angle 'γ' will be more compared to the other (eq. 3.11). So the surface needs a correction of 'x' so as to maintain an equilibrium gap of 'z', say. The correction needed for the surface can be estimated as follows.

From the geometry of the two Δs ABC and ABD,

$$\frac{h}{\sin \alpha} = \frac{y}{\sin \gamma}$$

or $y = h \operatorname{cosec} \alpha \sin \gamma$ (3.30)

again, since (eq. 6.11)

$$\frac{dh}{dt} = \frac{C}{h}$$

and if δh and δz are the machining rates achieved at the two surfaces under equilibrium conditions, then,

$$\frac{\delta h}{\delta z} = \frac{z}{h}$$ (3.31)

But from geometry of the triangles containing δh and δz

$$\frac{\delta h}{\sin \alpha} = \frac{\delta z}{\sin \gamma}$$

since both contain a side equal to the length S, feed-rate

or $$\frac{\delta h}{\delta z} = \frac{\sin \alpha}{\sin \gamma}$$ (3.32)

from eqs. 6.31 and 6.32

$$\frac{z}{h} = \frac{\sin \alpha}{\sin \gamma}$$

or $z = h \operatorname{cosec} \gamma \sin \alpha$ (3.33)

Hence, the necessary correction can be drawn from 6.30 and 6.33 as

$x = z - y = h(\cos ec\gamma \sin \alpha - \cos ec\alpha \sin \gamma)$ (3.34)

So, when a = 90°, i.e. first surface perpendicular to the feed direction, the correction needed for the second surface is

$$x = h(\cos ec\gamma - \sin \gamma) = h \frac{\cos^2 \gamma}{\sin \gamma} = h \cot \gamma \cos \gamma$$ (3.35)

Any curved surface to be generated need not be produced by trial and error, but can be corrected by finite-element methods considering the difference in slope between the element with respect to preceding element to give a solution (Fig. 6.19).

3.9 APPLICATION

This process is highly versatile to process extremely difficult-to-machine metals and its alloys (electrically conductive) not possible by conventional methods. Though the stock removal is lower as compared to conventional machining (since ECM needs removal atom by atom), yet proves to be more economical when machining vety hard materials with hardness above 420 BHN value (Fig. 6.20). Moreover, this process directly gives the surface quality which does not require further finishing operations and machining can be done even after heat-treatment process.
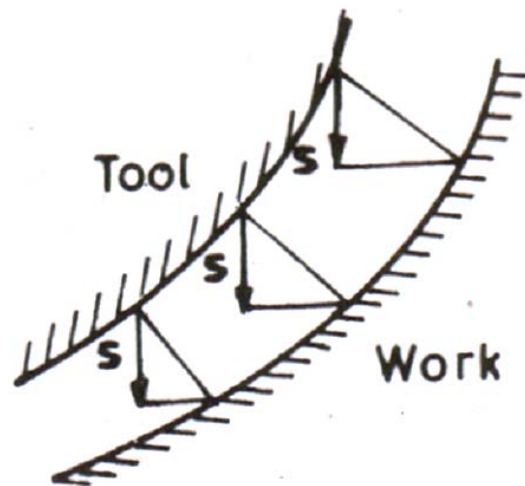
Fig. 3.19 Variation in Tool Profile with Respect to Work Surface

The ECM is used for die-sinking, profiling and contouring, multi hole drilling, trepanning, broaching, honing, steel mill applications, surfacing, sawing, contour machining of hard and hard-to-machine materials. It operates on constant feed system and the required motions are given depending upon the variety of difficult processing operations (Fig. 3.21).

As can be seen, this process have no tool wear, the machining rate is directly proportional to current (power) and the machining rate does not affect the surface finish (since reaction is in atomic level) unlike conventional and other processes. It is considered to be a high production machining system, and it does not require a finishing operation. Another biggest advantage of this process is that to produce crack and stress free surfaces (excepting intergranular attack), there is no thermal damage. It is indepen¬dent of hardness of work material and the machine operates at high unidirectional feed (for $3D$ profile also).
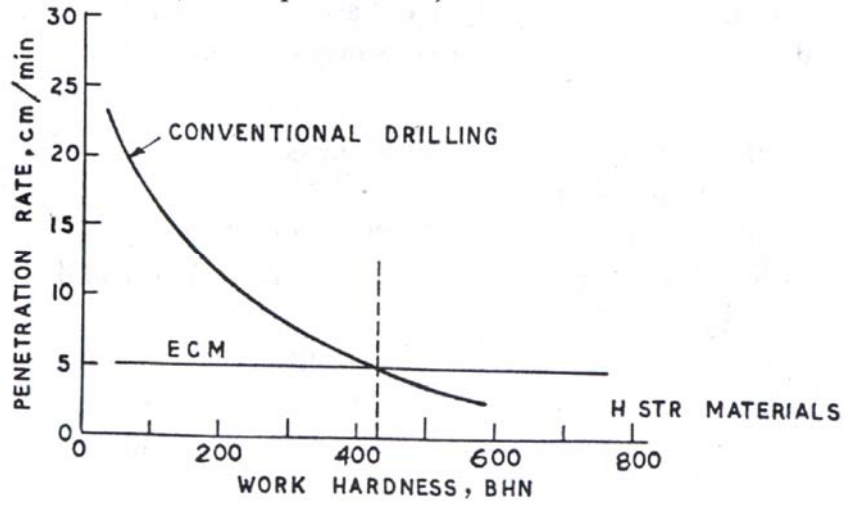
Fig. 3.20 Comparison of Penetration Rates in Conventional Drilling and ECM Process
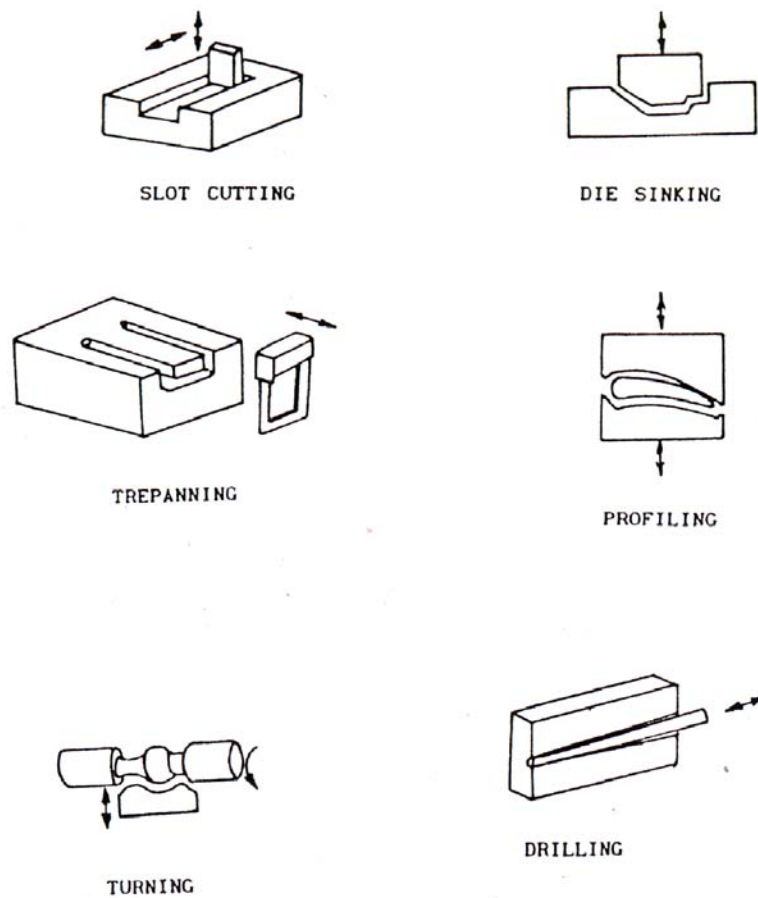
Fig. 3.21 Types of ECM Operation.

Another advantage of this process is that lay lines (here flow lines) of the roughness is along the liquid flow direction. Hence, the desired lay line orientation can be achieved easily and it also generates a burr-free surface.

The disadvantages, apart from considering its suitability for use in a specific work, lie in:

- Difficulty in learning to use the process.

- Heavy initial investment.

- Difficulty in designing a proper tooling system.

- Corrosion-free material requirement for the structure and electrolyte handling systems.

- Though the process provides high surface finish and stress-free surfaces, preferential etching of highly dissolving impurities present at the inter-granular boundaries may result in tunneling effect.

- Hydrogen liberation at the tool surface may cause hydrogen- enbrittlement of the surface.

- Spark damage may become sometimes more problematic.

- Fatigue property of the machined component may reduce as compared to conventional techniques, so may need further treatments.

3.10 OPERATIONAL SUMMARY

Power Supply

Type	Direct Current
Voltage	2 to 30 V
Current	50 to 40,000 A
Current density	10 to 500 A/cm^2

Electrolyte (Type and concentration)

Mostly used	NaCl 50 to 250 g/L
Frequently used	NaN0$_3$ at 120 to 500 g/L
Occasionally used	Proprietary mixtures
Temperature	26° to 50°C
Flow rate	16 lit/min/lOOA
Velocity	1,500 to 3000 m/min
Inlet pressure	130 to 2200 KPa

Outlet pressure	0 to 300 KPa
Frontal working gap	0.075 to 0.75 mm.
Side overcut	0.125 to 1 mm
Feed rate	0.50 to 13 mm/min
Electrode material	Copper, Brass, Bronze
Tolerance	
2-D shape	0.025 mm
3-D shape	0.050 mm
Surface Roughness, Ra	0.2 to 1.5 μm

3.11 SOME TYPICAL APPLICATION NOTES [5]

- Electrochemical sinking of the Disc for Turbine Rotor Blades.

- Thin wall mechanical slotting of the Collets, makes it difficult for manufacturing and costly, can be replaced by EC-sinking where the parts could be finished in one operation without burrs, deformation and stress.

- Difficult to maching Hollow Shafts are easier and faster by ECM.

- Chain Pinions (Sprockets) are processed in 50 sec with cycle time of 65 sec by 300 amp/part.

- EC-sinking is possible for machining internal profile of Internal Cams.

- Driving Joints are processed in two shapes within 44 sec (cycle time 28 sec) with 80 amp/part.

- Pump Glands are processed within 10 sec (cycle time 15 sec) with 250 amp/part.

- Connecting Rod is processed within 18 sec with cycle time of 46 sec.

- Splined Rear Axle Joint is processed in 30 sec and cycle time of 33 sec with 500 amp/part.

- Hydraulic Spools are processed in two steps within 50 sec with current of 280 amp/part.

- Gear Wheels are processed in 25 sec (cycle time of 28 sec) with 400 amp/part.

ELECTROCHEMICAL GRINDING (ECG)

4.1 INTRODUCTION

Conventional grinding produces components with good surface finish and dimensional tolerances but such components are also associated with burrs, comparatively large heat affected zone (HAZ), and thermal residual stresses. These defects are not found in electrochemically ground workpieces (anodes). During electrochemical grinding (JECG), material is removed by mechanical abrasive action (about 10%) and by electrochemical dissolution (about 90%) of anodic workpiece. As in any other electrochemical dissolution based process, workpiece should be electrically conductive. Electrolyte is recirculated in ECG, hence, an effective and efficient electrolyte supply and filtration system is needed. The commonly used electrolytes are sodium chloride (NaCl) and sodium nitrate ($NaNO_3$).

In ECG, there is a grinding wheel (cathode) similar to a conventional grinding wheel except that the bonding material is electrically conductive. Electrolyte is supplied through inter electrode gap (IEG) between the wheel and the workpiece. The height of abrasive particles protruding outside bonding material of the wheel helps in maintaining a constant IEG because the abrasive particles act as spacers. *Life of the ECG* wheel is about ten times more than that of the conventional grinding wheel. Two factors are responsible for such a high wheel-life: only 10% contribution by abrasive action towards the total material removal, and very small length of arc of contact.

In ECG, the area in which machining is taking place can be divided into 3 zones (*named as, zone I, zone II, and zone III*) as discussed in the following. Fig. 4.1 shows a schematic diagram for ECG set-up.

In **zone I** (Fig. 4.2), material removal is purely due to electrochemical dissolution and it occurs at leading edge of the ECG wheel. Rotation of the ECG wheel helps in drawing electrolyte into the IEG. As a result of electrochemical reaction in zone I, reaction products (including gases) contaminate electrolyte resulting in lower conductivity. In fact, presence of sludge, to some extent, increases conductivity of the electrolyte [Jain et al, 1990], while that of gases decreases it. Net result is a decrease in the value of conductivity of the electrolyte. It yields a lower value of IEG. As a result, abrasive particles touch the workpiece surface and start removing material by abrasive action. Thus, a small part of material is removed in the form of chips. Further,

electrolyte is trapped between the abrasive particles and workpiece surface, and it forms a tiny electrolytic cell as shown in Fig. 4.2. In each electrolytic cell, small amount of material from the workpiece is electrochemically dissolved.

The electrolyte is being forced into the IEG in **zone II** by rotational motion of the wheel. As a result, local electrolyte pressure increases in this part of the IEG (zone II). It suppresses formation of gas bubbles in the gap yielding higher MRR. Chemical Or electrochemical reaction may result in the formation of passive layer on the workpiece-surface. In this zone II, abrasive grains remove material from the work surface in the form of chips and also remove non-reactive oxide layer. Most of the metal oxides formed are insoluble in water, and electrically nonconductive.
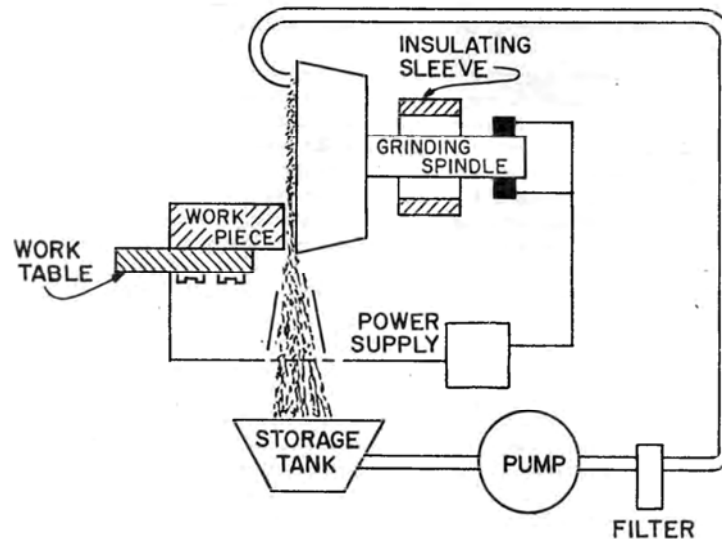
Fig. 4.1 Schematic diagram of electrochemical grinding set-up.

Removal of non-reactive oxide layer promotes electrolytic dissolution. It exposes fresh metal for further electrolytic action. Hence, it is also called [Bhattacharyya, 1973] as " mechanical assisted electrochemical grinding" process.

In zone III, material removal is totally by electrochemical dissolution. **Zone III** starts at the point where wheel lifts off the work-surface. In this zone, pressure is released slowly. This zone contributes to the removal of scratches or burrs that might have formed on the workpiece in **zone**

4.1 ECG MACHINE TOOL

The ECG systems are very similar to conventional grinders (Fig. 4.3). In ECG system, machining area is made up of non-corrosive materials. Power is supplied through spindle either

with the help of brushes or mercury coupling. The latter can carry more current than the previous one. The probability of short circuiting during ECG is very low because of the presence of protruding abrasives which create a positive IEG. Hence, in this system, there is less need of having short circuit cut-off devices.
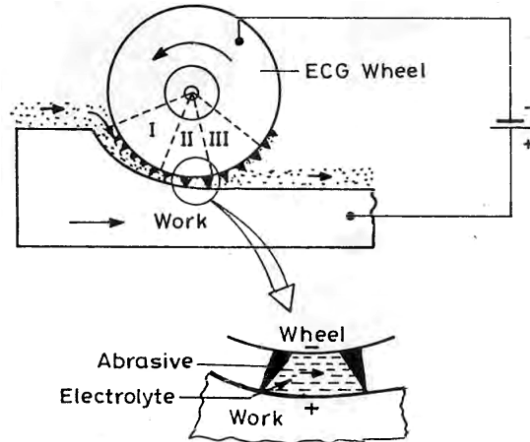
Fig. 4.2 Three machining zones and tiny electrochemical cell formation in ECG.

Five different kinds of ECG operations can be performed, viz electrochemical (EC) cylindrical grinding, electrochemical form grinding, EC surface grinding, EC face grinding and EC internal grinding. EC cylindrical grinding is the slowest process because of the limited area of contact between the
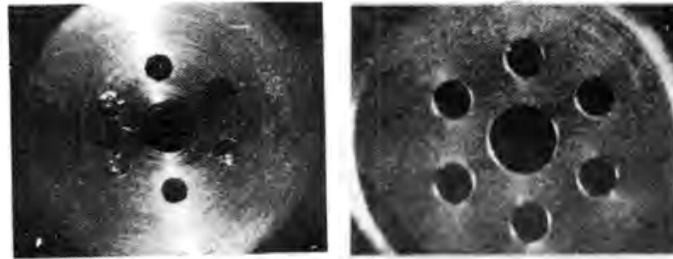
Fig. 4.3 Electrochemical grinder [*Hammond Machinery*, USA]

wheel and the workpiece. However, EC face grinding is the fastest process because of maximum area of contact between the anode and the cathode. Uneven wheel wear can be controlled by providing oscillating motion to the workpiece. In EC surface grinding, the workpiece reciprocates. EC internal grinding and EC form grinding are the same as conventional internal and form grinding operations except that the ECG wheel is electrically conducting and the electrolyte is present in the IEG. Metal bonded grinding wheels have many advantages over resinoid bonded wheels. In ECG wheel, the commonly used bonding materials are copper, brass, nickel, or copper impregnated resin. Such metal bonded wheels are effectively dressed using electrochemical process. To prepare (or dress) them, reverse the current (or make the wheel as anode) and do the grinding on the scrap piece of metal. It will deplate the metal bond. The commonly used abrasive is alumina (grit mesh size 60-80). ECG does not require frequent wheel dressing. Dissolution of bond metal usually makes mechanical shear unnecessary. Trueing of the metal bonded grinding wheel is done, in-process, during electrochemical dressing. Further, the electrolyte used in ECG should be chemically inert to the conductive wheel bond material and workpiece. Current rating of these machines is usually 50-3000 A.

4.2 PROCESS CHARACTERISTICS

Performance of ECG process depends on various process parameters such as wheel speed, workpiece feed, electrolyte type, concentration and delivery method, current density, wheel

pressure, etc. By selecting appropriate values of these parameters, MRR and surface finish obtainable during the process can be varied over a wide range [Kuppuswamy, 1976].

Current density is one of the most important parameters that influences the process performance. Material removal rate (MRR) in ECG is also governed by current density. With higher current density, both MRR and surface finish improve. If the applied voltage is very high (usual range is 4-15 V), it may deteriorate surface' finish of the machined workpiece as well as damage the tool (grinding wheel). Presence of such condition is percepted by spark formation at the front of the wheel, Selection of an appropriate feed rate to the tool is important. If it is higher than the required one, the abrasive particles will prematurely detach from the wheel, leading to excessive wheel wear. If it is lower than the required one, a large overcut (or poor tolerances) and poor surface finish will result. The IEG is usually a quarter of a millimetre while using a freshly dressed wheel. Surface speed of the wheel is in the range of 1200-1800 m/min. The depth of cut is usually below 2.5 mm and it is limited by the wheel contact arc length, which should never exceed 19 mm; otherwise electrolyte becomes ineffective because of higher concentration of H_2 gas bubbles and sludge [Benedict, 1987]. M RR achieved during ECG may be high as 10 times compared to conventional grinding on hard materials (hardness > 65 HRC). But tolerances obtained in ECG are poorer ($\pm$ 0.0025 mm). Minimum inside corner radius of 0.25 mm and outside corner radius of 0.025 mm can be produced by this process. Abrasive particles maintain electrical insulation between cathode and anode, and determine the effective gap between them (may be as low as 0.025 mm). Surface finish obtained by ECG ranges from 0.12 and 0.8 μm. The surface produced by ECG is free of grinding scratches and burrs. Surface finish produced on nonhomogeneous materials during ECG is better than that produced during conventional grinding. In spite of more initial investment, the cost of EC grinding is lower than that of conventional grinding due to much higher MRR during ECG. Risk of thermal damage is also reduced. Electrochemical grinding of WC-Co has been reported [Levinger and Malkin, 1979], The initial specific etching rate of cobalt phase is higher than that of WC phase. In addition to the direct dissolution of material, the electrolysis process in ECG weakens the cermet material by selective removal of cobalt. When the in-feed rate during ECG is less than the initial specific etching rate of cobalt phase, selective etching of cobalt occurs that reduces mechanical power requirement for machining. At higher in-feed velocities, the reduction in mechanical power requirement is marginal. Study of surface roughness produced during ECG [Geva et al., 1976]

clearly indicates that there is selective electrochemical etching of the metal phase (Cobalt). It weakens the composite material and, thereby, reduces the forces required for mechanical grinding. Kuppuswamy and Venkatesh [1979] conducted experimental study to investigate the effect of m agnetic field on electrolytic grinding using diamond, SiC, and Al_2O, wheels. It has been found that the magnetic field in case of a diamond wheel, improves the process performance but the same is not true for Al_2O_3 wheel. In case of SiC wheel, the improvement obtained is marginal. The magnetic field interacts with the moving charged particles and may affect the rates of both mass transport and charge transfer processes [Dash and King, 1972], The magneto-hydrodynamic force leads to stirring of electrolyte particularly in the neighbourhood of electrodes. It leads to enhanced mobility and hence an increased rate of electro-chemical reactions. Gedam and Noble [1971] concluded that fine grits and low concentration wheels show a tendency to draw more current and thereby achieve greater MRR than coarse grits and high concentration wheels. ECG is a cold process (bulk temperature $< 100°C$), thus prevents structural damage and grinding cracks. However, electrochemically ground specimens show relatively poor fatigue strength, possibly due to stray current attack of the surface, which leaves a series of 'pits' that would act as sites for fatigue crack initiation [DeBarr and Oliver, 1968].

Declogging of the grinding wheel can be done by reversing its polarity (making the tool as anode) for a short period. It may, however, result in longer machining time and degeneration of the wheel-shape.

4.3 APPLICATIONS

Electrochemical grinding is economical for grinding carbide cutting tool inserts. Microscopic study of electrochemically ground surfaces of the cemented carbide do not reveal any damage to the microstructure, microcracks, or any other defects. This process is also used to reprofile worn locomotive traction motor gears. Usually wear marks from the gear tooth surfaces are removed by removing as much as 0.38 mm thick layer of material. ECG does not have any effect on gear hardness. ECG is also used for burr-free sharpening of hypodermic needles, grinding of superalloy turbine blades, and form grinding of fragile aerospace honeycomb metals.

ELECTROCHEMICAL DEBURRING (ECDe)

5.1 INTRODUCTION

A designer during the design phase of a component usually considers the aspects like material, form, dimensional accuracy, surface texture and heat treatment, but not the surface integrity and edge quality [K. Takazawa, 1988]. However, the last two factors are very important from the point of view of performance and the life of the product. Fig. 5.1 shows the concepts of surface technology. In this chapter, s,ome discussion on how to achieve the desired edge quality (shape, dimension, tolerance and surface roughness) through electrochemical deburring is presented.

When a component is processed by a conventional machining method, usually, it is left with burrs specifically along the two intersecting surfaces. Such burrs are undesirable from the viewpoint of performance of a component as well as safety of an operator, or for that matter whosoever works with this component. Such burrs can be removed by one of the deburring processes. Deburring is an important phase for manufacturing quality products, especially in large scale industries. The problems of burrs are still persisting and unsolved in many industries. Attempts are made to reduce burr level by various means, viz. by fixing speed, feed rates, and tool life, but this could not be achieved for certain reasons. Hence, the quality of the products is affected.
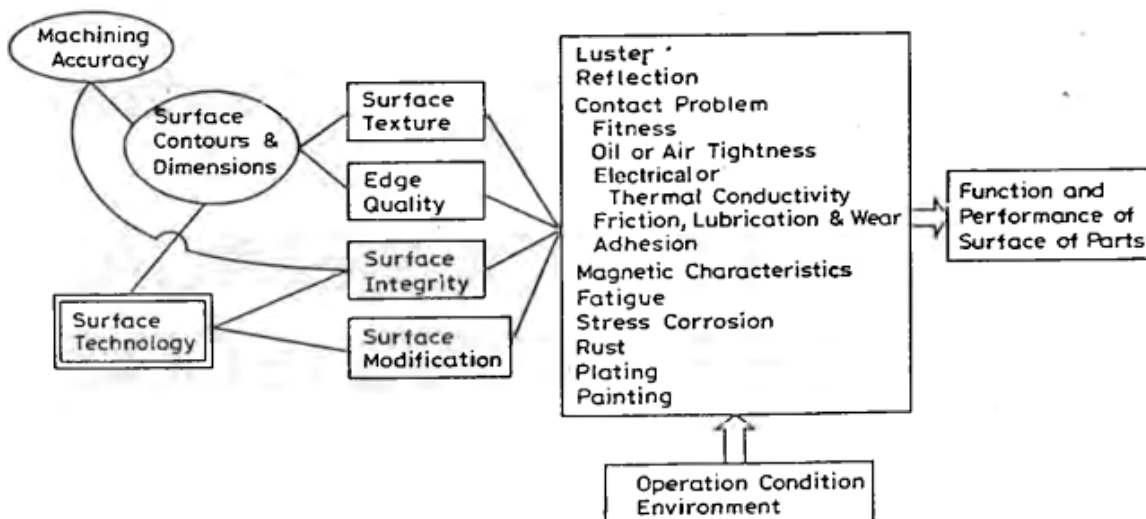
Fig. 5.1 Concepts of surface technology [K. Takazawa, 1988]

5.2 Definition of Burr:

Burrs are three-dimensional in nature (Fig. 5.2) having length (/), height (h) and thickness (t) as described in the following:

l (Burr length)   : length of the edge along the burr axis.

h (Burr height)   : distance of the burr projected above the parental surface.

t (Burr thickness)   : thickness or width of the burr where it joins the parental surface.

Burr Hardness   : Hardness of the burr in the vicinity of the base of the bun-.
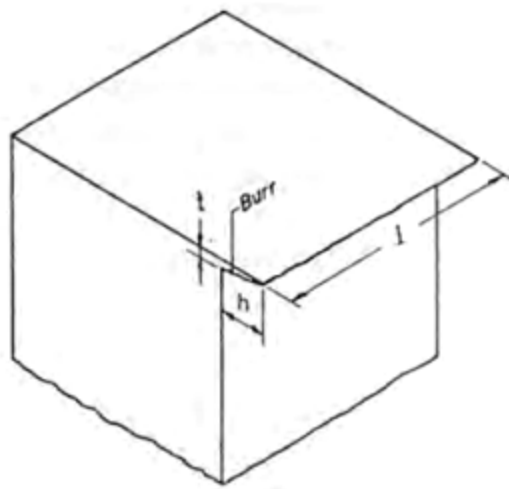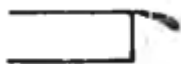
Fig. 5.2 Terminology of a burr [Naidu, 1991].

Types of Burrs Formed During Different Manufacturing Methods:

Types of Burrs	Figure of the Burr	Remarks
Compressive burr		The burr produced in blanking and piercing operations in which slug separates from the parent material under compressive stress.
Cutting off burr		A projection of material left when the workpiece falls from the stock.

Comer burr		Intersection of three or more surfaces.
Edge burr		Intersection of two surfaces
Entrance burr		Cutting tool enters in the workpiece.
Exit burr		Cutting tool exits the workpiece.
Feather burr		Fine or thin burr.
Flash burr		Portion of flash remaining on the part after trimming.
Hanging burr		Loose burr not firmly attached to the workpiece.
Roll over burr		Burr formed when it exits over a surface and allows the chips to be rolled away.
Tear burr		Formed from the sides of the tool as the tool tears the edge.

5.3 Basic Approach on Deburring

In the modem industrial technology, the deburring process has attained great importance because of rigid quality standards. In analyzing the specific situations, one has to know 'why deburring is required?' Burrs, to some extent, can be reduced by controlling cutting conditions, but cannot be eliminated completely. Hence, deburring becomes inevitable. However, deburring cost should not be very high. This requires careful considerations regarding effects of the presence of burrs

on functional, physiological and aesthetic requirements [Naidu, 1991], as outlined in the following chart.

```
                          ┌──────────────────────────┐
                          │       FUNCTIONAL         │
                          └──────────────────────────┘
          ┌───────────────────────┼───────────────────────┐
          ▼                       ▼                       ▼
┌───────────────────────┐ ┌───────────────────────┐ ┌───────────────────────┐
│   In manufacturing    │ │     Workpiece         │ │     Equipment         │
│ Handling, Machining,  │ │ Corrosion, after      │ │ Wear, and/or breakdown,│
│ Assembly, Positioning,│ │ coating,              │ │ by loosened burrs.    │
│ Checking, and Mounting│ │ Crack formation in    │ │                       │
│ are endangered        │ │ loading.              │ │                       │
└───────────────────────┘ └───────────────────────┘ └───────────────────────┘
```

```
                          ┌──────────────────────────┐
                          │      PHYSIOLOGICAL       │
                          └──────────────────────────┘
          ┌───────────────────────┼───────────────────────┐
          ▼                       ▼                       ▼
┌───────────────────────┐ ┌───────────────────────┐ ┌───────────────────────┐
│       Injury          │ │     AESTHETIC         │ │      Utility          │
│ Injury may take place │ │     Impression        │ │ Physiological shaping │
│ in consequent         │ │ Advertising, sale,    │ │ of gripping surface,  │
│ processing, assembly, │ │ and use.              │ │ tools, and handling   │
│ use, maintenance, and │ │                       │ │ elements.             │
└───────────────────────┘ └───────────────────────┘ └───────────────────────┘
```

5.4 CLASSIFICATION OF DEBURRING PROCESSES

Deburring processes can be classified (Fig. 5.3) as:

1. Mechanical deburring,
2. Abrasive deburring,
3. Chemical and Electro-chemical deburring, and
4. Thermal deburring.

5.3.1 Mechanical deburring, using cutting tools, brushes, scrapers, belt sanders, etc, is generally unreliable as it is labour oriented and is only a burr-minimizing process. It does not meet the requirements of high edge quality because of the existence of fine burrs even after mechanical deburring operation.

5.3.2 In abrasive deburring like tumbling, barrel finishing, vibratory deburring, liquid abrasive flow, sand blasting^etc, the selection of abrasive medium, its shape and quantity play an important role. Deburring by this method generally affects other areas on the component where deburring is not required and has limitations on edge quality. The reliability, uniformity and MRR of these processes are low, and tend to charge the workpiece with grits.

5.3.3 In thermal deburring (TDe), components to be deburred are placed in the deburring chamber. The chamber is closed and filled with combustible gas mixture of oxygen and hydrogen. After ignition by an electric spark, the gas burns in few milliseconds and the temperature attained is over 3500°C. Due to this short heat wave, burrs and sharp edges on the component burn away.

5.3.4 Chemical deburring is the process where the burrs are dissolved in chemical media. It also may affect the areas where material removal is not required.

Principle of anodic dissolution (ECM) has also been applied [Benedict, 1987; Rumyantsev and Davydev, 1989] for the removal of burrs. However, in case of electrochemical deburring (ECDe) as compared to ECM, magnitude of current, electrolyte flow rate, and electrolyte pressure are all low. Secondly, tool is stationary. Fig. 14.4 shows an ECDe system.

5.3.5 Electrochemical deburring is generally employed for far away located as well as inaccessible places where other deburring processes are not effective. This process involves the use of flowing electrolyte for conducting electric current for the electrochemical reaction to take place. The current rating and duration of the current flow to suit a particular component are determined after extensive trials for each type of the component. The electrolyte commonly used is either sodium chloride or sodium nitrate. Because of the corrosive nature of the electrolyte

5.4 DEBURRING PROCESS

Much of this research and development has now made the transition from the laboratory into the production.
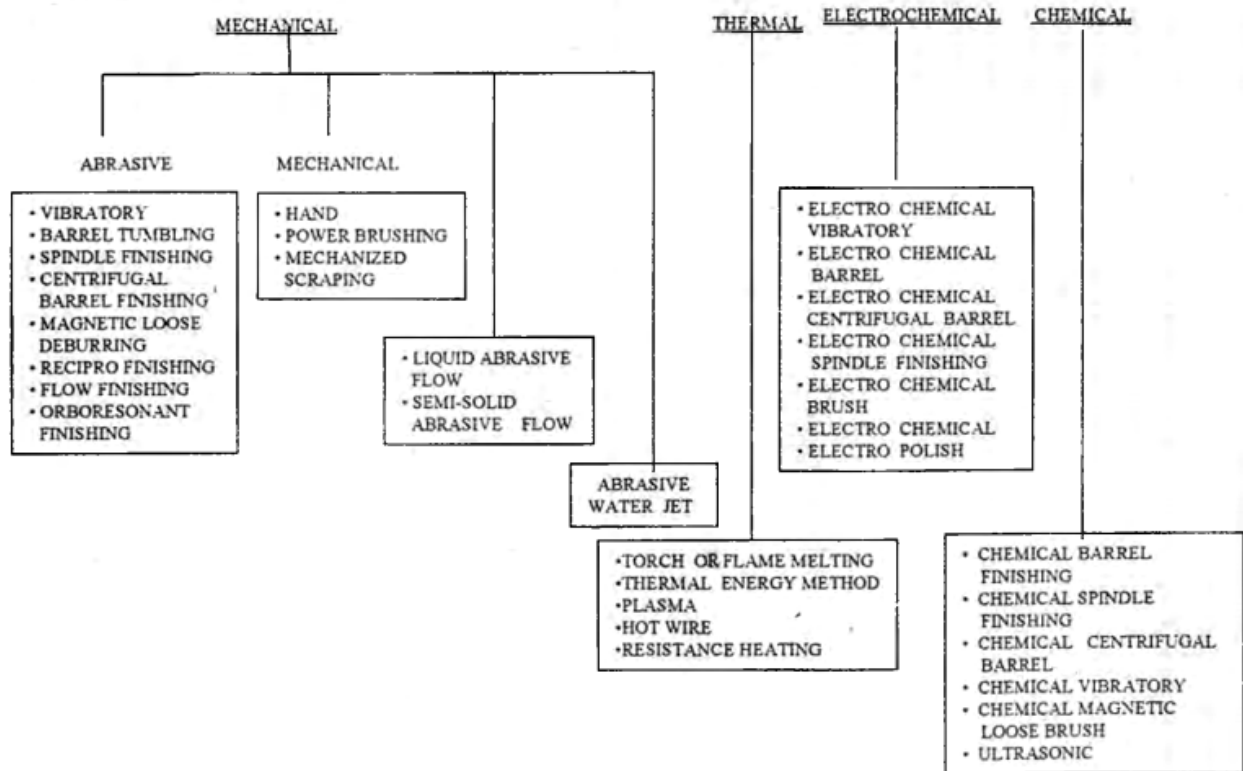
Fig. 5.3 Classification of deburring processes.

and ferrous hydroxide released by the process, machines are built with noncorrosive materials.
Electro polishing deburring (EPDe) is different from EC deburring. The metal removal and polishing simultaneously take place on all the surfaces in EPDe, whereas in ECDe, the metal removal is localised. In this process, a component which has roughness and some burrs, is subjected to selective electrochemical attack. As a result, microprofile is smoothened and levelled.

Selection of a process depends on the edge quality and other requirements of the component. Most of the modem industries are switching over to modem technologies like ECDe, EPDe and TDe due to obvious advantages including cost savings.

5.5 ELECTROCHEMICAL DEBURRING (ECDe)

This process has been tried out successfully on contours where the conventional deburring tools can not be used. The performance of the process is improved. with higher current intensities. It requires specially engineered equipment for its use as manufacturing unit. It consists of:

1. Electrolyte system which provides high velocity to the electrolyte flow,

2. Electrical power system which supplies the electrolyzing current,

3. Mechanical structure which locates and provides movement/mounting to the electrodes, and

4. Separator which separates the sludge.

5.6 Principle of working

When a voltage is applied between two metal electrodes immersed in an electrolyte, current flows through the electrolyte from one electrode to the other. Unlike the conduction of electric current in the metals in which only the electrons move through the structure of the material, 'ions' (electrically charged groups of atoms) physically migrate through the electrolyte. The transfer of electrons between the ions and electrodes completes the electrical circuit and also brings about the phenomenon of metal dissolution at the positive electrode or anode (workpiece). Metal detached atom by atom from the anode surface appears in the main body of the electrolyte as positive ions, or as precipitated semi-solid of the metal hydroxide, which is more common in electrochemical deburring process.

The tool is usually insulated on all surfaces except a part which is adjacent to the burr(s). Instead of insulated tool, a bit type of tool [Jain and Pandey, 1982] can also be used. The electrolyte is made to flow through inter electrode gap. However, setting of dimensions of the bare part of the tool, time of machining, and other machining conditions are all decided by 'trial and error? method. The inter electrode gap (IEG) is usually kept in the range of 0.1-0.3 mm. The deburring tool-tip should normally overlap with the area to be worked by 1.5 to 2.0 mm.

5.7 ECDe machine tool (M/T) is usually designed with multiple work stations served from a single power supply. The electrolyte is properly filtered out before its re-circulation. Criteria for selection of tool material used is the same as for general ECM.

It is considered as a high-tech method when compared to the conventional methods of deburring. Before applying ECDe method for a particular type of job, one should know about thickness, shape, and repeatability of burrs on the job in hand. Almost identical shape and size of the burrs should be on the job otherwise efficient burr removal may not take place. Further, the part of the tool supposed to remove burrs should be shaped as a replica of the contour of the work. Fig. 5.5 shows a tracing from the micrograph of a sample deburred electrochemically.
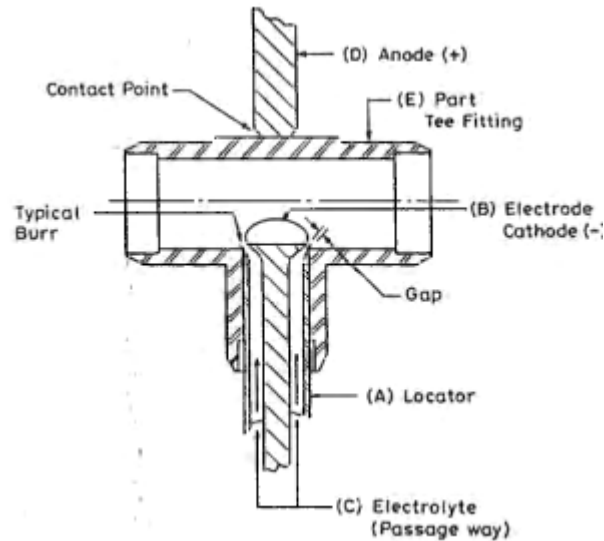
Fig. 5.4 Schematic diagram of electrochemical deburring.
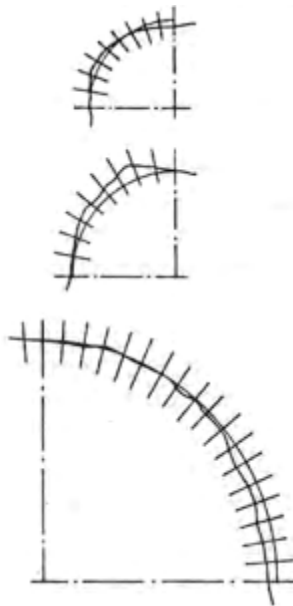
Fig. 5.5 Tracing from the micrograph of an electrochemically deburred samples [Rumyantsev and Davy dev, 1989],

In some cases, deburring can also be done with the help of a movable ECDe unit [Rumyanstev and Davydov, 1989] consisting of deburring gun, electrolyte supply tank, and power supply unit (= 50 A max. current). The deburring gun is supplied with electrodes of different diameter and length so that it can be used to deburr hard-to-get places. However, in some cases, tool of varying length may be needed. For this purpose, a flexible tool is used which consists of wire coiled into a closely wound spring. The details of the tool are shown in Fig. 5.6 (1-insulating

spherical tip, 2-copper tip with a hole for electrolyte supply, 3-spring, 4-PVC sleeve, 5-copper shank press fitted to the spring. The flexible electrode is attached to the gun by means of shank 5). The deburring gun is also used to deburr edges of sheet metals. Deburring speed may be as 400-500 mm/min.

The data in the following table may be useful for practical deburring purposes:
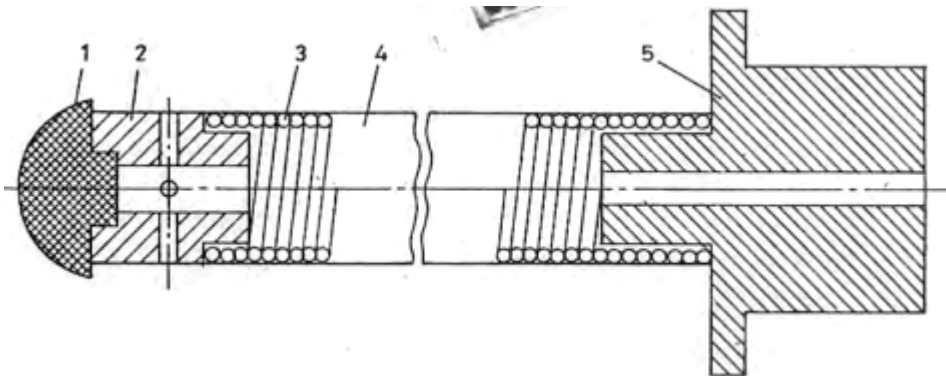
Fig. 5.6 A tool for a movable. electrochemical deburring unit [Rumyantsev and Davydev, 1989].

Material	Electrolyte	Applied Voltage	Current Density	Deburring Time
Carbon and low	5-15% $NaNO_3$			
carbon steel	+ 2-5% $NaNO_2$			
Copper alloys	5-15% $NaNO_3$	12-24V	5-10 A/cm^2	5 -100 s
Aluminium alloys	15-20% $NaNO_3$			
Stainless Steels	5% $NaNO_3$+NaCl			

ECDe is found suitable for removing burrs from tubes and pipes widely varying in configuration, length and cross-sectional area.

5.8 Functions of Electrolyte and its Importance

Depending upon the requirements of the process, sodium chloride (NaCl) and sodium nitrate

(NaNO$_3$) are generally used as electrolytes. The other electrolytes like hydrochloric acid, potassium chlorate, etc. have certain disadvantages in the process application. Sodium nitrate and sodium chloride have certain variations in usage [Naidu, 1991] which are as follows:

Details	Sodium Nitrate	Sodium Chloride
1. Voltage requirements	High	Low
2. Reaction	Normal	Aggressive slow
3. Increase of pH value	Fast	Slow
4. Machining efficiency • Low carbon steel • High carbon steel • Aluminium	 60-80% Good Good	 80-100% Poor Poor
5. Machined surface • Roughness • Colour • Edges • Dimensional accuracy • Reach • Effect on surrounding surface	 About 5 μm Dark grey Sharp & distinct Accurate Up to 1 mm Limiting stray machining and pitting of adjacent areas	 About 1 μm Bright grey Blunt & dull Not accurate Up to 5 mm Removes material from surrounding areas and pitting damages adjacent areas.
6. Cost	Costly	Not very expensive.

The deburred component shows a localized deposit (dark grey) which is a reaction product of the process. The composition of the reaction product while deburring ferrous component is Fe$_3$O$_4$. It is a magnetic oxide of iron and its thickness is less than 1 pm. The adhesion of the deposit is very strong and it can be removed only mechanically. In specific cases, this deposit can be removed from unhardened components (urialloyed or low alloyed steels) as follows:

1. Anneal under air flow for more than 40-60 min at 430°C,
2. Pickle in hydrochloric acid for 1/2 min,
3. Anodically clean in alkaline bath for about 2 min.

In most of the cases, the deposit is eleotrolytically conductive and does not come in the way of galvanic deposits. This deposit disappears during heat treatment of the components.

5.9 APPLICATIONS

ECDe has applications in industries like consumer appliances, biomedical, aerospace, automobile, etc. ECDe is used for the components like gears, splines, drilled holes and milled components, fuel supply and hydraulic system components, etc. It is very successful even in the situations where two holes cross each other like crank shaft. Apart from economics of the process, it gives higher reliability, reduced operation time, and more uniformity. This process can be automated in an easier way than other processes. Fig. 14.7 shows a gear before and after deburring.

5.10 SPECIFIC FEATURES OF ECDe M/C

Specific features of an ECDe M/C-are summarized as follows:

1. *Application:* Removal of thin and thick burrs at inaccessible and irregular areas within the restricted zone, and wherever edge rounding is required.

2. *Principle:* High velocity electrolyte (sodium chloride/sodium nitrate) is passed through the IEG between the tool-cathode and the component-anode connected to the electric potential. The undesired superfluous projections on the component are dissolved electrochemically within a preset cycle time of a few seconds. The dissolved burrs in the form of hydroxides settle down and the electrolyte is regenerated. The hydroxide is disposed through outlet drain.

3. *Equipment:* Consists of specially designed DC-power pack, working station, storage tank, and necessary controls. All the controls and safety requirements are interlocked in a logic system.

4. *Capacity:* It is decided based on the area of deburring and production quantity. Approximately 200 mm diameter gear with the tooth profile and spline slots are deburred within 45-60 s cycle time on a 500 A capacity machine.

5. *Consumables:* A 500 A capacity machine requires approximately 20 kg of electrolyte salt per week, working in two shifts. The cathode electrode wears out at the insulating areas where the component has heavy burrs, hence the life of the electrode is approximately

3000-25000 components per electrode. The cost of such electrode varies from Rs. 1000 to 5000.

6. *Adoption:* It can be adopted to any material through the selection of an appropriate electrolyte. Generally sodium nitrate ($NaNO_3$) is used on steels, cast iron and aluminum for a precise deburring, and sodium chloride ($NaCl$) is used on steels for an aggressive deburring.

Machine tool components
Matl: steel
Cycle time: 40 secs
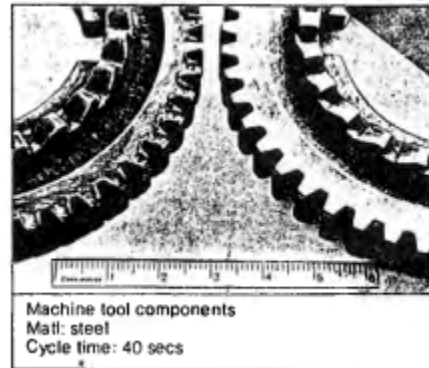
Fig. 5.7 A gear before and after deburring [Courtesy, EleChem Technik, Bangalore].

7. *Pollution:* Electrolyte is a domestic salt and solution is free from health hazard. The hydroxide removed from the drain valve is extensively being used as a raw material for the lapping paste.

8. *Quality:* The component having the burr root thickness less than 0.2 mm and the height less than or equal to 1 mm, can be precisely deburred by maintaining the edge rounding from 0.2-0.5 mm radius, and the cycle time for approximately 20-30s. If the burr size is larger than the above stated one, the edge quality after deburring would be of approximately 0.5-1.5 mm radius and cycle time required will be 66-90s depending upon the burr level. There will be discoloration at the adjacent area but no material. Removal; however, as the cycle time increases more than 30s, there will be slight material removal (approximately'0.05 mm) on a width of 1-2 mm adjacent to the deburred area. It can be controlled through tooling, if desired.

9. *Components Cleaning:* Before deburring, the components should be free from loose burrs which damage the electrodes, and from grease/oil which contaminates the electrolyte. Hence, it is preferred to thoroughly wash the components just before deburring. After

deburring, it should be dipped immediately in running water followed by dewatering fluid, thus protecting against corrosion.

Deburring is advised to be done usually before any surface treatment. There will be no hydrogen embrittlement.

Electrochemical honing(ECH)

6.1 INTERDUCTION

ECH is one of the most potential micro-finishing process in which material is removed by anodic dissolution combined with mechanical abrasion of bonded abrasive grains (capability to machine material of any hardness, production of stress-free surface with good finish and higher MRR) with the capabilities of mechanical honing (ability to correct shape/geometry-related errors, controlled generation of functional surfaces having cross-hatch lay patterns and compressive residual stresses) in a single process. At the same time, it overcomes some limitations of ECM along with certain limitations of mechanical honing (reduced tool life, low productivity due to frequent failure of honing sticks, inability to finish hardened workpiece and possibility of mechanical damage to the workpiece). ECH, therefore, provides a higher productivity alternative with many benefits that may produce surfaces that are not attainable by either of the processes when used individually.

Electrochemical honing (ECH) has capabilities and potential to be developed as an alternative of conventional gear finishing processes and can play an important role as high-precision gear finishing method because being a hybrid machining process it has potential to overcome most the limitations of conventional gear finishing methods and at the same time offers most of the capabilities of the conventional gear finishing methods. Electrochemical Honing (ECH) is one of the most potential hybrid electrochemical-mechanical process, is based on the interaction of Electrochemical Machining (ECM) and mechanical honing. In ECH, most of the material is removed by electrolytic dissolution action of ECM. But during ECM, a thin micro-film of metal oxide is formed on the workpiece. This film is insulating in nature and protects the workpiece surface from further being removed. With the help of bonded abrasives, honing acts as scrubbing agent to remove the thin insulation layer from high spots and thus produces fresh metal for further electrolytic dissolution. The typical range of process parameters for ECH is given below in Table 2.

Power Supply	Electrolyte
Type: DC Voltage: 6-30 V Current: 100-3000 A Current density:15.5-465 A/cm^2	Type: $NaNO_3$, NaCl Concentration: 120 g/L ($NaNO_3$), 240 g/L (NaCl) Temperature: 25-38^{0}C Pressure: 500-1000 kPa Flow rate: Upto 95 L/min IEG: 0.076-0.25 mm

Table 1: Typical value of ECH parameters.

6.2 Equipment and working principle:

Honing is a subtractive type manufacturing process in which material is removed by the cutting action of bonded abrasive grains and is used to improve the form, dimensional precision and surface quality of a workpiece under constant surface contact with the tool. Different honing techniques namely *longitudinal stroke honing* is used for connecting rod holes, brake drum, cylinder liners, etc.; *short stroke honing* is used for crank shaft, rotor shaft; *profile honing* is used for tracks of inner and outer ball bearing rings; *surface honing* for finishing roller guideways, guide rails; *gear honing*, etc. are commonly used in Industries.
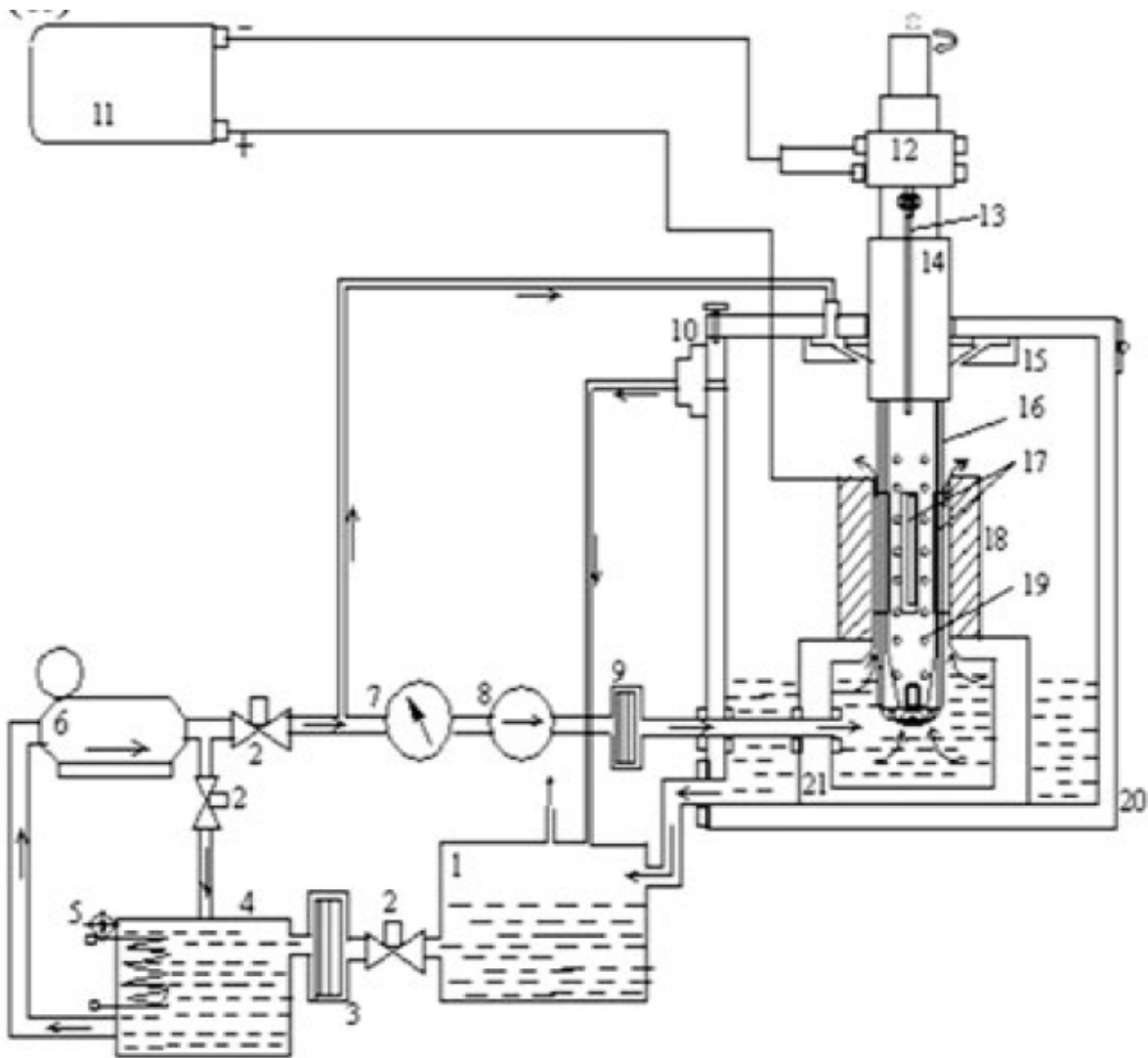
1 Electrolyte settling tank; 2 Flow control valve; 3 1st stage filter cum magnetic separator; 4 Electrolyte storage tank; 5 Temperature control system; 6 Stainless steel electrolyte supply pump; 7 Pressure gauge; 8 Flow meter; 9 2nd stage filter cum magnetic separator; 10 Mist collector; 11 DC power source; 12 Carbon brush and slip ring

assembly; 13 Copper connector; 14 Seal hub; 15 Hydraulic cum mechanical seal; 16 Tool body; 17 Honing sticks; 18 Workpiece; 19 Electrolyte exit holes; 20 Work chamber; 21 Fixture cum electrolyte inlet sleeve

Figure 6.1 presents a schematic of the ECH set-up for finishing of an internal cylinder. It consists of five major subsystems: (i) DC power supply; (ii) tool for ECH process; (iii) the kinematic system for tool motion; (iv) electrolyte supply and cleaning system; and (v) machining chamber for holding and positioning workpiece. A power supply unit provides a DC voltage (3–40 V) and constant current (up to 200 A) across the electrolyte flooded inter-electrode gap. The positive terminal of the power supply is connected to the workpiece by means of a carbon-brush and slip ring assembly, while the negative terminal is directly connected to a brass ring mounted over the axle of the cathodic tool. An ECH tool for finishing of cylindrical workpieces typically consists of a Teflon (PTFE) body over which a hollow stainless steel sleeve is placed having provision for an even number of equally spaced honing sticks to protrude out circumferentially by a light spring mechanism which can be used to adjust the required honing pressure. These honing sticks being electrically non-conducting maintain a uniform inter-electrode gap and preferentially remove the non-conductive passive layer of metal oxide from the high spots to correct errors/deviations in geometry/shape of the cylindrical workpiece. The tool is provided a precisely controlled combination of rotation and reciprocation simultaneously. Rotary motion is provided by a speed-controlled DC servo motor, while the reciprocating motion is provided by a microprocessor-controlled stepper motor.

6.3 Advantages, Limitations and Applications

6.3.1 ECH offers many useful advantages as follows:

(i) Material of any hardness (but electrically conducting) can be finished by ECH;

(ii) It produces surfaces with a distinct cross-hatch lay pattern that is beneficial for oil retention; (iii) ECH not only produces high-quality surface finish and surface integrity but also has the ability to correct errors/deviations in geometry/shape such as out of roundness or circularity, taper, bell-mouth hole, barrel-shaped hole, axial distortion and boring tool marks for cylindrical surfaces and the ability to correct form errors (i.e. deviations in lead and profile) and location errors (i.e. pitch deviations and run-out) for cylindrical and conical gears;

 (iv) It is faster when compared to ECM and mechanical honing. ECH can finish materials up to 5–10 times faster than mechanical honing and four times faster than internal grinding. The benefit is more pronounced for higher material hardness;

(v) Low heat generation thus making it suitable for the processing of parts that are susceptible to heat distortions;

(vi) increased life of abrasive sticks/tool due to the limited contribution of mechanical honing to the process; and

(vii) Low working pressure implies less distortion while finishing thin-walled sections. Despite the numerous advantages,

6.3.2 ECH does exhibit some limitations as follows:

(i) It can be used for finishing electrically conductive materials only;

(ii) It is more costly than the mechanical honing due to the cost of the electrical and fluid handling elements, need for corrosion protection, costly tooling and longer set-up time. This makes ECH more economical for longer production runs than for tool room and job-shop conditions;

(iii) It cannot finish blind holes easily; and

(iv) ECH cannot correct location of hole or perpendicularity.

Materials that can be finished by ECH include cast tool steels, high-alloy steels, carbide, titanium alloys, Incoloy 901, 17-7PH stainless steel, Inconel and gun steels. ECH is an ideal choice for superfinishing, improving the surface integrity and increasing the service life of the critical components such as internal cylinders, transmission gears, carbide bushings and sleeves, rollers, petrochemical reactors. moulds and dies, gun barrels and pressure vessels, which are made of very hard and/or tough wear-resistant materials, most of which are susceptible to thermal distortions. Therefore, ECH is widely used in the automobile industry, aerospace, petrochemical industry, power generation and fluid power industries. It has been successfully used for finishing bore sizes ranging from 9.5 to 300 mm and length up to 600 mm, ECH can achieve surface roughness up to 50 nm and tolerances of ±0.002 mm.

MODULE-III

Electro Discharge Machining: Mechanism of Material removal, Basic EDM circuitry and principle of operation, Analysis of relaxation circuits, Concept of critical resistance, Machining accuracy and surface finish, Tool Material, Dielectric Fluid, Application and limitations.

Introduction to Wire Cut Electrodischarge Machine (WEDM)

Laser Beam Machining: Lasing process and principle, Population Inversion, Principle of Ruby laser, Nd:YAG Laser and CO_2 Laser, Power Control and laser output.

Electro Discharge Machining

1.1 PROCESS

Electrical Discharge Machining (spark erosion machining! is mainly a technique used for the manufacture of a multitude of ever changing geometries very often produced as unit jobs or in small batches. Controlled machining by electrical sparks was first introduced by Lazarenko in Russia in 1944. The first British patent was granted to Rudorff in 1950. USA, Japan and Switzerland developed their machines around 1950. A machine for spark machining by 'method x' vas patented in USA in 1952.

The basic concepts of EDMing process is cratering out of metals (Fig. 1.1) affected by the sudden stoppage of the electron beam by the solid metal surface of the anode. The portion of the anode facing the direct electrical pulse reaches the boiling point. Even in the case of medium long pulse the rate of temperature increase in tens of millions of degree per second which means dealing with an explosion process (Fig 1.2). The shock wave produced spreads from the centre of the explosion inside the metal and on its way crushes the metal and deforms crystals. In the very small duration of the process the entire energy can only be expended in the surface layers of the anode. Actually, the mechanism of thermal conductivity has no time to start before the violent process of energy transfer is completed. When a suitable unipolar (pulsed) voltage is applied across two electrodes separated by a dielectric fluid, the latter breaks town. The
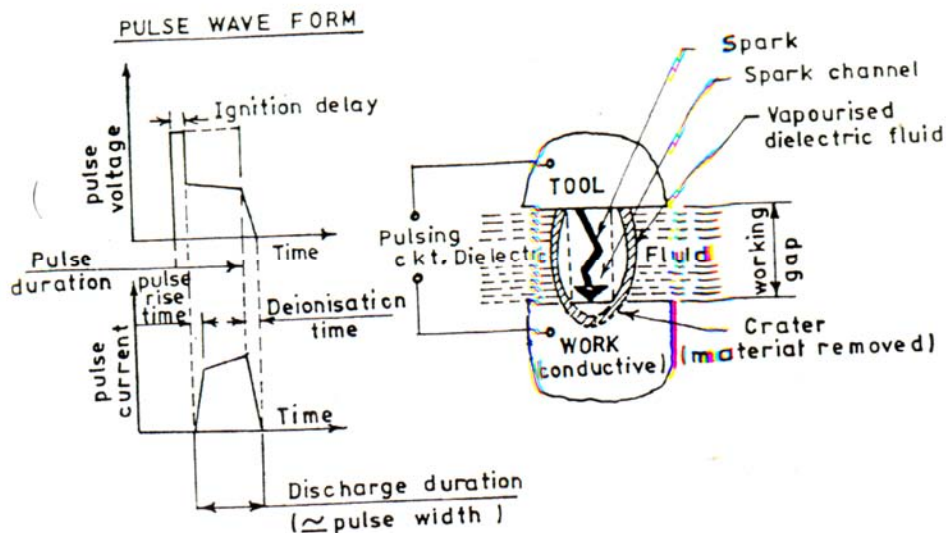
Fig. 1.1 Scheme of EDM Process (Single Discharge Condition)

Fig. 1.2 Incandescent Particles are being ejected from the Spark Gap

electrons, so liberated, are accelerated in presence of the electric field collide with the dielectric molecules, causing the latter to be robbed off their one or two electrons each and immunize. The process grows and multiplies with secondary emission followed by an avalanche of electrons and ions. The resistance of the dielectric layer drops as it is ionized resulting into ultimate breakdown. The electric energy is discharged into the gap and multifarious actions take place- electrodynamic waves set in and travel at high speed causing shock-impact and high temperature rise at the electrode surfaces. The instantaneous temperature may reach as high as 10,000°C causing localized vaporization of the electrodes. The whole process can be represented as shown in Jig. 8.3. To machine some of the hardest materials, electrical discharge machining process has following important advantages which make it widely used in practice:
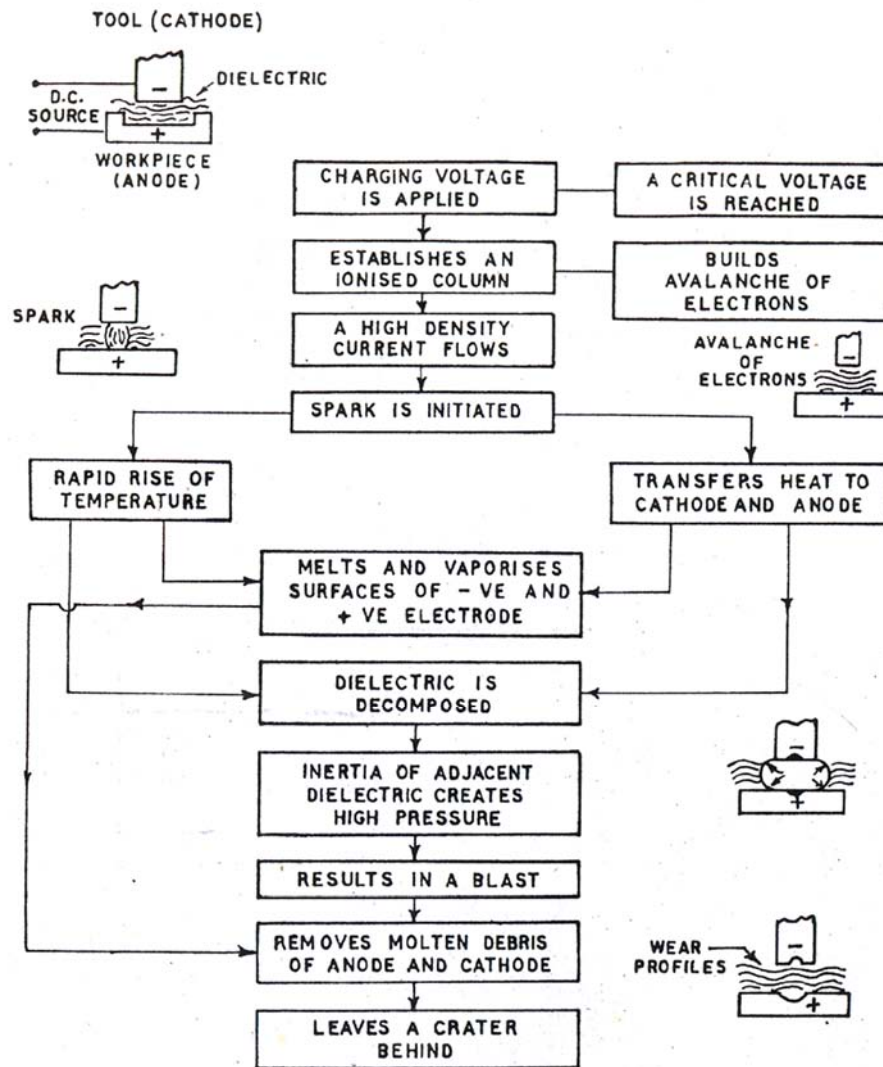
Fig. 1.3 Stages of EDM Action

1. The process can be applied, in general, to any electrically conductive material. Other properties like strength, brittleness, etc. do not impose any restrictions to the application of the process.

2. The process provides a simple and straightforward method of form producing drop-forging, drawing and extruding dies and complex cavities in moulds and dies for plastics, die casting, glass and ceramic manufacturing.

3. Though the process involves temperature, rise at the local spots to about 10,000° C which can vaporise the localised material to machine, there is no heating of the bulk materials. However, the 'heat-affected- zone'(HAZ) surrounding the local points extends in the bulk to a depth of about few microns.

4. The high rates of heating and cooling at the treated surface renders some extrahardness (Case-hardening) to the surface and this becomes a point of advantage in favour of the process.

5. Simple geometrical shape configurations can easily be produced by piercing or die-sinking in hardened die-plates with required accuracy and surface finish. Thus elimination of much complicated grinding and lapping is possible.

6. No mechanical stress is developed in the work material as there in no physical contract between the tool and work-piece. This permits machining fragile and slender work-pieces.

7. The process reduces time of machining in comparison with conventional grinding, honing or contour grinding, etc.

8. The crater-type non-directional (layless) surface pattern is said to retain lubricants, rendering the process particularly suitable for the finishing operations.

9. The surface finish produced by EDM process can be controlled to the required extent, minimising the extra cost involved in additional operation for achieving improved surface-finish.

10. Wire-cut EDMing process has revolutionized the production of hard surfacing on soft tough and cheaper backing material for blanking/ piercing die and punches. The hard surfacing materials are cut out of thin sheets of hard and wear resisting materials end enables to maintain proper clearance while cutting.

All these **advantages** enumerated above emphasise the importance of EDM in modem manufacturing technology. Yet, the process is not free from drawbacks and successful utilization of the process requires careful preparation of workpiece, proper planning of electrode and choice of dielectric even when the machining is to be done in the best available machine.

1.2 OPERATING PRINCIPLES

The EDMing process involves finite discrete periodic sparks between tool-electrode and conductive work-electrode separated by a thin film of liquid dielectric that causes the removal of work material. For consideration of mechanism of material removal, there exists three different theories briefly discussed as follows:

1.2.1 Theories of Material Removal Concepts

(a) High Pressure Theory

In this, due to sudden stoppage of electrodynamic waves, high impulsive pressure responsible for the erosion of electrodes is released on the electrode surface.

Pressure of electrical discharge reported might be as high as 1,000 kgf/ mm^2 was predicted, but expected plastic deformation was not found on the surface. From the energy distribution of discharge spectrum, the pressure in the arc column remain between 10 and 100 kgf/cm^2. Actually the pressure is less than that reported because the acting area of discharge pressure is thought to be wider than the crater area. It is obtained that duration during which pressure acts is longer than discharge periods. Later as the maximum force was measured to be about 60 kgf and that the impose was proportional to the discharge power. To conclude, in smaller energy discharges, the discharge pressure alone would not be sufficient to erode the material, but in conjunction with some other factor, such as heat, the pressure might blow out molten metal from the electrode surface.

(b)   Static Field Theory

Two charged electrodes experience an electrostatic force according to Coulomb's law. Accordingly, the force between the electrodes produce stress on the electrodes which, when the gap is very small, may cross the ultimate stress limit of the electrode material resulting in a tensile rupture.

For discharge durations less than 2 μsec during initial intervals, the tensile rupture hypothesis of Williams correlates well with the experimental erosion results. The forces involved in tensile rupture erosion arise because the extremely high current densities beneath the surface of the anode produce a strong electric field gradient, which acts on the positive ions of the crystal lattice. When this force reaches the tensile strength of the material, a tensile fracture occurs removing one or several particles. For discharge durations greater than a few micro seconds, it is found that the tensile rupture theory does not explain the observed electrode erosion. However, this field theory is found to be incorrect because forces into metal lattice due to colliding electrons belong to the force created by the static field.

The observational data of Williams lead one to set aside thermal action as the primary factor in anode erosion in metals with melting points above 600°C at low currents. The possibility of explosive force or a cathode 'flare' action remains to be explored. The crater form at the anode is primarily dependent on the current distribution under the anode surface. This current distribution, for a given discharge area, can vary only as a result of skin effect which is a negligible factor in non-ferromagnetic materials but not in ferromagnetic ones, where the magnitude of current below the anode surface is substantially decreased. Quantitative data show that an ionic force can be sufficient to cause rupture. It is possible that explosive forces play some part and these data supply some confirmation for an electric field force hypothesis, especially for low discharge durations.

(c)   High Temperature Theory

According to this theory, due to the bombardment of high energetic (kinetic) electrons on the electrode surface, the spot attains high temperature (about 10,000°C) especially with materials of

low thermal conductivity. At this high temperature, material at that spot instantaneously melts and vaporises leaving a crater on the surface. The ratio between the energy expended at the anode and the total discharged energy are related to various parameters like gap between the electrodes mean-free-path-of electrons, cathode and anode work-functions etc. This high temperature is not generated by electron bombardments alone. The joule-heating by high density current is also considered to contribute.

Gradually high temperature theory became promising. Many experiments were carried out for exploring this theory. Dependence of discharge voltage on gap length was found out. Single discharge experiments were carried out and short-time contest between electrode was found to occur quite often. It is also observed that contract occurs about 1-5 ms after the end of the discharge by the formation of crater rime and high temperature and high pressure prevail till that time.

In the mechanism of electrical erosion by considering electron bombardment [10], the anode spot is melted, vaporised and blown off

producing a crater. It was established that the energy given to anode per unit area (W_a) and whole discharge energy (W_0) bear the following relation

$$\frac{W_a}{W_0} = l - \left[\frac{3}{8} \left(\frac{d}{\lambda} - b \right) \frac{m}{m_g} - \frac{F_c - F_a}{V_c} \right] \qquad (1.1)$$

where d is the gap between electrodes, λ the mean free path of electron, $b = l / \lambda$, l the cathode fall area, m the mass of electron. m_g the mass of gas molecule, F_a, F_c are anode and cathode work-functions, respectively and V_c the cathode fall.

This equation coincides with experimental results qualitatively and by increasing the ratio W_a/W_0, the erosion rate is increased while electrode wear decreased. It is also reported 50-50 share remain between electron bombardment and Joule heating in causing high temperatures. Many calculated the melting depth, vaporising depth and heat efficiency when a-constant energy was given on the surface.

Williams observed cathode-crater volume dependence on the melting point of cathode material. Melting-point and discharge duration effects suggested on involvement of thermal energy irrespective of fero and non-ferromagnetic cathode materials in contrast to his earlier field theory and tensile rupture theory on anode erosion.

Above theories give no exact individually and realistic view of the spark machining phenomena; however, these can be combined for the description of the process, the high temperature theory being the predominating one.

However, the thermal theory is quite acceptable which can take care to explain the major portion of the stock removal phenomenon and the figure below show the evidence of vaporisation during sparking (thermal).

But any thermal model developed so far could only from the gap during explain about 25-80% of the material removal. However, the first two postulation cannot fully disregarded but might contribute towards the unaccountable material removal through thermal model. So works one still on progress to determine an agreeable combined model with the practice.

The present state-of-art deals with a thermal metal removal mechanism (Fig. 1.2) explicitly given in the flow diagram (Fig. 8.3) and the power distribution scheme (Fig. 1.4) which contribute to the material removal mechanism are given below.
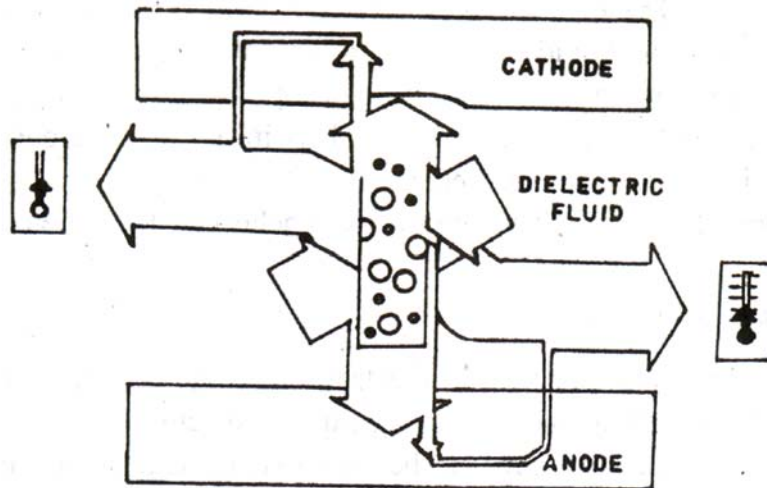
Fig 1.4 Electrical Power Distribution in the Spark Gap

1.3 DIELECTRIC FLUID

Since the process of removal of materials (both from work and tool) mainly depends on thermal evaporation and melting, the presence of oxygen in the atmosphere surrounding the spark would lead to formation of metal oxides which adversely affect the continuation or generation of repetitive sparks (most of metal oxides are bad conductor). Hence, it is pertinent to use a dielectric fluid which contain no oxygen for liberation during the process, to help ionization, without disturbing the process. But the performance (mainly the failure) of the dielectric to suit the purpose is extremely important.

The failure of dielectrics under electric, stress, termed as breakdown, is found to spread over a wide range of applied stresses, depending upon its environment and mode of use.

In general, the main basic mechanism of dielectric breakdown in the three states of matter are: (i) intrinsic, (ii) thermal and (iii) discharge or avalanche.

1.4 Breakdown Mechanism

The earlier theories of breakdown in liquids have assumed that it occurs by avalanche ionization of the atoms induced by conduction electrons accelerated in the applied field. The cathode electrode is assumed to be source of these electrons which are emitted either by field-effect or by Schottky-effect. The electron liberated from the cathode gains from the applied field more energy than it loses in vibrational collisions with the molecules of the liquid dielectric. These electrons are accelerated until they gain sufficient energy to ionize the liquid molecules and initiate an electron avalanche. Considering this mechanism, Lawis analytically showed that the vibrational collisions account for the major energy loss in the hydrocarbons where bond vibration is the main absorbent.

The applied field E, at which an avalanche can be initiated and is given as

$$eE\lambda = ch\gamma \tag{1.2}$$

where λ is the mean free path of electron of charge e, c the velocity of light and $h\gamma$ ionization quantum for the liquid molecule.

The theory satisfactorily predicts the order to magnitude of the breakdown strength of hydrocarbons. But this does not account for the ignition-delay observed between the application of a pulse of voltage greater than the breakdown voltage and the actual onset of breakdown. Horaten et al showed experimentally that ignition delay depends on the energy per unit volume added to the gap. Breakdown in gas is introduced by collisional ionization of the molecules. But collisional ionization of liquid molecules by electrons is not possible due to insufficient kinetic energy of the electrons. During the ignition delay a pre-breakdown electron current flows from the cathode to anode. This low current heats the liquid to form a vapour bubble of sufficient pressure in between the electrodes. Then a spark takes place in the vapor bubble, according to the high pressure gas-discharge mechanism. With changing gap width, amount of pre-breakdown energy changes, thus influencing the ignition delay.

1.5 ELECTRODE MATERIAL

As already discussed, the tool electrode in EDM process is the means of providing electrical energy to the work-material, as well as the necessary form to the latter. The work-surface sometimes being the inverse profile of the tool, its accuracy depends on the form stability of the tool under the severe, electrical and flushing stress conditions. Moreover, the share of heat that the tool receives (Fig. 1.4) from the plasma channel, is to be dissipated away faster unlike work-material in order to reduce surface temperature to minimise evaporation and melting of the tool material responsible for its wear rate. So it is necessary to be made of highly thermal conductive materials over and above its first character of higher electrical conductivity. Then it is evident that the-tool material should have high melting point to reduce its wear-rate, as shown in Fig. 1.5.
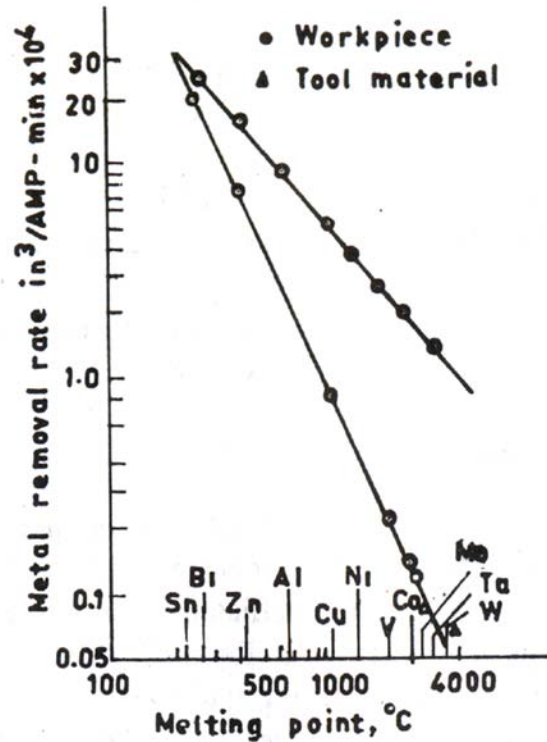
Fig. 1.5 Effect of Melting Point on Erosion Rate

However, from the material science point of view, higher thermal conductivity and higher melting point are sometime two contradicting characters for pure elements. So a proper choice is necessary to be made, since the electrode cost can represent more than 50% of the total machining cost.

Therefore, the basic desirable characters of the tool-material are:

High electrical conductivity

High thermal conductivity

High melting temperature

Cheapness

Easier manufacturability

Theoretically, any material that is a good electrical conductor can be used as a tool with more or less advantages. In general, tool or electrode materials can be classified into four groups:

(i) Metallic electrodes   : Electrolyte copper

Tellurium or chromium copper

Copper tungsten

Brass

Aluminium

Aluminium alloy (Silumin)

Tungsten (mostly coated or wire)

Silver tungsten

Steel

(ii)   Non-metallic   : Graphites

(iii)   Combined metallic and   : Copper-graphite

         non-metallic

(iv)   Metallic coating as insulators   : Copper on moulded plastic and

                                                Cooper on ceramic.

1.5.1 Metallic Electrodes

Copper Electrodes: It is one of the oldest and commonly preferred as tool material. Its melting point at 1083°C density = 8.9 g/cm^3 and electrical resistivity of 0.0167 ohm mm^2/m, coefficient of expansion of 4.318 x 10^{-4} mm mm/K and its abundant availability is the reason behind its use.

Copper being difficult to cast for tool material and since at its molten state it tends to absorb oxygen from oxides, the tool is preferred to be made out of rolled or forged forms, generally marketed in four forms: tough, pitch, oxygen free, phosporized or arsenised. Most copper marketed for commercial use contains traces of silicon or other hardeners (impurities as well) and small percentage of arsenic (0.4%). These affect to reduce the conductivity of copper seriously.

Oxygen-free copper is about 99.9% pure and exhibits extremely high conductivity. Phosporized copper contains residual phosphorus and exhibits lower conductivity than electrolytic tough pitch copper.

Cold forgings/rolling products are preferred. Hot forging, however, is to be cold forged to restrike copper electrodes at room temperature to resume final size, shape and accuracy. It is to be noted that the tool electrodes must be annealed to make them more malleable before each forming operation. So precautions are to be taken to prevent oxide formation on the surface of copper. A suggested method is to heat the electrode to 500- 600°C and then quickly quenched in rubbing alcohol. This will also keep the surface absolute clean.

Copper is machinable but wheel loading in grinding seriously affect surface finish and accuracy. Copper is most often used when higher surface finish in work-material is required. The tool can be polished to about 0.25 micron Ra to provide best surface integrity in the work-material.

However, high porosity of copper electrode and hydrogen entitlement of copper during operation are to be avoided.

Electrolytic copper can be machined as readily as coppers containing selenium, lead or tellurium. The recommended materials for better machining are:

Tellurium Copper	- 99.5% copper and 0.6% tellurium
Leaded Copper	- 99% copper and 0.1% lead .
Selenium Copper	- 99.4% copper and 0.6% selenium.

These three coppers are utilized for most EDMing applications. The amount of temper applied to each determines the best performance of a given EDMing operation. Copper with half-hard temper exhibits the best overall performance. Under high current, soft copper will temper and begins to warp. So it is required to put chillers at the hot spots when softer electrodes are used.

Copper-tungsten electrodes (Cu : W varies between 50 : 50 and 20 : 50), however, do not exhibit warpage problems. This is used when small holes are to be drilled using a tubular tool. Although, expensive Cu-W can be used for those applications where the use of alternate electrode material would be impractical. Because of its low flexural strength and high rigidity, it is a preferred material for slots. Small pieces of Cu-W can be silver soldered an steel shanks to form intricate tool shapes.

Copper-tungsten has high density (15-18 gm/cm^3) along with high strength (BHN : 85 - 240 kg/mm^2 Rb 94), good thermal and electrical conductivity (resistivity : 0.045 ~ 0.55 ohm mm^2/m) high density enables it impart high surface finish. It is commonly recommended for EDMing of dies with fine contoured details.

Brass Electrodes: Free machined brass is often used as an electrode material. Because of its high wear-rate it is not preferred for generation of 3-D surfaces. It has been seen to be one of the best tool materials for machining titanuim-alloys at low material-removal-rate conditions.

The high wear rate is attributed by the presence of low melting alloy of element Zn. However, the plasma channel stability (machining stability) is achieved nicely with brass tool since its high-rate or erosion allow zinc- vapours in the plasma channel might reduce arc resistance and helps quicker ionization also.

Silver Tunpten: This has very similar characteristics to those of the Cu- W. It contains very high percentage of tungsten and hence extremely costly which restricts applications. However, the

lower comer wear helps to produce very sharp comers (small comer radius) if required and is better than Cu-W.

Tungsten: Because of its high melting point exhibit extremely low erosion rate but its high cost only restricts it for use in producing fine holes or wire cutting operations where high order accuracy is required. Wire electrodes of Tungsten of less than 0.01 mm are available for use owing to its high strength character. To enable its use Tungsten coated electrodes are being developed for use.

Aluminium: In spite of high thermal and electrical conductivity and low density it has not found a suitable place in EDMing tool because of its low melting temperature and higher tarnishing property.

When machining large 3D cavities which do not require higher surface finish, one can use aluminium alloy known as SILUMIN as tool material.

It has a composition of about

A1: 85%; Si: 11%; Mg: 0.4% to 0.6 %; Zn: 1% ;

Ti: 1%; Mo, Fe and Cu: 1%.

This is easily castable. Shrinkage of about 1% can be off-set by cold-forming preceded by annealing at 540°C followed by water cooling. It is also easily machinable.

Steel: Steel sometimes is used as electrodes even if it has lower efficiency as compared to copper or graphite.

In case of irregular parting lines for plastic moulds and die casting dies are matched to prevent flash by using upper part of the mould or die as an electrode.

1.5.2 Non-metallic Electrode

Since the introduction of pulse generator, graphite has become the most important electrode material.

It has electrical resistivity in between 5 and 10 ohm mm2/m and low density between 1.6 and 1.85 g/cm3. Its high vaporisation temperature of about 3600°C makes it possible for its use to achieve high stock removal. Moreover, it has low thermal coefficient of expansion 2 to 4 x 10'4°C, i.e. 1/6 that of Cu.

One has to be careful, since graphite electrode materials are available in various types and grades. These can be broadly classified into three major categories having grain sizes ranging between 10 and 45 micron.

Low or coarse density: 1.6 to 1.7 gm/cm^3 — used for forging dies

Medium density:	1.7 to 1.8 gm/cm^3 — production applicant
High or fine density:	1.8 to 1.85 gm/cm^3 — for moulds and dies

Since these are manufactured by isostatic compression, the density is dependent on the pressure. The coarse density graphites are anisotropic whereas high density graphites are isotropic, which seriously affects the electrode-wear-rate. Coarse graphite is normally used for large-volume EDMing operation requiring few or no fine details of the contour. Fine graphites are to be used when fine details are required on the work surface.

These tools are generally used for machining steel, to give high stock removal with high surface integrity (will be discussed later). While machining tungsten-carbide, a satisfactory result is obtained with good flushing conditions to prevent micro-cracks. This is because excessive carborization and uncontrollable arcing during EDMing operations. The excess deposition of carbon on work-surface leads to hot spots which does not allow deionization process of the dielectric in use. So it is recommended to use higher-density graphite electrodes below 20 amp. for machining of tungsten-carbides.

But graphites must be kept free from moisture and not allowed to become saturated with dielectric or any other petrochemical contaminants. These precautions insures longer life and reliable optimization of EDM parameters.

One should not use carbon in place, since it is amorphous to produce excessive arcing and tool wear, carbon exists in three allotropic forms: amorphous, graphite and diamond. Since carbon has ability to chemically self-bond can be easily converted to crystalline form graphite under high isostatic pressure. It is an excellent conductor with higher melting point as compared to metals and has no reaction to highly corrosive chemicals.

It is inexpensive and easily machinable as well. Graphite is made from petroleum coke, a prime raw material. The coke is subjected to very high temperatures to remove impurities. It is then crushed and mixed with coal-tar pitch and various other additives. This mixture is then compressed and shaped by moulding or extruding into bars, rods or plates. The carbon is then converted into graphite by heat treatment at 2760°C. The result is a solid porous mass of graphite capable of being impregnated with other materials, such as copper, tin, etc. Moreover, graphite is easily machinable by turning, milling and even grinding. Surface finish in the order of about 0.51 micron Ra is achievable for medium to fine density graphite electrodes to impart higher surface finish in the work material. When machining work pieces in large numbers using graphite electrodes it is economical to use moulded graphites electrodes of specialized forms, reducing its machining costs.

Advantages of graphites are:

1. It is not affected by thermal shocks and can return mechanical properties (rigid, tough)

2. It does not distort because of high melting point and chemically does not react.

3. Easily machinable by conventional methods.

4. Lower density provides higher size of the electrode.

5. Low cost operation.

The disadvantages are:

1. It being a brittle material special cares must be taken at sharp comers during manufacture.

2. It is an abrasive material. So precaution must be taken to protect slides of machine-tools from graphite dust.

3. Machining in graphite produce dust of carbon to pollute the atmosphere.

4. It being acid resistance or chemically inert, cannot be etched to produce finer surfaces on the tool.

5. High porosity allows the dielectric to saturate the tool which produces internal stress when fluids inside evaporates.

6. High porosity also allows moisture entrapped inside the tool which affects the machining performance if care is not taken.

1.5.3 Combined Metallic and Non-metallic Electrode

The graphite tools are highly efficient for EDMing operation with fewer drawbacks. These can be easily eliminated by taking the advantage of its capability of being impregnated by copper, tin, etc. to make it less porous and brittle. If impregnated with copper to form copper-graphite under vacuum to form a less brittle material, it possesses an electrical resistivity of 3 to 5 ohm mm2/m, density between 2.4 and 3.2 g/cm^3 and ultimate strength of 700 to 900 kg/m^2 as compared to copper having ultimate strength of 200 to 700 kg/cm^2. It has some added advantages over graphite as already discussed, however bit costlier. Coated copper graphite tools are tried to make it more inexpensive as compared to the above. The quality of surface contour or graphite easily achievable and the added advantage of copper tools for higher surface finish operations can be achieved in a combined form by thin type tools.

1.5.4 Electroformed Electrodes

In the electroforming of copper spark erosion electrodes, the electrode having once been electrodes (cathodes) in the electroforming bath, become electrodes again in another electrical but not electrolytic process.

These electrodes are much like moulds or dies in helping to shape metal. Also, the majority of the spark machining work which uses intricate electrodes (rather than simple rods for piercing holes) is aimed at the manufacture of moulds and dies in wider scene. Unlike die electroforming (a

building-up process) die EDMing is a scooping-out procedure but is also based on a positive. Electrode making like master-making when die electroforming is, therefore, technically and economically a key problem of spark eroding. This is accentuated by the fact that, through electrode wear, several identical electrodes are needed for each cavity, though there is some re-use of worn masters for the roughing stages of identical repeat cavities. We may consider (copper) electroforming as a solution to the electrode problem—though immediately bring in a master problem. Of course, some intricate cavities are eroded in stages by the use of several succeeding electrodes of simpler shape, thus making electrode manufacture easier.

More recent developments

Meanwhile spark erosion technology has progressed. Copper was first superseded by harder tungsten copper as a most favoured electrode material. An electroformed P.R. copper even hardened than the usual Rockwell B/ C boundary area (180-220 Vickers), achieved by adding traces of molybdenum to the electrolyte, did not overcome its teething troubles. Spark erosion machines change from using relaxation circuits to faster and more efficient (ratio of work erosion : electrode wear) impulse circuits. Though some descriptions of this change do not exclude the continued use of sprayed and electroformed electrodes, it is generally accepted that only the special purpose high thermal/electrical conductivity graphite fired at 2,000°C and then machined into the required electrode shape will do justice to the fast machines, though there now appears to be a possibility of moulding these graphite (new field for electroformed moulds?). For special cases the use of electroforming, or of heavy deposition are still reported. When spark eroding round holes of exceptional accuracy into semiconductors, wear on the costly stainless steel electrodes was prevented by grinding these just under size and building them up by acid copper plating, using the principles of wave-guide making skills and facilities. This copper layer wears quickly in use but, before it is entirely burnt away, erosion is interrupted, the remaining copper is stripped off. The report points out that the throwing power limitations of acid copper are not as restrictive as usual. Electroformed nickel electrodes for electrochemical machining are a possibility, e.g. for forging dies for turbine blades.

1.5.5 Observations

An important parameter influencing the wear of the tool electrode is the polarity of workpiece and tool. Observations of this on different work-tool pairs indicate that the behaviour of metals vary differently on this point. However, this depends on kind of electrode metal, pulse current, pulse duration and also on the average voltage. A report published by Cincinnati Milling Machine reveals the effect of polarity on machining performance. Of course, the data sampling were through an Electrojet Drilling Machine from the same company which used Relaxation type power supply. However, the facts remain but the^ quantitative data may differ with modem EDM machines which needs verification. The result is shown in Fig. 8.6 which makes that for case of machining Fe with Cu (tool) in direct polarity (Cu-negative and Fe-positive) the machining stability is with wear-ratio of 0.5 at 12 Amp current setting whereas in reverse-polarity (Fe-negative and Cu-positive) the

machining stability is 'Good' but with higher wear ratio of 1.3 for the same current setting. It is also observed for other materials as well. Before an explanation is sought let us see how other researchers feel about it.

1.5.6   Explanation

It has been explained that since the anode temperature is higher than the cathode, unipolar pulses are struck between tool and work. The loss of energy from cathode in the form of electron emission (cold cathode emission) are accelerated in the applied electric field to strike the work surface to impart the kinetic energy to generate high temperature. The entire process is dependent on the emission of electrons, striking of electrons to cause any change.

It has de-referred and according to T-F theory the electron emission will depend on the work-function of the emitter (and its temperature) and
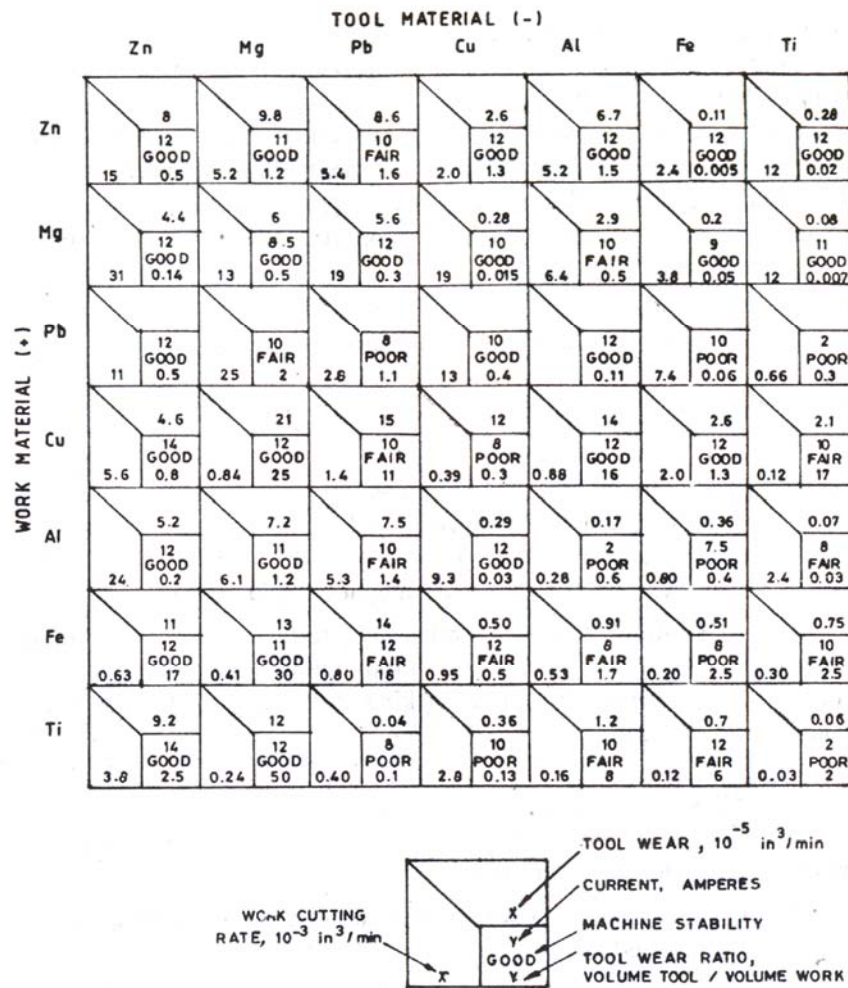
TOOL MATERIAL (–)

Each cell is read as: tool wear (10^{-5} in³/min) / current (amperes) / machine stability / tool wear ratio (volume tool / volume work); the value to the left of each cell is the WCnK cutting rate (10^{-3} in³/min).

WORK MATERIAL (+)	Zn	Mg	Pb	Cu	Al	Fe	Ti
Zn	8 / 12 GOOD / 0.5 (15)	9.8 / 11 GOOD / 1.2 (5.2)	8.6 / 10 FAIR / 1.6 (5.4)	2.6 / 12 GOOD / 1.3 (2.0)	6.7 / 12 GOOD / 1.5 (5.2)	0.11 / 12 GOOD / 0.005 (2.4)	0.28 / 12 GOOD / 0.02 (12)
Mg	4.4 / 12 GOOD / 0.14 (31)	6 / 8.5 GOOD / 0.5 (13)	5.6 / 12 GOOD / 0.3 (19)	0.28 / 10 GOOD / 0.015 (19)	2.9 / 10 FAIR / 0.5 (6.4)	0.2 / 9 GOOD / 0.05 (3.8)	0.08 / 11 GOOD / 0.007 (12)
Pb	12 GOOD / 0.5 (11)	10 FAIR / 2 (25)	8 POOR / 1.1 (2.8)	10 GOOD / 0.4 (13)	12 GOOD / 0.11 (7.4)	10 POOR / 0.06 (0.66)	2 POOR / 0.3
Cu	4.6 / 14 GOOD / 0.8 (5.6)	21 / 12 GOOD / 25 (0.84)	15 / 10 FAIR / 11 (1.4)	12 / 8 POOR / 0.3 (0.39)	14 / 12 GOOD / 16 (0.88)	2.6 / 12 GOOD / 1.3 (2.0)	2.1 / 10 FAIR / 17 (0.12)
Al	5.2 / 12 GOOD / 0.2 (24)	7.2 / 11 GOOD / 1.2 (6.1)	7.5 / 10 FAIR / 1.4 (5.3)	0.29 / 12 GOOD / 0.03 (9.3)	0.17 / 2 POOR / 0.6 (0.28)	0.36 / 7.5 POOR / 0.4 (0.80)	0.07 / 8 FAIR / 0.03 (2.4)
Fe	11 / 12 GOOD / 17 (0.63)	13 / 11 GOOD / 30 (0.41)	14 / 12 FAIR / 18 (0.80)	0.50 / 12 FAIR / 0.5 (0.95)	0.91 / 8 FAIR / 1.7 (0.53)	0.51 / 8 POOR / 2.5 (0.20)	0.75 / 10 FAIR / 2.5 (0.30)
Ti	9.2 / 14 GOOD / 2.5 (3.8)	12 / 12 GOOD / 50 (0.24)	0.04 / 8 POOR / 0.1 (0.40)	0.36 / 10 POOR / 0.13 (2.8)	1.2 / 10 FAIR / 8 (0.16)	0.7 / 12 FAIR / 6 (0.12)	0.06 / 2 POOR / 2 (0.03)

Legend:
TOOL WEAR, 10^{-5} in³/min
CURRENT, AMPERES
MACHINE STABILITY
TOOL WEAR RATIO, VOLUME TOOL / VOLUME WORK
WCnK CUTTING RATE, 10^{-3} in³/min

Fig. 1.6 Electro-discharge Machining Characteristics of Various Electrode Material Combinations

the field strength. In case of similar electrode and work material, the electron emission in general, is from cathode. But in case of dissimilarity, the electron emission, since depends on work-function of the materials for electron emission from it, will be from the electro-negative materials. In case of machining Fe with Cu, the electron emission will start from Fe since it is electro-negative to Cu. So under direct polarity tool wear should be higher. To avert the phenomenon the polarity is to be reversed to have the electron emission from Cu (tool). However, this may change under very high voltage conditions.

After the electrons are liberated, the process of ionisation start to break-down the dielectric medium to produce the spark. The spark causes the evaporation of the work material. The evaporated material will produce metal ions. The material removed is proportional to the energy supplied which can be written in the form

$$MR \; \alpha \; \frac{1}{2} \; \text{Total energy of the string electrons}$$

$$MR \; \alpha \; \frac{1}{2} n_e m_e v_e^2$$

where MR = material removed per pulse

n_e = number of electron striking the work during sparking period

m_e = mass of the electron

v_e = velocity of electron dependent on field strength.

This evaporation of work material will produce equivalent amount of positive ions which will in turn might move to the tool and will strike the tool with some energy equal to its kinetic energy which in turn cause some tool wear. Hence,

$$TR \; \alpha \; \frac{1}{2} n_+ m_+ v_+^2$$

where TR = tool wear per pulse

n_+ = number of positive ion striking the work during sparking period.

v_+ = velocity with which the positive metallic ion strike the tool.

However, $m_+ \gg mg; \; v_+ \ll v_e$ for the same applied voltage.

So a conditional equation may be written in the form

$$MR \; \geq \; \text{or} \; \leq TW$$

or, $\dfrac{1}{2}n_e m_e v_e^2 \leq$ or $\geq \dfrac{1}{2}n_+ m_+ v_+^2$

n_+ will depend on n_e and n_+ is small for lower pulse width conditions, i.e. *MR* > *TW*. Increase in the pulse width, since n_+ goes on increasing, so that both sides are equal showing wear ratio equal to unity. On further increase in pulse width right hand side of the equation may exceed the left hand side showing the wear ratio more than unity (Fig. 1.7). Under this condition if one would try to change the polarity, the wear-ratio will again try to reverse i.e. less than unity and the machining ought to be due to positive ions bombardment rather than electron bombardment.
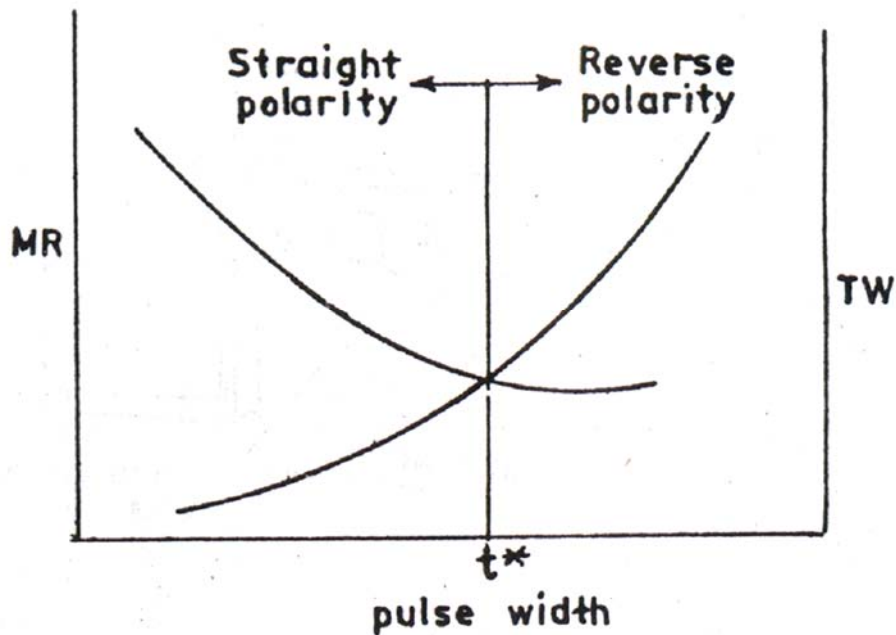
Fig. 1.7 A scheme of MRR and TWR as a Function of Pulse Width

1.6 EQUIPMENT

The basic units constituting an EDM equipment are (Fig. 1.8):

- Machine tool structure with work positioning unit.

- Servo head and for tool feed.

- Power supply.

- Dielectric fluid system.

The machine tool Structure will depend on the work-tool configuration to perform the required activities. The table below shows the three main categories into which spark-machining operations can be divided:

- Die sinking by EDM.

- Cutting by EDM.

- Grinding by EDM.

All the operations are explicitly shown in Fig. 1.9. Each operation is unique of its nature. So the system must accommodate suitable fixture for work as well as tool and at the same time provide the required motions to the tool as well as to the work.
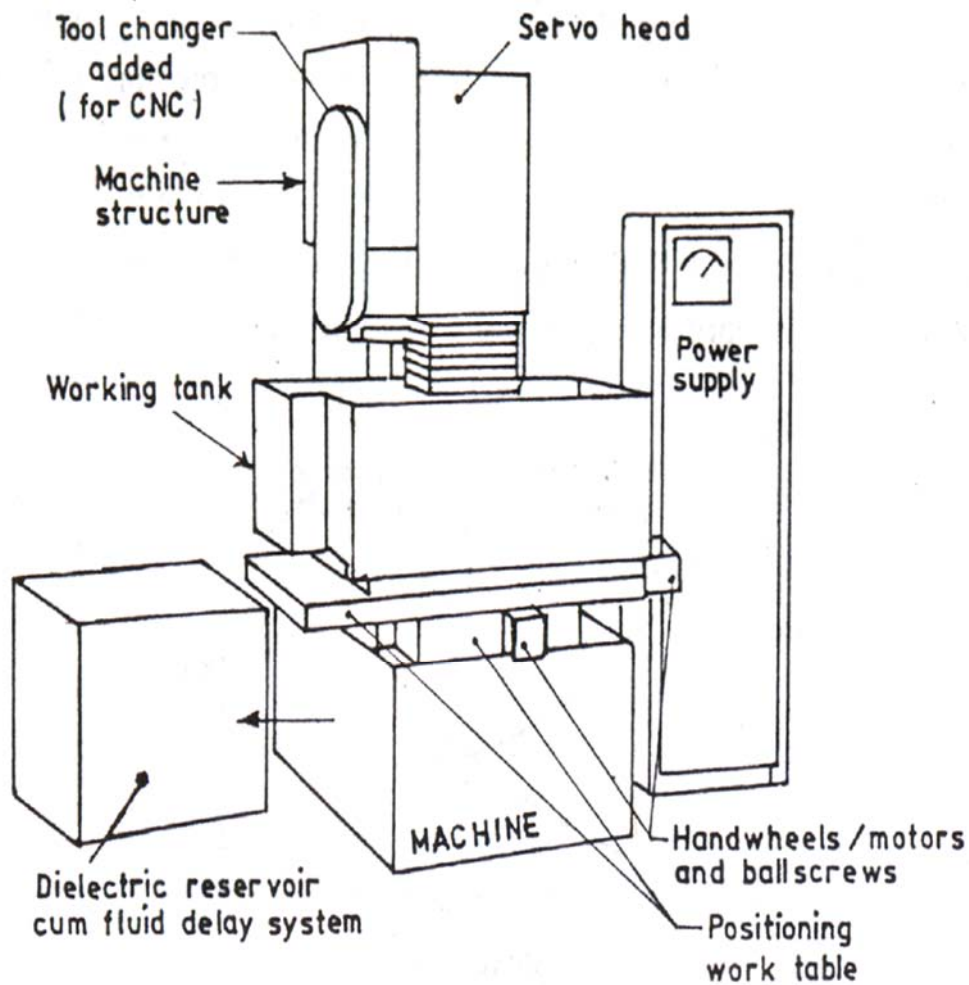
Fig.1.8 Scheme of an EDM Equipment
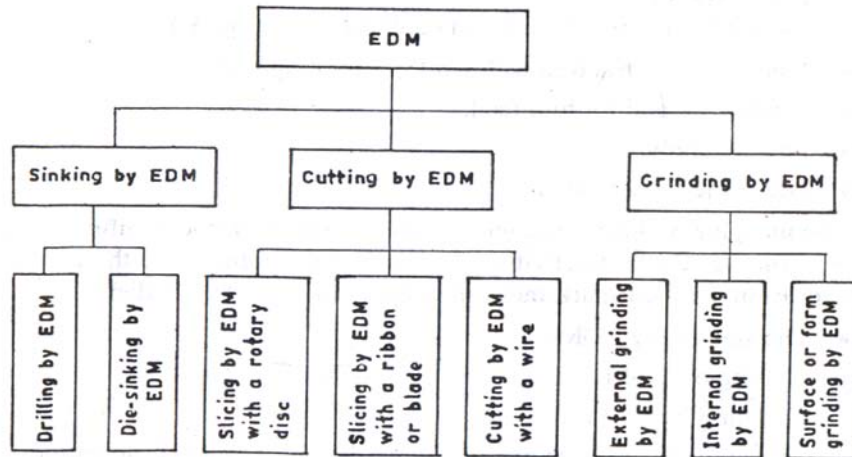
Fig. 1.9 (a) Different Categories of EDM Machines

The servo head is necessary to bring in the stability in the EDMing. It is never meant to maintain uniform gap but to maintain gap voltage or gap
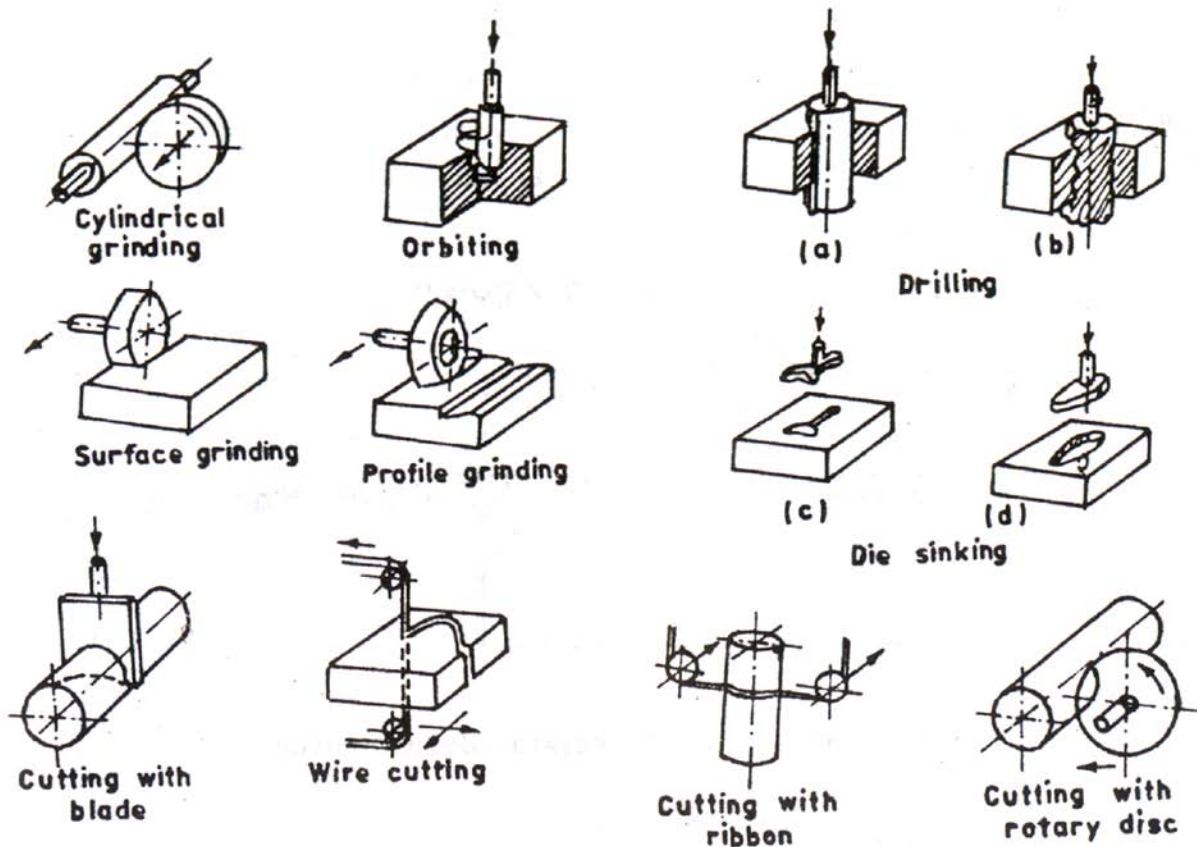
Fig. 1.9 (b) Different EDM Operations

energy constant since the dielectric parameter constantly fluctuate because of pollution and temperature changes. The dielectric fluid system consist of dielectric tank, a pumping unit and a filtering unit to handle basically two types of dielectric used:

Hydrocarbons (i) *Mineral oil* — With low viscosity (5 - 20 cts) at 20° C without any aromatics or other additives. Roughing operations with heavy oils are efficient.

(ii) *White spirit or kerosene* — Very low viscosity (2 cst at 20°C). This is well suitable for finishing and superfinishing operations recommended for machining WC when short duration charges are required.

Water: Deionized water is a dielectric mainly reserved for micro-machining and for wire cutting. However, when water is used as a dielectric fluid and addition accessory is a deionizing unit.

1.6.1 Power Generator

Power Generator is one of the most important part of an EDM system. Its primary function is to convert an alternating current (AC) into a pulsed direct current (DC) required to produce the unidirectional spark discharges between the gaps of a tool and work serving as the electrode.
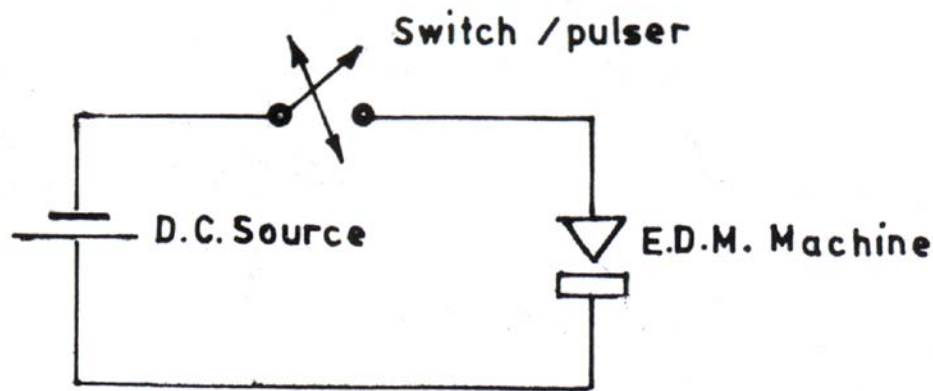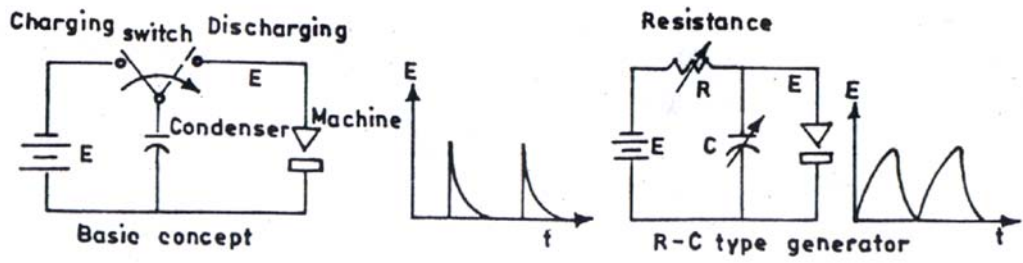

Fig. 8.10 A Pulse Generator-Basic Concept
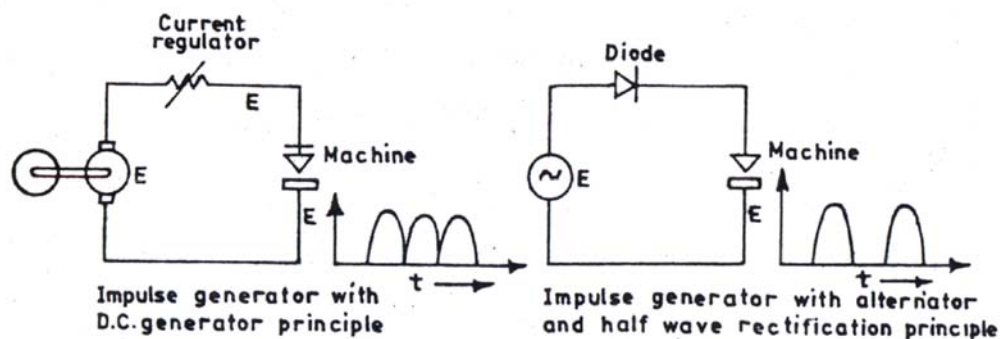
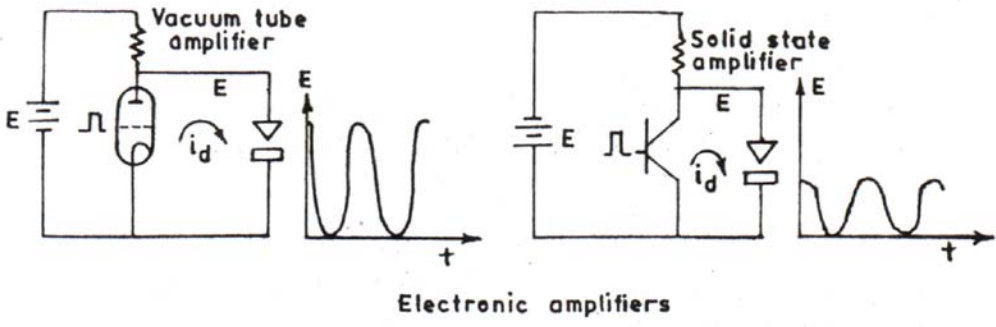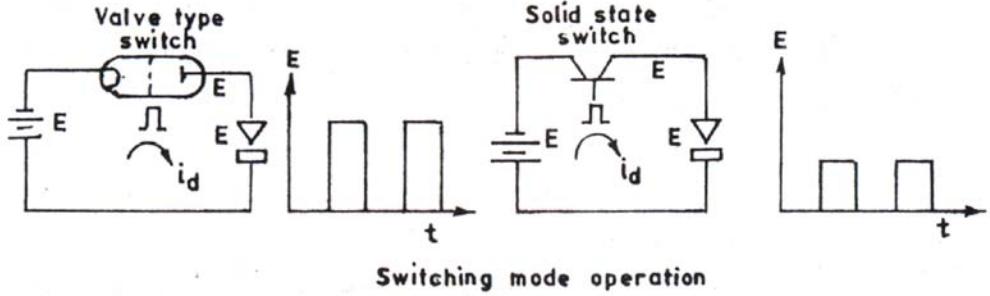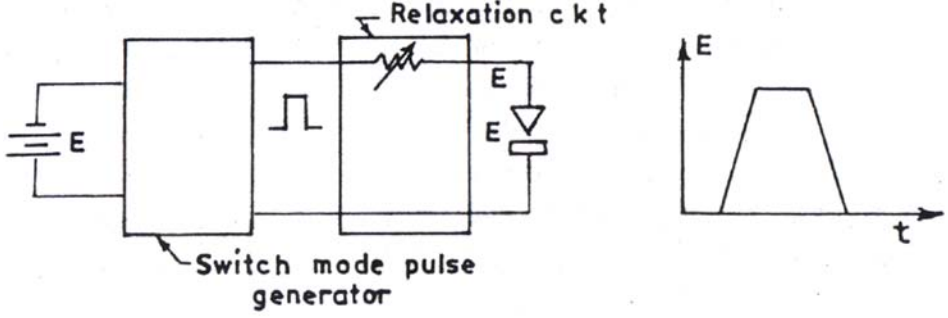(a) Impulse generator

(b) Relaxation generator

Electronic amplifiers

Switching mode operation

(c) Electronic pulse generators

(d) Hybrid generators

Fig. 1.11 Scheme of Different Pulse Generators for EDM

This pulsing unit in practice is of four different types (Fig. 8.11) as: e Rotary Impulse Generator

- Relaxation Generator

- Pulse Generator

- Hybrid Generator.

(a) *Rotary Impulse Generator*

It supplies the voltage waveform based on the principles as in the case of DC Generators, given by

$$E = \frac{\phi z N}{60} \times \frac{P}{A} \tag{1.3}$$

where (*p* is the flux per pole, z the total number of armature conductors, *N* the armature rotation (rpm), *P* the number of poles and *A* the number of parallel paths.

Here the frequency of operation is limited by *N* and *P* and cannot be increased much because of the limitation in *N*. Moreover, the wave form is near sinusoidal. This leads to arcing unless the poles are asymmetrically staggered to provide off time for deionization. The circuit is modified using a half wave rectified AC output from a AC generator, where the frequency of operation is denoted by

$$f = \frac{PN}{120} \, \text{Hz} \tag{1.4}$$

where *P* is the total number of magnetic poles and *N* the rotational speed of rotor, rpm.

In half wave rectification the frequency remains same but the pulse off time is half of the cycle time controlled by *N* and *P*. However, the voltage waveform remains as before sinusoidal.

This type of generator supplies very high voltage in excess of 110 V. Arcing is frequent since the voltage waveform is uncontrollable, so the tool-wear-rate is extremely high, more than 100% of MRR. This type of generators are still in vogue in some Russian and Japanese machines. The use is being restricted since uneconomical, high inaccuracy in machining process and high surface damage.

(b) *Relaxation Type Generator*

This type of generators are quite common because of its simplicity and lowest cost. This uses a 'resistance' and a 'condenser' to generate a nearly a saw tooth voltage wave form (Fig. 8.11b). The condenser gets charged from no voltage to a required voltage when it is connected to a DC source. Then the charged condenser is connected to the machine to discharge its charge to the

spark gap is the machine and so relaxed to zero voltage (voltage which cannot sustain the spark). The next discharge will not occur unless the condenser in charged again. The switch is replaced by the resistance which varies the charging current. This helps in controlling the idle period (charging time), discharge period and the pulse energy content,

(a) Charging Circuit   (b) Discharging Circuit
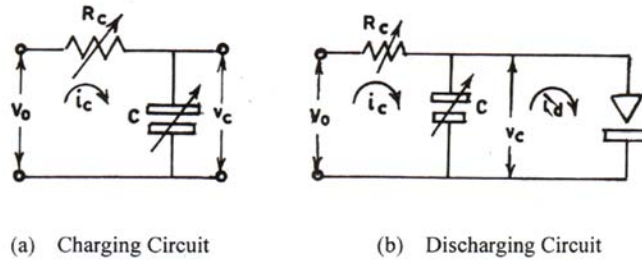
Fig. 1.12 Relaxation Generator

$$E_p = \frac{1}{2}CV^2$$

where E_p is the pulse energy, C the condenser value and V the voltage to which the condenser is charged.

Mechanism of Relaxation Generator

In Fig. 1.12 (a), R_c is the charging or Balast resistance and C stores the charge during the idle period (i.e. when there is no discharge in the spark gap) and delivers it to the spark gap when a threshould voltage to produce the spark is reached. To analyse the circuit, consider each side of the circuit separately.

Let us consider the charging circuit (Fig 1.12b).

If,

V_o = D.C. source voltage, volts,

i_c = value of charging current at any instant of time t, amp.,

V_c = condenser voltage achieved at the same time t, volt,

C = condenser value, Farad,

R_c = charging resistance, ohm.

Now, from circuit therogy

$$i_c = \frac{V_0 - V_c}{R_c} = C\frac{dV_c}{dt}$$

or $\dfrac{dV_c}{V_0 - V_c} = \dfrac{1}{CR_c} dt$

Integrating between the limits, i.v. $v = 0$ and $v = V_c$ at t at $t = 0$ at $t = t_c$

$$\int_0^{v_c} \dfrac{dv}{V_0 - v} = \dfrac{1}{CR_c} \int_0^{t_c} dt$$

or, $\left[\log \left(V_0 - V_c \right) \right]_0^{V_c} = -\dfrac{1}{CR_c} t_c$

or, $\log \dfrac{\left(V_0 - V_c \right)}{V_0} = -\dfrac{1}{CR_c} t_c$

or, $\dfrac{\left(V_0 - V_c \right)}{V_0} = e^{-(1/CR_c)t_c}$

or, $V_c = V_0 \left(1 - e^{-(t_c/CR_c)} \right)$ (1.6)

This shows the experimental rise of condenser voltage and

$$i_c = \dfrac{V_0 - v}{R_c} = \dfrac{V_0 - V_0 \left(1 - e \right)^{-(t/CR_c)}}{R_c}$$

or, $i_c = \dfrac{V_0}{R_c} e^{-(t/CR_c)}$ (1.7)

This shows the exponential decaying of charging current (Fig. 8.13).

Discharging ckt

Let us assume the load (machine) is $\mathbf{v_0}$ [1] purely a resistive load (Fig. 8.14) and the condenser is charged to voltage V_{co} which is sufficient to breakdown the dielectric to create a discharge. If V_d is the value of condenser voltage at any instant of time t and R the load Resistance, then
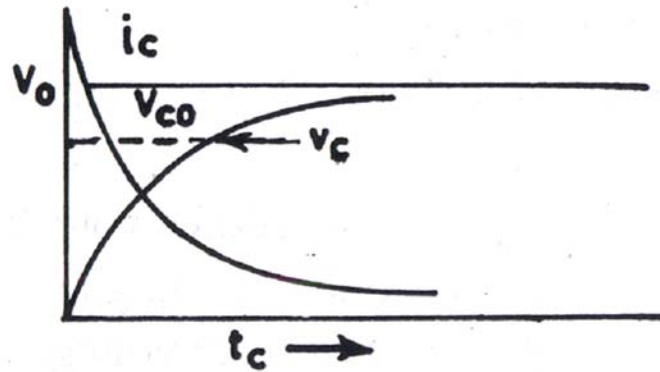
Fig. 1.13 Voltage and Current

$$\frac{V_d}{R} = i_d = -C\frac{dV_d}{dt}$$
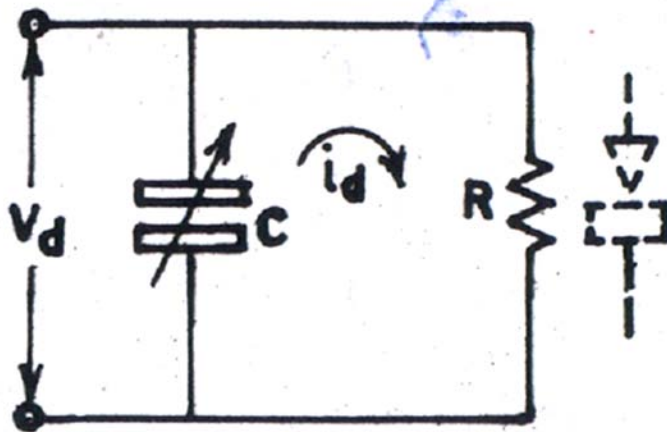
(since the condenser voltage is full)

Fig. 1.14 Discharging Circuit

or, $\quad \dfrac{dV_d}{V_d} = -\dfrac{1}{CR}dt$

integratingthis between the limits,

i.e. $V_d = V_{co}$ at $t_d = 0$ and $V_d = V_d$ at $t = t_d$

$$\int_{V_{co}}^{V_d} \frac{dV_d}{V_d} = -\frac{1}{CR}\int_0^1 dt$$

or, $\left[\log V_d\right]_{V_{co}}^{V_d} = \left[\dfrac{t}{CR}\right]_0^{t_d}$

or, $\log \dfrac{V_d}{V_{co}} = -\dfrac{t_d}{CR}$
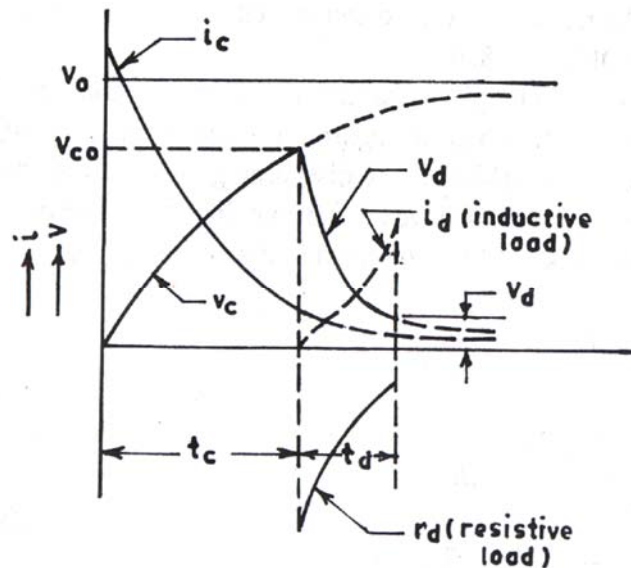
or, $V_d = V_{co}e^{-(t_d/CR)}$ \hfill (1.8)

This shows exponential decaying of condenser current and voltage,

or, $i_d = \dfrac{V_d}{R}$

or, $i_d = \dfrac{V_{co}}{R} e^{-(t_d/CR)}$ \hfill (1.9)

This also shows an exponential decaying of discharge current (Fig. 1.15).

Fig. 1.15 Charging and Discharging Wave-form for a Pure Resistive Load

Had we assumed an inductive (pure) load then the i_d curve would have been as shown by the dotted line, i.e. inductance would oppose the discharge current. So the i_d will be equal to zero when condenser voltage
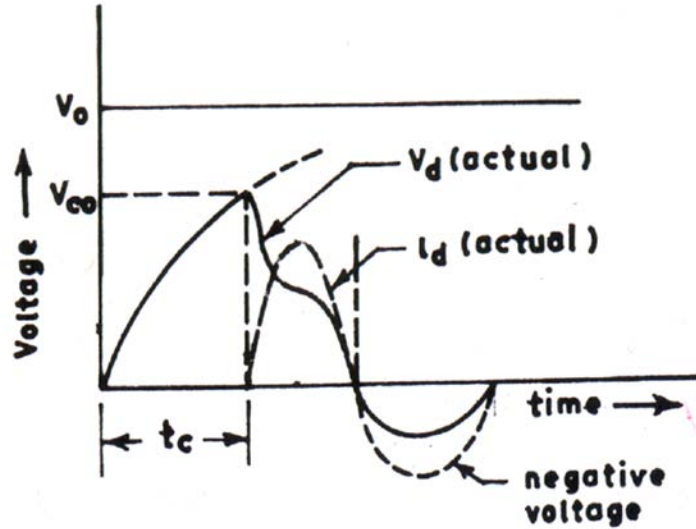
Fig. 1.16 Voltage and Current Wave-form in Actual Machine

is maximum at V_{co} whereas id is maximum at V_{co} for resistive load when the condenser voltage is maximum and id is zero for resistive load when the condenser voltage reaches zero.

R-L-C ckt

Let us see how the nature of voltage and current variation is seen in actual, relaxation type EDM (Fig. 1.16).

It is seen that the charging characteristics remain the same but the discharging characteristics with a *negative voltage in the discharging ckt*. shows the inductive load (*R-L*). So the discharging circuit as assumed earlier is neither resistive nor pure inductive but the combination as shown.

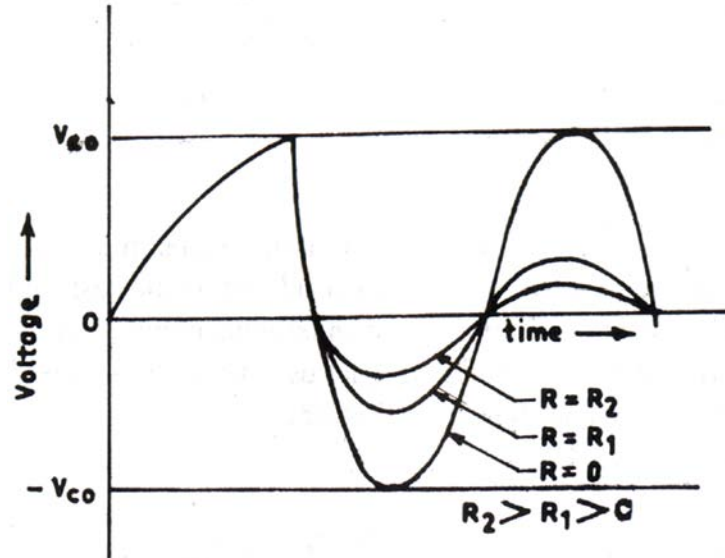Now if e is the back E.M.F. generated in the circuit, then,

$$\frac{V_c - e}{R} = i = -C\frac{dV_d}{dt}$$

But, $\quad e = L\frac{d_1}{dt} = LC\frac{d^2V_d}{dt^2}$

or, $\quad \dfrac{d^2V_d}{dt^2} + \dfrac{R}{L}\dfrac{dV_d}{dt} + \dfrac{1}{L}V_c = 0$ $\hspace{3cm}$ (1.10)

This equation is a case of damped vibration. If it is a pure inductive *ckt*, i.e. *R = 0*, then eqn. 1.10 takes the form

$$\frac{d^2V_d}{dt^2} + \frac{1}{LC}V_c = 0 \hspace{3cm} (1.11)$$

Fig. 1.17 Wave-form with a Pure Inductive Load

This is a case of simple harmonic fluctuation of voltage with a time period of $\sqrt{(1/LC)}$.

So the condenser once charged will not recharge and the voltage will oscillate between V_{co} and -V_{co} (Fig. 1.17) showing a deterioration of material removal and increased tool wear. Hence the vibration has to be damped effectively to prevent reversal of spar and also to allow continuous charging and discharging of the condenser. This means the introduction of R in the circuit is a primary requirement, and the more the value of R, it is better in reducing reversal of spark (tool wear). But,

$$R = R_1 + R_s$$

where R_1 is the line resistance and R_s the spark resistance.

Here the spark resistance cannot be changed but the line resistance can be increased to reduce the tool wear. Which in the other way proves that *when Relaxation generators are used for high power generation, i.e. for higher MRR the tool wear rate becomes very high, so that they are not prescribable for high production rate, though they are simple and less costly at the initial stage.* For this reason the electronic pulse generators have come into the market for its higher eroding capacity with less tool wear. However, no one can eliminate the relaxation generator for its simplicity and is seen in most machines.

Condition for maximum power generation in Relaxation Generator
The material removal depends on the pulse energy. Now" the energy supplied to the spark gap to cause erosion is equal to $\{(1/2)\ (C\ V_{co})\}$. We see that energy supply is maximum when $V_{co} = V_a$ (source voltage). But from eqn. 3.

$V_{co} = V_o$ when $t = \infty$

i.e. we have to wait for infinite time to dissipate maximum energy to the spark-gap. So, the MRR would not be considered on the basis of maximum energy condition but on the basis of maximum power dissipated in the spark-gap. In order to determine this let us start with the energy gain by the condenser while charging it for time dt as

$$dE_c = i_c v_c dt \tag{1.12}$$

or, $$dE_c = \frac{V_o}{R_c}\left[e^{-\{t/(R_c C)\}}\right]V_o\left[1-\left\{e^{-\{t/(R_c C)\}}\right\}\right]dt \tag{1.13}$$

$$= \frac{V_o^2}{R_c}\left[e^{-\{t/(R_c C)\}} - e^{-\{2t/(R_c C)\}}\right]dt$$

Now, we can obtain the total energy gain during the time t by integrating between the limits, i.e. $E_c = 0$ at t - 0 and $E_c = 0$ at t - t_c.

$$\int_0^E DE_c = \frac{V_o}{R_c}\int_0^{t_c}\left[e^{-\{t/(R_c C)\}} - e^{-\{2t/(R_c C)\}}\right]dt$$

where γ_c is the time constant of the charging circuit = $R_c C$

$$E = \frac{V_o}{R_c}\left[-\gamma_c \, e^{-(t/\gamma_c)} + \frac{\gamma_c}{2} - e^{-(2t/\gamma_c)}\right]_0^{t_c} dt$$

$$E = \frac{V_o}{R_c}\left[\frac{\gamma_c}{2} - e^{-(t/\gamma_c)} + \frac{\gamma_c}{2}e^{-(2t/\gamma_c)}\right]$$

$$= \frac{V_o}{R_c}\gamma_c\left[\frac{1}{2} - e^{-(t/\gamma_c)} + \frac{1}{2}e^{-(2t/\gamma_c)}\right]$$

Now average power stored

$$P_{avg} = \frac{E}{t_c} = \frac{V_o}{R_c}\left(\frac{\gamma_c}{t_c}\right)\left[\frac{1}{2} - e^{-(t_c/\gamma_c)} + \frac{1}{2}e^{-(2t_c/\gamma_c)}\right] \tag{1.14}$$

putting $(t_c/\gamma_c) = x$, and for maximisation of average power, i.e

$$\frac{dP_{avg}}{dx} = 0$$

or, $\quad \frac{1}{2x} - (1+\frac{1}{x})\ e^{-x} + (1+\frac{1}{2x})\ e^{-2x} = 0$

This transcendental equation has two solutions: $x = 0$ and $x = 1.26$. In first case.

$$\frac{t_c}{\gamma_c} = 0 \ \ or \ t_c = 0 \qquad\qquad\qquad (8.15)$$

To make charging time $t_c = 0$ means the charging resistance R_c to approach zero, below its critical value, when the voltage across the gap will (Fig. 8.18) stay at the supply level and a large current will flow, the gap will not relax. Hence, it would result in arcing.
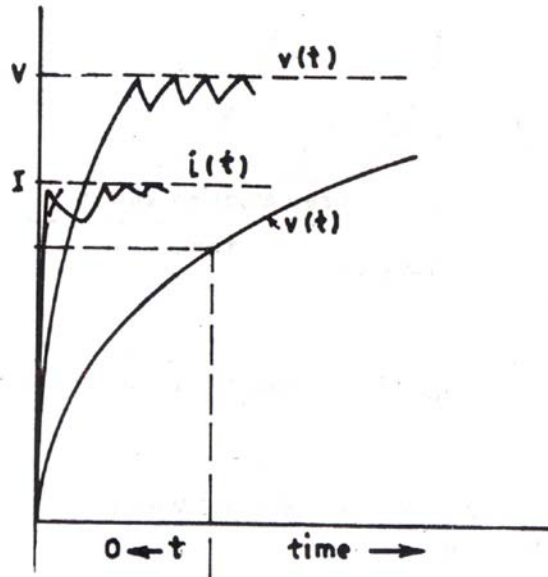
Fig. 1.18 Effect of Decrease in Charging Time

In second case, the power dissipation is maximum when $\dfrac{t_c}{\gamma_c} = 1.26$,

which proves that $V_{co} = 0.716$.

Therefore, the maximum power to the spark gap is dissipated if the condenser is allowed to charge to about 3/4th of source voltage.

This implies that if the nature of pulses is to be changed from the saw-¬tooth shape to the rectangular one (for maximisation of power transfer), the circuit should be made to relax at fixed intervals of time. This is difficult to achieve hence, the adoption of electronic pulse generators.

Frequency of Operation in Relaxation Circuit

The charging time t can be calculated from eq. 1.15 as

$$t_c = \frac{R_c C}{\log\left(1 - \frac{V_{co}}{V_o}\right)}$$
(1.16)

This charging time (Fig. 8.19) is the idle time for EDM.
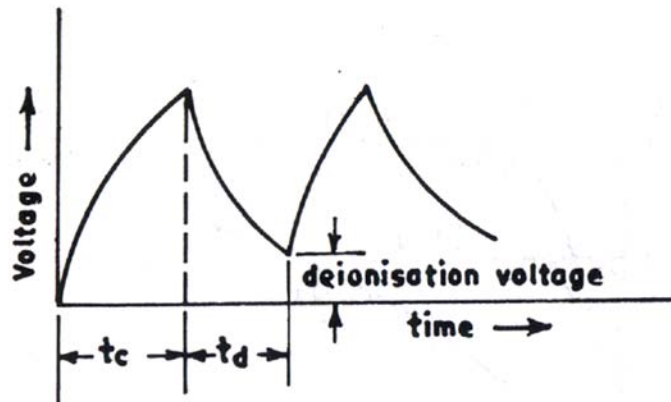
Fig.8.19 Actual Operation

Again the discharge period or the pulse width can be calculated from eq. 8.16 and may be written as,

$$t = \frac{R_c C}{\log\left(\frac{V_d}{V_{co}}\right)}$$
(1.17)

One thing must be clear here, that for effective discharge, i.e. for maximum power dissipation, $V_{co} = V_g$ and V_d is to be assumed to be equal or less than the deionisation voltage (i.e. voltage at which the ion column collapse).

So the frequency of operation can be written as (1.18)

$$f = \frac{1}{t_c + t_d} = \frac{1}{\dfrac{R_c C}{\log\left(1 - \dfrac{V_{co}}{V_o}\right)} + \dfrac{RC}{\log\left(\dfrac{V_d}{V_{co}}\right)}} \qquad (1.18)$$

But for higher condenser setting and higher charging resistance value in R-C type generator the discharge period is very small compared to the charging period, i.e. $t_d \ll t_c$. So

$$f = \frac{\log\left(1 - \dfrac{V_{co}}{V_o}\right)}{R_c C} \qquad (1.19)$$

(c) *Electronic Pulse Generator*

It has been observed that the Relaxation Generator with its simplicity could not meet the demand for higher production which reflected in high amount of tool wear, so restricted only for low removal-rate machining system.

To search for higher production with lower tool wear rate there were innumerable circuit modifications of Relaxation Generators using diodes and inductances in different forms, but were of no use and the use of electronic pulse generators were tried.

Electronic Amplifiers: This was tried with valves as well as solid state devices in class A and B operations. Different waveforms were tried to see the effect on productivity and improved wear ratio. These were found to be much more better as compared to R-C type generators. However, as shown in Fig. 1.11c the load current is taken care by the amplifier since the operate on linear mode operations of the amplifier. So the machine power has to be taken care by the amplifier itself, i.e. if it is required to have a 1 kW machine the amplifier should be designed to handle 1 kW at - least. Then the cost of the amplifier type generator would escalate with power. For this reason designer thought of switching the operation from linear mode to saturation mode of the devices

Rectangular Pulse Generator: This uses the principle of switching a valve or a solid state devices (transfer) in saturation mode as shown in the configurations as shown in Fig. 1.1 Id. These are electronic switches which can be operated at high frequency to give rectangular pulses swinging between zero and supply voltage, *E*.

In the configuration, it is evident when we apply no voltage on the grid the valve or base of the transistor, or allow no grid current or base current, the resistance across plate and base or collector and emitter is infinity representing the switch in the off-position. So the voltage across the machine is zero. Now if small voltage is applied to a saturation current to flow through grid or base, the resistance across plate and base or emitter and collector becomes extremely small = zero representing the switch to be in on position. So the voltage across the machine is *E* and allowing

the discharge current i_d to flow to erode the material. This i_d will flow till the switch is on i.e. when the resistance across the electronic switch is practically zero. So during the machining process there is hardly any loss of power across the electronic switch. But the current is limited by the handling capacity of the electronic switch. Now, if the handling power of the operation is to be increased, use a electron switching bank as shown in Fig. 1.20.
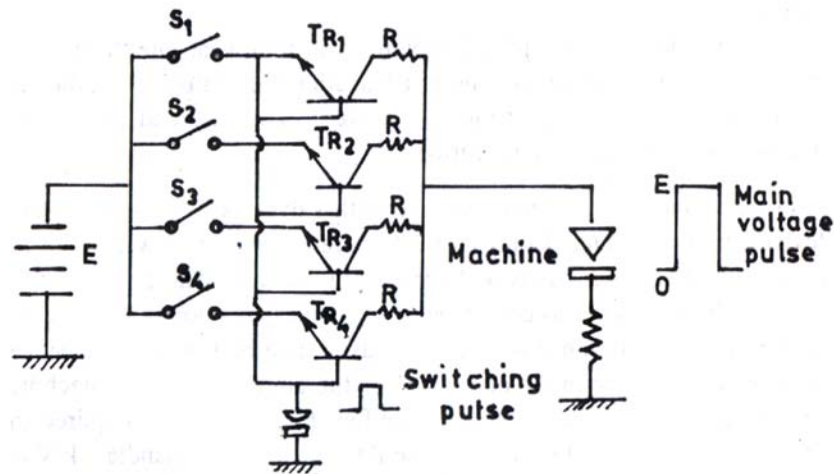
Fig. 1.20 Switching Bank of Transistors in Electronic Type Pulse Generator

In this, there are banks of transistors (or valves) of similar character, say $V_{CEO} = 100$ V and $I_{CE} = 10$ Amp. If the mechanical switch 5, is on the transistor T_R is operated by the switching pulse, so that a voltage pulse of 100 V is applied across the machine. The resistance R is so chosen that

the current flow is limited by 10 amp so that the transistor T_{R_1} is safe. Now if switches S_1, and S_2 are 'on', transistors T_{R_1} and T_{R_2} simultaneously switched on by the same switching pulse to give a voltage pulse of 100 V across the machine to allow 20 amp of current to flow to throw the machine to work at double the power, likewise the handling capacity of the machine can be increased by paralleling required number transistors in the active circuit. Thus the rectangular pulse generators have flourished in the EDM market with controllable tool wear phenomenon through easily programmable pulses.

Now, review the different pulsing conditions by different generators to observe the gradual improvements in the generator performance to decide if any further developments is required to idealise the process.

1.6.2 Waveforms in EDM Process

Different wave forms supplied by different generator are schematically shown in Fig. 8.21. In the case of rotating impulse-generators the rectified sinusoidal voltage wave form is given across the spark gap to produce the spark. Due to the inductive circuitry (generator as well as the sparking load) there is a spark oscillation even after the pulse is withdrawn give rise to extremely high tool

wear and arcing becomes frequent if the second pulse comes before complete dampening of the oscillation. So the inherent problem with this type of generator is to allow low frequency operation. Even if the material removal per pulse can be made high by increasing the peak voltage the flow frequency operation makes the MRR low with high thermal distortion of the work material.

In case of a relaxation generator (Fig. 1.21b) the spark oscillation is much more reduced, however, there will be a negative kick due to inductive load. So the tool wear will be less than the previous. The negative kick can be dampened easily as discussed in the previous sections. One can go for higher frequency. The charging time is equal to ignition delay, so the ionization process is slower and depends on charging time constant. If one tries to reduce the charging time, it might lead to arcing once again. By the square pulse generators the pulse wave form is much more defined and easily controlable and phenomena of sparking arc easily predictable. But a part of pulse width t_d is spoiled for ionizing the fluid.
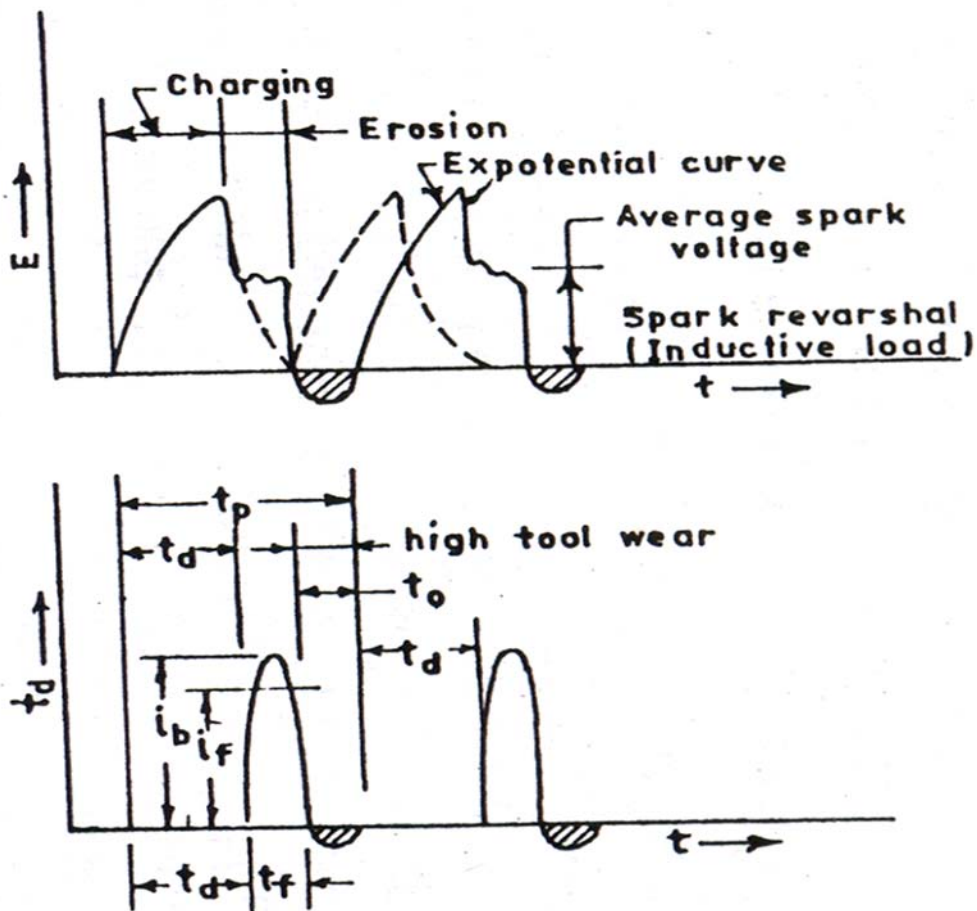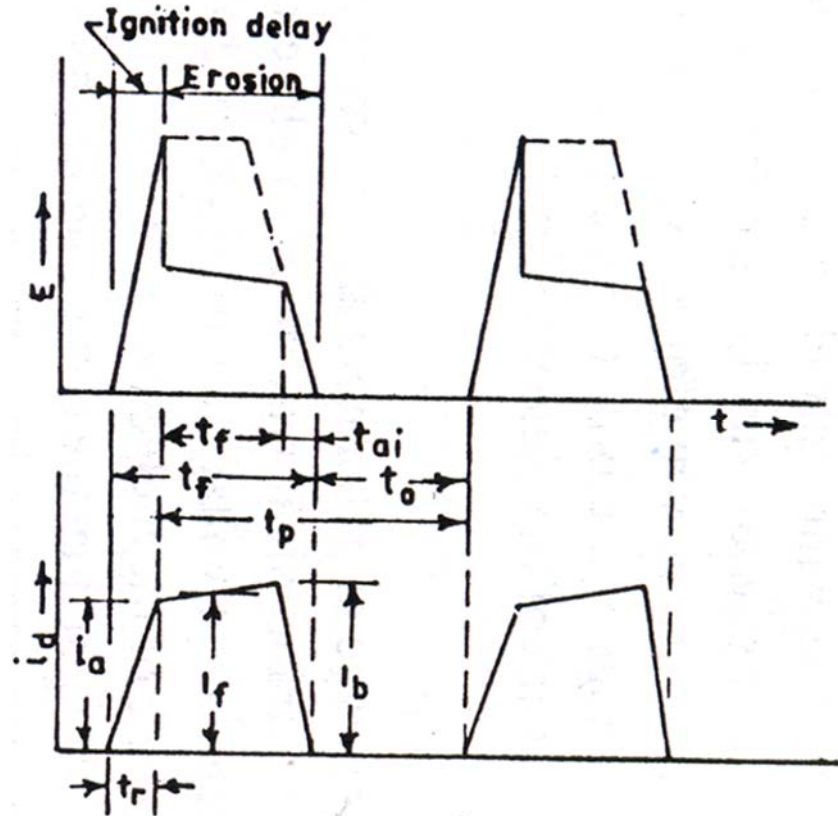

(a) Impulse generator
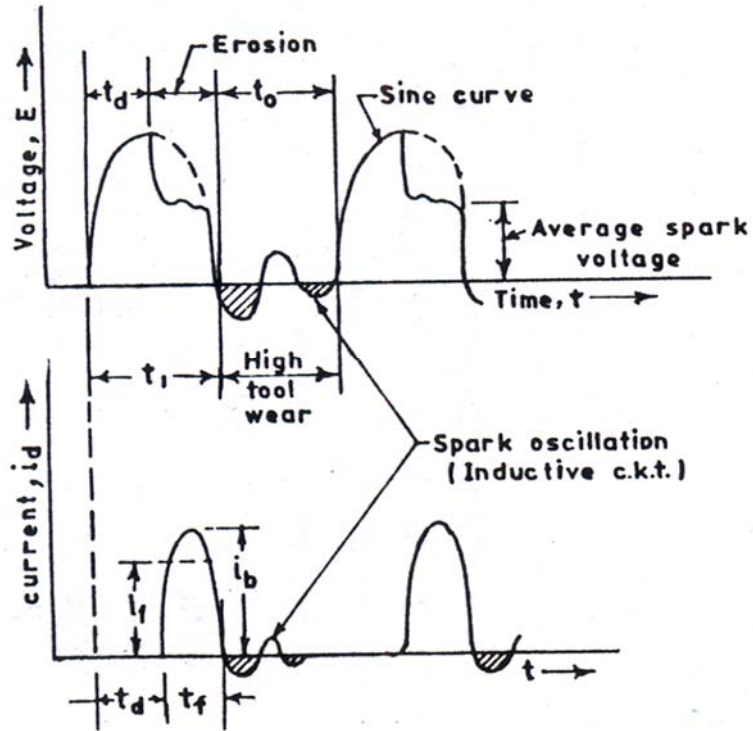
(b) Relaxation generator
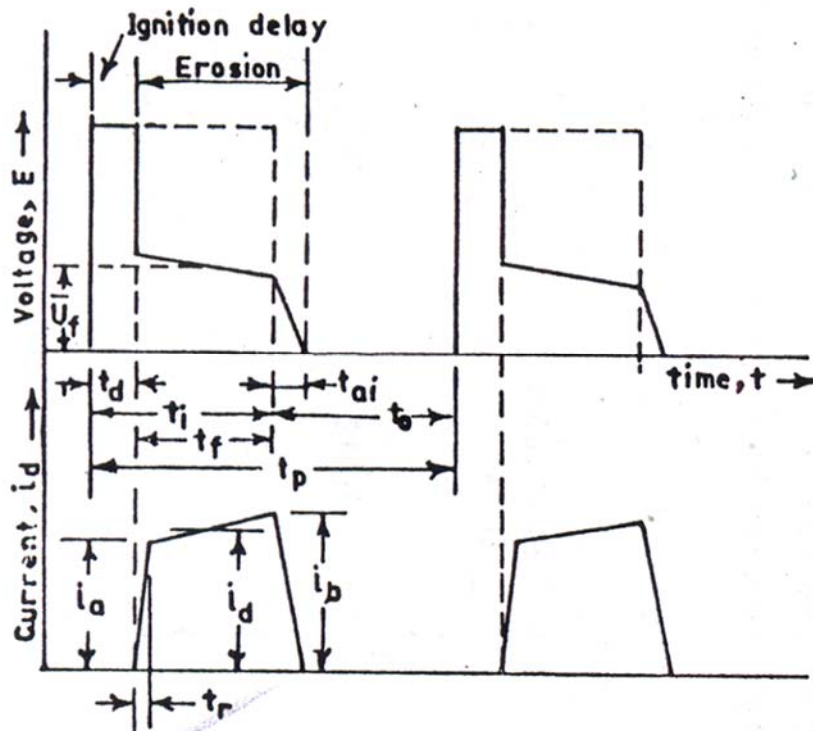
(c) Rectangular pulse generator

(d) Hybrid pulse generator

Fig. 1.21

N.B.: Dotted line gives the actual wave form supplied to the spark gap and firm line shows the wave form in actual machinery conditions

t_p – Pulse cycle time $\qquad$ t_o – Pulse interval $\qquad$ U_f – Average gap voltage =

$$\frac{1}{t_f}\int_{t_f} dt$$

t_i – pulse duration $\qquad$ t_r – Pulse rise time $\qquad$ i_f – Average pulse current =

$$\frac{1}{t_f}\int_{t_f} i_d \, dt$$

t_d – Ignition delay time $\qquad$ E_l – Instantaneous pulse voltage $\qquad$ i_a – Instantaneous pulse current

t_f – Discharge duration $\qquad$ i_d – Instantaneous pulse current $\qquad$ i_b – Final current

Moreover even after the removal of the voltage waveform is withdraw suddenly the deionisation of the fluid will lead to persist the spark for a period of t_d. So if $t_o \leq t_d$, even if the pulse is off the sparking will continue to produce the arcing. However, the tool wear is controllable easily since negative voltage is not present as before. The application of sudden voltage to the gap, along with electron and a sudden discharge formation there might lead to a phenomenon of mass transfer from tool to cause tool wear. So the tool wear cannot be completely eliminated however controllable to minimum. The difficulty with this is that the voltage wavefrom does not match with the current waveform. So there is a necessity of slope control of the voltage waveform to take care of the ionisation and deionisation characteristics of the dielectric fluid.

1.6 .3 Hybrid Generator

The hypothetical wave forms for this type of generators are shown in Fig. 1.21d. This type of generator uses a trapezoidal waveform in place of a square waveform. Instead of sudden rise of voltage a slope is provided to match with the ionisation characteristic of the dielectric fluid. The voltage pulse is withdrawn by a time factor of t_{dc} so that the condenser discharging character matches with the deionisation characteristic of the fluid, so that we get a pulse waveform matching with ionisation sparking and' deionisation characteristics of the dielectric fluid. The voltage waveform matches with current waveform. This becomes easier to predict the ideal performance of an EDM machine. Moreover, with the change of dielectric fluid property with time of machining (because of pollution and temperature etc.) the waveform can be changed through charging resistance or condenser value or both to match with the stochastic change of the dielectric fluid (Fig. 1.22).
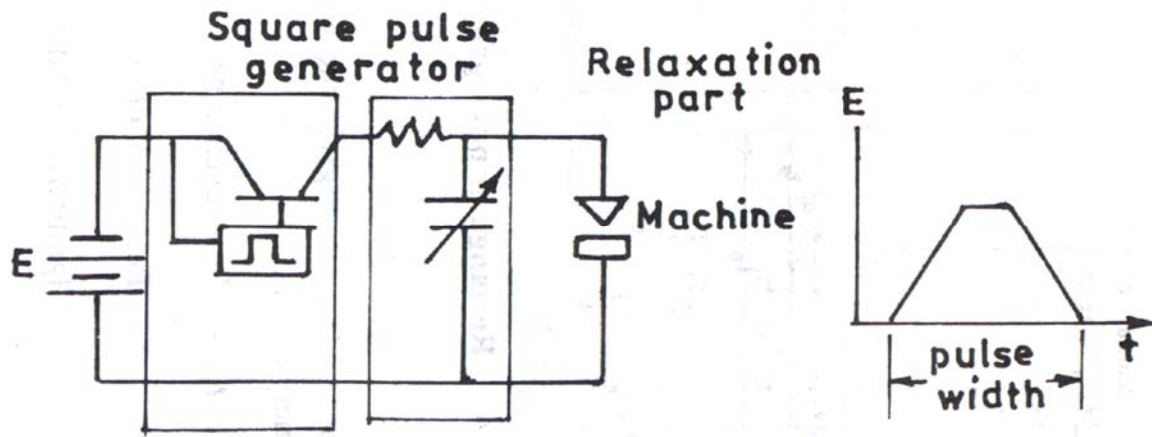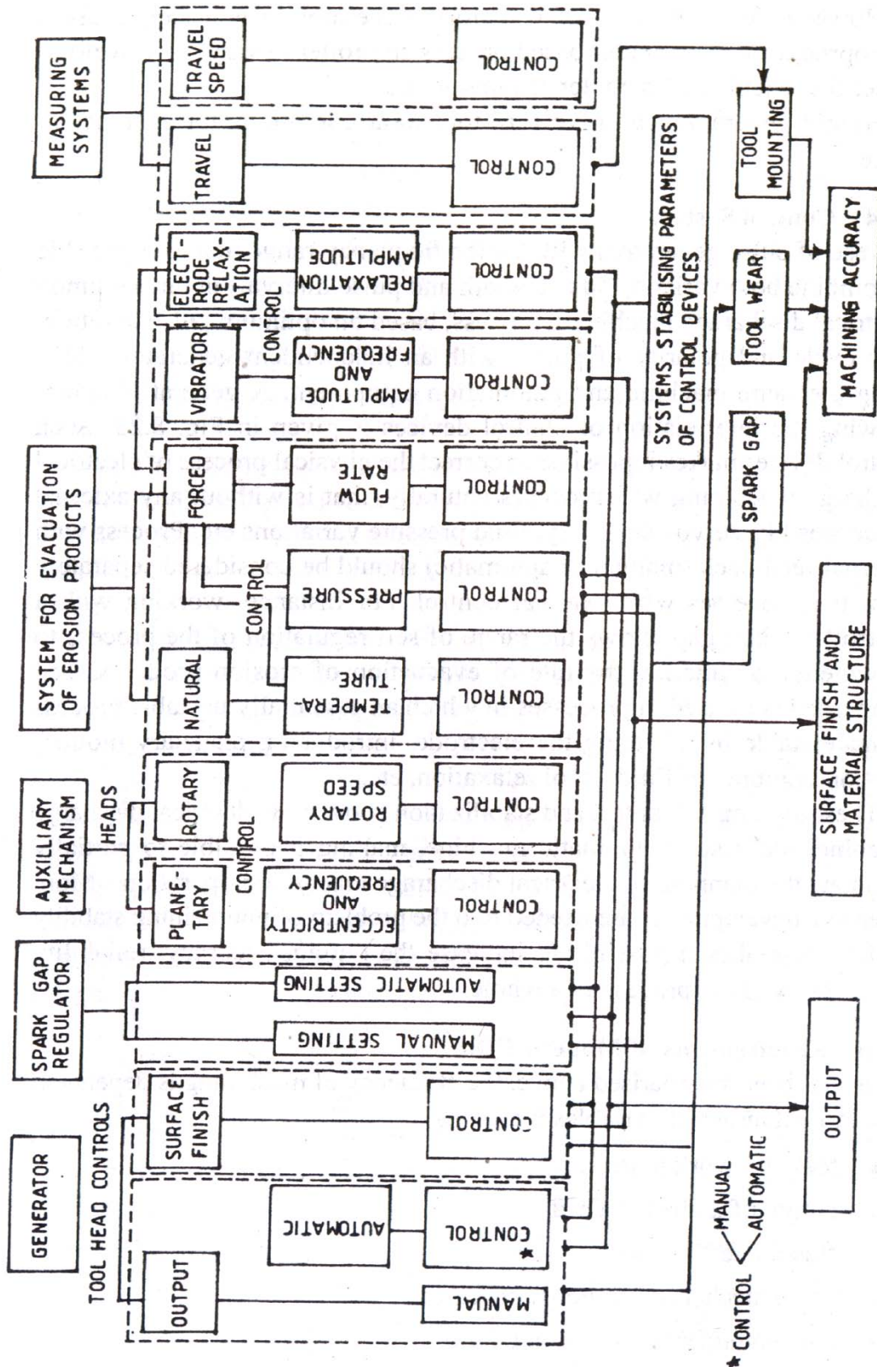

Fig. 1.22 An Ideal Pulse Generator

Fig. 1.23 Required controlled and monitored quantities in an EDM machine

generator, it is easier to use a microprocessor or computer based process controller to vary the waveform as per the machining character requirements.

Hybrid generators can give zero-tool wear conditions for all times to come.

1.6.4 Control System

Ths use of pulse generators with a wide frequency range makes it possible to combine both variation (pulse width and pulse interval) in one common electrical discharge machining process, based on optimum pulse duration, duty cycle and polarity of pulses with an independent generator whilst using the same machine and automation equipment. A generatl diagram showing the interrelation of control devices is given in Fig. 8.23. Such control devices makes it possible to correct the physical process of electrical discharge machining which occurs naturally, that is without any external influences like servo-sensitivity, fluid pressure variations etc. Process with external feed-back (manual or automatic) should be considered separately from the processes with external control. For instance, working with a controlled spark gap allows the range of self regulation of the process to be widened by altering the rate of evacuation of erosion products. The same trend is utilised in processes in which an essentially unstable process is made stable by vibrating the electrode, introducing planetary motion, rotation pumping of fluids, tool relaxation, etc.

These systems of control and stabilization convert an electrical discharge machine into a semi-automatic machine, making it possible to partially automate the planning of electrical discharage machining operations. More extensive developments are needed into the problem of maintaining stability artificially makes it possible to increase the output, accuracy, reliability and stability of the process as a whole.

1.6.5 Requirements of Modern EDM

So, as has been summarised above, the efficiency of machining is dependent on a large number of variables including

- tool and work materials

- nature of dielectric fluid

- flushing efficiency

- servo mechanism response speed

- the parameters of machining pulse.

These variables are to some extent interdependent and to try to generalise about the effects each is of little value. The best that can be done, at the present time, is to characterise the efficiency of the process by recording empirical data on a number of different jobs. Statistical attempts have been

made to evaluate the relative importance of each variable and these have thrown some light on the subject, but considerable research needs to be done on the physical mechanisms which are responsible for material removal.

The net result of the variability of the process has led to commercial equipment with a large number of controls to optimise the cutting on any particular job and inevitably EDM equipment is expensive. In its simplest form, a modem EDM has the following facilities.

(1) It should have a power supply capable of switching current of 1-100 A at 100 V at frequencies of 500-250 kH$_z$. At the higher frequencies, the required current is the lowest, for the finishing cuts. Automatic reduction of switched current (when machining becomes difficult owing to flushing inadequacies) is advantageous. A basic requirement of EDM generator is that it must provide a pre-spark over-voltage to define spark gap length.

(2) It must have vertical (in case of die sinking) or horizontal (in case of wore-cut) feed-control servomechanism which must maintain the tool near the optimum distance from the work-piece so that spark can occur and cause useful erosion. If the gap is too small, there are frequent short circuits between the tool and workpiece, causing loss of machining pulses, and possible 'Burning' of the workpiece because of overcurrent and mechanical forces on the elctrodes. Too large gap causes loss of potential machining pulses, since the available voltage unable to breakdown the dielectric fluid. Since the gap is being fed down, it cannot be sensed with an ordinary transducer, but is usually sensed by measuring the average voltage U_f and while this voltage is within certain limits, no correction signal is fed to the feed drive(s).

(3) It has a dielectric fluid-filtering and flushing system. A liquid, as opposed to a gaseous, dielectric will provide higher accuracy cutting, flushing away of debris and concentration of the discharge (enhancing its erosive effect), as well as serving as a cooling fluid in high current cutting. Flushing is necessary to remove debris which tends to short circuit the electrodes, particularly in the case of deep cavities, where pressure flushing is essential.

(4) It must have a lateral-positioning mechanism, x and y co-ordinate slides are usually provided to position the workpiece relative to the electrode, which is generally on a vertical feed axis above the work-table.

(5) In addition to the above the following features are often provided on commercial machine:

(a) Vibrator — providing very low amplitude oscillations in the tool axis, to assist flushing.

(b) Tool rotation — with circular holes, more accurate shape is produced if the tool is slowly rotated during machining.

(c) Independent adjustment of short-circuit and open-circuit limits. In some machines, it is possible to preset and adjust the mean gap voltages at which short circuit lift and open

circuit feed drives operate. These controls are sometimes known as 'gap and feed-rate' controls respectively.

(d) Dampening control — A hydraulic damper to assist stabilising during difficult machining periods e.g. at the start of a cut.

1.6.6 Generalised Electronic System

Based on the above consideration a modern EDM machine should have provisions to interrelate the functions necessary to implement the requirements. The elctronic system in general is schematically shown in Fig. 1.24.

The system centers on the bank of transistors or thyristers which are sequentially switched so as to apply a series of voltage pulses from the power pack to the electrodes. In a thyristorised generator, the major difficulty associated is that of turning of each thyristor at a suitable time after fixing however is not at all any problem for a transistorized one. The switching is controlled by a logic network which is programmed so that both the pulse rate and pulse width may be manually controlled within the speed limits imposed by the spark-gap characteristics.

1.6.7 NC Control

The use of numerical control with EDM machines is recognized as a method to increase table-positioning efficiency, such as that used in the case of multiple cavity work, and to cut dies and punches with travelling wire EDM. Numerical control is also in orbit—EDM machine tables, especially for large-mold workpieces. The addition of NC to the vertical ram movement makes it possible to EDM at different angles. Using an automatic electrode changer with the NC machines makes the EDM process completely automatic from roughing to finishing operation.
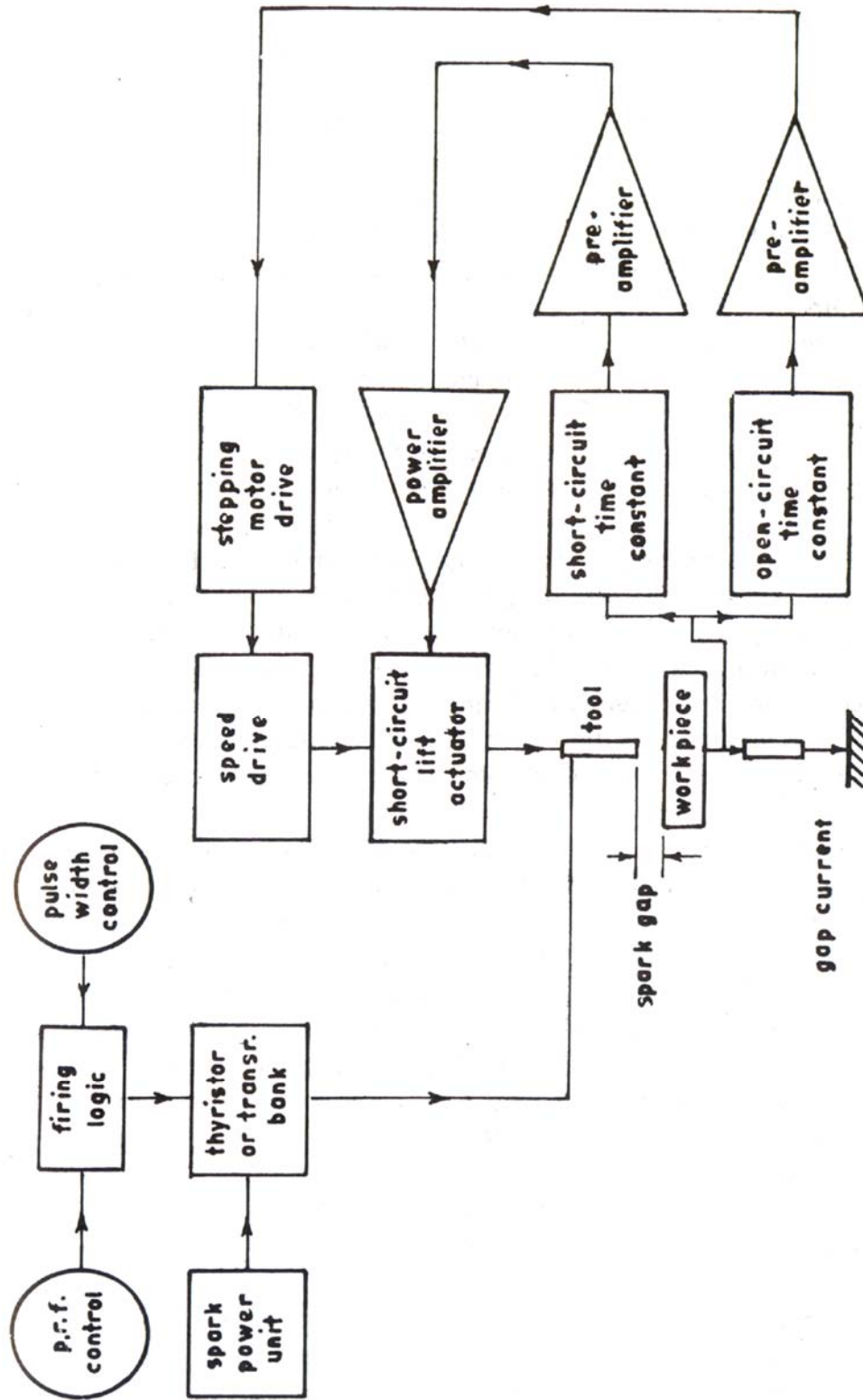
Fig. 1.24 Block Diagram of Electronic System

WIRE CUT ELECTRODISCHARGE MACHINE (WEDM)

2. Introduction

Sometimes called travelling wire EDM electrical discharge wire cutting is a process that is similar in configuration to bandswing except in the case of WEDM the "saw" is a wire electrode of small diameter. Material removal is affected as a result of spark erosion as the wire electrode is fed (from a spool) through the workpiece. In most cases, horizontal movement of the worktable, controlled by CNC on modem machines, determines the path of cut as illustrated in Fig. 8.26. However, some WED machines move the wire horizontally to define the path of cut, leaving the part stationary. On both types of machining configurations, the wire electrode moves vertically over sapphire or diamond wire guides, one above and one below the workpiece. The electrode wire is used only once, then discarded because the wire looses its form after one pass through the workpiece. A steady stream of deionized water or other fluid is used to cool the workpiece and electrode wire and to flush the cut area.

Viewed from above, the electrode wire cuts a slot or "kerf". The width of the kerf is the wire\diameter plus EDM overcut as illustrated in Fig. 8.27.
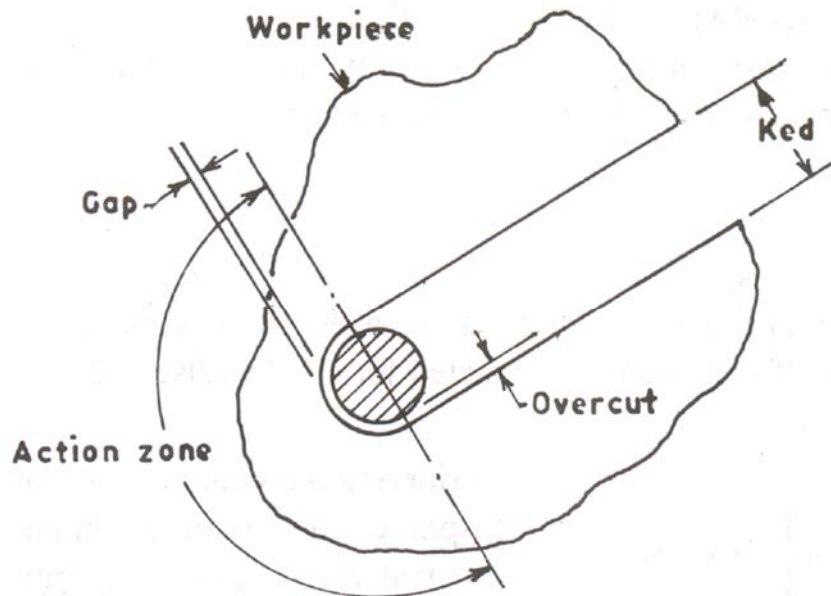
Fig. 2.1 Definition of Kerf in Wire-cut EDM

Strater or threading holes are required. In steel or other material a drilled hole suffices for carbide; the hole may have to be produced by EDM or micro EDM.

2.1 PROCESS PARAMETERS AND THEIR EFFECTS

2.1.1 Operating Parameters

Operating process involves the removal of work and tool as a measure of electrical energy input.

$$MRR = \phi(E)\, f = \phi \int_o^{\tau_p} v\, i\, dt$$

Eq.2.1

where ϕ = function, E = electrical energy, v = voltage, i = instantaneous current, d_t = time interval, τ_p = pulse width and f torque.

And,

$$TWR = Tool\ wear\ out = \psi(E) \cdot f = \psi \int_o^{\tau_p} v\, i\, dt$$

Eq. 2.2

Based on the above considerations, it is well understood that the objective functions, i.e. MRR, TWR and topological parameter are governed by the energy content of the pulses and the rate at which they are supplied. In

addition to these some other controlling parameters like servo sensitivity, gap width and dielectric parameters etc. also contribute to the objective functions.

So under unknown-or unpredictable circumstances i.e. when appropriate science to describe the process is absent, one tries with empirical formulae generated through insito experimental procedures.

2.1.2 Evaluation

(a) *Experimental Approach*

Material Removal Rate: Metal is removed from work in the form of crater (Fig. 8.2) and can be estimated for single pulse and rate at which it is given, i.e.*f*.

Considering the volume of a crater as part of sphere, the crater parameter can be estimated as a measure of energy.

$$h_c = K_1 W_p^n \tag{2.3}$$
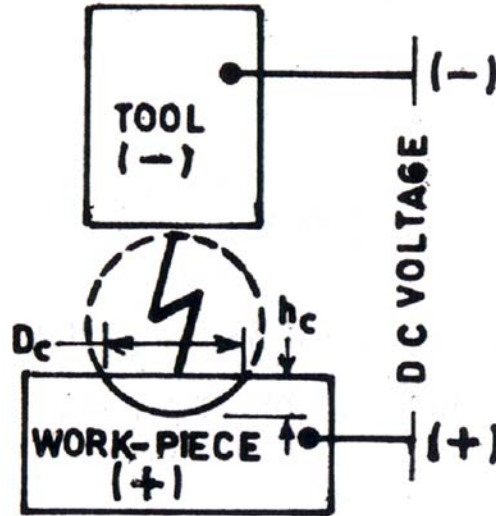
$$D_c = K_2 W_p^n \tag{2.4}$$

Fig. 2.2 Scheme of Crater Formation

where

W_p = pulse energy, Joule

h_c = height of crater, mm

D_c = diameter of crater, mm

K_1 , K_2 = constants depending on electrode materials and dielectric

n = constant depending on work tool combination

So the volume of crater V_c from simple geometry

$$V_c = \frac{\pi}{6} h_c \left(\frac{3}{4} D_2^2 + h_c^2 \right) \mathrm{mm}^3 \tag{2.5}$$

$$= \frac{\pi}{6} K_1 \left(\frac{3}{4} K_2^2 + K_1^2 \right) \mathrm{mm}^3 \tag{2.6}$$

So K_1 , K_2 and n values are to be determined from experiments and the material removal rate can be written in the form

$$MRR = V_c . f . \eta \tag{2.7}$$

Where f is the frequency of operation and η = efficiency of the machine at any setting.

Tool Wear Rate:　　　Similarly the tool wear can be determined. This is required to account for tooling cost, machining accuracy and estimate the time of machining for a desired depth of cut.

However, there are three types of wear observed in an electrode, end, comer and side wear explicitly defined in Fig. 8.29.
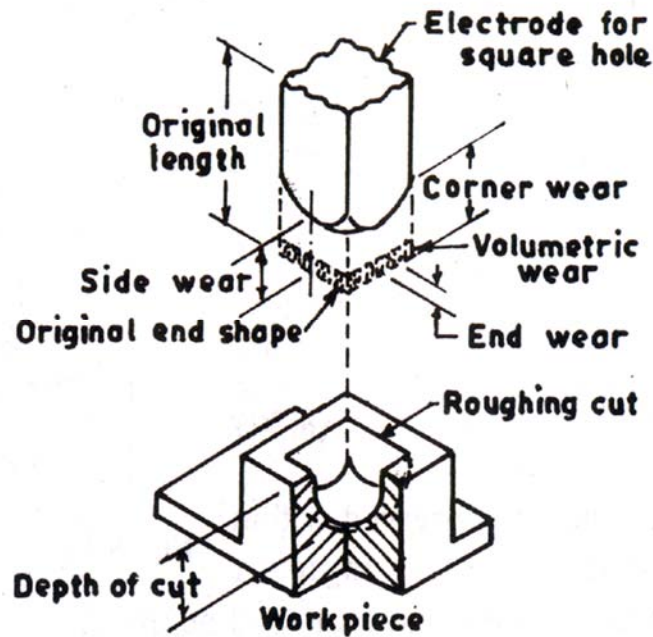
Fig. 2.3 Types of Electrode Wear in EDM Process

Taper: In this process tapering effect is observed due to side sparks (Fig. 2.4). Sometimes it is more pronounced as compared to frontal sparks under high dielectric pollution.

In this case, overcut at any instant is given by

$$\delta = K_3 \left(\frac{\pi}{4} d^2 \right) h \tag{2.8}$$

where *h* is the depth of machining at any instant.
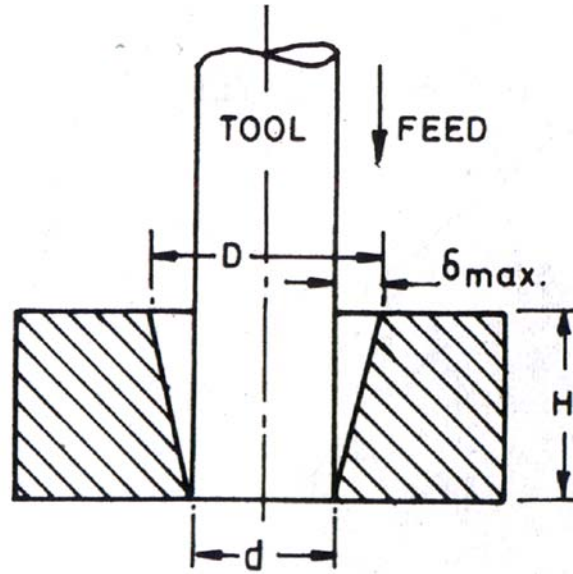
Fig. 2.4 Scheme of Taper

Hence

$$\delta_{max} = K_3 \left(\frac{\pi}{4} D^2 \right) h \tag{2.9}$$

So, taper $T_p = \dfrac{D-d}{2H} = \dfrac{\delta_{max}}{H} = K_3 \dfrac{\pi}{4} D^2$ (2.10)

The taper is observed for a bare tool for straight hole drilling. However, this can be eliminated with side electrical insulation.

Surface Finish: The quality of the machine surface mainly depends on the energy of the pulse and frequency of operation. The roughness is generally observed as (Fig. 2.5),

$$H_m \propto h_c$$

$$\propto \frac{1}{f}$$

Therefore

$$H_m = K_4 \frac{h_c}{f} = \frac{K_4 K_1 W_p^n}{f} \tag{2.11}$$
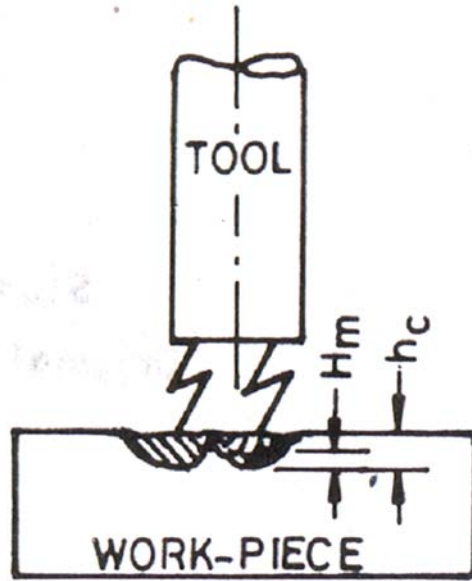
Fig. 2.5 Scheme of Finish

However, roughness is observed within a bandwidth depending on single or multispark conditions. In the experimental approach it is very difficult to predict some of the very important parameters like surface integrity problems associated with the process, e.g. recast layer, structural transformation, micro crack etc. evident from the Fig. 2.6.
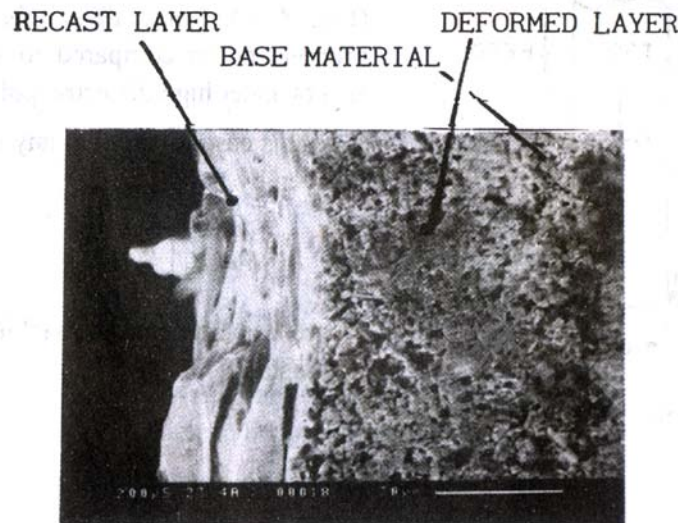
Fig. 2.6 SEM Analysis of Surface Processed by EDM

To analyse these microscopic parameters in addition to the microscopic surface topological phenomena one has to take the shelter under analytical approach.

(b) *Analytical Methods*

In EDM process a thermal balance as per Fig. 2.7 can be made as given below (ref. Snoyes and Van Dijck).
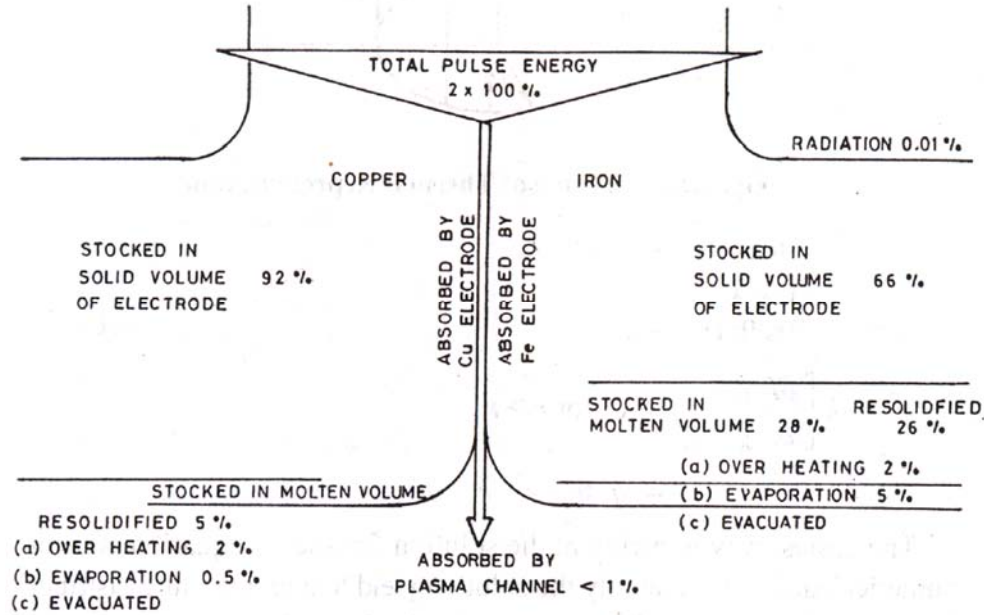
Fig. 2.7 Thermal Balance of EDM Process

To analyse the process, there are several thermal models with different techniques for the analytical or numerical solution with relevant boundary conditions. However, in general the thermal analysis for cycles of the EDM process is based on two dimensional transient heat conduction in a body of the work piece subjected to the uniform heat flux over a small circular portion on its upper surface (Fig.2.8).

From the above representation, the governing equation from the axi- symmetric form is given by,

$$\rho C_p(T)\frac{\delta T}{\delta t} = \left[\frac{1}{r}\frac{\delta}{\delta r}(k\,r)\frac{\delta T}{\delta r} + \left(\frac{\delta}{\delta z}\right) + \frac{\delta}{\delta z}\left(k.\frac{\delta T}{\delta z}\right)\right] \tag{2.12}$$

with the initial condition

$$T(r, z, 0) = 0$$

and boundary conditions,

Fig. 2.8 Scheme of Thermal Representation

$$T(0,z,0) = \text{finite}$$

$$T(r_2,z,0) = 0$$

$$T(r,0,t) = 0$$

$$k\left[\frac{\delta T}{\delta z}\right]_{(r,1,t)} = 0 \text{ for } r > r_1$$

$$= q \text{ for } r > r_1$$

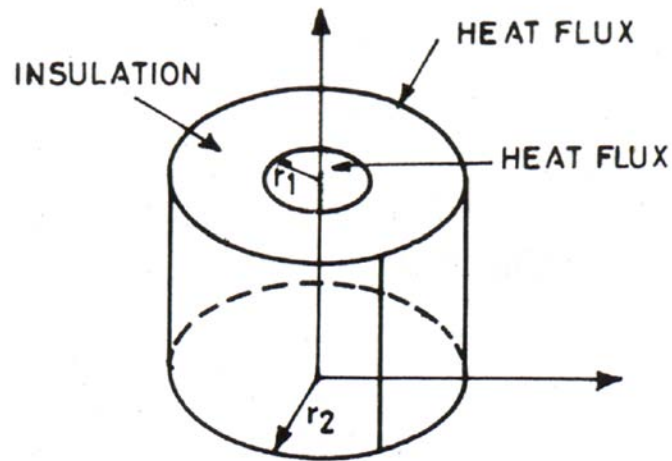The easiest way to arrive at the solution for such a equation is through numerical analysis. Generally the solution yield to a temperature distribution in work and tool material as mentioned below (Fig. 2.9).

For the above case, one can predict material removal and as well as structural damage or changes.

Further the temperature can also be predicted within the bulk of the material as mentioned below considering different thermal properties of different materials (Fig. 2.10).

With the availability of computation facilities numerical solution even for complicated situations like simultaneous conductive, convective and radiative heat transfer (cooling) arising out of the presence of liquid dielectric can easily be made to realise the actual situation.

2.3 GAP FLUSHING

The effectiveness of flushing has a large effect on MRR V_w, tool wear V_v and conference accuracy.

The different effects on flushing are easier to understand from the action of the dielectric fluid discussed earlier and its most important properties in relation to EDM process are:
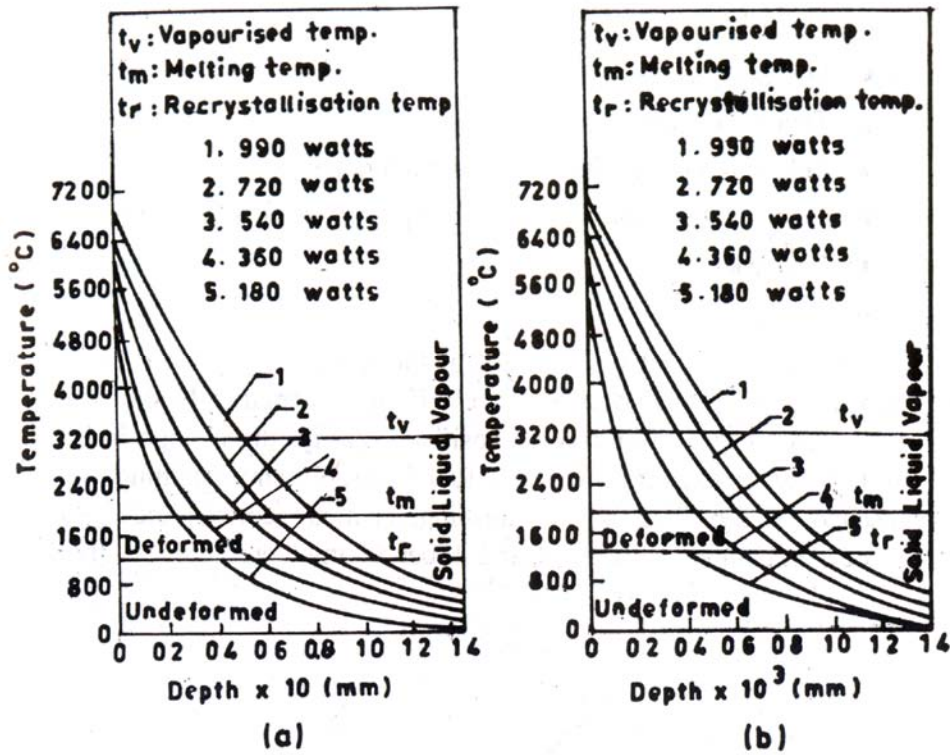
(a) For pulse width of 440 ps   (b) For pulse width of 880 ps

Fig. 2.9 Temperature Rise in Work Material
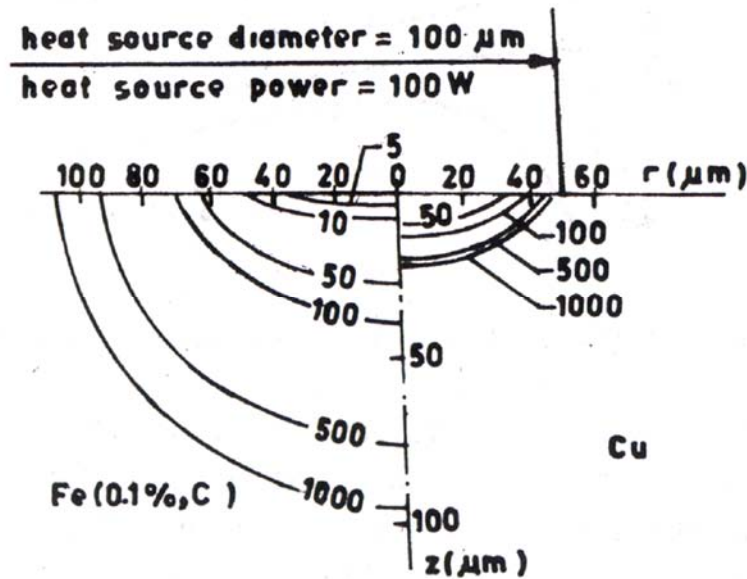
Fig. 2.10 Melting Point Isotherm in Steel and Copper (Stochastic)

- Electrical breakdown strength stability

- Viscosity

- Specific heat

- Thermal conductivity

- Temperature stability and distillation range

- Gas absorbing and solid solvency properties Health hazards

- Fire risk

- Cost

The effect of inlet pressure P_{in} of the dielectric liquid on both metal removal rate V_w and volumetric wear V_v are schematically shown in Fig. 8.37 [13]. With copper tool of positive polarity, the change in both V_w and V_v are greatest in range of 1 to 1.5 bar. When machining with low discharge energy W_e pulses for finishing, the metal removal rate V_w exhibits a local maximum between 0 and 1 bar of inlet pressure. As the pulse
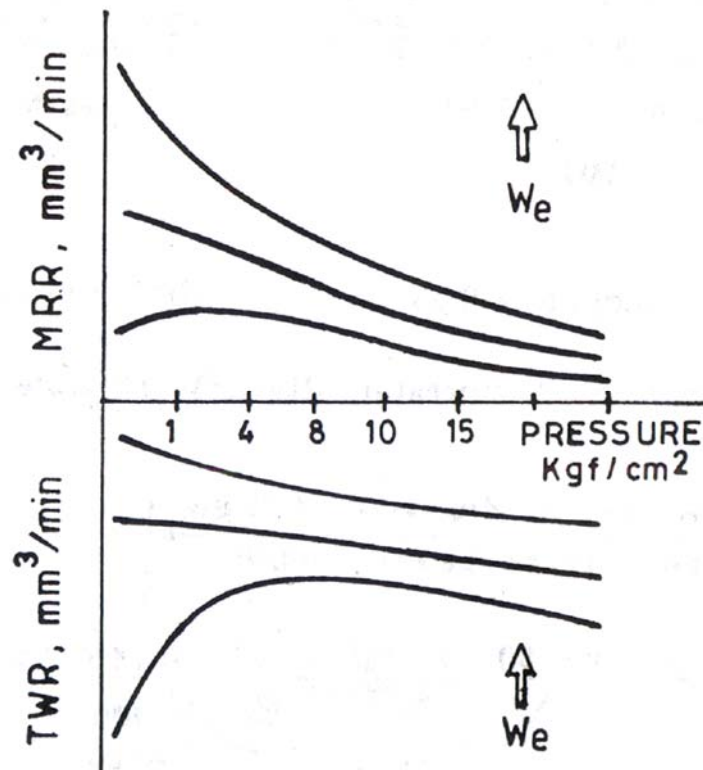
Fig. 2.11 MRR and Volumetric Wear Ratio vs Inlet Pressure

discharge energy is increased the maximum moves towards the left of the graph, that in towards lower inlet pressures, until the local maximum disappears and the curve is one of a monotonously

decreasing shape. The variations in electrode wear with increasing pulse energy are very similar to those of the metal removal rate.

When finishing [13], there is very little self-cleaning of the gap due to shock waves from the discharges, because pulse energies are low. Small local products can quickly develop in which erosion pocket accumulate, causing short circuits and generally impairing working efficiency. If the dielectric fluid is forced at low velocity through the gap, then these local pockets are flushed and accumulation of erosion products is prevented, thus short circuit pulses become rarer, working efficiency rises and metal- removal-rate increases. For the some reason, cooling of the tool is improved and tool wear reduces.

Higher flushing (higher velocity) hinder the formation of ionized bridges across the gap and result in higher ignition delay. Consequently, the energy (or frequency) of the discharges decreases and so balance. the effect of increased working efficiency. Where these opposing effects balance each other a minimum value of MRR (and, often, nearly a minimum for tool wear ratio) is observed. Further increases in flow rate long then the ignition delay time with consequent reductions in MRR.

The effects of increasing pulse energy are stronger shock waves and larger forward gaps produced by reductions in the breakdown strength of the more contaminated dielectric fluid. This explains why the self-clearing effect in roughing EDM is more effective than in finishing with lower discharge energies.

If clean fluid is pumped into the gap, the breakdown strength of the gap increases and the forward gap dimension decreases. With increasing discharge energy, metal particles accumulate faster and adhere to one another in increasing the incidence of spontaneously occurring short circuits, so that working efficiency reduces and metal removal rate falls rapidly. Increased numbers of short-circuit pulses locally heat the tool surface and rapidly increase the wear ratio.

From these observations the following practical rule can be formulated thpt the gap flushing should be continuous for finishing and intermittent for roughing.

2.3.1 Practical Flushing Techniques

With modem controlled pulse generators, the kinetic energy of the fluid shock wave produced by the collapse of the discharge channel is not sufficient to self clear the gap for longer than a few minutes. Therefore, in all cases, as uniform flushing conditions as possible should be attempted. An essential condition for this is that the machining allowance all around the periphery of the tool should be equal.

Flushing methods can be classified according to:

1.   Time, i.e. continuous or intermittent,

2.   Flow, i.e. pressure, vacuum or displacement.

2.3.2 Pressure (or Injection) Flushing

Pressurized clean dielectric is pumped into the EDM gap via either a predrilled hole in the tool (Fig. 8.12a) or the workpiece (Fig. 12b). The liquid flows upwards in the peripheral gap sweeping the erosion products into the open work tank. Occasionally, debris builds up in the gap on
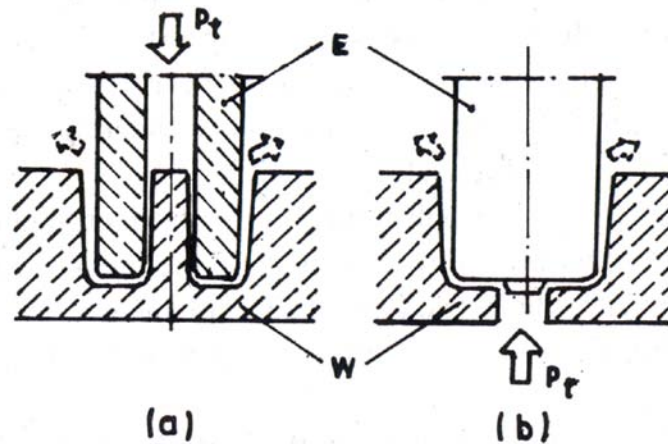
Fig. 2.12 Two typical Cases of Pressure Flushing

either tool or workpiece surface and so-called "evacuation-discharges" result. The gap gradually enlarges because of this kind of discharge; with more of these discharges taking place in the "down-stream" part of the gap, because of the higher debris content of the dielectric fluid having passed further through the gap, a tapered hole is always, produced even though the tool used is parallel sided.

2.3.3 Vacuum (or Suction) Flushing

Incontrast to pressure flushing, vacuum flushing sucks used dielectric fluid laden with erosion products either through the electrode (directly or indirectly through the electrode holder) Fig2.12a) or through the workpiece (Fig. 2.12b). Clean dielectric fluid from the work tank flows into the peripheral gap to replace the used dielectric sucked out. Since this peripheral gap is flushed with clean (or at worst only slightly contaminated) fluid, very few evacuation discharges occur down the sodes of the tool, though some taper may occur at the bottom of the cavity. Obviously, vacuum flushing produces an almost constant side gap.
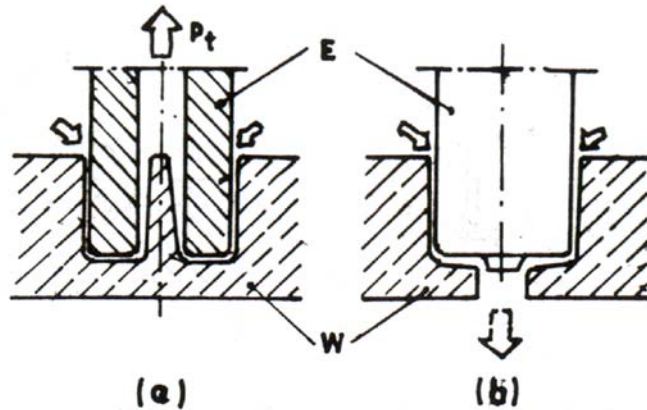
Fig. 2.13 Typical Cases of Vacum Flushing

2.3.4 Side Flushing

There are some applications in which the drilling of flushing holes through tool or workpiece are not possible (for example when EDMing coining dies or deep narrow slots or processes in plastics molding dies). In these cases the gap has to be flushed using carefully adjusted nozzles forcing sets of fluid to flow evently around the periphery of the tool electrode (Fig. 2.14a). The nozzle surrounds between a sixth to a third of the tool periphery. The direction of the jet of dielectric fluid has to be carefully adjusted to coincide with the angle of the gap so that the flow is directed parallel to the surfaces which define the gap (Fie. 2.15a)

Fig. 2.14 Side Flushing of a Coining Die

If the direction of flushing is not parallel with the electrode surface (Fig. 2.15a) and (b), then turbulence results and only a small proportion of the dielectric fluid actually enters the gap, so that the actual flushing will be inadequate. Another disadvantageous result of the fluid jet being applied perpendicular to the side of a tool is that deflection and/or vibration of the tool may occur (Fig. 2.15b).
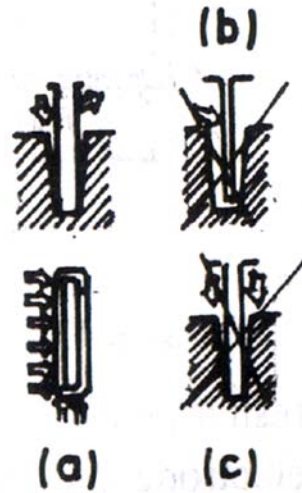
Fig. 2.15c Side Flushing for Deep Narrow Slots

An important working rule is to avoid directing the jets of fluid symmetrically to opposite' sides of a tool since the flows will tend to cancel each other at the bottom of the cavity with the consequence that erosion products are not flushed away (Fig. 2.15c).
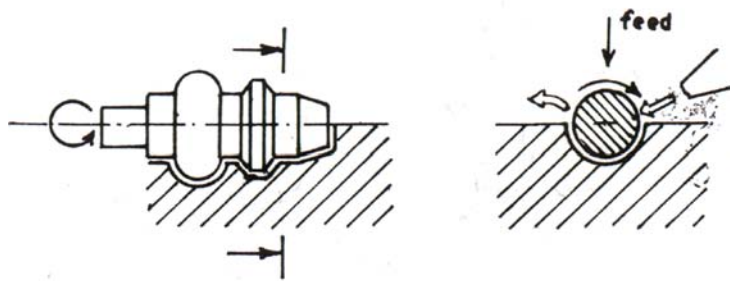
Fig. 2.16 Side Flushing with Electrode Rotation

Figure 2.16 shows a special application of side flushing in which clean dielectric fluid is assisted into the EDM gap by rotation of the electrode and the viscosity of the fluid. Many geometrical variations of this technique are possible and commonly used, particularly in wire cut EDM where the longitudinal feed of the wire introduces fresh dielectric fluid into the EDM gap.

8.8.5 Reciprocating Electrode Flushing

When EDMing deep cavities, the tool can be moved periodically up and down, thus, introducing fresh dielectric fluid into the gap and expelling contaminated eielectric fluid from the gap respectively. At each cycle (Fig.
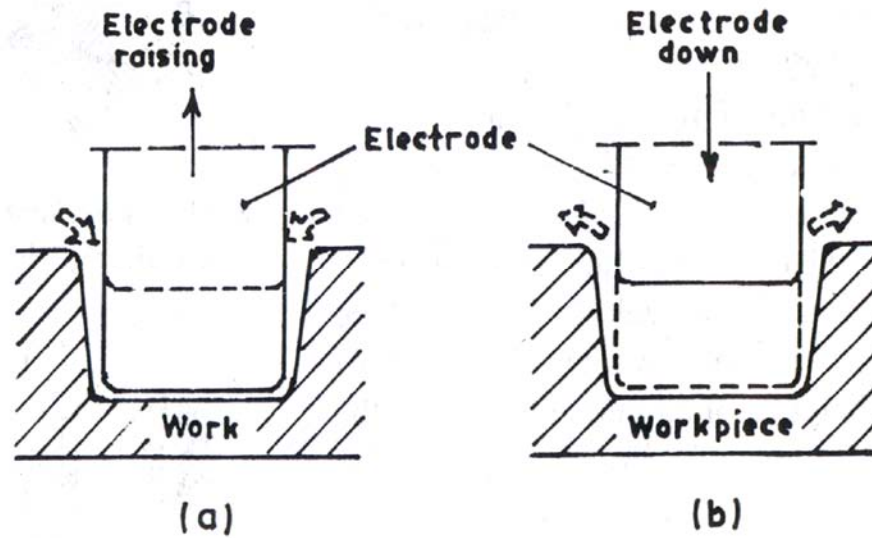
Fig. 2.17 Two Subsequent of Displacement Flushing

2.17) fresh liquid is mixed with contaminated fluid by the upward movement of the electrode and the mixture is partially expelled from the cavity by the downward movement. So at each strode the contamination of the dielectric fluid by the EDM debris is reduced.

Side flushing and reciprocating electrode flushing may be used together so that erosion debris leaves from the opposite side of the gap from the inlet jet. Evaluation discharge cause tapering similar to that experienced in pressure flushing, though the flushing is less effective and the side tapering rather larger with this method than with pressure flushing.

………….2.4 **OPERATIONAL SUMMARY**

Independently Controlled Parameters

Open circuit voltage	:50 to 300 V
Frequency	:50 Hz to 500 kHz or equivalent duty- cycle setting of on and off times per pulse
Dielectric type	: Hydrocarbon(petroleum) oils, deionized water, kerosene, gas (dry) (see table 12.3-10)
Dielectric flow pressure	: 711 mm vacuum to 480 kPa pr.
Electrode materials	:Graphite, copper, brass, zinc-tin, steel,, copper-tungsten, copper-graphite, silver- tungsten, tungsten
Servo drive gap	: 0.013 to 0.13 mm

Sensitivity Control Capacitance	: (on some style machines) from trial cuis
Polarity	: "Standards" is positive on workpiece, negative on electrode
Dependent Variables and Results Average current	: 0.1 to 500 A (A few large machines use multiple 500 A power packs, with separate leads.)
Spark gap	: 0.013 to 0.13 mm
Overcut	: 0.005 to 0.50 mm per side
Material removal rate	: 0.05 to 24.5 cm^3/hr
Wear ratio (ratio of workpiece erosion to electrode erosion)	:0.5:1 to 100:1
Source roughness	: R_0, 0.2 to 6.3 μu
Depth of recast and affected zone	: 0.005 to 0.13 mm
Corner radius	: 0.025 mm or equal to overcut
Taper	: 0.0005 to 0.005 mm/mm/side. With proper tooling, taper can be eliminated.

Laser Beam Machinrig (LBM)

3.1 PROCESS

Laser is acronym for the phenomenon called light amplification by stimulated emission of radiation. The phenomenon was first developed by Albert Einstein. However, the first laser was made possible only in 1960 by Maiman. Since then the laser has seen developments.

A laser beam can melt and vaporise diamond when focused by lens system, the energy density being of the order of 100,000 kW/cm^2. Such tremendous energy release is due to certain atoms which have higher energy level and oscillate with particular frequency. When such atoms impinge with electromagnetic waves having resonant frequency. The waves absorb energy from the atoms and become highly powerful. Such waves with increased energy are called "Maser" (Microwave amplification by stimulated emission of radiation). Laser was invented amplifying ordinary light waves on similar principles, i.e. to transmit the light waves with constant frequencies and wavelengths throughout without interference. Such light waves, i.e. laser may be concentrated for the release of tremendous energy.

3.2 BASIC MECHANISM OF LASER GENERATION

Laser light is generated by the transitions between high and low level of energy in various media. The mechanism deals with lasers converting electrical energy into a high energy density beam of light through stimulation and amplification. In addition, population inversion is another necessary condition for the lasing medium. Stimulation occurs when electrons in the lasing medium are excited by an external source such as electrical arc or flash lamp, resulting in emission of photons shown in Fig.3.1 The energy required to raise an electron from one energy state to another is provided by an excitation process or pumping. This achieved by lasing medium's absorption of energy from mechanical, chemical and light sources. The lasing medium typically contains ions, atoms and molecules whose electrons are conducive to change in energy level.

Amplifications of light in laser are accomplished by an optical resonator, which is composed of cavity with the lasing medium set between two high precision aligned mirrors. One mirror is fully reflective and other mirror is partially transmissive to allow output of the beam. Mirror channel the light back into the lasing medium as photon passes back and fourth through the lasing medium, they stimulate more and more emissions. Photons that are not aligned with the resonator are not redirected by the mirror to stimulate more emission, so that the cavity will only amplify those photons with proper orientation, and a coherent beam develop quickly. The details of the amplification phenomenon are shown in the Fig.3.2.

Population inversion is a prerequisite for laser light generation. The distribution of population of atoms at normal temperature is such that majority of atoms are in ground state with

few atoms in the higher excited state. Population inversion mechanism is shown in the Fig.3.3. Population distribution at thermal equilibrium can be changed by applying external energy to atoms such that there are selectively large no of atoms in some higher excited state than in the lower energy level as shown in the figure. This situation is called population inversion. As the population inversion is non-equilibrium state, the situation will not exist for long time and atoms form the higher excited state soon transformed to lower energy levels following the thermal equilibrium population distribution. Therefore, the stimulation emission is required for continuous population inversion.

The action of stimulation, amplification and population inversion is to produce a stream of photons with common characteristics, namely laser beam. This laser beam possesses temporal, spatial and energy properties that are different then diffuse light. These properties make the laser beam useful for many applications such as communication, measurement and materials processing, etc.
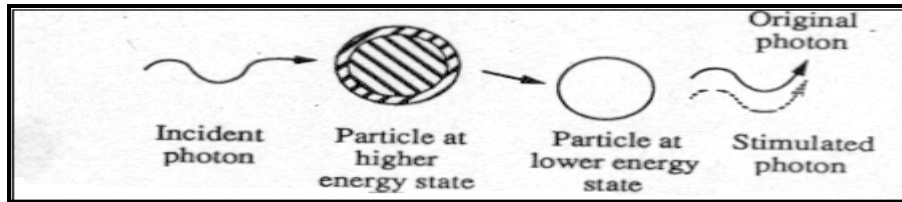
Fig. 3.1 Stimulation emission process
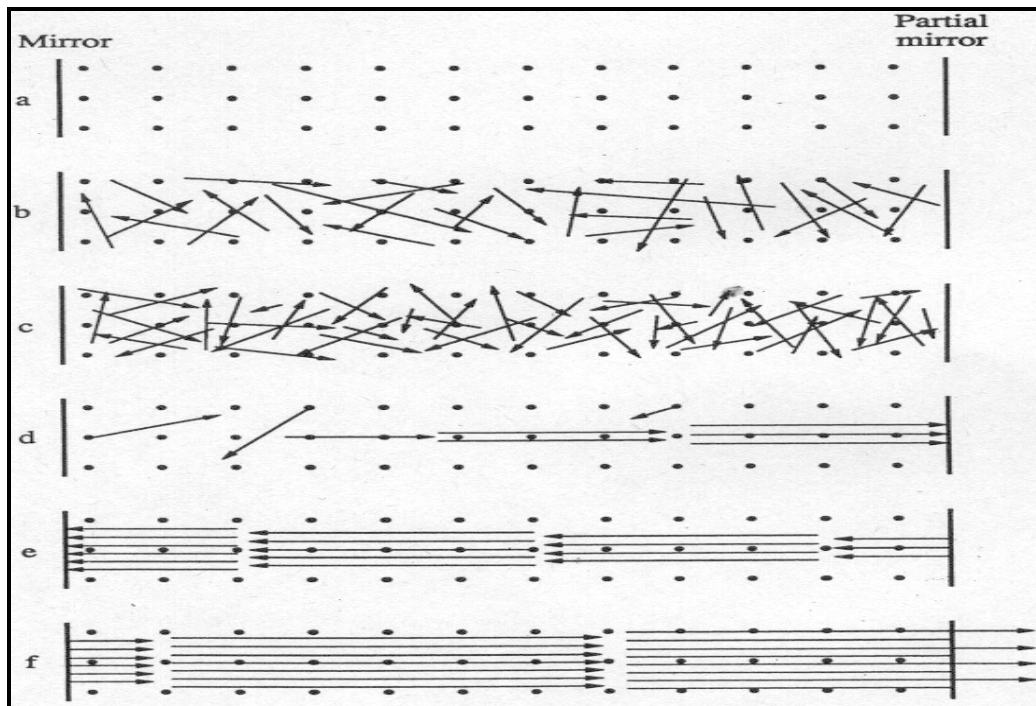
Fig. 3.2 Amplification, (a) Laser off, (b) & (c) Initial random states, (d) Initial stimulation, (e) Amplification, (f) Coherent beam
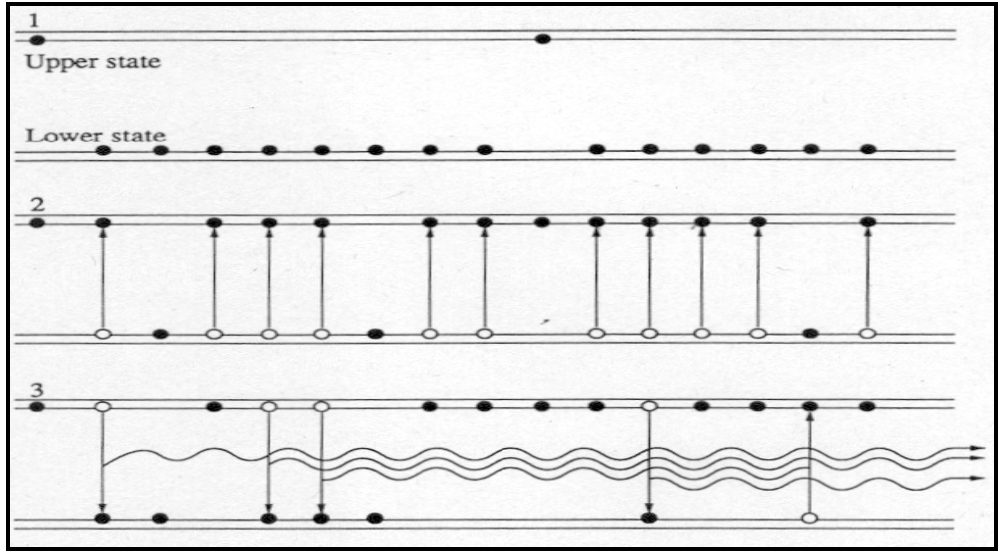
Fig. 3.3 Mechanism of population inversion

(1. Normal state. 2. Excitation state. 3. State of stimulated emission.)

3.2 LASING PROCESS

Operation of the laser depends on the utilization and, to some extent, manipulation of the naturally occurring transitions between the energy levels of a quantified system, such as atom.

In the Bohr-Sommerfeld model of the atom, negatively charged electrons orbit along specific paths (orbital) around a positively charge nucleus. The positions of the discrete orbitals depend upon a complex set of conditions, such as the number of electrons surrounding the nucleus, the existence of nearby atoms, and the presence of electric and magnetic fields. Each orbital defines a unique stationary energy state in tire atom. The atom is said to be in its ground state when all the electrons occupy orbitals that have lowest potential energies. At absolute zero ($0°K$) all electrons are in ground state. The electrons at the ground state can be excited to higher-energy state by absorbing energy of various form (Table 3.1) such as through vibrations at elevated temperature, by collision with other atoms or free electrons, via chemical reactions with other atom, or through absorption of photons (Fig. 3 4).
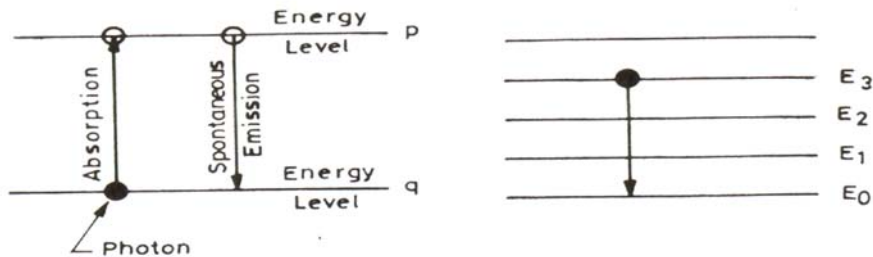
Fig. 3.4 Energy Diagram from an Atom Showing Level-to-Level Transition

For example, by the absorption of photon when the electrons are excited to higher state, they will almost immediately decay back to the ground state in about 10 ns and happens spontaneously. Spontaneous decay often results in spontaneous emission of photons. These have exactly the same frequency as the exciting photons. Light created from atoms may be in random direction but at well-defined wavelengths called "emission lines". These emission lines can intensify when more electrons are pumped (excited) to the higher energy state.

In an atom, some transitions are possible than the other. There are well established selection rules in quantum mechanics that predicts the probability of any given transition under various circumstances. This ultimately would determine the intensity of an absorption of emission line. However, sometimes the excited atom may be trapped in an energy state forbidding it for any downward transition. So the atom can linger in this so-called metastable state from micro to milliseconds range before decaying to a lower energy state.

The existence of metastable states can upset the thermodynamic equilibrium which normally prevails in atomic system. If enough electrons get hung up in a metastable state, its population would exceed the population of atoms in ground state. Thus creating a condition for "Population Inversion", which in thermodynamically unstable. When more energy at higher energy state is available for an avalanche waiting to happen, all that needed is some kind of stimulus to set the downward transition. Like stimulated absorption and spontaneous emission, Einstein proposed the powerful thermodynamic argument for the third kind of transition-stimulated emission (Fig. 3.5).Any device left to itself as considered above, the medium becomes a super-radiant mixture of spontaneous emission and stimulated emission, but
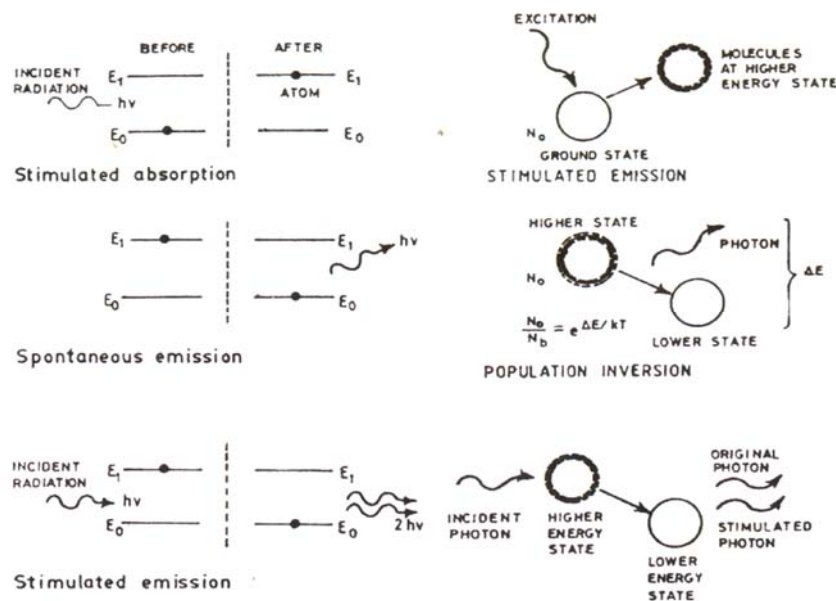
Fig. 3.5 Spontaneous and Stimulated Emission

is not a laser in customary sense of the word since the light radiate in all possible directions. Even if the population inversion persists, the medium will have a small gain, albeit the radiation have the laser like qualities. To achieve more efficient stimulated emission, the most effective ways is to contain the radiation is to place the laser medium inside a Fabry-Perot (Fig. 3.6) interferometer.
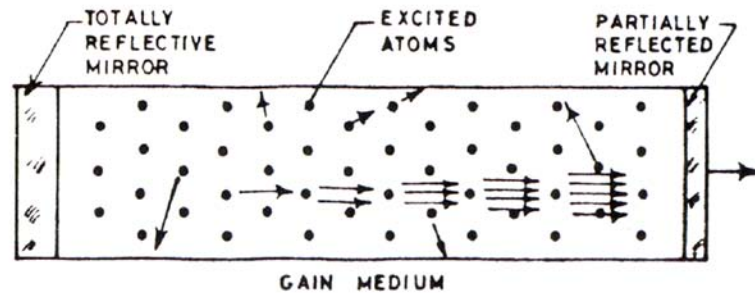
Fig. 3.6 A Fabry-Perot Interferometer, Laser Resonator

The resonant condition transforms the interferometer into a highly selective filter. The selectivity depends on the reflectivities of the mirrors. At resonant wavelengths, the reflectivity inside the cavity can be very high and create an excellent feedback environment for the laser gain medium.

Under the condition, the population inversion is high enough to overcome all the losses inside the cavity. The so-called threshold condition would be met and lasing will begin. To couple light out of the cavity, one of the mirrors is usually made partially reflective (a small hole in an otherwise totally reflective mirror would also suffice).

Because laser light consists mostly of stimulated emission with each pass through the gain medium, it is

- coherent—special and temporal
- high collimation-—high directional property
- intense—for any material processing application.

3.3 LASING MATERIALS

Many materials exhibit lasing action. However, only a limited number is used in metal working. Solids, liquids and gases can be used as lasing materials. The lasers are also classified according to the type of material used. In metal working, the solid state and gas lasers are generally used. Table 3.1 shows the classification and their functional relationships.

Solid state lasers consists of a host material which may be crystalline solid or glass doped with an active material whose atoms provide the lasing action. For example, the Nd-YAG lasers consists of a single Neodymimum. In ruby laser the aluminium oxide contains Cr^{3+} ions as active material.

Solid state lasers are pumped optically, generally by flash tube (Fig. 3.7). The flash tubes are mounted in a reflecting cavity parallel to the lasing rod.

In one of the arrangements, two flash or even more flash tubes are maintained on the foci of an elliptical reflecting cavity with the lasing rod parallel to the central axis. Gas lasers consists of optically transparent tube fitted with a single gas or a mixture of gases of the lasing material (Fig. 3.8). The gases used commercially are He-Ne, Argon, CO_2 etc. T'.i.e power source is the electric discharge between electrodes or flash tubes.

Table 3.1 Laser Classification and their Relationships
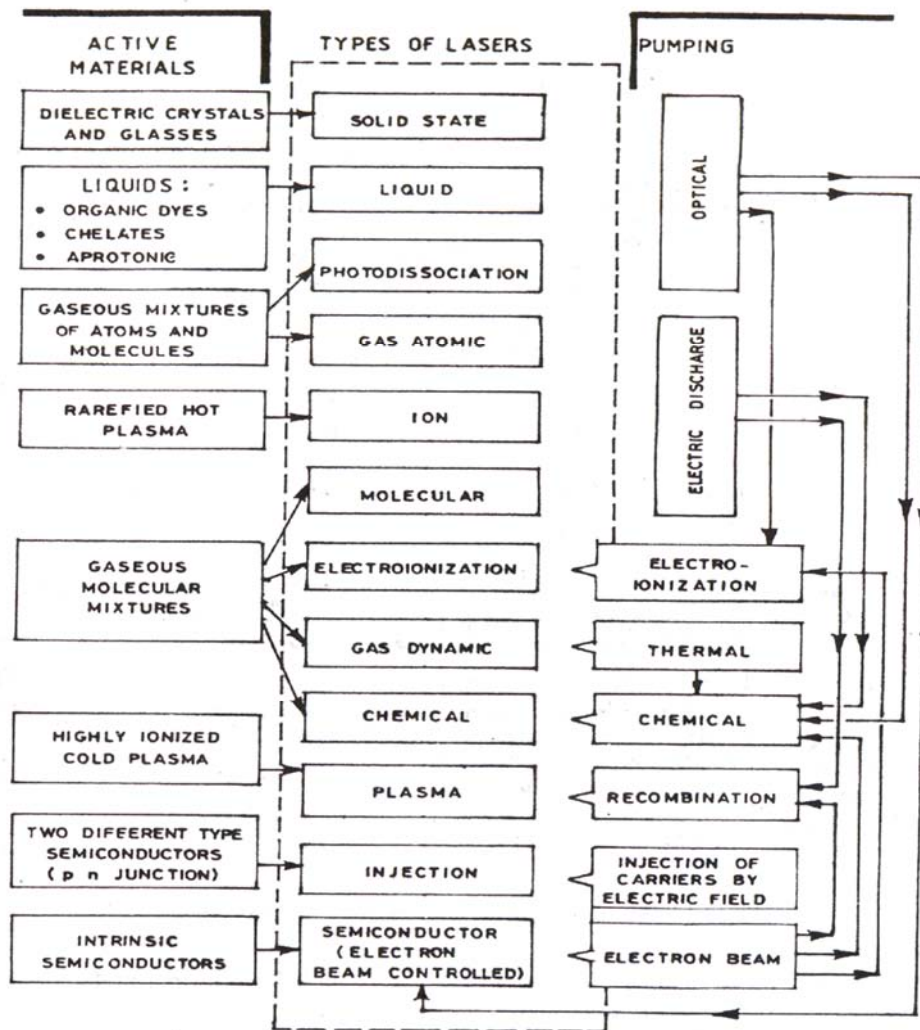
The power output is dependent on the length of the laser tube. Thus C02 laser can develop about 50 W for every meter length of tube. The problem of length could be overcome by arranging the short length tubes in a
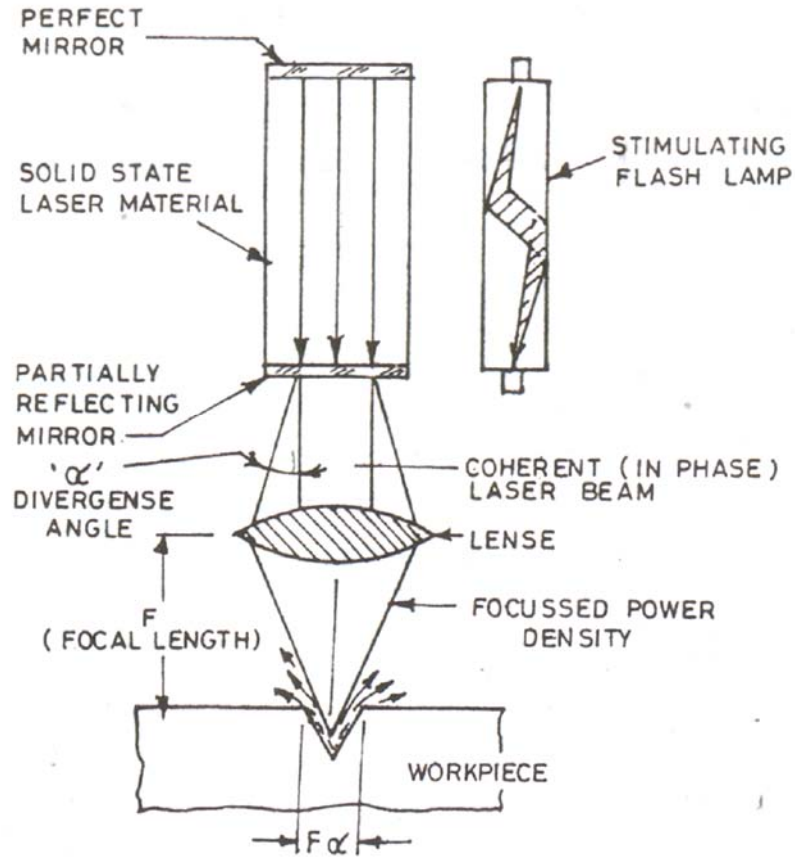
Fig. 3.7 Solid State Laser- A Schematic Diagram
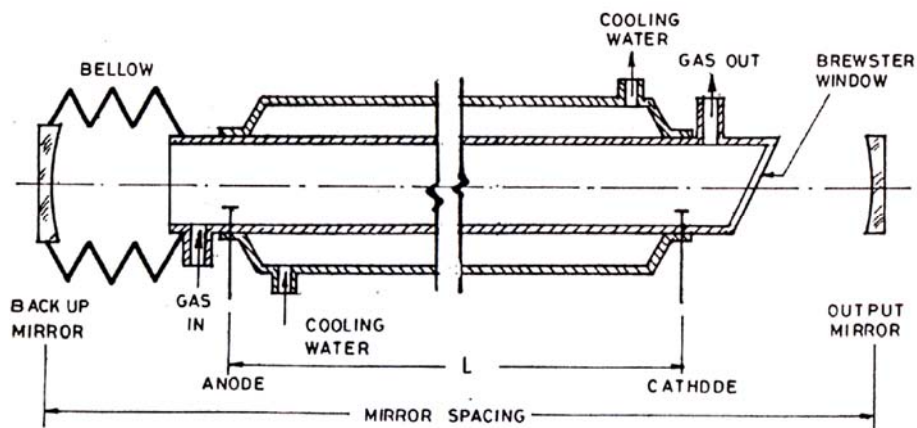
Fig. 3.8 Schematic Diagram of a Gas Laser

zigzag fashion with a reflecting surface at each end. Thus Ferranti Electric Inc. developed 400 W CO_2 laser in a length of 120 m.

A typical high power CO_2 laser contains three gases, namely CO_2, N_2 and He. CO_2 gives the molecular action to generate photons, N_2 reinforces and sustains this action and He provides intra-cavity cooling. In gas lasers, stabilization of discharge is very necessary which requires cooling of gas. There are also other types of gas lasers with axial gas flow and cross gas flow arrangements. Lasers are now available in a variety of power ratings, i.e. from a few milliwatts to 20 kW in the continuous wave (CW) mode and much higher

intensity in pulsed form (Table 3.2).

Table 3.2 Typical Laser Systems

Gas Lasers

Type	Wave-length (μm)	Beam divergence (mr a d)	Beam diameter $(1/e^2\ pt,\ mm)$	Operating mode	Ripit rate (pps)	Pulse Width (s)	Power (W) TEM 00	Multi mode
		0.8	1.1				0.001	
H_eN_e	0.6328			CW				
		1.0	1.4				0.005	
		2	10	CW			200	250
CO_3	10.6	2	10	Pulsed	1000	0.001		600
		2	10	Q-Switch		0.5×10^{-6}		100000
			30	CW				1000
CO_2 (Tea)			0.25	Pulsed	400	0.4×10^{-6}		100000

Solid State Lasers

Type	Wave-length	Beam divergence	Beam diameter	Operating mode	Max pulse Engy (J)	Output Peak Power (W)	Characteristics Pulse width (μs)	Rep rate (pps)
Ruby	0.6943	10	6	Pulsed	80	10^5	300-600	1
$Cr^{3+}Al_2O_3$				Q-Switch	20	10^9	0.015	2 (ppm)

				Pulsed	125	10^6	500-10ms	1
Nd^{3+} glass	1.06	10	6	Q-Switch	30	10^9	0.015	2 (ppm)
		3	4	Q-Switch	0.005	5×10^3	0.1	500000
Nd^{3+} YAG	1.64	8	4	Pulsed	30			20
		3	4	CW (TEM_{00}-20W, Multi Mode-150W)				

Laser action can be obtained over the entire frequency range from ultraviolet to infrared. Figure 9.6 shows some of the lasing materials and their frequency range. Lasers commonly used in metal working have wavelengths ranging from 0.6 to 10.6 μm.
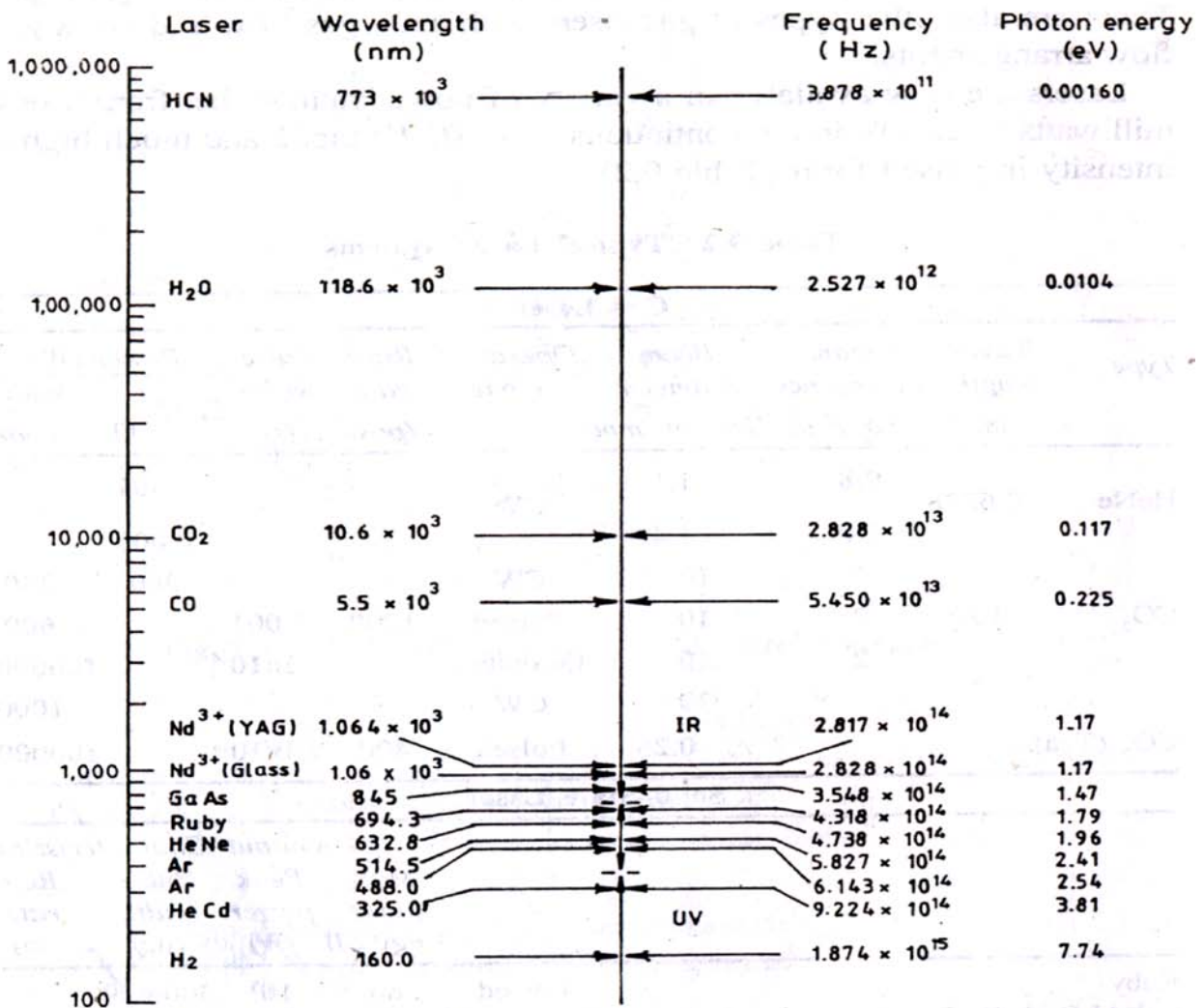
Fig. 3.9 Typical Available Lasers and their Radiation Properties

3.4 PROCESSING WITH LASERS

The general arrangement of using a laser for material processing is shown in Fig. 9.7.

A: Laser Head
B: Rotating Mirror and Lens Assembly
C: Rotating Mirror
D: Work Table
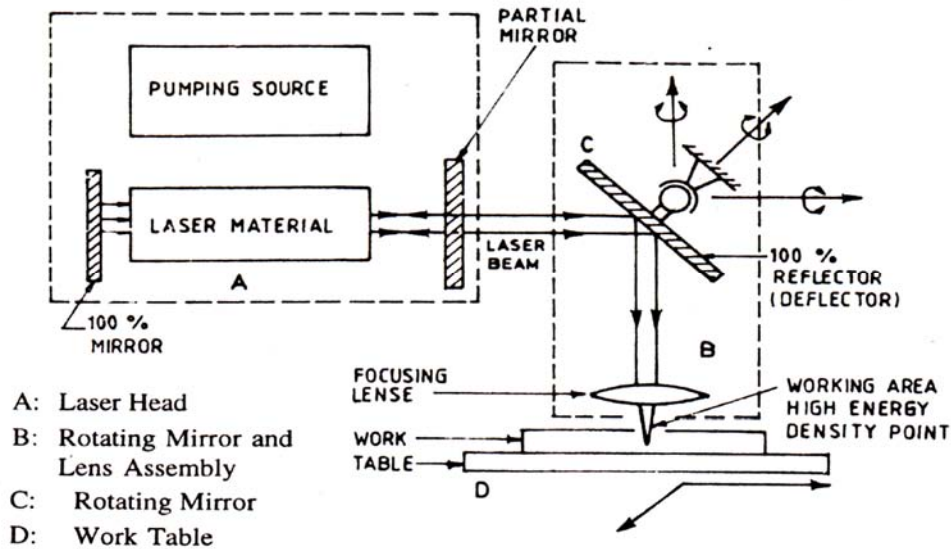
Fig. 3.10 A Schematic Representation of a Material Processing Laser Work Station

Because of their special characteristics, lasers give rise to certain advantages in metal processing. Table 3.3 lists these advantages.

Table 3.3 Characteristics of Laser Beam and Laser Beam Machining

SI. No.	Special characteristics of laser beam	Cutting process characteristics
1.	Can be focused to maximum intensity or to lower intensity as needed	High cutting speed narrow kerf straight sides little affect
2.	Can be moved rapidly on the work	Cutting of complex shapes No tool/work contact, precision location
3.	When projected some distance from the lens	Remote cutting over long stand-off distances
4.	Dedicated to an on-line process	No re-routing necessary
5.	Time shared between stations	Cut, then weld using same beam use for additional cutting stations
6.	Power shared on a job or between stations	Two or more cuts simultaneously

3.5 Nd:YAG Laser Generation Process

Solid state lasers use ions suspended in a crystalline matrix to produce laser light. Nd:YAG laser is one of the most widely accepted solid state laser used for micro machining. The name of this laser represents the composition of the crystal gain material i.e. Neodymium (Nd) doped Yttrium Aluminum Garnet (YAG). In Nd:YAG lasers, Neodymium atoms (lasing media) are embedded in a YAG crystal host ($Y_3Al_5O_{12}$). The Neodymium atoms are doped in this host. The concentration Nd in YAG crystal is 1% by weight .

The YAG crystal has excellent thermal, mechanical and optical properties to produce efficiently a high quality coherent laser beam. The Nd:YAG laser's strongest advantage over other lasers is its ability to produce a continuous beam at room temperature, which allows the laser to be used in typical work place environments without any major modifications. These properties have all contributed to the wide acceptance of the Nd:YAG laser in cutting, micro-machining and other processing applications. It is operated at 1064 nm wavelength. There are two types of YAG lasers, continuous wave and pulse mode. This is having distinctly different output characteristics and material processing capabilities. Peak power, pulse energy and pulse repetition rate are useful indicators for determining the processing speed and capability of pulsed Nd:YAG lasers. The efficiency of this laser is comparatively high. To achieve high power and low divergence from Nd:YAG rod it is necessary to cascade several rods and to pump each optically. A typical schematic Nd:YAG laser diagram is shown in fig. 3.11

The solid-state laser usually uses krypton or xenon flash lamps for optical pumping. Krypton lamps have low operating current and high-energy efficiency, so they are useful for continuous wave operation. Two mirrors are provided in case of Nd:YAG laser the back mirror has reflectivity of 100% and the front mirror has reflectivity of about 80%. To improve the beam-quality, aperture is used in the resonator to eliminate highly amplified divergent light when it is operated on fundamental mode (TEM_{00}). The safety shutter is provided to block the lasing action for long period. To control the heat generation a cooling system is provided for operation of Nd:YAG lasers. With an efficiency of 3%, a typical Nd:YAG produces thirty times as much waste heat as laser output.

The out put characteristics of a Nd:YAG laser can be altered by varying the pumping discharge waveform. Laser beam pulse frequency and shape can be tailored by using Q-switching, where a shutter moves rapidly in and out of the path of the beam. In this manner, beam output is

interrupted until a high level of population inversion energy storage is achieved in the resonator. Fiber optics materials for beam delivery and transportation can be used for Nd:YAG laser radiation.
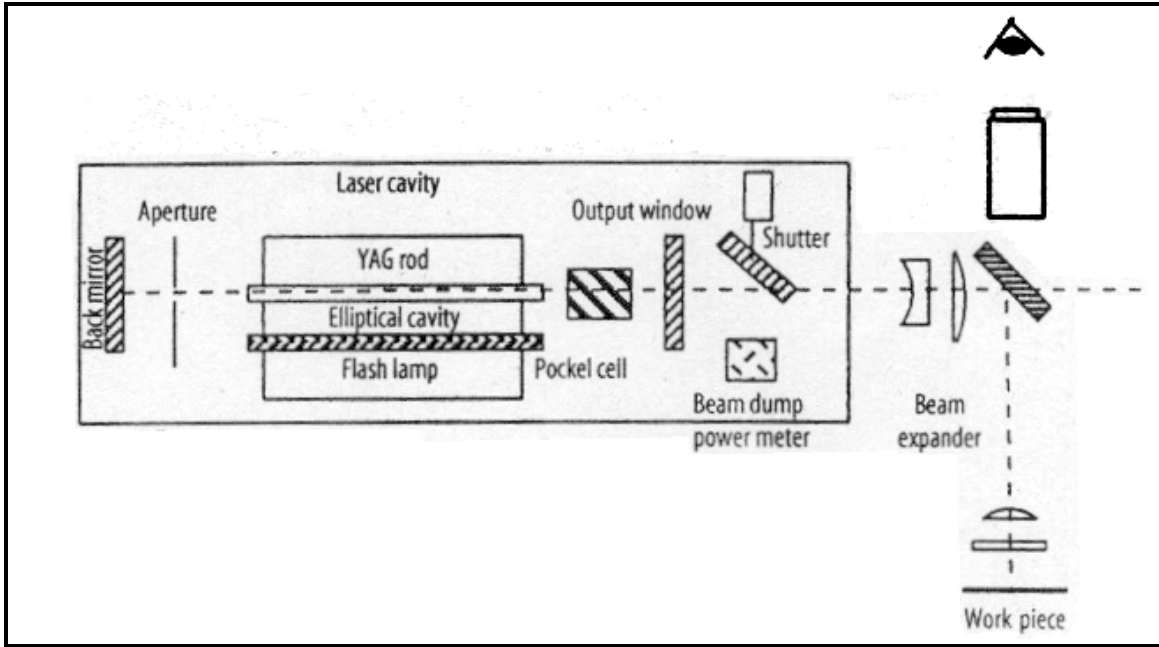
Fig. 3.11 General Construction of Nd:YAG Laser [ ]

3.6 Carbon dioxide

Gas lasers based on molecules emitting light on transitions between vibrational energy levels differ in important ways from the electronic-transition gas lasers. The most important functional differences are their longer wavelengths in the infrared and the higher efficiency of some irrational transition lasers.1he best known of this large family of lasers is the carbon dioxide (CO_2) laser. widely used in industry and medicine. Chemical lasers also are vibrational lasers, but their different characteristics make them more important as potential high-energy laser weapons. The commercial importance of the CO2 Laser comes from its combination of high efficiency and high output power. Typically 5-20% of input power emerges in the output beam ,the highest of any gas laser. although lower than some semiconductor lasers. This high efficiency limits both power consumption and heat dissipation. so industrial CO2 Lasers can generate continuous powers from 1 W to 10 kW. Typical powers are below I kW.

In addition to being efficient, the CO2 laser lends itself to efficient removal of waste heat left over from laser excitation. Flowing gas through the laser can remove waste heat efficiently, by transferring the heat to flowing air surrounding the tube, flowing water, or in some cases, exhausting the laser gas directly to the atmosphere . CO2 Lasers emit at wavelengths between 9 and 11 Um. The strongest emission is near 10.6 um which is often li1ed as the nominal

wavelength. These wavelengths are strongly absorbed by organic materials ceramics water, and tissue; Therefore, tens of watts often suffice for applications such as cutting plastics or performing surgery. By contrast, most metals reflect strongly at 10nm. so metal working requires higher powers at that wavelength than at shorter wavelength. Years of engineering development have made the CO_2 laser a practical tool for moderate-to-high-power commercial application. Laser weapons require considerably higher powers-officially classified, but unofficially at powers of 100 kW and greater-available from various chemical lasers.

3.6.1 EXCITATION

The standard technique for creating a population inversion in CO_2. and most other vibrational lasers is to apply an electric discharge through the gas. Typical voltages are kilovolts or more, and as in electronic-transition lasers, a higher voltage may be needed to break down the gas and initiate the discharge. Total gas pressure must be kept below about one-tenth of atmosphere to sustain a stable continuous discharge, and this is the standard operating mode for most commercial CO_2 lasers.

The addition of other gases aids in energy transfer to and from CO_2 molecules Molecular nitrogen absorbs energy from the electric discharge more efficiently than CO_2 does. Because nitrogen's lowest vibrational mode has nearly the game energy as the upper laser level of CO_2. It readily transfers the energy to the CO_2 during a collision. Thus, adding nitrogen to the CO_2 in the laser discharge enhances the excitation process.

Helium is added to the gas mixture in a CO_2 laser because its thermal conductivity is much higher than CO_2 so it can efficiently remove waste heat from the gas mixture. He also plays a role m depopulating the lower laser level, thereby increasing the population inversion.

An alternative way of exciting CO_2 is by thermal expansion of a hot laser gas, in what is called a gas-dynamic laser Very rapid expansion of hot gas at temperatures of about 11OO'C and pressures above 10 atm through a fine nozzle into a near vacuurn produces a population inversion in the cool. low-pressure zone. This approach can generate high powers in the laboratory but has not found commercial application.

3.6.2 TYPES OF CO2 LASERS

Several types of CO_2 lasers have been developed for particular applications. Like other gas lasers, commercial CO_2 lasers usually generate a continuous beam. but they also can be pulsed by modulating the discharge voltage.

The simplest type is a sealed-tube CO_2 laser with longitudinal discharge passing along the length of the tube. as shown in figure below.

Waveguide Co_2 lasers are a variation on sealed Co_2 lasers in which the discharge and laser gas are concentrated in a laser bore a few millimeters across. which functions as a waveguide for

10-nm light, The wave guide design reduces the diffraction losses that otherwise would occur in a laser with output aperture a relatively small number of wavelengths across.

Flowing gas Co_2 lasers can provide higher powers than static sealed lasers because the gas is blown through the tube. The heated gas in the tube is constantly being replaced new, cool gas. The key variables in flowing-gas CO_2 laser are the speed and direction of flow. Typically flow is longitudinal, along the length of the laser. Because this gas flow through a wide aperture, it does not have to flow as fast as in a ***longitudinal-flow laser***.

Gas-dynamic CO_2 lasers are quite distinct from other CO_2 lasers because they rely on a different excitation mechanism. Hot CO_2 at high pressure is expanded through a small nozzle into a near-vacuum. a process that produces a population inversion as the expanding gas cools.

Transversely excited atmospheric (TEA) CO_2 lasers, unlike other types, are designed for pulsed operation at gas pressures of 1 atm or more the electrodes are placed on opposite sides of the laser axis. as in other transversely excited lasers, but the discharge fires pulses into the gas lasting nanoseconds to about 1 ns, producing laser pulses of the same length. TEA CO_2 lasers cannot generate a continuous beam, but they are attractive sources of intense pulses of 40 ns to about 1 ns.
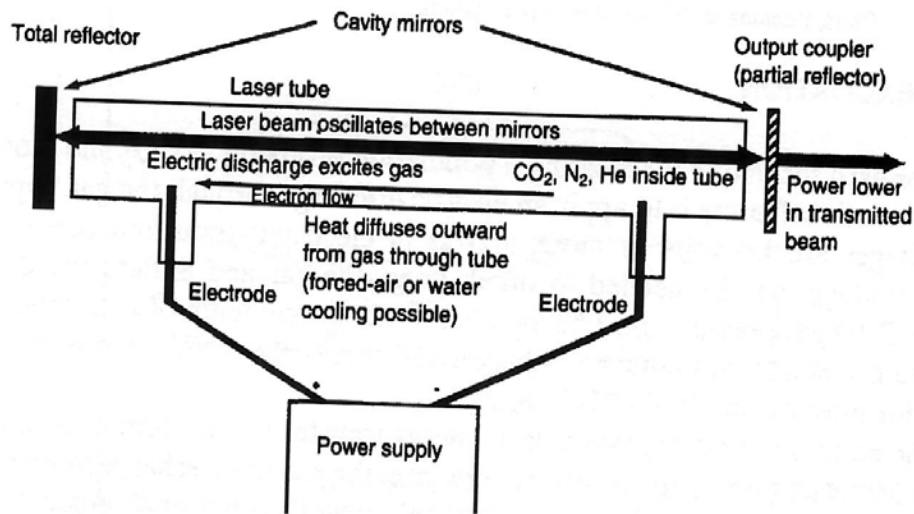
3.12 Sealed tube CO2 laser with Longitudinal discharge

3.8 MACHINING APPLICATIONS OF LASER

Besides the usual applications in communications, ranging navigation, meteorology, metrology etc. laser has a wide range of machining applications. Metal processing by laser may categorised as follows:

(a)   Material removal (drilling, trimming, and evaporated),

(b)   Material shaping (cutting, scribing and controlled fracturing,

(c)   Welding,

(d)   Thermokinetic change (annealing, photo-chemistry, grain size controls, diffusion. Zone melting etc.

3.8.1 Drilling Holes by Laser

Micro sized holes can be laser drilled in difficult to machine or refractory materials. This is the biggest area of application in laser machining.

Hole drilling by lasers is a process of melting and vaporising unwanted material by means of narrow pulsed laser operating at 2 to 100 pulses/s. Because of the very nature of melting and vaporisation processes, very high accuracy is not possible. The shape of the hole drilled by laser is shown in Fig. 3.13.

(a)   Cross section   (b)   Axial section
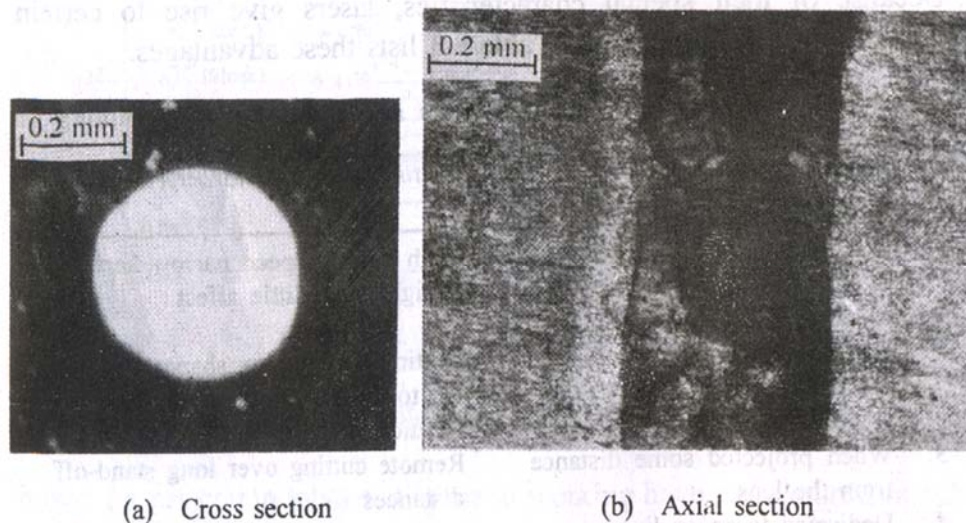
Fig. 3.13 Quality of Hole Drilled by Laser

It is essentially a tapered hole, bell shaped at the top. The hole generally has on its surface a layer of material which had melted and later cooled and solidified. In case of brittle materials this layer have cracks as well.

3.8.2 Advantages of Laser Drilling

The advantages of laser drilling are:

1.   No physical contact between work-tool pair, hence there is no possibility of breakage or wear of tool.

2.   Precision location is ensured by focusing of the beam.

3.   Large aspect ratio (depth to diameter) can be achieved.

4.   Very small holes can be drilled in very hard materials like diamond in seconds.

Further, it has been suggested to use unidirectional multiple pulses for deep hole production. The reasons are:

1.   Single shot vaporisation and material removal by laser in punching a deep hole would require much more energy than that contained in the single pulse.

2.   Time required for heat transmission through the hole thickness is much longer than the short timed pulse.

3.   Uniform diffusion of heat in all directional would occur instead of concentration in the drilled out cylindrical volume.

3.9 OPERATING SUMMARY

Selection

Application	Type of laser
Large holes up to 1.5 mm dia. Large holes	Ruby, Nd-glass, Nd-YAG
(trepanned)	Nd-YAG, CO_2
Small holes > 0.25 mm dia.	Ruby, Nd-glass, Nd-YAG
Drilling (punching or percussion)	Nd-YAG, Ruby
Thick cutting	CO_2 with gas assist
Thin slitting of metals	Nd-YAG
Thin slitting of plastics	CO_2
Plastics	CO_2
Metals	Nd-YAG, Ruby, Nd-Glass
Organics, Nonmetals	Pulsed CO_2
Ceramics	Pulsed CO_2, Nd-YAG

Relative Power to Evaporate Equal Volumes in Equal Time

Aluminium	1.0
Titanium	1.5
Iron	1.8
Molybdenum	2.2
Tungsten	2.9

Operating Parameters

Lasing Materials :	Ruby	Nd-YAG	Nd-Glass	CO_2
Type :	Solid state Smallest spot, High peak power, high absorption for metals.	Solid state	Solid state	Gas High efficiency
Composition :	0.03-0.07% Nd in Al_2O_3	1% Nd doped Yittrium Aluminium Garnet	2-6% Nd in Glass	CO_2+He +N_2 (Typically 3:8:4)
Wavelength (radiation) Efficiency	0.69 μm 1% max.	1.064 μm 2%	1.064 μm 2%	10.6 μm 10-15%
Beam Mode	Pulsed or CW	Pulsed or Cw	Pulsed	Pulsed or CW
Spot Size :	0.015 mm	0.015 mm	0.025 mm	0.075 mm
Pulse Reptn. Rate (Normal operation)	1-10 pps 10-100 W	1-300 pps or CW 10-1000 W	1-3 pps 10-100 W	CW 0.1-10 kW
Beam Output :				
Peak Power :	200 kW	400 kW	200 kW	100 kW
Beam	5-7 mRad.	1-5 m Rad	5-7 mRad	0.1-10 mRadian
Divergence Excitation	Optical Pumping through Krypton, Elect. Xenon or Tungsten-halogen lamps Discharge.			

Process Capability Drilling Diameter	0.005 to 1.25 mm but larger may be achieved by trepanning)
Drilling Depth	up to 20 mm
Drilling Angle to Surface	15 to 90°
Drilling Taper	5-20% of hole diameter.
Drilling L/D Ratio	Up to 50 : 1
Drilling Length, trepanning	Up to 6.5 mm

Drilling Tolerance	± 5-20% of hole diameter
Minimum Corner Radius	0.25 mm

MODULE – IV

Electron Beam Machining: Basic Principle, Controlling Parameters and focal distance, Application

Ion Beam Machining: Principle and Mechanism, Application

Plasma Arc Machining: Generation of Plasma, Equipment's, Torch, Classification, Direct and indirect torches and application, parameters effecting cutting, Advantages.

Electron Beam Machining (EBM)

1.1 INTRODUCTION

A comparatively recent innovation in the field of metal processing has been the use of high energy density beams. Electron beam is one of the three such sources. The major user of this beam has been the field of welding technology where the high concentration of energy provided considerable advantages like deep penetration, low distortion and clean welds. However the facilities provided by these heat sources, particularly the electron and laser beams, made these very suitable for other applications also. Some of these are the availability of energy in the form of controlled energy pulses, the capability to vary the current density at will, very fine beam focusing to small diameters to a longer focal length as compared to laser beam, if required and clean atmosphere of evacuated electron beam chamber.

The other applications of electron beam, besides welding, are:

(a) High speed perforation of small dia holes

(b) Through thickness cutting of any kind of material

(c) Engraving of metals and ceramics

(d) Thin film machining

(e) Surface treatment including surface alloying.

The various hole drilling and surface machining capabilities of electron beam are :

(i)   High speed perforation in any kind of material.

(ii) Perforation of small diameter holes in thick materials.

(iii) Drilling of tapered holes

(iv) Perforation of inclined holes

(v)   Non-circular hole drilling

(vi) Engraving of metal, ceramic and vaporised layers

(vii)   Machining of thin films to produce resistor network in IC chip manufacture.

These capabilities of electron beam have been utilized in specific applications and in some applications the process has shown definite advantages over the other competing processes. One major drawback in some of these applications has been the requirement of high degree of vacuum essential or satisfactory operation of this process because of degassing.

However, in the field of welding, negligible distortion and very narrow and deep welds produced by electron beam have made it suitable for many

1.2 PROCESS TECHNOLOGY

The process involves generation of a beam of rapidly moving electrons in an electron gun. High velocity of electrons is achieved by use of accelerating voltage of the order of 100 kV. The narrow beam so produced moves inside a vacuum (of the order of 10^{-6} torr) the beam retains its narrow configuration over a long distance. When this beam hits the work piece it results in the development of intense heat resulting in fusion and partial vaporisation of material. Depending upon the beam strength it may penetrate up to considerable depth. Either the work piece can be moved under the beam using a numerically controlled table or the beam itself can be deflected using a magnetic deflection coil. Generally deflection method is used only or small movements. The scheme is shown in Fig. 1.1.
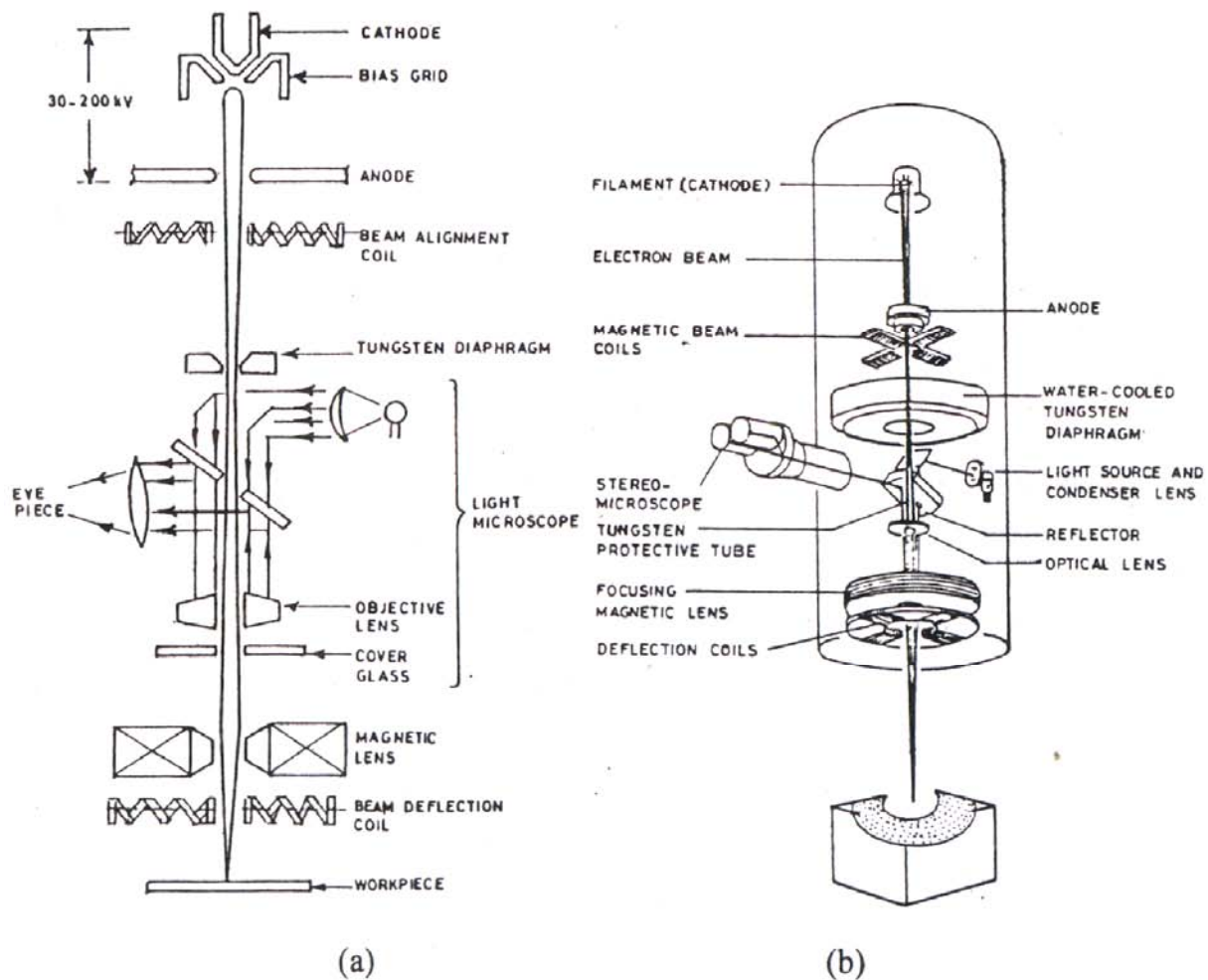
Fig. 1.1 Electron Beam Gun Construction Scheme

1.3 GUN CONSTRUCTION

The main features of the welding gun, first constructed by Steigerwald are shown in Fig. 1.1. It consists of a tungsten cathode which is heated by a low voltage current. On heating it emits electrons mainly by thermionic emission. These electrons move towards the anode which is kept at a potential difference of 30-200 kV. Such high voltage accelerates the electrons to a high velocity. The use of a grid around the cathode helps in further narrowing the beam and this grid is also used for controlling the beam current. The beam passes through central hole in the anode. A tungsten diaphragm, with a small central hole, separates this portion of the gun from the rest of it. Light microscope helps in focusing the beam on work piece initially. The magnetic lens further converges the beam into a narrow spot on the work piece. A beam deflection coil can be used to deflect the beam further either onto a different spot on the work piece or for moving it along a contour.

The parameters which have significant influence on the beam intensity are the beam current, the beam diameter when it is focused on the work piece (normally known as spot diameter) and the focal distance of the magnetic lens. Every electron beam machine has provision for adjusting these three parameters. However, the limit of these adjustments should be clearly understood in order to use these wisely.

1.4 CURRENT CONTROL

The heated cathode emits electrons depending upon the thermionic emission capability of the cathode given by Richardson-Dushman equation, i.e.

$$J = AT^2 e^{-(EW/KT)} \qquad\qquad (1.1)$$

where

J = current density (amp/cm^2) of the emitted current

W = work function of the material of the cathode (volts)

T = absolute temperature of cathode (K-Kelvin)

E = electronic charge (coulomb)

K = Boltzmann constant (1.3 x 10^{-23} J/K)

A = constant (⊔ 120 amp/cm^2 (degree)^2

Although the above equation gives the density of the current emitted by the cathode in free space, the presence of electric field around the cathode alters this current density very much. Thus one factor which controls the beam current is the grid voltage. The more negative the grid

is with respect to the cathode, the more it restricts the emission of electrons. This charges the area on the cathode from where the electrons are emitted besides

changing the magnitude of total beam current which is dependent on the electrons emitted from cathode. Thus a decrease in beam spot size is not independent of beam current and it is generally associated with a decrease in beam current. The design of grid bias and its shape itself affects the electron gun performance appreciably. However, we thus conclude that a simple way of controlling beam current is to change grid bias voltage.

1.5 CONTROL OF SPOT DIAMETER

The spot size is a complex function of beam current, accelerating voltage, magnetic lens, ampere turns, distance between gun and work piece (throw-distance) etc. Following are the three effects which contribute to change in spot diameter.

(a)   *Effect of thermal velocities*: It is well known that all the electrons associated with the electrons will be distributed around some mean value. This will result in different electrons converging at different points along the longitudinal axis of the beam. Hence the spot size will get spread out and the minimum spot size thus obtained is given by

$$\delta T = 2r_T = \left(2r_c / r_i\right)\xi\sqrt{KT / EV}\tag{1.2}$$

where δT is the minimum spot diameter, r_c the cathode spot radius, r. radius of beam at magnetic lens, ξ the throw distance, V is anode voltage and K, T are Boltzman constant and cathode temperature, respectively.

(b)   *Space charge spreading of target*: Electrons converging in a conical beam to a point at the target will be subjected to mutual repulsion which limits the minimum spot size attainable. The repulsion becomes increasingly severe with increasing current in the beam. An approximately formula for the minimum spot size at the target is as follows:

$$\delta_s / 2 = r_s = 5.9 \times 10^4 \xi^{5/2} I^{5/4} V^{-15/8} r_i^{-3/2}\tag{1.3}$$

where distances are in cm, potential in volts and current in ampere.

(c)   *Spherical aberration of the focusing lens*: Spherical aberration results in the marginal rays crossing the axis at a different position from the rays.

This causes an ideal point image to be confused in a disc whose minimum diameter is given by

$$\delta_s = 2.5 \ r_i^3 \left[\xi / \left\{f\left(S+D\right)\right\}^2\right]\tag{1.4}$$

where *S* and *D* are lens pole piece separation and bore diameter, respectively, in the case of magnetic lens and *f* is the focal length of the magnetic lens.

The combined effect of the three degradation in spot leads to the following formula for minimum spot diameter

$$\delta = \sqrt{\delta_T^2 + \delta_S^2 + \delta_S^2}$$ (1.5)

1.6 CONTROL OF FOCAL DISTANCE OF MAGNETIC LENS

The general formula for the focal length of a magnetic lens is

$$f / (S + D) = 25v / (NT)^2$$ (1.6)

where *V* is the electron accelerating voltage (150 kV or so) and *NT* is the ampere turns in the lens winding.

The discussion above briefly explains how the three different gun parameters like beam current, spot diameter and focal length of focusing lens are controlled and what are the limits imposed on these. However, an exact theoretical determination of these parameters for a particular setting on a machine is very difficult. This demands some trial runs on the machine to find out spot diameter, focal length and beam current under different setting of machine. The above mentioned equations can be used as guide for knowing the trend.in variation of these values with changes in operating parameters.

1.7 CURRENT PULSING

In many application like hole drilling and perforation, a current pulse having fixed amount of energy is required. As has been explained earlier, the increase in grid bias (or the negative voltage at the grid) reduces the beam current and decreases the spot size. The grid bias can be increased to an extent so as to reduce the beam current to zero. This effect is used to supply constant energy electron beam pulses. A pulse of high negative bias is applied at grid which in turn produces an electron beam pulse by switching on and off the beam.

1.8 APPLICATION

The areas where electron beam machining has found application are drilling of large number of small diameter holes at a very rapid rate such as perforated screens used for filters, drilling of large number of cooling
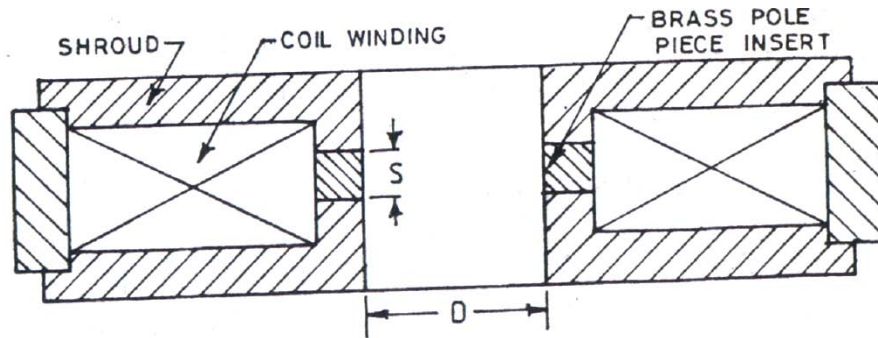
Fig. 1.2 Construction of Magnetic Lens

holes in the leading edges of a turbine blade. Another application reported is drilling holes in spinning head for the production of glass fiber. There were 6000 holes of 0.8 mm dia. on the periphery of 3 mm thick 200 mm j dia. spinning head. The drilling speed was 20 poles/sec.

Engraving of resistor network for production is for production of thin film hybrid circuits and also such machining of thin films used for production IC's are some other application examples.

A machine for electron beam machining reported in the literature had a 1 kW rating. It had highly stabilized voltage supply to give very small spot diameter. The capabilities of this machine reported were: (1) Pulse generation of 10 ps to 20 ps duration up to a frequency of 10 kHz. (2) Range of possible hole size between 25 pm dia. in 20 (im thick foil to 1 mm hole in 5 pm thick sheet.

The machine had the provision of complex numerical control like with facilities for monitoring the current pulse etc. so that proper coordination l of hole positioning, pulsing etc. can be done. With this a high drilling rate of few hundred holes per second can be attained. In fact, for application like perforation of synthetic leather, a machine with the capacity of producing few tens of thousand holes per second has been reported. Figures 10.3 and 10.4 give some of the data on the hole drilling capabilities of such machines.
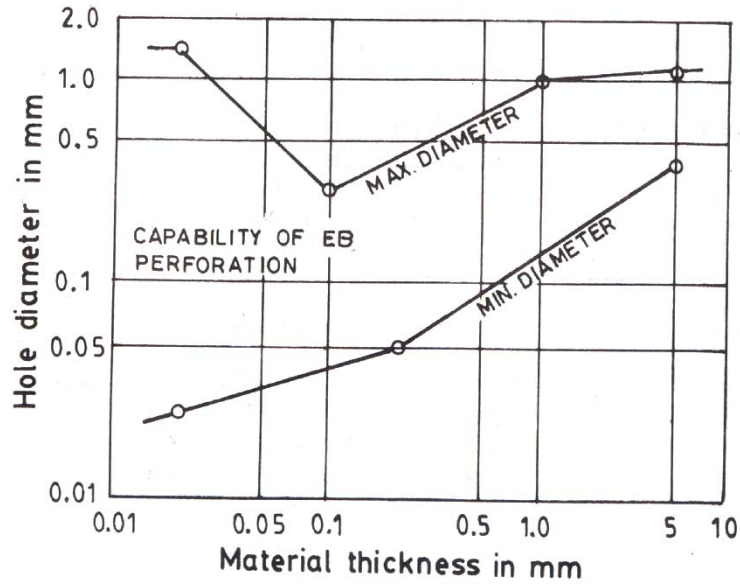
Fig. 1.3 Capability Range of Perforations Valid for Steel Nickel Alloys
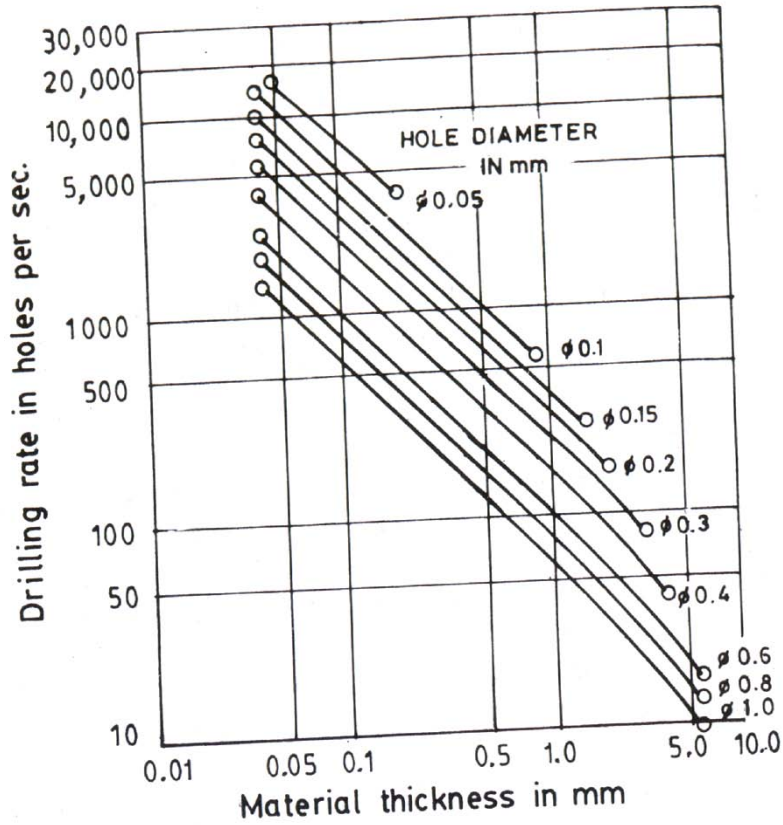
Fig. 1.4 EB Perforation EB Rate of Steel and Nickel Alloys

Ion Beam Machining (IBM)

2.1   INTRODUCTION

Ion-Beam Machining (IBM) is an electro-thermal process, which in real sense uses charged particles in vacuum to remove the material from the work surface. This process is different from other thermal-thermal processes like E.B.M. and E.D.M. since it uses sputtering of ions primarily as the method to remove material from the work-surface, whereas, the bombardment of electrons in EDM and EBM, bombardment of heated ions in PAM or bombardment of photons in LBM shall heat, melt and vaporise work materials.

In the process, sputtering is the main phenomenon widely used to remove the work-material from any surface. In the process, the surface atoms are dislodged from incident bombarding ions. Thus it is not a thermo-electric process. Here ions are formed by knocking of electrons from the atoms and are accelerated in an electric field which collide with the work surface. A transfer of kinetic energy takes place on the work surface to its atoms to.finally dislodge it off the surface atoms. Energetic ions cause rearrangement of atoms of the solid in displacement cascades, remove near surface atoms by sputtering and may be incorporated with over turn or back off the work surface.

The foregone explanation reveals that by sputtering a high yield of ions is required since that well increase the sputtering yield and remove work more faster. Sputtering ions is also assisted by striking of metals but since they have comparatively low velocities, they cannot be used to dislodge sizable quantities of work. Thus sputtering coefficient or sputtering yield Y, is defined as,

$$Y = \frac{\text{Number of atoms removed}}{\text{Number of striking ions}} \qquad (2.1)$$

The yield can increase if the atomic weight of the bombarding ion is more due to high momentum transfer and the angle of grazing or incidence, i.e. the angle of incidence on the work surface material. It is found that disordering of atoms transforms crystalline structure into amorphous phase as observed in covalently bonded elements.

2.2 BEAM SOURCE

Since the primary element of interest is ion, it is necessary to get an ion by knocking out electrons to get cations or for anions. Here the principle of electron discharge through a gases or Glow-discharge characterized by high voltage is used as a source of energetic electrons.

To generate a glow-discharge the primary set up comprises of two electrodes in an enclosure. Pressure of the gas inside the glass chamber is specified reduced pressure ranging from 10~3 to 10-s atm. This range is termed as "soft vacuum". The voltage across the two electrodes is of the order of 1 kV to l00 kV range. This result into an electron beam. The beam power can be varied over a wide range. The ability of soft vacuum to produce varied glows and spaces need be exploited for two reasons.

- It is technically advantageous in material processing, and
- economically advantageous in engineering.

Thus a true optimisation is required to increase effectiveness of the system.

However, for an optimality of the process the following are searched and expedited.

(a) Electrode Characteristics

Two electrodes mounted in a vessel (glass or metallic) at reduced pressure have a voltage characteristics at a specified current. This is given by,

$$EC = pd \tag{2.2}$$

where p = pressure of gas in torr (1 torr = 1 mm Hg) and

d = dimension between the electrodes, cm.

The actual function depends on (i) nature of the gas, (ii) material of electrodes, (iii) electrode geometry and (iv) time and temperature.

Usually, plant or hollow cathode type arrangements are made, the latter being more useful for thin beam glow discharge sources. Scaling of a given geometry does not change the characteristics when plotted and is used to engineer a source of specified beam. However limitations come from heating, which causes density decrease of plasma and gas.

(b) Discharge Mechanism

Ionized gas emit positive ions (Fig. 2.1) which are accelerated in the electric field of the "cathode face" towards the cathode. Most of the applied voltage appears in the region. Its dimension mostly depends upon the applied voltage ion current density, mass of ions.

• The fast ions may interact with natural gas molecules by charge exchange to become fast neutrals (possibly exited) and both may go on to strike the cathode. The energy ranges from zero to maximum and cause secondary electrons to be emitted there. Photons invalid in the plasma or else where like at the anode due to electron bombardment and after striking the cathode cause electron bombardment and after striking the cathode cause electron (secondary) release. This process is termed responsible for high efficiency of hollow cathode.
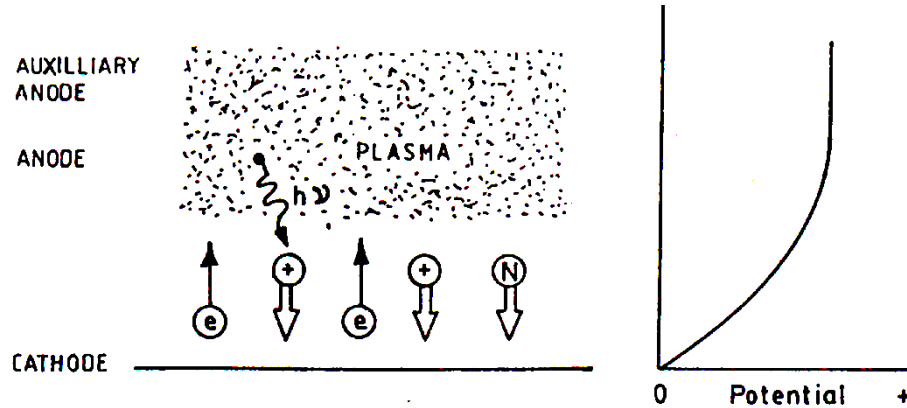
Fig. 2.1 Scheme of Discharge Mechanism

• Secondary electrons are accelerated towards the plasma in the cathode fall. Either they or further secondary electrons released are responsible for maintaining plasma ionization of gas. The degree of ionization can be augmented by means of an auxiliary discharge to a second anode at different potential to the first. In this way regulation or control of the main discharge may be obtained. As trajectories of fast ions and electrons are normal to the cathode surface, cathode curvature can be employed to focus fast electrons in a specified way.

• When the separation of side ways boundaries is of the same order as the cathode fall dimension, the plasma boundary becomes concave towards cathode causing concentrated thin beam of electrons, fast in nature. Division of broad and thin beams are based on cathode fall dimensions. As voltage is increased and pressure reduced, the beam becomes more penetrating due to reduced collisions and reduction in gas density.

(c) Cathode Electron Emission

Electron emissions at the cathode occurs due to neutrals, photons and ions so that effective coefficient of secondary electron emission gives total yeild per bombarding ion and depends on voltage,

$$Y = Y_1 + n_n \ V_n + \eta_p \ V_p \tag{2.3}$$

gas, geometry and cathode material. The general increase of voltage tends to make ion gems efficient at low voltage.

(d)   Cathode Sputtering

Role of cathode emission cannot be precisely assessed due to complexity of the glow. The sputtered atoms collide with the gas present and are transported by diffusion. Ionized are subjected to electric field. Rate of cathode erosion depends on the distribution of ion bombardment over the cathode. Cathode is rotated to reduce erosion. Corrosion are obtained to the order of 10^{-7} cc/sec/kW. It can be reduced by light gases like Hydrogen and Helium. Condensation causes a need to maintenance.

(e)   Regulating and Control Electrodes

An auxiliary cathode (+ve or -ve with respect to main anode). Acceleration of the electrons should take place at an appropriate boundary of plasma. Effectiveness depends on influence to increase discharge at anode boundary. Position, shape, polarity and electrical characteristics are parameters for optimization. Reduced working pressure by hollow electrodes can be exploited to reduce probability of change exchange collisions accelerated in the main cathode fall.

2.3   ION GUNS

Guns are designed to correct the target in some desired direction. Energies range for 1 keV to 100 keV current from milli amps to amps.

Ion guns are less penetrating, less homogenoeous and difficult to manipulate magnetically. They are similar in design to electron guns. Broad and thin beams are available. Auxiliary anode provides regulation. Ion guns require a special electrode outside the cathode to stabilize discharge. The ions coming out will form a plasma after ionizing the gas. Types are as shown in Fig. 2.2.

2.4   ION BEAM SET-UP

(a) The Unit

The gun and its associated equipment are shown in Fig. 2.3. The gun is intended to work in the range 1 to 10 kV (or more depending on the insulator) to continuous power consumption of 10 to 100 watt/cm2 of cathode. The electrode geometry may be spherically or cylindrically or cylindrically curved to produce a spot or line focus, or it may plane or convex downwards to

produce a parallel beam. The anode guard ring may be adjusted to obtain the best beam shape under given conditions.

(a) Broad beam guns: wire mesh for cathode. Restricted geometry only if they modify cathode fall.

(b) Hollow anode structure: thin pencil beam, rotation produces beam geometry.

(c) Thin beam hollow: relatively large cathode ionization is independently maintained to get non-energetic beam.
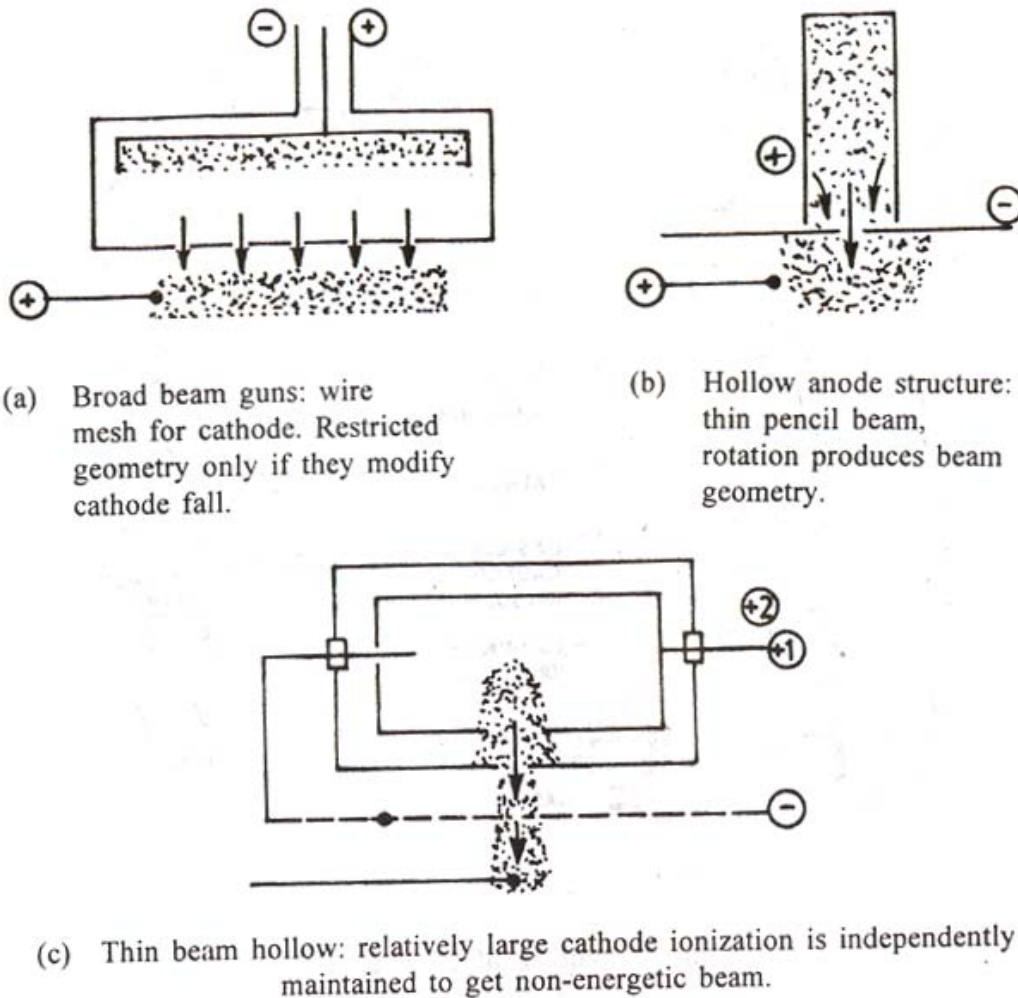
Fig.2 .2 Different Types of Ion-Gun

Metal parts of the gun are conveniently made from stainless steel because of its low thermal conductivity. Thin sheet construction permits operating temperature to be established quickly. Heat dissipation in the cathode is radiated away. The gun stem (cryogenic stainless steel tubing) and insulator assembly may be longer than shown, in order to avoid heating of the rubber seals. The cathode voltage dropper resistor should be chosen to drop about 20% of the applied voltage. It should be connected close to the cathode support rod in order to minimise stray capacitance.

The whole assembly should be mounted in an interlocked enclosure to protect the operator from electrical hazard or X-radiation.

The characteristics shown in the figure (Fig. 2.4) indicate the strong dependence pressure. Practical operation is facilitated by employing adequate pumping speed at the chamber (at least one litre per second).
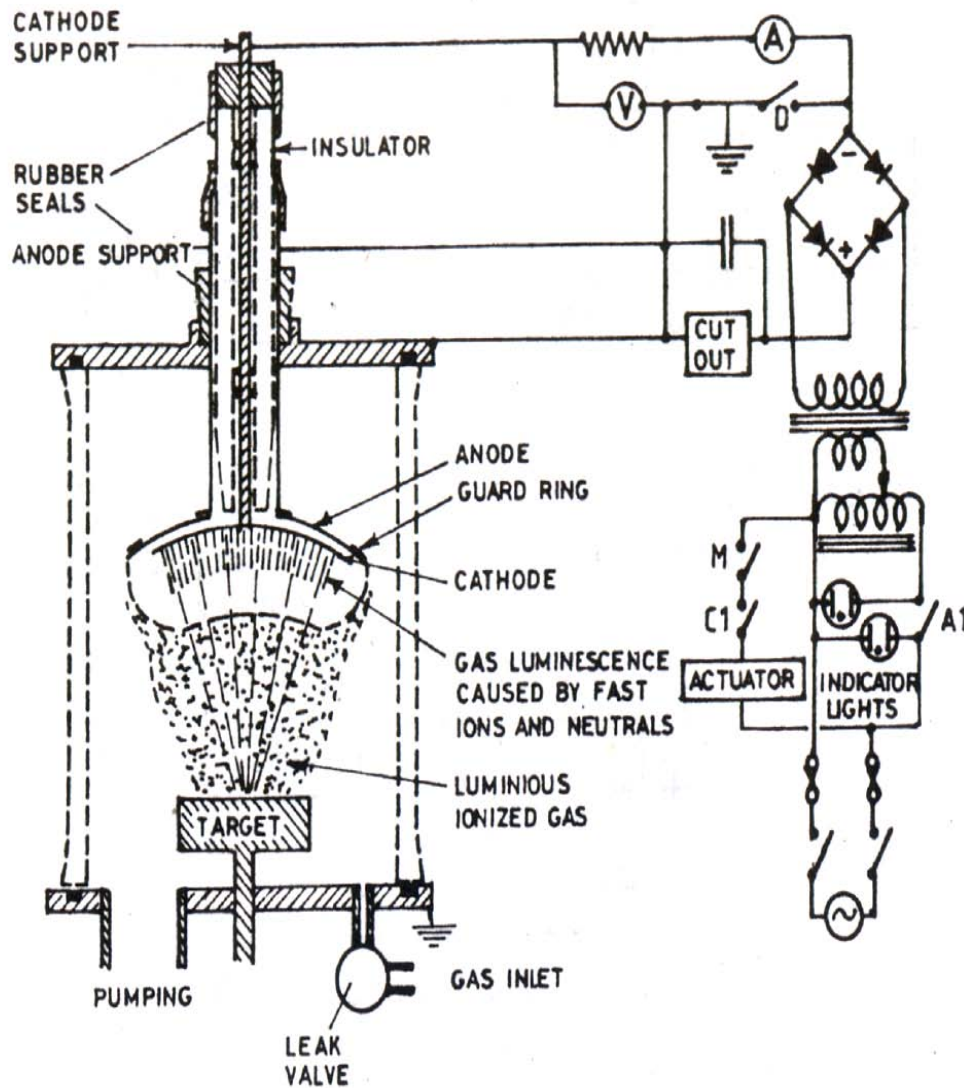
Fig. 2.3 A Scheme of Ion Beam Unit
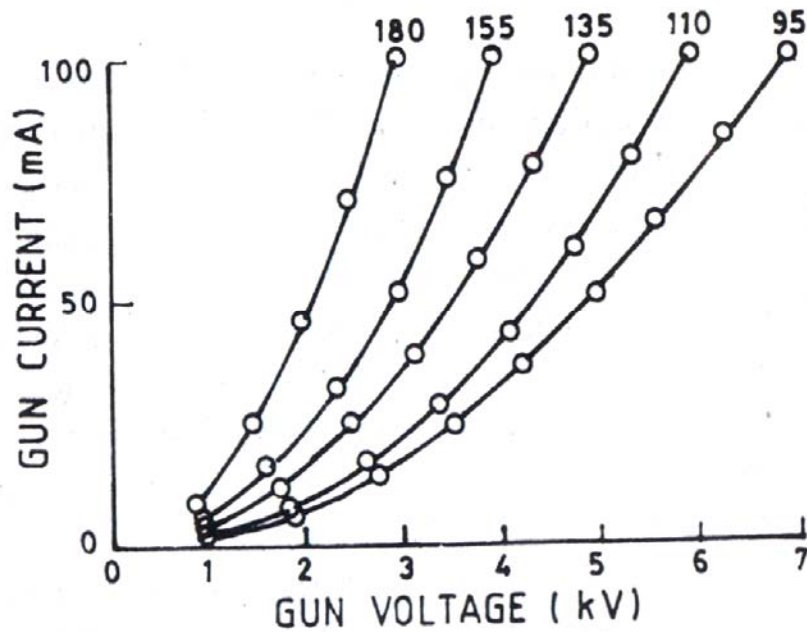
Fig. 2.4 Current and Voltage Dependence on Pressure in Milli-bar

Gassy applications are difficult to undertake with simple system of this type, but heat-treatment, melting and moderate evaporation work are possible (particularly if the pumping speed is high). Electrical characteristics with auxiliary anode may be determined and closed loop regulation may be adopted (a signal can be taken from the cut-out or a series resistor in the positive conducted) with or without an ambient discharge by switching in a charged capacitor through an appropriate charging resistor (few hundred ohms) connected to the cathode.

(b) Getter Ion Pumps

High vacuum pumps that employs chemically active material layers which are continuously/intermittently deposited on the wall of the pump and when chemisorb (chemically absorb) active gases while inert gases are cleaned up by ionizing them in an electric discharge and during +ve ions to the walls where neutralized ions are buried by fresh deposits of material.

2.5 SPUTTERING RATE (MRR)

$W = 6.24 \times 10^{15}\ Y.J.S.$ atoms/sec   (2.4)

(for single energetic ions)

where Y = sputtering yield atom/ion, J = ion current density mA/cm^2 and S = sputtering area in cm^2.

2.6 APPLICATIONS

(a)	Rates poor in	- Drilling
	Good in	- Shallow contouring
	Fair in	- Deep cutting
(b)	Rating	
	Fair	- Al, Steel, Super alloys, Titanium, Refractory plastics and glass
	Good	- Ceramics
(c)	M.R.R	- 2×10^{-4} mm/min
	Tolerance	- 0.005 m
	Surface finish, CLA	- Super
	Surface damage	- 0.005 m
	Comer radius	- 0.002 mm
	Safety	- Fair
	Micro drilling D < 0.03 mm	- Fair
	Small hole drill 0.15 > D > 0.3	- Good
(d)	Widely used for :	-
	(a) Cleaning	- Removing surface contamination
	(b) Polishing glass	- Not to crystalline
	(c) Etching	- Study of micro structure wire dies
	(d) Micromachining	- Integrate circles, bearings
	(e) Sputter deposition	- atomic deposition i.e. thin film metal deposition

2.7 ADVANTAGES
   (a) Process is almost universal.
   (b) No chemical reagents etchants.
   (c) No undercutting.
   (d) Etching rates and controllable.

2.8 DISADVANTAGES
   (a) Relatively expensive.
   (b) Slow etching rates.
   (c) Little possibility of some thermal or reaction damage.

Plasma Arc Cutting (PAM)

3.1 PROCESS

Plasma arc cutting began in the early 1950s when it was discovered that the performance of an electric gas cutting arc could be greatly improved if it was directed through a water-cooled copper nozzle (Fig. 11.1) located between an electrode (cathode) and the work piece (anode). The nozzle constricted the arc into a small cross-section which increased both the arc temperature and voltage. After passing through the nozzle, the arc emerged as a high velocity, intensely hot plasma jet.

(a) The system   (b) The nozzle
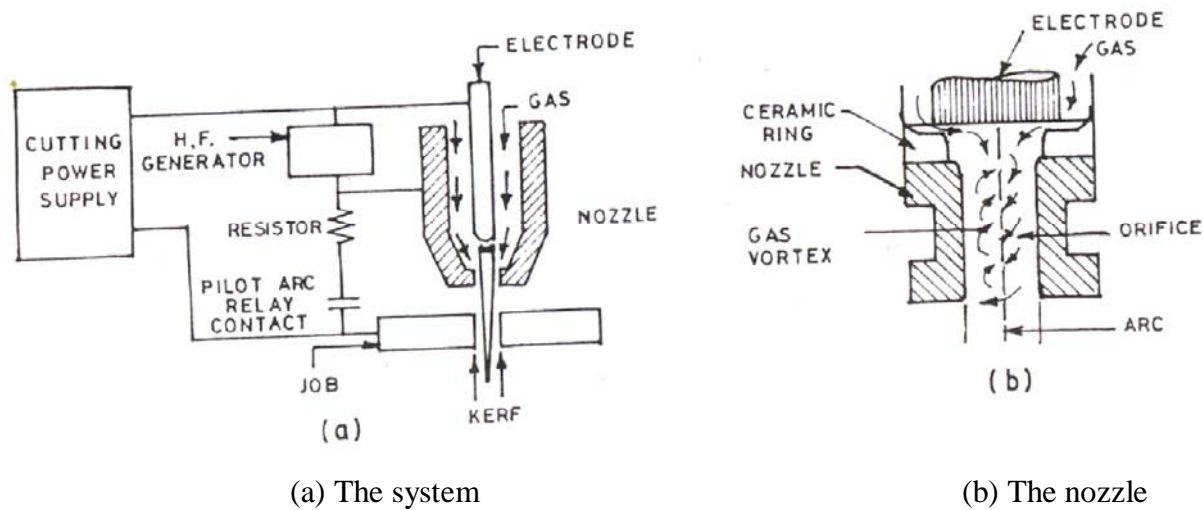
Fig. 3.1 Scheme of Plasma Arc Cutting System

The cutting action of the torch is provided by this plasma jet. Often called the fourth state of matter, plasma is an extremely hot gas in a highly ionized state, produced by passing a high voltage electric arc through a gaseous mixture consisting of hydrogen, nitrogen, argon, etc. Unlike Oxy-fuel cutting, this method does not make use of the heat of chemical reaction (oxidation). It uses the energy of plasma to melt the metal and thereby cut. Plasma arc has, therefore, emerged as a method of cutting of stainless steel, aluminium and nonferrous metals which, because of the chemical reaction produced were impossible to cut with any oxy-gas flame.

3.2 PRINCIPLES (PLASMA ARC)

An arc is a stable form of electric discharge between two electrodes in a gaseous medium. A feature of a gaseous conduction is a continuous interchange of energy between electrons, ions and neutral particles, the interchange occurring during the collision resulting from their

disorderly movement caused by beating. Structurally, in an arc there are anode, cathode and a column of quasi neutral plasma. Due to thermionic or auto electronic emission, electrons are discharged by the cathode. The electrons lose part of their energy to the ions, neutral atoms and molecules in multiple collisions causing ionization as well as dissociation of the gaseous medium. There is a consequent rise of temperature in the gaseous plasma varying from 4x10 to 20×10^3 deg. K or more.

An attempt to artificially increase the temperature of the arc has led to the development of plasmatrons or plasma torches and their extensive use in industry.

The plasmatrons are based on the forced cooling and construction of the arc column with steam, or gas flow. There are two types of plasmatrons direct and indirect arcs. In both types (Fig. 11.2) of plasmatrons, one of the electrodes (cathode) is in the form of a rod with refractory tip attached to it.

1. ELECTRODE
2. GAS CHAMBER
3. INSULATING SPACER
4. NOZZLE
5. WORKPIECE
6. POWER SOURCE
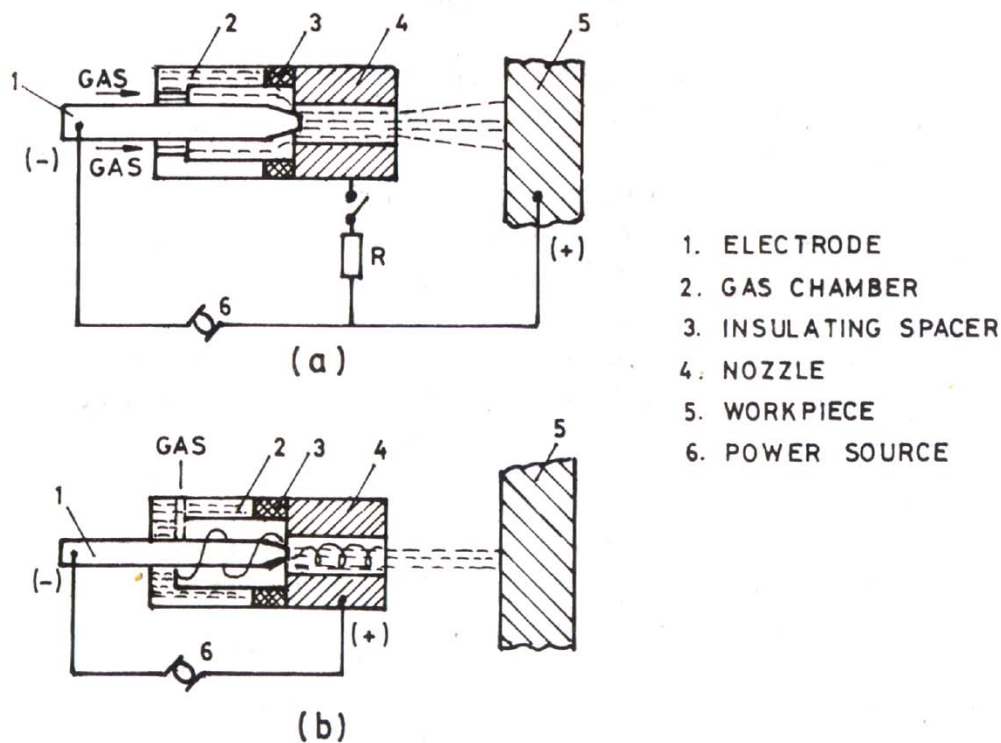
Fig. 3.2 Schematic Diagram of Plasmatron: (a) Direct Arc System and (b) Indirect Arc System

In the indirect arc type, the nozzle is the anode while the work piece is the anode in the direct type.

3.3 PLASMA ARC TORCHES (PLASMATRON)

3.3.1 Indirect Arc Plasma Torches

The arc established between the electrode and the torch is forced through the nozzle by the working gas fed into the chamber. The anode spot of the arc moves on the inside wall of the nozzle passing, whereas the column if firmly stabilized along the axis of the electrode and torch.

In passing through the nozzle, part of the working gas becomes heated, ionized, and emerges from the torch as the plasma jet. The outer layer of the gas flowing around the arc column remains relatively cool and forms an electric and thermal insulation between the plasma jet and nozzle bore, thus protecting the nozzle from erosion. In addition, the external coat of gas intensively cools the arc column due to which the cross-section of the column decreases and the current density diameter of the column the constricting action of the arc intrinsic magnetic field also increases:

$$p_m = \frac{36 \times 10^{13}}{\pi} \times \frac{I^2}{D_{con}^2 C^2} N/cm^2 \tag{3.1}$$

where P *is the inward pressure of the magnetic field,* I *the arc current (Amp),* D *the conductive*

diameter of column and C *the speed of light (= 3 x 10^{10} cm/s).*

Thus the thermal constriction in the plasmatron (thermal pinching effect) induces an increased magnetic constriction (magnetic pinch effect). The current density reaches l00A/mm and the temperature reaches several thousand degrees.

Emerging from the torch the plasma jet widens slightly. This leads to the appearance of an axial pressure gradient of the arc magnetic field, accelerating the plasma jet to supersonic speeds.

3.3.2 Direct Arc Plasmatrons Torches

In direct arc plasma torches the work piece is the anode, whereas the nozzle is electrically neutral, being used for the construction and stabilization of the arc only. In contrast to the indirect-arc plasma torches, the plasma jet of the direct-arc type is brought into coincidence with the arc column and for that reason has a higher temperature and thermal power.

Since it is difficult to strike an arc between the electrode and work piece directly through the narrow torch passage, first an auxiliary arc is commonly excited between the electrode and the nozzle and then, as soon as the arc flame reaches the work piece, it automatically strikes the main arc between the electrode and the work piece, while the auxiliary arc is switched off.

Indirect-arc plasimtorches are used for working non-conducting materials (for flame spraying, spheroidizing, heating, etc.). Direct-arc torches has a higher efficiency and arc preferred for cutting, welding, depositing, et£. In this case, gas is admitted into the chamber through tangential holes and flows spirally, enveloping the arc column in a vortex flow.

In many cases plasma torches with a double or combined gas flow are used for welding and cutting. They have two nozzles. The gas applied to the internal nozzle can be termed the primary, and the external nozzle can be termed the primary, and the external nozzle gas, the secondary.

Primary and secondary gases can differ in the designation, composition and flow rate. In the cutting process the primary (usually inert) gas protects the tungsten cathode from the environment, the secondary (usually active, molecular) in the plasma forming, cutting gas. In welding, the gas applied to the external nozzle additionally constricts the plasma jet found by the primary gas and protects the weld zone from the environment.

A number of plasmatron types (26 types) are explicitly schematically described in Fig.3.3
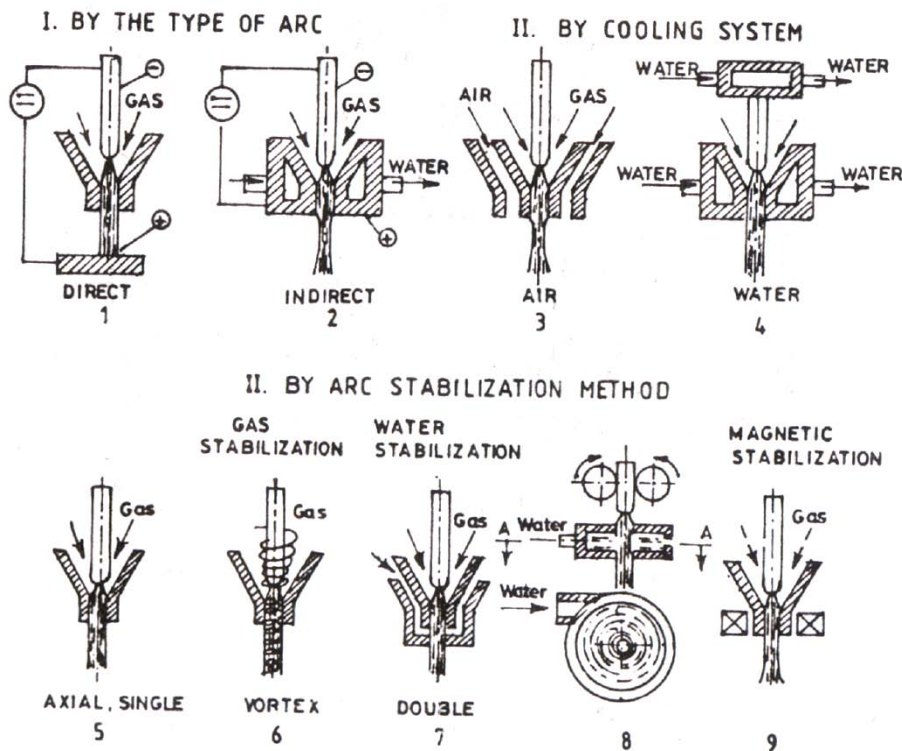
Fig. 3.3 (Contd.)

IV. BY THE TYPE OF THE ELECTRODE-CATHODE

ROD-TYPE

CONSUMABLE | GAS-SHIELDED | FILM-SHIELDED | HOLLOW | DISK-TYPE | RING-TYPE
10 | 11 | 12 | 13 | 14 | 15

V. BY PLASMA-FORMING MEDIUM

INERT

Ar   He

16

REDUCING

H_2 N_2 C_nH_{2n+2} NH_3

17

OXIDIZING

O_2 (H_2+O_2)

CO_2 H_2O

18

VI. BY THE TYPE OF CURRENT

Gas   Gas   Gas   Gas   Gas

19 | 20 | 21 | 22

ON DIRECT CURRENT | ON ALTERNATING CURRENT

Water   Gas   Gas   Gas

23 | 24 | 25 | 26

COMBINED | HIGH FREQUENCY
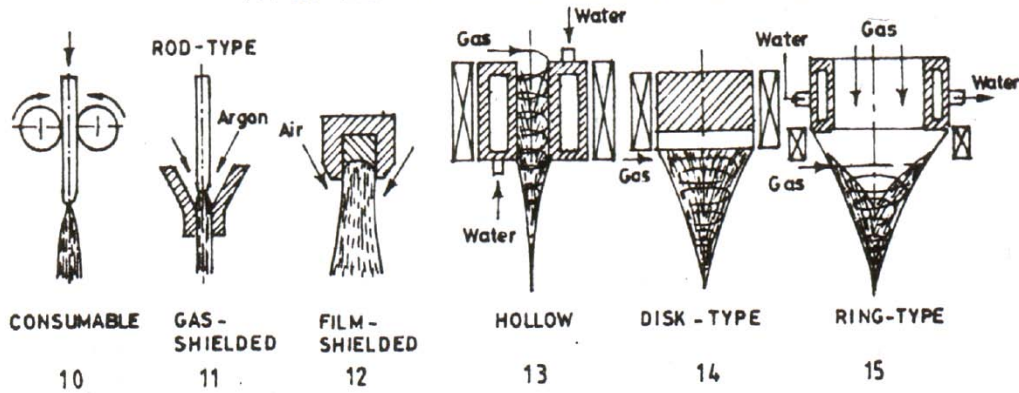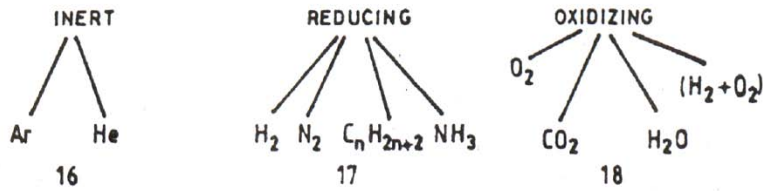
Fig. 3-3 Classification of Plasma torches

3.4 PARAMETER AFFECTING CUTTING

3.4.1 Plasma-Forming (Cutting) Gases

The quality and the speed of cutting, far from being fully dependent on the power parameters of plasma arc, are much influenced by thermo-physical and chemico-metallurgical properties of the plasma-forming (cutting) gases. Natural and artificial mixture which are various combinations of the four principal gases, argon, nitrogen, hydrogen and oxygen have been used as plasma-forming media. Thermophysical properties of these gases as well as those of air and water (steam) are shown in Table 3.1.

Due to high heat capacity, hydrogen has the maximum heat content enthalpy at a comparatively low temperature of plasma, and due to high heat conductivity it makes it possible to achieve the best conditions for the transfer of the plasma arc column power to the metal ($i.e. \eta_u$). That is why, the arc power being the same, the cutting speed will be higher in hydrogen and in mixtures based on hydrogen than in other gases. The plasma jet with hydrogen as the basic agent pressures high energy of gas at the maximum arc length. For this reason hydrogen-containing mixtures should be used for cutting thick, high-alloy steel plates and such good heat conductors as copper and aluminium. In addition, hydrogen provides for a smooth cutting surfaces. From the economy point of view most advantageous is the use of cheap hydrogen con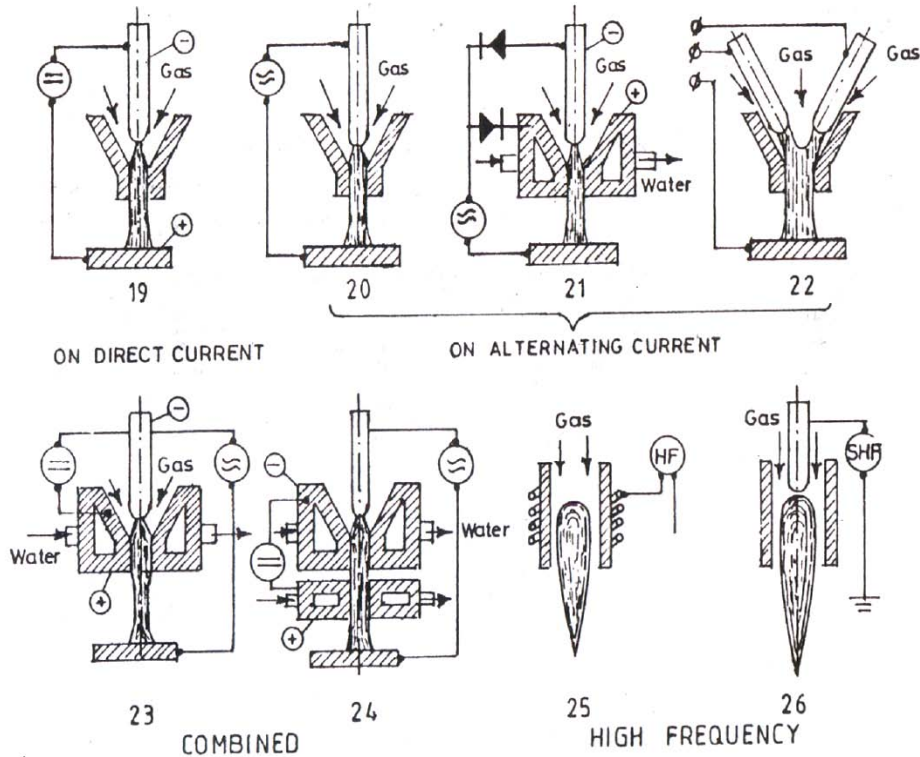taining gases such as ammonia, consisting of 75% H and 25% N. In contrast to pure hydrogen, ammonia is explosion proof, cheap and easily available. The consumption of hydrogen containing gases depends on the cutting current and is 2 to 4 m^3/hr. However, hydrogen containing gases also possess significant disadvantages. As a consequence of the high thermal conductivity of hydrogen, the thermal and electrical insulation of the plasmatron nozzle from the arc column is disrupted even at comparatively small power supply, which results in the nozzle destruction. Sometimes a gas mixture containing hydrogen and a maximum of 20% argon is also used. It has been suggested that due to the thermal diffusion, argon, being much heavier than hydrogen, accumulates at the nozzle walls, providing for a thermal protection of the nozzle, since its electric and thermal conductivity" is comparatively low. Cutting of carbon steels, stainless steels and aluminium of medium thickness in many cases is performed with the use of commercial nitrogen. The quality of plasma cutting in nitrogen is somewhat worse and the speed is considerably less than in hydrogen-containing gases. In addition, an appreciable increase in nitrogen content was noted in the fused layer of the cut at a depth of 0.15 mm. Commercial nitrogen is cheap.

Table 11.1 Properties of Plasma-Forming (Cutting) Gases

Gas	Atomic or molecular weight	Heat conductivity λ J/cm.s ×10⁻⁵ 293°K	K at 1 atm ×10⁻² 10000°K	Enthalpy max × 10⁻²	I, J/g at 293°K	at 1 atm ×10⁴ 10000°K	×10⁴ 15000°K
Ar	39.940	16.84	0.55	—	152.90	0.59	3.4
H₂	2.016	174.70	4.19	16.34 at 3800°K	4148.00	46.09	138.27
N₂	28.016	24.43	2.63	6.08 at 7000°K	305.87	5.03	12.15
O₂	32.000	25.14	—	—	268.16	3.27	8.92
AIR	29.000	25.14	5.87	20.95 at 7000°K	290.37	4.94	11.52
H₂O (steam)	18.016	24.68 at 373°K	—	—	544.9	8.04	23.25

Table 11.2 Properties of most Common Metals

Metal	Atomic weight	Density gm/cm³	T_m °K	T_b °K	Sp heat J/g °K at 293°K	L_m J/g	λ J/cm.s °K	Sp. energy ×10⁻⁶ cm³/J
Aluminium	27	2.7	930	2670	0.5	390	2.34	95
Copper	63.5	8.96	1356	2850	0.34	212	3.84	17
Steel	55.9	7.86	1810	3170	0.46	270	0.73	44

The simplest and most economical is the use of air plasma. Air has oxygen and nitrogen. Its maximum heat conductivity (at 7000 K) is higher than that of hydrogen (at 3800 K). Therefore,

the air-plasma jet is noted for a higher concentration of energy and greater as compared with the hydrogen jet.

With oxygen in the plasma, heat is applied to the cut not from the arc alone but also due to heat of oxidation reaction. Furthermore, dross adherence on the bottom edge of the cut is substantially reduced. The speed of cutting steels with the air plasma is 1.5 to 2.5 times greater than with the use of nitrogen as the cutting gas and ensures better quality. The plasmatron is to be specially designed (normally zirconium cathode) to operate on compressed air.

Air plasma can be advantageously employed for cutting non-ferrous alloyed metals but at a sacrifice of the quality of the cut surface. With thicknesses in excess of 40-50 mm for copper and 80-100 mm for aluminium the air plasma cutting process cannot complete with the cutting in hydrogen containing mixtures because of a decrease in the cutting speed.

Water is an ideal plasma-forming medium which is a cheap combination of hydrogen and oxygen. Despite long-period research work carried out to determine the feasibility of using water for plasma cutting, plasmatrons with the water stabilization of the arc have not yet found wide application since they are rather complicated and unreliable. From the economy point of view the least efficient plasma-forming gas is argon, since it is scarce, expensive and low-enthalpic. However, for the reason of the low voltage of the arc, at present it is extensively used for the manual cutting of non-ferrous metals and alloyed steels of small and medium thicknesses both as a sole agent or in conjunction with commercial nitrogen.

3.4.2 Stand-off Distance

Increase of the stand-off distance reduces the depth of the penetration, and hence narrows the cut width at the bottom. With an excessive reduction of the stand-off distance, the plasmatron can be damaged by the metal spatter. The optimum stand-off distance depends on the thickness of the metal being cut and varies between 5 and 10 mm.

3.4.3 Speed of Cutting

There exists an optimum correlation between the metal thickness, arc power and speed of cutting. The increase of the cutting speed leads to a reduced depth of immersion of the aic column and of the anode region, to
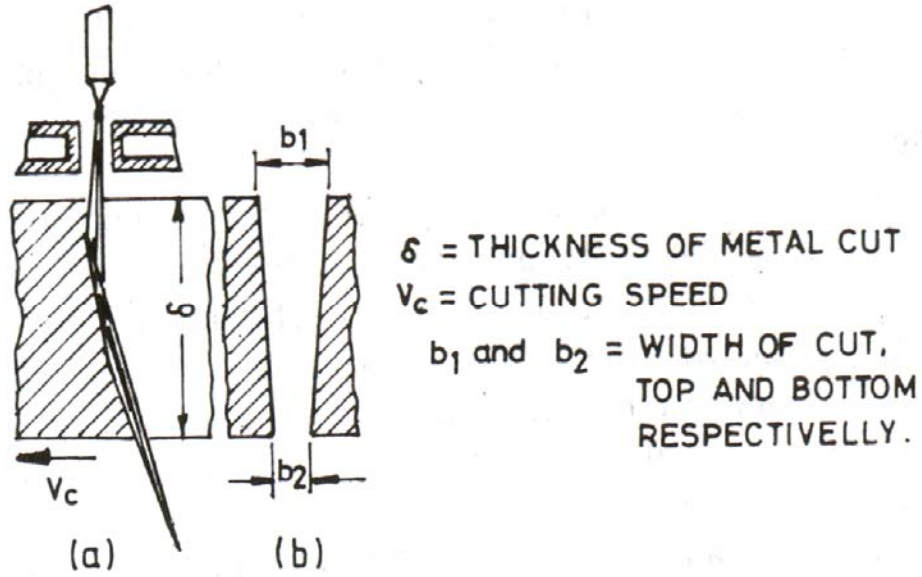
Fig. 3.4 (a) Cut Formation and (b) Cut Cross-section in PAM

a lag of melting front at the bottom, and consequently to a narrowing of the cut in the lower portion and, in case of excessive speed, to incomplete cutting. Figure 11.4 shows the cut formation when the speed is higher than the optimum speed. On the other hand, the reduction of speed below the optimum will cause the opening of the cut at the cut bottom. Usually the optimum cutting speed is approximately one and a half to two times below the maximum one.

Table 3.2 shows typical plasma cutting parameters.

To cut 25 mm thick	Orifice dia (mm)	Current DCSP (amp)	Cutting speed (mm/s)	Power (KW)
Aluminium alloys	4	400	38	80
Stainless steel	4	400	21	80
Carbon steel	4	425	21	85

The optimum parameters of cutting can be selected proceeding from the balance of heat power spent on the melting and evaporation of a volume of metal equal to the volume of cut formed per unit time:

$$\eta_u \; I \; V = \gamma \; b_{av} \; \delta \; \Delta S \; V \; W \, / \, S \qquad\qquad (3.2)$$

where

η_u = factor of arc power utilization = 0.4 (usually)

γ = metal density, g/cm

b_{av} = average width of cut = thickness of metal cut, cm/s

V = maximum speed of cutting, cm/s

ΔS = amount of heat spent on a unit of mass of metal removed from cut, J/g.

3.5 ADVANTAGES OF PLASMA ARC CUTTING

1.   In plasma arc cutting, the material being cut becomes molten and is either blown away by the high velocity gas stream or is evaporated due to the high temperature of the plasma arc. The method can, therefore, the applied to any metals and even to non-conducting materials like concrete etc.

2.   Carbon steels thinner the 50 mm can be cut at accelerated speeds (10 times faster than oxy-fuel cutting).

3.   Due to the high speed of cutting the deformation of sheet metals is reduced while the width of the cut is minimum and the quality is high.

4.   Owing to the high productivity of the plasma-arc cutting and the emergent tedency to use cheap and easily available plasma-forming media (air, water, ammonia and others) plasma-arc cutting is finding ever increasing application. Arc plasma-arc cutting is finding ever increasing application. Arc plasma torches give the highest temperature (around 14000 C) available for many practicable sources.

5.   Metal cutting is performed with the direct plasma arc which has a highly constricted arc column and, therefore, a greater concentration of the thermal flux. The penetration is high and starts cutting almost at once (there is no need for the local heating of the metal to its ignition temperature).

6.   With the optimum correlation between the metal thickness, arc power and speed of cutting, the plasma arc column penetrates the entire metal thickness, and its anode region is at the level of the lower surface of the sheet. The cut is near perfect with the vertical side edges without the dross adherence. It leaves a narrower kerf.

7.   Plasma cutting can be used for stack cutting, plate beveling, shape cutting and piercing. It can also be used for underwater cutting.

3.6 OPERATIONAL SUMMARY

Power Supply

Type	Direct Current
Wattage	Up to 200 kW
Current	50 to 1000 A
Primary Gas	
Type	Argon-nitrogen (4 : 1), Hydrogen
Flow	0.40 to 5.65 m^3/hr
Shielding Gas	

Type	Nitrogen, oxygen, air, CO^2 and water
Flow	Up to 11 m^3/hr
Water Shield Flow	
(in place of Shielding Gas)	Up to 60 L/hr
Plasma Temperature	20,000 to 50,000 °F or 11,000 to 30,000 °C
Cutting Speed	50 to 6000 mm/min
Standoff Distance	6 to 10 mm
Nozzle Orifice Size	1.5 to 6.5 mm
Kerf Width	1.5 to 3 mm for thin plate
	4.75 mm for 25 mm plate
	19 mm for 150 mm plate
Kerf Angle	
Normal	2° to 7°
Special	1° to 2°
Accuracy	± 0.8 mm on 6 to 35 mm
	± 3.0 mm on 150 to 200 mm
Corner Radius	4 mm min. but increases with cutting speeds up to 38 mm at 6000 mm/min

Reference's

1. Advance machining process, V K Jain, Allied publishing Pvt, Ltd
2. Ghosh & Mallik, Manufacturing Science, EWP, East West press Pvt. Ltd.
3. Paday and Hsan, Morden machining process, TMH.
4. P K Mishra, Nonconventional Machining process, Narosa publication House.
5. Manufacturing Technology, HMT
6. Manufacturing process, Amstesd, ostwaed and Begemen, John wiley & sons.
7. Processes and materials of Manufacturing – Lindberg, PHI
8. Laser Machining, George Chryssolouris, Mechanical Engineering Series, Springer
9. Introduction to Laser Technology, Hitz, IEEE press.
10. www.newagepublishers.com/samplechapter/001566.pdf

11. Lavoi, F.J., Abrasive Jet Machining, Machine Design, September, 1973, pp 135-159.

12. LaCourte, N., Abrasive-jet Machining-A Solution for Problem Jobs, Tooling and Prodn., Nov, 1979, pp 104-106.

13. Neema, M.L. and P.C. Pandey, Erosion of Glass when Acted upon by a Abrasive Jet, Proc. Int. Conf. on Wear of Mat., April 1977, pp. 387—391.

14. Engel, P.A., Impact Wear of Mateirals, Elsevier Scientific Publishing Co., Amsterdam, 1976.

15. Goldsmith, W., Impact'. The Theory and Physical Behaviour of Colliding Bodies, Edward Arnold Pb. Ltd., 1960.

16. Kinslow, R.C. (Ed), High Velocity Impact Phenomena, Academic Press, New York, 1970.

17. Rozenberg, L.D. et al, Ultrasonic Cutting, CB Publication, N.Y., 1964.

18. Markov, A.I. (ed. Neppiras, E.A.), Ultrasonic Machining of Intractable Materials, London Iliffe Book Ltd., 1966.

19. Lavoi, F.J., Water Jet Machining, Machine Design, Feb. 1973, pp. 89-93.

20. BHRA, Jet Cutting Technology.

21. Sringer, G.S., Erosion by Liquid Impact, John Wiley & Sons, 1974.

22. Preece, C.N. (ed), The Mechanics of Liquid Impact, Treatise on Material Science and Technology, Vol. 16, Academic Press, 1979.

23. De Barr, A.E., Electrochemical Machining, Macdonald Pb., London, 1968.

24. Wilson, J.F., Practical and Theory of Electrochemical Machining, Wiley—Interscience, New York, 1971.

25. McGeogh, J.A., Principles of Electrochemical Machining, Chapman and Hall, London, 1974.

26. Rumyantsev, E. and Davydev, A., Electrochemical Machining of Metals, MIR Pb., Moscow, 1989.

27. BOSCH report.

28. Lazarenko, B.R. and Lazarenko, N.I., Electrical Efosion of Metals, No. 1, Gosenergoizdat, 1994.

29. Ruderft, D.W., Electric Spark Erosion as Applied to Metal Machining Engineers" Digest, Vol. 14, No. 10, Oct. 1953, pp. 373-377.

30. Lazarenko, B.R. and Lozorenko, N.I. The Physics of the Electric Spark Method of Machining Metals; Pb of ministry of Elect. Industry, USSR, Moscow, 1946. 4. Lazarenko, B.R. (Ed), Electrospark Machining of Metals; Vol. 2, Consultant Bureau Pb., New York, 1964.

31. Brume, M., Advances in Electroerosion, Discovery, 20(3), 1959, 126.

32. Kurafuji, H., Development of Researches and Applications of Spark Erosion and Electrolytic Machining in Japan; Annals of 14th CIRP Gen, Assembly, Sept. 1964.

33. Williams, E.M. Woodford, J.B. and Smith, R.E., Recent Development in Theory and Design of Electrical Spark Machine Tools; Tr. AIEE, Vol. 73, IGA Pt. II, May 1954, pp. 83-88.

34. Anderson, J.C., Dielectric, Chapman & Hall, UK, 1964.

35. Lewia, T.J., Jn. of Electrochemical Society, 107, 185, 1960.

36. Horsten, H.J.A. et at., Annals CIRP 20,43, 1971.

37. Thija, A., Van Dijck, F. and Snoeys, R., Investigation of polarity effects in EDM, Paper No. 73, p.7, CIRP, Feb. 1973.

38. Motoki, K. and Hashiguchi, K., Energy Distribution at the Gap in Electric Discharge Machining, Annals of CIRP, Vol. XIV, 1967, pp. 485-489.

39. Lee, T.H., T.F. Theory of Electron Emission in High-current Arcs, Jn. Appl. Phys., Vol. 30, No.2, Feb. 1959, pp. 166-171.

40. Kaldes, F., Flushing the Gap in EDM, Pt. I EDM Digest Jan/Feb 1983.

41. Application of High Power Laser, SPIE Pb., Vol. 527, 1984.

42. Manufacturing Application of Laser, SPIE Pb., Vol. 621, 1986.

43. High Power Lasers & Their Industrial Applications, SPIE Pb., Vol. 650, 1986.

44. Laser Technologies in Industries, SPIE Pb., Vol. 952 (Pt. II), 1988.

45. High Power Lasers & Laser Machining, SPIE Pb., Vol. 1132, 1989.

46. Lasers in Industries, Charschan, S.S. Van Nostrand, 1972.

47. Laser Machining, by G. Chryssolous; Springer Pb., 1991.

48. Laser Material Processing, by W.M. Steen; Springer Pb., 1991.

49. Laser in Manufacturing, Ed. by A. Quenzer, 1986, Proc. 3rd. Int. Conf., Paris; ISBN 3-540-16326-3.

50. Laser in Manufacturing, Ed. by W.M. Steen, 1987, Proc. 4th Int. Conf., Birmingham; ISBN 3-540-17854-6.

51. Laser in Manufacturing, Ed. by H.H.gel, 1988, Proc. 5th Int. Conf., Stuttgard; ISBN 3-540-50310-2.

52. Laser in Manufacturing, Ed. by W.M. Steen, 1989, Proc. 6th Int. Conf., Birmingham; ISBN 3-540-51241-1.

53. Laser in Manufacturing, by J.A. Luxon, D.E. Parker and P.D. Plotkwaski; ISBN 3-540-17427-3.

54. The Changing Frontiers of Laser Material Processing, Ed. by C.M. Banas, G.L. Whitney, Proc. ICALEO'86, Arlington, 1986; ISBN 3-540-17563-6.

55. Laser Material Processing, Ed. G. Bruck, Proc. ICALEO'88 USA, 1988; ISBN 3-540-51537-2.

56. Laser in Manufacturing, Ed. A. Gomersall, 1986; ISBN 3-540-16678-5.

57. Fundamentals of Laser Interaction II, Ed. F. Ehlotzky, 1989; ISBN 3-540-51430-9.

58. Electron Beam Welding by Maleka, McGraw-Hill Book Co., Lond. 1971.

59. Handbook of Electron Beam Welding-by R. Bakish and S.S. White, 1964.

60. Proceedings of 3rd Electron Beam Processing Seminar 1974 by R.M. Silva; publisher Universal Technology Corporation, Dayton, Ohio.

61. State of art of electron beam technology for metal removal, welding and heat treatment processes by K..H. Steigerwald in Proceedings of 20th IMTDR Conference 1980.

62. Arata, A., Plasma, Electron and Laser Beam Technology, ASM Pb., 1985.

63. Esibyan, E.M., Plasma-Arc Equipment, MIR Pb., 1973.

64. Anisimovich, L.A., A Physicist ABC on Plasma, MIR Pb., 1985.

65. Arata, A., Plasma, Electron and Laser Beam Technology, ASM Pb., 1985.

66. Dugdale, R.A., Glow Discharge material Processing, MB Mon. ME/5, Mills & Boon Ltd., London, 1971.

67. Benedict G.F. (1987), Non-traditional Manufacturing Processes, Marcel Dekker Inc., London.

68. Bhattacharyya A. (1973), New Technology, The Institution of Engineers (I), Calcutta.

69. Buttner A. and Lindenback D.A. (1969), Electrolytic dressing of diamond wheels for use in steel grinding, Ind. Diamond Rev., pp. 450-454.

70. Dash J. and King W.W. (1972), Electrothinning and electrodeposition of metals in magnetic fields, J. Electrochem Soc., Vol. 119, pp. 51-56.

71. DeBarr A.E. and Oliver D.A. (1968), Electrochemical Machining, MacDonald, London.

72. Gedam A. and Noble C.F. (1971), An assessment of the influence of some wheel variables in peripheral electrochemical grinding, Int. J. Mach. Tool Des. Res, Vol. 11, pp. 1-12.

73. Kuppuswamy G. (1976), Electrochemical grinding: an investigation of the metal removal rate, Proc. 7th AIMTDR Conf. held at Coimbatore (India) pp. 337-340.

74. Kuppuswamy G. and Venkatesh V.C. (1979), Wheel parameters and effect of magnetic field on electrolytic grinding, J. Inst. Engrs. (I), Part ME(l), Vol. 60, pp. 17-20.

75. Levinger R. and Malkin S. (1979), Electrochemical grinding of WC-Co cemented carbides, ASME Paper No. 78-WA/PROD-26, WAM, San Francisco, pp. 1-10.

76. McGeough J.A. (1988), Advanced Methods of Machining, Chapman and Hall, London.

77. Pandey P.C. and Shan H.S. (1980), Modern Machining Processes, TataMcGrawHill, New Delhi.

78. Jain V.K., Tandon S. and Kumar Prashant (1990), Experimental investigation into electrochemical spark machining of composites, Trans. ASME, J. Engg. Ind., Vol. 12, pp. 194-197.

79. Verma M.M. (1981), A study of process parameters in electrochemical grinding, M. Tech. Thesis, IIT Kanpur (India).

80. Benedict G.F. (1987), Non-traditional Manufacturing Processes, Marcel Dekker Inc., New York.

81. Naidu M.G.J. (1991), Electrochemical deburring for quality production, Proc. Winter School on AM T (Eds.: Jain V.K. and Choudhury S.K.), IIT Kanpur (India).

82. Pandey P.C. and Shan H.S. (1980), M odem Machining Processes, TataMcGraw Hill, New Delhi.

83. Pramanik D.K., Dasgupta R.K. and Basu S.K. (1982), A study of electrochemical deburring using a moving electrode, Wear, Vol. 82, pp. 309-316.

84. Rumyantsev E. and Davydev A. (1989), Electrochemical Machining o f M etals, Mir Publishers, Moscow.

85. Takazawa K. (1988), The challenge of burr technology and its worldwide trends, Bull. JSPE, Vol. 22, No. 3, pp. 165-170.

86. Tool Design Manual fo r Electrochemical Deburring, Chemtoal Inc., Minnesota, U.S.A.

Reference's

1. Advance machining process, V K Jain, Allied publishing Pvt, Ltd
2. Ghosh & Mallik, Manufacturing Science, EWP, East West press Pvt. Ltd.
3. Paday and Hsan, Morden machining process, TMH.
4. P K Mishra, Nonconventional Machining process, Narosa publication House.
5. Manufacturing Technology, HMT
6. Manufacturing process, Amstesd, ostwaed and Begemen, John wiley & sons.
7. Processes and materials of Manufacturing – Lindberg, PHI
8. Laser Machining, George Chryssolouris, Mechanical Engineering Series, Springer
9. Introduction to Laser Technology, Hitz, IEEE press.
10. www.newagepublishers.com/samplechapter/001566.pdf

11. Lavoi, F.J., Abrasive Jet Machining, Machine Design, September, 1973, pp 135-159.

12. LaCourte, N., Abrasive-jet Machining-A Solution for Problem Jobs, Tooling and Prodn., Nov, 1979, pp 104-106.

13. Neema, M.L. and P.C. Pandey, Erosion of Glass when Acted upon by a Abrasive Jet, Proc. Int. Conf. on Wear of Mat., April 1977, pp. 387—391.

14. Engel, P.A., Impact Wear of Mateirals, Elsevier Scientific Publishing Co., Amsterdam, 1976.

15. Goldsmith, W., Impact'. The Theory and Physical Behaviour of Colliding Bodies, Edward Arnold Pb. Ltd., 1960.

16. Kinslow, R.C. (Ed), High Velocity Impact Phenomena, Academic Press, New York, 1970.

17. Rozenberg, L.D. et al, Ultrasonic Cutting, CB Publication, N.Y., 1964.

18. Markov, A.I. (ed. Neppiras, E.A.), Ultrasonic Machining of Intractable Materials, London Iliffe Book Ltd., 1966.

19. Lavoi, F.J., Water Jet Machining, Machine Design, Feb. 1973, pp. 89-93.

20. BHRA, Jet Cutting Technology.

21. Sringer, G.S., Erosion by Liquid Impact, John Wiley & Sons, 1974.

22. Preece, C.N. (ed), The Mechanics of Liquid Impact, Treatise on Material Science and Technology, Vol. 16, Academic Press, 1979.

23. De Barr, A.E., Electrochemical Machining, Macdonald Pb., London, 1968.

24. Wilson, J.F., Practical and Theory of Electrochemical Machining, Wiley—Interscience, New York, 1971.

25. McGeogh, J.A., Principles of Electrochemical Machining, Chapman and Hall, London, 1974.

26. Rumyantsev, E. and Davydev, A., Electrochemical Machining of Metals, MIR Pb., Moscow, 1989.

27. BOSCH report.

28. Lazarenko, B.R. and Lazarenko, N.I., Electrical Efosion of Metals, No. 1, Gosenergoizdat, 1994.

29. Ruderft, D.W., Electric Spark Erosion as Applied to Metal Machining Engineers" Digest, Vol. 14, No. 10, Oct. 1953, pp. 373-377.

30. Lazarenko, B.R. and Lozorenko, N.I. The Physics of the Electric Spark Method of Machining Metals; Pb of ministry of Elect. Industry, USSR, Moscow, 1946. 4. Lazarenko, B.R. (Ed), Electrospark Machining of Metals; Vol. 2, Consultant Bureau Pb., New York, 1964.

31. Brume, M., Advances in Electroerosion, Discovery, 20(3), 1959, 126.

32. Kurafuji, H., Development of Researches and Applications of Spark Erosion and Electrolytic Machining in Japan; Annals of 14th CIRP Gen, Assembly, Sept. 1964.

33. Williams, E.M. Woodford, J.B. and Smith, R.E., Recent Development in Theory and Design of Electrical Spark Machine Tools; Tr. AIEE, Vol. 73, IGA Pt. II, May 1954, pp. 83-88.

34. Anderson, J.C., Dielectric, Chapman & Hall, UK, 1964.

35. Lewia, T.J., Jn. of Electrochemical Society, 107, 185, 1960.

36. Horsten, H.J.A. et at., Annals CIRP 20,43, 1971.

37. Thija, A., Van Dijck, F. and Snoeys, R., Investigation of polarity effects in EDM, Paper No. 73, p.7, CIRP, Feb. 1973.

38. Motoki, K. and Hashiguchi, K., Energy Distribution at the Gap in Electric Discharge Machining, Annals of CIRP, Vol. XIV, 1967, pp. 485-489.

39. Lee, T.H., T.F. Theory of Electron Emission in High-current Arcs, Jn. Appl. Phys., Vol. 30, No.2, Feb. 1959, pp. 166-171.

40. Kaldes, F., Flushing the Gap in EDM, Pt. I EDM Digest Jan/Feb 1983.

41. Application of High Power Laser, SPIE Pb., Vol. 527, 1984.

42. Manufacturing Application of Laser, SPIE Pb., Vol. 621, 1986.

43. High Power Lasers & Their Industrial Applications, SPIE Pb., Vol. 650, 1986.

44. Laser Technologies in Industries, SPIE Pb., Vol. 952 (Pt. II), 1988.

45. High Power Lasers & Laser Machining, SPIE Pb., Vol. 1132, 1989.

46. Lasers in Industries, Charschan, S.S. Van Nostrand, 1972.

47. Laser Machining, by G. Chryssolous; Springer Pb., 1991.

48. Laser Material Processing, by W.M. Steen; Springer Pb., 1991.

49. Laser in Manufacturing, Ed. by A. Quenzer, 1986, Proc. 3rd. Int. Conf., Paris; ISBN 3-540-16326-3.

50. Laser in Manufacturing, Ed. by W.M. Steen, 1987, Proc. 4th Int. Conf., Birmingham; ISBN 3-540-17854-6.

51. Laser in Manufacturing, Ed. by H.H.gel, 1988, Proc. 5th Int. Conf., Stuttgard; ISBN 3-540-50310-2.

52. Laser in Manufacturing, Ed. by W.M. Steen, 1989, Proc. 6th Int. Conf., Birmingham; ISBN 3-540-51241-1.

53. Laser in Manufacturing, by J.A. Luxon, D.E. Parker and P.D. Plotkwaski; ISBN 3-540-17427-3.

54. The Changing Frontiers of Laser Material Processing, Ed. by C.M. Banas, G.L. Whitney, Proc. ICALEO'86, Arlington, 1986; ISBN 3-540-17563-6.

55. Laser Material Processing, Ed. G. Bruck, Proc. ICALEO'88 USA, 1988; ISBN 3-540-51537-2.

56. Laser in Manufacturing, Ed. A. Gomersall, 1986; ISBN 3-540-16678-5.

57. Fundamentals of Laser Interaction II, Ed. F. Ehlotzky, 1989; ISBN 3-540-51430-9.

58. Electron Beam Welding by Maleka, McGraw-Hill Book Co., Lond. 1971.

59. Handbook of Electron Beam Welding-by R. Bakish and S.S. White, 1964.

60. Proceedings of 3rd Electron Beam Processing Seminar 1974 by R.M. Silva; publisher Universal Technology Corporation, Dayton, Ohio.

61. State of art of electron beam technology for metal removal, welding and heat treatment processes by K..H. Steigerwald in Proceedings of 20th IMTDR Conference 1980.

62. Arata, A., Plasma, Electron and Laser Beam Technology, ASM Pb., 1985.

63. Esibyan, E.M., Plasma-Arc Equipment, MIR Pb., 1973.

64. Anisimovich, L.A., A Physicist ABC on Plasma, MIR Pb., 1985.

65. Arata, A., Plasma, Electron and Laser Beam Technology, ASM Pb., 1985.

66. Dugdale, R.A., Glow Discharge material Processing, MB Mon. ME/5, Mills & Boon Ltd., London, 1971.

67. Benedict G.F. (1987), Non-traditional Manufacturing Processes, Marcel Dekker Inc., London.

68. Bhattacharyya A. (1973), New Technology, The Institution of Engineers (I), Calcutta.

69. Buttner A. and Lindenback D.A. (1969), Electrolytic dressing of diamond wheels for use in steel grinding, Ind. Diamond Rev., pp. 450-454.

70. Dash J. and King W.W. (1972), Electrothinning and electrodeposition of metals in magnetic fields, J. Electrochem Soc., Vol. 119, pp. 51-56.

71. DeBarr A.E. and Oliver D.A. (1968), Electrochemical Machining, MacDonald, London.

72. Gedam A. and Noble C.F. (1971), An assessment of the influence of some wheel variables in peripheral electrochemical grinding, Int. J. Mach. Tool Des. Res, Vol. 11, pp. 1-12.

73. Kuppuswamy G. (1976), Electrochemical grinding: an investigation of the metal removal rate, Proc. 7th AIMTDR Conf. held at Coimbatore (India) pp. 337-340.

74. Kuppuswamy G. and Venkatesh V.C. (1979), Wheel parameters and effect of magnetic field on electrolytic grinding, J. Inst. Engrs. (I), Part ME(l), Vol. 60, pp. 17-20.

75. Levinger R. and Malkin S. (1979), Electrochemical grinding of WC-Co cemented carbides, ASME Paper No. 78-WA/PROD-26, WAM, San Francisco, pp. 1-10.

76. McGeough J.A. (1988), Advanced Methods of Machining, Chapman and Hall, London.

77. Pandey P.C. and Shan H.S. (1980), Modern Machining Processes, TataMcGrawHill, New Delhi.

78. Jain V.K., Tandon S. and Kumar Prashant (1990), Experimental investigation into electrochemical spark machining of composites, Trans. ASME, J. Engg. Ind., Vol. 12, pp. 194-197.

79. Verma M.M. (1981), A study of process parameters in electrochemical grinding, M. Tech. Thesis, IIT Kanpur (India).

80. Benedict G.F. (1987), Non-traditional Manufacturing Processes, Marcel Dekker Inc., New York.

81. Naidu M.G.J. (1991), Electrochemical deburring for quality production, Proc. Winter School on AM T (Eds.: Jain V.K. and Choudhury S.K.), IIT Kanpur (India).

82. Pandey P.C. and Shan H.S. (1980), M odem Machining Processes, TataMcGraw Hill, New Delhi.

83. Pramanik D.K., Dasgupta R.K. and Basu S.K. (1982), A study of electrochemical deburring using a moving electrode, Wear, Vol. 82, pp. 309-316.

84. Rumyantsev E. and Davydev A. (1989), Electrochemical Machining o f M etals, Mir Publishers, Moscow.

85. Takazawa K. (1988), The challenge of burr technology and its worldwide trends, Bull. JSPE, Vol. 22, No. 3, pp. 165-170.

86. Tool Design Manual fo r Electrochemical Deburring, Chemtoal Inc., Minnesota, U.S.A.